
# Qualification of innovative floating substructures for 10MW wind turbines and water depths greater than 50m

| | |
|---|---|
| Project acronym | LIFES50+ |
| Grant agreement | 640741 |
| | Collaborative project |
| Start date | 2015-06-01 |
| Duration | 40 months |

Deliverable D7.7 Identification of critical environmental conditions and design load cases

| | |
|---|---|
| Lead Beneficiary | USTUTT |
| Due date | 2018-06-31 |
| Delivery date | 2018-07-04 |
| Dissemination level | Public |
| Status | Final |
| Classification | Unrestricted |
| Keywords | Floating wind, critical environmental conditions, design load cases, simulation requirements |
| Company document number | Click here to enter text. |

The research leading to these results has received funding from the European Union Horizon2020 programme under the agreement H2020-LCE-2014-1-640741.

## Disclaimer



## Document information

| Version | Date | Description | |
|---|---|---|---|
| 01 | 2018-05-15 | Advanced draft | |
| | | Prepared by | Kolja Müller, Ricardo Faerron-Guzmán |
| | | Reviewed by | Mathias Marley, Jonas Gullaksen Straume, Andreas Manjock |
| | | Approved by | Kolja Müller |
| 02 | 2018-06-12 | First version for review | |
| | | Prepared by | Kolja Müller, Ricardo Faerron-Guzmán, Andreas Manjock, Michael Borg |
| | | Reviewed by | Henrik Bredmose, Wiliam Jonse, Andreas Manjock |
| | | Approved by | Kolja Müller |
| 03 | 2018-07-03 | Final version | |
| | | Prepared by | Kolja Müller, Ricardo Faerron-Guzmán, Andreas Manjock |
| | | Reviewed by | Andreas Manjock, Josean Galvan Fernandez |
| | | Approved by | Kolja Müller |
| 04 | 2018-07-04 | Final version for QA before submission | |
| | | Prepared by | Kolja Müller |
| | | Reviewed by | Jan Arthur Norbeck |
| | | Approved by | Petter Andreas Berthelsen |



| Authors | Organization |
|---|---|
| Kolja Müller | University of Stuttgart |
| Ricardo Faerron-Guzmán | University of Stuttgart |
| Michael Borg | DTU |
| Andreas Manjock | DNV GL |

| Contributors | Organization |
|---|---|
| Trond Landbø | Olav Olsen |
| Håkon Andersen | Olav Olsen |
| Mathias Marley | Olav Olsen |
| Jonas Gullaksen Straume | Olav Olsen |
| Luca Vita | DNV GL |
| William Matthew Nipper | DNV GL |
| Henrik Bredmose | DTU |
| German Perez | Tecnalia |
| Josean Galvan | Tecnalia |
| Miren Sanchez | Tecnalia |
| Inigo Mendikoa | Tecnalia |
| Lina Hagemann | University of Stuttgart |

Definitions & Abbreviations

| | |
|---|---|
| AHD | additional hydrodynamic damping |
| ANOVA | Analysis of Variance |
| AST | Administrative Support Team |
| CAD | Computer-Aided Design |
| DEL | Damage Equivalent Load |
| DLC | Design Load Case |
| DNV | Det Norske Veritas |
| DOF | Degree of Freedom |
| DTU | Danmarks Tekniske Universitet |
| FAIRTEN1 | Fairlead 1 tension (leading fairlead for wind/wave direction = 0°) |
| FLS | Fatigue Limit State |
| FOWT | Floating Offshore Wind Turbine |
| GL | Germanischer Lloyd |
| IC | Initial Condition |
| LCOE | Levelized Cost of Energy |
| LR1 | Load range 1 (below rated) |
| LR2 | Load range 2 (transition / around rated) |
| LR3 | Load range 3 (above rated) |
| NREL | National Renewable Energy Laboratory |
| OC3 | Offshore Code Comparison Collaboration |
| PC | Project Coordinator |
| PM | Project Manager |
| PtfmHeave | Platform Heave motion DOF |
| PtfmPitch | Platform Pitch motion DOF |
| PtfmRoll | Platform Roll motion DOF |
| PtfmSurge | Platform Surge motion DOF |
| PtfmSway | Platform Sway motion DOF |
| PtfmYaw | Platform Yaw motion DOF |
| RNA | Rotor Nacelle Assembly |
| RootMyb1 | Blade root flap-wise bending moment, Blade 1 |
| TLP | Tension Leg Platform |
| TTDspFA | Tower Top Displacement Fore-Aft |
| TTDspSS | Tower Top Displacement Side-Side |
| TwrBsMyt | Tower Base Fore-Aft Bending Moment |
| TwrBsRes | Tower Base Resulting Bending Moment |
| ULS | Ultimate Limit State |
| WPL | Work Package Leader |

## Executive Summary

The design process for new substructure concepts is highly complicated, as relevant environmental conditions and simulation settings for numerical load assessment must be defined for each concept individually. This is due to the novel state of the FOWT technology and the outstanding of large scale deployment and validation of simulation tools with full-scale measurements of different substructure concepts. This lack of experience with the technology makes it important to carefully select design conditions for the system to provide a conservative yet cost effective design.

In order to support the designers of FOWT systems, this report provides methodologies to help the designer identify reduced sets of critical design-driving load cases, and the therein relevant environmental conditions and simulation requirements.

These methodologies are derived and applied based on the two selected concepts of LIFES50+ phase I: the LIFES50+ OO-Star Wind Floater Semi 10MW and the NAUTILUS-10 floating support structure. The derived critical design load cases are the DLC 1.2 (fatigue loads during power production and normal sea state), DLC 1.6 (ultimate loads during power production and severe sea state) and DLC 6.1 (ultimate loads during parked conditions and 50yr wind and wave environment). A global Monte Carlo based sensitivity analysis methodology is implemented for the determination of relevant environmental conditions of FOWT and more in-depth statistical methods such as Bootstrap and analysis of the backwards standard deviation are used for the determination of convergence behavior of the simulations. Finally, based on results from this task as well as previous tasks in LIFES50+, methodologies for determining the environmental impact on the LCOE as well as upscaling considerations are given.

Next to the methodologies, the results of the substantial simulation studies performed in this work provide the reader with specific recommendations for the simulation setup of both fatigue and ultimate limit state (FLS, ULS) simulations regarding run-in-times, required number of seeds, simulation length, and relevant environmental conditions. The determination of relevant environmental conditions may be a complex and numerically intensive task, which is why global sensitivity analysis is proposed as part of the design process. This may also support the definition of a more thorough, probabilistic design process which is considered to lead to more cost effective FOWT substructures.

It is highlighted that the reduced set of load cases cannot be taken to be sufficient for a complete design and do not present a possibility to reduce the overall design effort. The effort of identifying critical load cases is seen as advantageous in the early design stage, where a large variety of design possibilities is considered, and fast evaluations are key in order to find an optimized solution.

## Contents

## Disclaimer

The proposed critical simulation settings, conditions and recommendations presented in this document are related to the experiences collected as part of the LIFES50+ project. They were established from work focussing on selected sites (and the related environmental conditions and design basis) as well as on selected floater-turbine configurations and may not necessarily applicable to other systems or sites.

# 1 Introduction

The design of floating offshore wind turbines (FOWT) is a complex and highly iterative task. As the combined system of wind turbine, controller, tower, substructure and mooring lines is strongly interacting with the environment composed of wind, waves and currents, a highly complex load case setup is necessary to (1) consider all relevant environmental load scenarios for both fatigue and ultimate loading and to (2) ensure that numerical solutions are sufficiently accurate and converged. Each individual concept is expected to show fundamentally different sensitivities towards the environment, which is why it is difficult to outline one general set of simulation load cases and related simulation requirements that is applicable in the same way for all concepts. This is why at the current state; available guidelines may not be as specific in the description of the design load cases (DLCs) as would be desirable by designers. Rather than going through a well-defined list of load conditions for each load case, the designers have the responsibility to identify relevant load conditions and simulation requirements (i.e. settings such as run-in-time, simulation length and seed number) for each of the load cases for their concept.

As a stated goal of the LIFES50+ project is to provide recommended practices in the design of FOWT, the present study provides procedures for (1) the derivation of relevant design load cases for the early design, (2) the derivation of relevant environmental conditions within these relevant design load cases and (3) the assessment of simulation requirements for the load calculation. Because the consideration of all relevant environmental conditions is often not feasible due to the large simulation effort, but a probabilistic design is aspired to provide cost competitive designs, another focus of this work was (4) the derivation of a probabilistic load assessment methodology for FOWT under consideration of a large number of environmental conditions.

By applying the methodologies to the public models of the two selected semisubmersible concepts from LIFES50+ phase I, the present study also gives more applicable recommendations for load simulations of FOWT. Because of the huge number of possible combinations of environmental conditions, operational conditions and simulation parameters in time domain simulations, this study seeks for potential in reducing of computational effort whilst maintaining acceptable accuracy levels of the load results. This may be achieved by sensitivity analyses and statistical approaches, which are applied and based on the simulation results. To enable designers to perform similar evaluations, guidance is given in selecting suitable configurations for a FOWT load setup in order to perform similar studies.

The document is organized as follows:

Chapter 2 gives an overview on past research on simulation requirements and critical environmental conditions. Also, the relevance of the load case definition is outlined as part of the certification process. Based on previous experience within LIFES50+, a reduced set of three critical design load cases is derived which is the focus of this study.

Chapter 3 summarizes the numerical setup and the two baseline concepts used throughout this work. The fundamental differences between the concepts and their numerical models are also highlighted.

Chapter 4 focusses on FLS simulation studies. Studies are performed to identify simulation requirements for the assessment of initial conditions and transient effects. This is followed by global load sensitivity analysis considering up to 7 environmental parameters. Based on this an in-depth study is presented investigating more closely the influence of the wave period. Also, the load sensitivity towards the wave peak shape parameter is investigated. Finally, the required number of seeds and combination of seeds with different simulation times is determined.

Closely linked to the previous chapter, chapter 5 investigates simulation requirements and critical environmental conditions for both concepts for ULS assessment. An additional item investigated for ULS is the impact of marine growth.

Chapter 6 provides a link to the work performed in other work packages with respect to the interaction between the found critical environmental conditions and LCOE as well as upscaling.

The derived recommendations from the work are summarized in chapter 7 and the conclusions and an outlook are given in chapter 8.

Significant parts of the studies presented herein have been compiled as part of WP4 efforts (i.e. definition of design driving load cases was also investigated in (Pegalajar-Jurado, et al., 2018) and will be part of LIFES50+ deliverable 4.6 (in preparation), simulation requirements are used throughout simulations performed in various deliverables, robustness check of public models was performed for the models presented in (Yu, et al., 2018)) and are included in this document to provide a more comprehensive overview.

# 2 Review

## 2.1 Simulation requirements

This section provides an overview on the work that has previously been done in the field of research, related to the simulation requirements for design load simulations of FOWT. They are sorted into the two principal topics, which are the critical environmental conditions (section 2.1.1), and the resolution requirements (section 2.1.2). Other items such as model requirements and/or techniques for data processing (e.g. consideration of half-cycles) are not addressed here.

The considered studies in this chapter are in particular:

- (Barj, et al., 2014), (Haid, et al., 2013): investigated a 5-MW turbine installed on a OC3-Hywind spar buoy
- (Kvittem & Moan, 2015): investigated a 5-MW turbine installed on a semi-submersible (similar to WindFloat)
- (Bachynski, et al., 2014): investigated a 5-MW turbine installed on a spar, tension leg and two semi-submersible platforms
- (Stewart, et al., 2013): made recommendations on the simulation length for a 5-MW turbine installed on a OC3-Hywind spar buoy
- (Stewart, 2016): made recommendations on the simulation length for a 5-MW turbine installed on a OC3-Hywind spar buoy and a semi-submersible platform

### 2.1.1 Critical environmental conditions

One existing guideline that is commonly used for the design of offshore wind turbine substructures is the IEC-61400-3 (International Electrical Commision, 2009) which was developed for offshore wind

turbine support structures that are fixed to the sea floor. This guideline, however, may not be sufficient for floating offshore wind turbines due to the larger movements in the waves and the lower natural frequencies of the system. The floating specific standard IEC-61400-3-2 is currently under development but is not published officially yet. Therefore, it is important to investigate the environmental conditions of the simulation for floating systems, since certain given parameters might be too conservative or not conservative enough for FOWT.

Several environmental conditions were investigated in earlier work. The most relevant ones being wind speed, wave height and wave period. However, next to these, directionality in the form of wind-wave misalignment is typically considered as an important item that needs special consideration for each individual platform. For example, (Barj, et al., 2014) found that 90° misalignment has a considerable impact on the side-side loading for both ULS and FLS conditions. Regarding wave direction impact on mooring line loads, it was found that the more significant loads are to be expected when wave impact is directed along the mooring lines. Additionally, (Kvittem & Moan, 2015) investigated the impact of wind directionality and found this to be of similar importance as wave directionality. Contrary to results from (Barj, et al., 2014), they found aligned wind and wave to give the most conservative loads. However, this disagreement may result from the different load definition used in the two studies. They note that loading in the substructure may be more dependent on directionality than the loading on the turbine´s tower and blades. Also, (Bachynski, et al., 2014) noted the most conservative loads on the tower for aligned wind and wave conditions, while acknowledging that the platform orientation with respect to wave impact direction is important. Platforms with large displacements (e.g. semi-submersible platforms) show the least fatigue loads at the tower base.

Regarding the consideration of wind and wave misalignment, (Stewart, 2016) also found that for both the OC3 Hywind Spar and for a semi-submersible with a 5MW NREL reference turbine, considering only aligned waves under predicts the side-side tower and over predicts the fore-aft fatigue damage. A recommendation is made to take only the aligned and 90-degree wave misalignment cases along with their pertinent probabilities.

It is noted that any conclusions with respect to critical environmental conditions will be depending on (among others) the absolute and relative severity of the environmental variables under consideration, the concept under consideration (i.e. chosen RNA, tower, floating substructure, mooring configuration and materials used). It is recommended to perform extensive sensitivity analyses before deciding which load cases should be considered as the most relevant.

### 2.1.2 Resolution requirements

In the setup of design simulations, the resolution (i.e. simulation length, Number of seeds, Binning of environmental conditions) of the relevant environmental conditions is important to obtain converged solutions. If the resolution of, for example, the wind speed is too coarse, important effects such as the 3p tower excitation may not be considered which may lead to an over- or –worse- underestimation of fatigue damage or ultimate loading. The most relevant conditions are typically wind speed, wave height, wave period and wind/wave misalignment. For floating wind, it becomes important to reassess the required resolution for different environmental variables specifically for each concept as they may be fundamentally different as for wind speed.

Regarding the **wind speed**, (Kvittem & Moan, 2015) found 2.0 m/s bins to provide results within 12% error margin for fatigue loads on the platform and tower base. They highlight the importance of including 3P resonance effects when turning to larger bins. In addition, they found 1.5 m **wave height** bins to provide results within 6% error margin for fatigue loads on the platform and tower base. Finally, for the

**wave period**, they also found 2.0 s bins to provide results within 5% error margin for fatigue loads on the platform and tower base.

**Wave direction** bins were investigated for an OC3 Hywind spar type floating wind turbine by (Barj, et al., 2014). They found that, based on 10-min simulations, for determining extreme loads for turbine and anchor loads, it should be sufficient to simulate only two bins (0° and 90°) for wave direction, when wind direction is held constant. They also noted that using two bins should suffice for the determination of lifetime fatigue but highlighted that the two directions with the largest damage contribution need to be considered.

(Stewart, et al., 2013) investigated the **simulation length requirements** for the OC3 Hywind Spar with a 5MW NREL reference turbine and found that for increasing the standard 10 minutes simulation lengths no significant variation is to be expected. However, it is mentioned that relatively greater number of unclosed cycles counted during the fatigue estimation in shorter simulations have an important role on the fatigue estimation. This is similar to the findings for onshore turbines, such as presented by (Söker, et al., 2004). Here, they investigated how taking individual fatigue from one time series neglects the loading effect of the wind speed varying from one ten minutes average to another respectively from one measurement load case to another, in other words the effect of low cycle fatigue. For the onshore turbines analysed, it was found that low cycle fatigue can contribute significantly to materials with large sensitivity to load cycles with large ranges such as fibre plastics and cast modular iron components.

Furthermore, the **number of considered seeds** was also investigated by (Stewart, et al., 2013). They showed that for the maximum loads of the OC3 Hywind Spar, 10 simulations (of 10min) are necessary to be within 2% of the true value of the maximum fore-aft tower base bending moment.

Similar to (Stewart, et al., 2013), (Stewart, 2016) further analysed the simulation length requirement not only for the OC3 Hywind Spar, but also for a semi-submersible with a 5MW NREL reference turbine. He found that for the semi-submersible, the shorter simulations with repeating 10 minutes wind files can create situations where the simulations never achieve full oscillations of the platform. This may be a reason to use longer simulations if anchor/mooring line tension is an important factor. However, he does note that, longer simulation lengths other than 10 minutes with constant mean wind speed and turbulence intensity would not represent reality, since these statistics change over the 10 minutes spans.

(Haid, et al., 2013) also focussed on **simulation length requirements** and the **number of considered seeds** in order to obtain converged load results. They used periodic 10-min wind fields in combination with 1-6 hours wave environments and investigated the impact on the response statistics. To investigate the dependence of aerodynamically derived loads on simulation length, they compared loads statistics from 10x1-hour, 12x50-min, 15x40-min, 20x30-min, 30x20-min, and 60x10-min FAST simulations. A land-based turbine was used for this study to ensure a comparison based on only aerodynamic loads. To investigate the dependence on simulation length of loads due to hydrodynamics and floating platform motion, they evaluated loads statistics from simulations with a length of 10 minutes, 20 minutes, 1 hour, 3 hours, and 6 hours, with the numbers of independent wave and wind seeds chosen to yield the same amount of random information in each group of simulations. The results showed that when the total simulation length for the wind and waves is constant, the ultimate loads do not intensify with increasing simulation length. Based on bootstrap analysis, the authors suggest that approximately ten 10-min simulations for each wind speed bin should be used to obtain converged statistics. They also found that the length of the wind files does not have a significant effect on the loads acting on the turbine, as long as the total simulation time was kept constant. For fatigue loads, the impact of the simulation length was found to be below 5% for all observed locations.

In addition to this study, (Kvittem & Moan, 2015) found that for locations on the platform and tower base, 10x10min simulations were sufficient to be within an error margin of 10%, when calculating the lifetime damage.

Another item of interest is the requirements for the determination of **initial conditions (IC)** and the **run-in-time** for the simulations. It might be thought that to yield stationary response in the low-frequent modes a significant amount of simulation time is needed. However, (Haid, et al., 2013) recommended that the initial simulation time which should be ignored is at least of 60 seconds for the FOWT analyzed, when proper ICs are used for rotor speed, blade pitch, out-of-plane blade deflection, and platform surge, pitch and heave displacements under specific wind and wave conditions. The methodology on how this conclusion was taken is not explained in the report. As 60s is typically less than one cycle of natural periods, technically, the ICs should then include some offset in the motion as well.

## 2.2 Relevance of load case definition

Load cases are an inherent part of the wind turbine standards and define the specific design load criteria for the structural design according to defined classes of environmental impacts. These generic external conditions describing wind, waves, currents, etc. and their related meteorological parameters in different classes of severeness and enables the calculation of reproducible and comparable load sets. The definition of extreme events – in wind industry standards a recurrence period of 50 years has been established – in combination with partial safety factors reflect a generally accepted safety level which enables a safe energy production during life time, typically 20 to 25 years. The intention of the load case definitions is to cover all load relevant situations within the designated life time of the system. These are basically normal operation, extreme events, failure modes and grid impacts in combination with operation and stand-still conditions. In line with the growth of turbine size, structural elasticity and complexity of modern wind turbines the load case definitions in international standards such as the IEC61400-3 (e.g. (International Electrotechnical Commission , 2009)) series or DNV GL standards (e.g. (DNV-OS-J103, 2013)) ) have been extended continuously. This was done e.g. by replacing stationary wind conditions by turbulent wind fields and introducing extrapolation methods for the determination of extreme load levels. A full load case setup for final design or for certification of a floating wind turbine according to above mentioned standards could easily reach $10^4$ different load case variations. Such a setup includes e.g. a complete representation of the wind and wave spectra with all relevant combinations and directionalities. This procedure ensures that all situations with a potential to generate critical design loading are covered by the load case setup.

Adding to the load cases of the installed system, load cases focussing on other stages of the life cycle could also be of value, covering items such as construction, temporary storage/mooring and towing cases. These may be of relevance but are not covered in this work.

## 2.3 Critical environmental conditions for FOWT global evaluation

When setting up a load case definition a classical trilemma must to be solved: Finding an optimal relation between calculation accuracy, calculation time and calculation data volume. As mentioned above a full load case setup according to a certification standard could lead to more than $10^4$ load cases, several terabytes of time series data and several weeks of computation time (depending on the hard ware equipment). Therefore, it should be clarified prior to the definition of load case setup for which purpose the load results will be used later on. The potential for reduction of calculation effort is obviously depending on the envisaged design stage of the FOWT. In concept development simplified models, application of scaling or extrapolation methods might be sufficient. In front end design or in academic analysis projects the load case table and the variation of calculation parameters could be reduced to a handful of (assumed/experienced) design driving configurations. If the load simulation results should be applied in a

final design calculation or within a type or project certification process the complete set of standard load cases, including the defined combinations of environmental and operational parameters should be performed to achieve the required accuracy for these development stages.

### 2.3.1 Summary of experiences

In this section experiences in simulating FOWT from research and demonstration projects have been selected. The review focuses on the four main floater types designed and build in the recent years: Semisubmersible, tension leg platform (TLP), barge and spar buoy. Today no floater type has been clearly established as a favourable design with respect to Levelised Cost Of Energy (LCOE). The recommendations given in this section have been extracted from the simulation calculations with the *LIFES50+ OO-Star Wind Floater Semi 10MW* and the *NAUTILUS-10* concept, see section 3.1. Additionally, observations have been applied made by DNV GL with different floating concepts, see DNVGL-RP-0286 for further details. The recommendations given in this section are based on experiences with a few selected design concepts under limited environmental conditions. They are not applicable generally to the addressed floater concepts and a sensitivity study as described in section 4 and section 5 shall be performed in any case for each new design concept.

However, there are several differences observed in FOWT simulations compared to bottom fixed offshore wind turbines and as well among the different floater types considered.

**Semi-submersible**

This floater type is buoyancy and ballast stabilised and large parts of the structure's volume is located below sea level. The platform type is typically characterised by strong motions induced by sea states. Tower bottom and floater hull loads are typically dominated by storm load cases, such as DLC 6.1. Wave lengths which are a portion of the distance between structure buoyancy columns could cause strong excitation. These "splitting periods" could cause significant ULS loads. Extreme wave heights might not necessarily result in maximum loads. Instead specific wave periods at lower wave heights could provide dimensioning loads. Therefore, a careful selection of wave periods, especially towards large periods (low frequency) is recommended. Wind-wave misalignment is relevant to consider, and beside collinear wind-wave directionality also misaligned seas lead typically to high FLS and ULS loading. The mooring system loading often receive little impact by wind loads and is dominated by combinations of wave loads and currents.

**Tension leg platform (TLP)**

TLP designs are well known in the Oil&Gas industry and have been designed primary for very deep waters. The floater is stabilised by vertical tendons which are fixed to the sea bed. This design provides a relative stiff positioning of the full submerged floater, especially in heave, pitch and roll direction. Many TLP designs show a weakness of the platform yaw motion degree of freedom. The sensitivity to environmental impacts is often close to bottom fixed offshore wind turbines, in the DOFs mentioned. Whilst the RNA loads are driven by wind, the support structure (tower, floater, station keeping) is driven by sea states. Wind-wave misalignment of 90° could result in strong loading because of the lack of aerodynamic damping. Due to unfavourable parking positions service limit states (SLS) could result in extreme loads. Furthermore, leakage and tendon failures become critical for the structure. Severe sea states and 50-year sea states are often design driver of the tower bottom and the floater. A special TLP effect is tendon slack (loss of pretension). The relation of tendon slack and varying sea levels is important for the tendon structural integrity and should be considered in the load case setup for TLP's. Consideration of currents is relevant for tendon ULS and FLS loads.

**Barge**

The barge type is purely buoyancy stabilised and uses often similar station keeping systems as the semi-submersible type. The barge type tends to strong, wave elevation induced platform motions with high inclinations in pitch and roll direction. In FLS simulations both wind and wave load typically contributes to structural fatigue. In ULS simulations wave impact from 50-years events is dominating hull and mooring loads for the considered barge type (DLC 6.1 and DLC 6.2). Large platform pitch angles result in extreme loads of the RNA and the tower. Perpendicular directions of wind and waves (wind-wave misalignment 90°) are critical due to the lack of aerodynamic damping. A global sensitivity analysis to wind-wave misalignment for each barge type design is recommended. For extreme sea state (ESS) and severe sea state (SSS), all the points on the environmental contour of wave height and wave period should be considered and not just the largest wave heights and associated wave periods.

**Spar buoy**

The slender structure design of spar buoys is generating its stability by a massive ballast located typically at the spar foot at high draught. Mooring lines are attached at fairleads above the ballast area. Compared to the other floater types described above, fatigue loads of the spar buoy are influenced by wind and wave conditions at balanced portion, both RNA and support structure. The spar buoy type is responding typically sensitive to wind-wave misalignment. A full analysis with at least 15° variation steps of the directionality of wind and waves is highly recommended. Collinear wind and waves as well as currents in line and opposing wind direction lead to extreme pitch angles which results in ULS design drivers for RNA and support structure. Spar buoy designs are often characterised by weak yaw resistance. This could lead to additional ULS loading for the rotor. The tower and the spar could receive extreme loads at maximum rotor thrust, e.g. DLC 1.6. System failures (DLC 2.x) and emergency shut downs (DLC 5.1) might result in extreme pitch/roll motions and related extreme loading. For the mooring lines or catenaries yaw excitation due to high wind turbulence or inflow errors could be an issue.

### 2.3.2 Global ULS analysis

A numerical study (Frias Calvo, 2017) was carried out on the *LIFES50+ OO-Star Wind Floater Semi 10MW* (Yu, et al., 2018) to investigate the ULS loads and dominating DLCs in terms of ultimate loads. The Gulf of Maine site defined in the LIFES50+ project (Krieger, et al., 2015) was considered. The aero-hydro-servo-elastic HAWC2 simulation tool (Kim, 2013) was used to perform dynamic calculations. In the model set up for this study, the wind turbine and tower were modelled with a Timoshenko beam finite element formulation, and aerodynamic loads on these components were calculated using a modified blade element momentum method detailed by (Larsen, 2013). The mooring lines are represented with a cable finite element model, including hydrodynamic loading through application of the Morison equation. Hydrodynamic loads on the floating support structure were calculated using a first-order potential flow solution by WAMIT, combined with the drag term from the Morison equation. No second order hydrodynamic loads were considered apart from the contributions of the Morison equation. The DTU Wind Energy controller was tuned to maintain stable operation across the wind turbine operating envelope and avoid the negative damping phenomenon (Pegalajar-Jurado, et al., 2018).

#### 2.3.2.1 Design load cases

The selection of DLCs was based on the LIFES50+ Design Basis (Krieger, et al., 2015) and the DTU Wind Energy Offshore Design Load Basis (Natarajan, 2016). The IEC 61400-3 DLCs were selected to assess the ultimate loads in ULS and ALS conditions. Table 2-1 defines the ULS DLCs and Table 2-2 defines the ALS DLCs. For DLCs with extreme operating gusts (EOG) in total seven scenarios were considered, corresponding to gust time periods equivalent to the platforms six rigid body natural periods

(multiplied by 1.5) and the standard 10.5 seconds duration. Similarly, for DLCs with extreme direction change (EDC) and extreme coherent gust with direction change (ECD), the gust time duration was set to the yaw natural period of the floating wind turbine. Further details on the definition of all DLCs may be found in (Frias Calvo, 2017).

**Table 2-1: Ultimate limit state DLCs**

| Name | Load | PSF | Description | WSP $[m/s]$ | Yaw $[deg]$ | Turb. | Seeds | Shear | Gust | SS | WWD | T$[s]$ |
|---|---|---|---|---|---|---|---|---|---|---|---|---|
| DLC13 | U | 1.35 | Power production with ETM | 4:2:26 | -10/0/+10 | ETM | 6 | 0.14 | None | NSS | UNI | 3600 |
| DLC14 | U | 1.35 | Power production in ECD | Vr -2, Vr, Vr +2 | Direction Change | None | None | 0.14 | ECD | NSS | Initially aligned with wind | 1000 |
| DLC15 | U | 1.35 | Power production with EWS | 4:2:26 | 0 | None | None | Eq. in IEC | None | NSS | UNI | 1000 |
| DLC16 | U | 1.35 | Power production in severe sea states | 4:2:26 | -10/0/+10 | NTM | 6 | 0.14 | None | SSS | UNI | 3600 |
| DLC21 | U | 1.35 | Power production with grid loss | 4:2:26 | -10/0/+10 | NTM | 4 | 0.14 | None | NSS | UNI | 3600 |
| DLC23 | U | 1.1 | Power production with grid loss during EOG | Vr -2, Vr, Vr +2 Vout | 0 | None | 5 gusts at 3 diff. starting points | 0.14 | EOG | NSS | UNI | 1000 |
| DLC32 | U | 1.35 | Start-up in EOG | Vin, Vr+-2, Vout | 0 | None | None | 0.14 | EOG | NSS | UNI | 1000 |
| DLC33 | U | 1.35 | Start-up in EDC | Vin, Vr+-2, Vout | 0 | None | None | 0.14 | EDC | NSS | Initially aligned with wind | 1000 |
| DLC42 | U | 1.35 | Shut-down with EOG | Vin, Vr, Vout | 0 | None | None | 0.14 | EOG | NSS | UNI | 1000 |
| DLC51 | U | 1.35 | Emergency shut-down | Vr+-2, Vout | 0 | NTM | 12 | 0.14 | None | NSS | UNI | 1000 |
| DLC61 | U | 1.35 | Parked in extreme wind | V50 | -10/+10 | 11% | 6 | 0.11 | None | ESS | UNI | 3600 |

Table 2-2: Accidental limit state DLCs

| Name | Load | PSF | Description | WSP $[m/s]$ | Yaw $[deg]$ | Turb. | Seeds | Shear | Gust | SS | WWD | T$[s]$ |
|---|---|---|---|---|---|---|---|---|---|---|---|---|
| DLC91 | U | 1.1 | Power production transient condition | 4:2:26 | -10/0/+10 | NTM | 6 | 0.14 | None | NSS | UNI | 3600 |
| DLC92 | U | 1.1 | Power production redundancy check condition | 4:2:26 | -10/0/+10 | NTM | 6 | 0.14 | None | NSS | UNI | 3600 |
| DLC101 | U | 1.1 | Parked transient condition | V50 | -10/0/+10 | 11% | 1 | 0.11 | None | ESS | UNI | 3600 |
| DLC102 | U | 1.1 | Parked redundancy check condition | V50 | -10/0/+10 | 11% | 1 | 0.11 | None | ESS | UNI | 3600 |

#### 2.3.2.2 Important results

Figure 2.1 presents the maximum fore-aft and side-side bending moments in the tower bottom, Figure 2.2 presents the maximum fore-aft and side-side accelerations of the tower top, and Figure 2.3 presents the mooring line arrangement and maximum fairlead tensions.

The analysis of the results showed a strong influence of the controller on loads within the wind turbine and tower during gust events and extreme turbulence conditions. The tuning of the controller to avoid platform motion instabilities resulted in a slower controller response to disturbances. This slower response rate resulted in higher loads in the tower bottom, tower top and blade root bending moments. This is highly dependent on the concept and could be mitigated by including the RNA acceleration into a feedback loop. A better tuned controller might thus change the found loads of this study.

A challenge in this study was the definition of the gusts, due to the large number of possible combinations of duration and time-lag. Thus, it is not certain if the largest loads possible were induced in the present work, and whether these gusts are realistic in nature. A probabilistic approach may be considered in the future to reduce uncertainties here.

DLC 10.1 and DLC 10.2, corresponding to a mooring line failure with a parked wind turbine, were initially found to be the dominant DLCs in generating largest loads and accelerations in the majority of sensors analysed. Further analysis of results showed that blade edgewise instabilities in these DLCs with a wind direction of 10 degrees led to the large loads and accelerations. This issue was also observed during the design of the DTU 10MW Reference Wind Turbine (Bak, et al., 2013). The bars denoted '*DLC 10.1*' and '*DLC 10.2*' in Figure 2.1, Figure 2.2 and Figure 2.3 represent the largest response for these DLCs, excluding the case with a wind direction of 10 degrees. Thus, whilst this instability is specific to the turbine used here, the scenario of a mooring line failure may still be a design-driving case for floating wind turbines with catenary mooring systems.

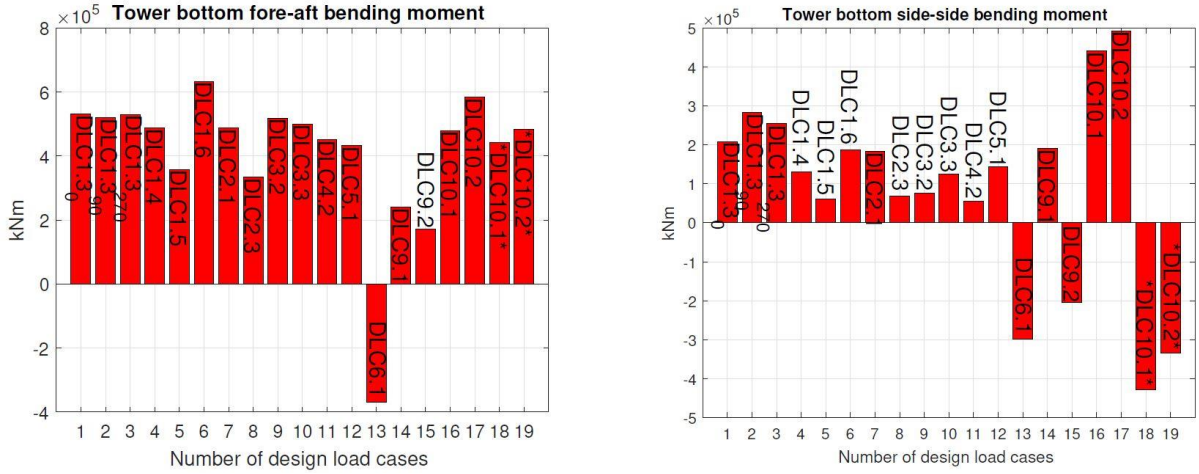


Figure 2.1: Tower bottom bending moments

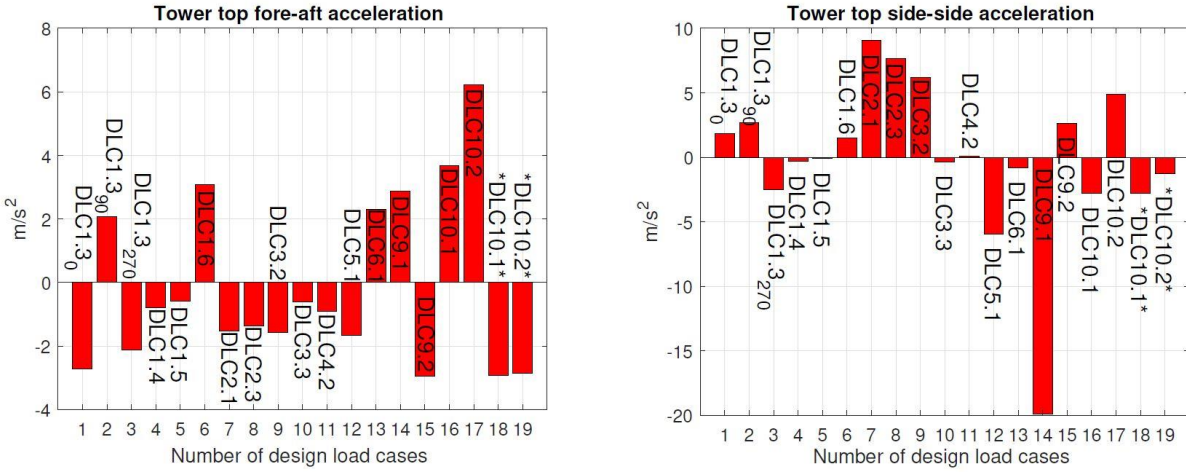


Figure 2.2: Tower top accelerations

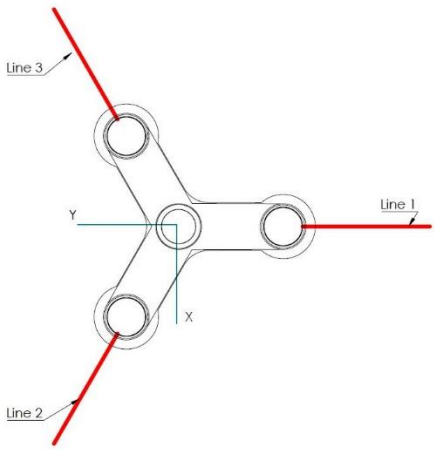


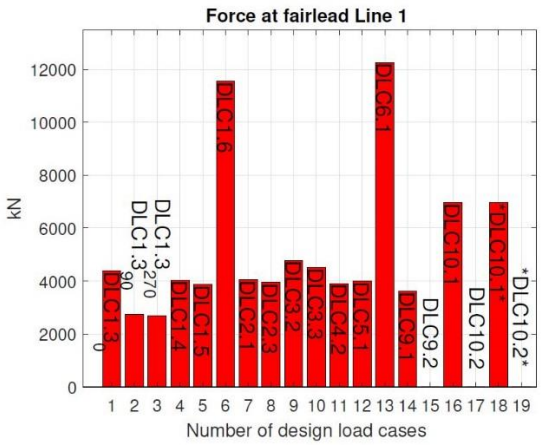

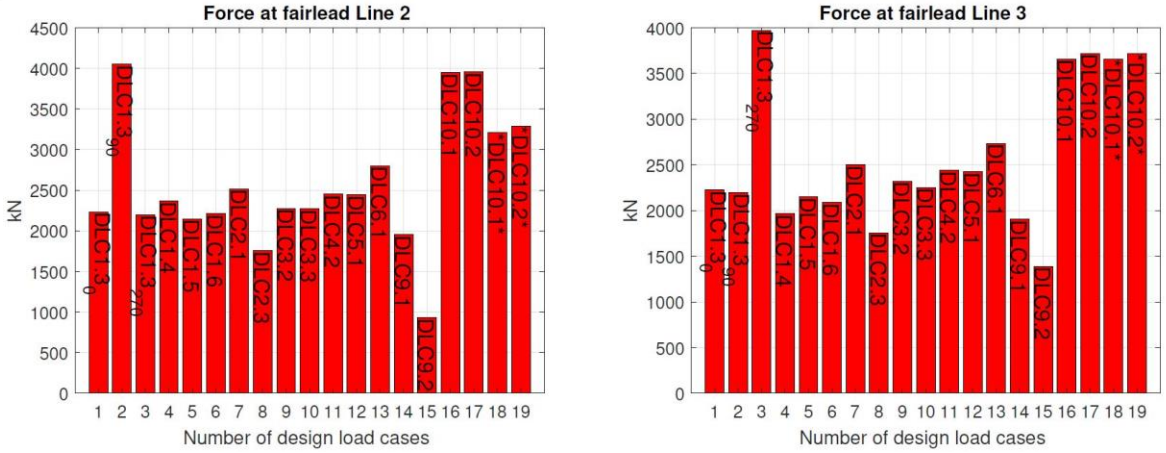


**Figure 2.3: Mooring line arrangement and fairlead tensions**

# 3 Considered setup

## 3.1 Turbine and platform concepts

The considered systems are the DTU 10MW reference wind turbine and either the *LIFES50+ OO-Star Wind Floater Semi 10MW* or the *NAUTILUS-10* floating support structure. The lifetime for the considered systems is set to 25 years. The used DTU 10MW RWT is an upwind HAWT with variable speed, collective pitch and a rated rotor speed range of 6-9.6 RPM. The cut-in, rated and cut-out wind speeds are 4.0 m/s, 11.4 m/s and 25.0 m/s. (Bak, 2013).

The semi-submersible *LIFES50+ OO-Star Wind Floater Semi 10MW* consists of a concrete platform with star-shaped base pontoon connecting the central column with the three outer columns. Three mooring lines with additional weights hold the platform in place. The tower design used in this concept is a stiff-stiff design. The corresponding natural frequencies are shown in Table 3-1. Figure 3.1 shows a sketch of the CAD model used within LIFES50+ as well as a rendered view of the concept. A controller developed at the University of Stuttgart with tailored input parameters was used for this study. There is no active ballasting included in this concept. The natural frequencies have been calculated by FAST based on an elastic blade and tower model mounted on a stiff floater. Note that this modelling leads to increased natural frequencies for the tower, which may alter the results of the model used in this work compared to a commercial design.

The *NAUTILUS-10* concept is a steel semi-submersible floater with four columns, a squared ring pontoon connecting them at their lower ends, an X-shaped main deck consisting of four rectangular shaped connections between column's upper ends and an embedded transition piece. The substructure is moored to the seabed using four conventional catenary steel chain mooring lines arranged in a symmetrical configuration. An active ballast system with closed-loop control has been designed to mitigate wind-induced thrust forces, restoring the system to optimal efficiency following changes in wind velocity and direction and keeping the verticality of the tower. The platform trim system pumps sea water in or out independently into each of the individual columns to adjust the draft (target floater air gap) and to compensate for the mean wind thrust loading on the turbine rotor and substructure. The tower design used in this concept is a stiff-stiff design. The corresponding natural frequencies are shown in Table 3-1. Figure 3.2 shows a sketch of the CAD model used within LIFES50+ as well as a rendered view of the concept. The DTU Wind Energy Controller (Hansen & Henriksen, 2013) with tailored input parameters was used for this study. The natural frequencies have been calculated by FAST based on an elastic blade

and tower model mounted on a stiff floater. Note that this modelling leads to increased natural frequencies for the tower, which may alter the results of the model used in this work compared to a commercial design.

**Table 3-1: Properties the two considered platform concepts (Yu, et al., 2018)[1]**

| Property | *LIFES50+ OO-Star Wind Floater Semi 10MW* | | *NAUTILUS-10* | |
|---|---|---|---|---|
| Total mass [kg] | 2.3618E+07 | | 9.337E+06[2] | |
| Natural frequencies or period surge | 0.0055 Hz | 181.8 s | 0.0080 Hz | 125.0 s |
| Natural frequencies or period heave | 0.0490 Hz | 20.4 s | 0.0530 Hz | 18.8 s |
| Natural frequencies or period pitch | 0.0320 Hz | 31.3 s | 0.0330 Hz | 30.3 s |
| Natural frequencies or period yaw | 0.0086 Hz | 116.3 s | 0.0100 Hz | 100 s |
| Natural frequencies or period tower | 0.7860 Hz | 1.3 s | 0.5410 Hz | 1.8 s |

Different models were available for the different concepts and due to new findings, some relevant variations in the simulation studies are to be taken into account when trying to compare the results presented in this document:

- Different hydrodynamic modelling was applied for both concepts (1st order potential flow & second order hydrodynamics & global drag for *Nautilus-10* concept rather than first order potential flow & Morison drag for *OO-Star Wind Floater Semi 10MW* concept)
- Non-consideration of currents for the *Nautilus-10* concept
- Using a different minimum wave period for the ULS analysis
- Using different controllers (DTU controller for *Nautilus-10*, SWE controller for *LIFES50+ OO-Star Wind Floater Semi 10MW*)
- Consideration of the maximum of fairlead tension loads for the evaluation for the *Nautilus-10* concept rather than leading fairlead tension for the *LIFES50+ OO-Star Wind Floater Semi 10MW* concept
- Consideration of the tower-base-resulting bending moment for *Nautilus-10* concept rather than the fore-aft and side-side moment for the *LIFES50+ OO-Star Wind Floater Semi 10MW* concept.

[1] Assuming stiff floater for both concepts
[2] including fully loaded active and passive ballast

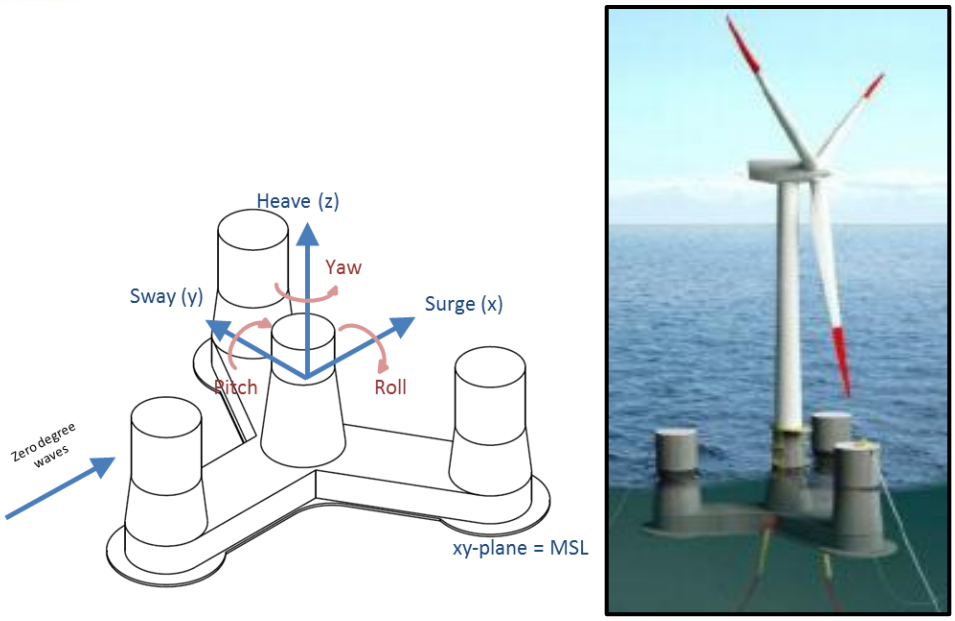


Figure 3.1: LIFES50+ OO-Star Wind Floater Semi 10MW (Yu, et al., 2018), (Olsen, n.d.)

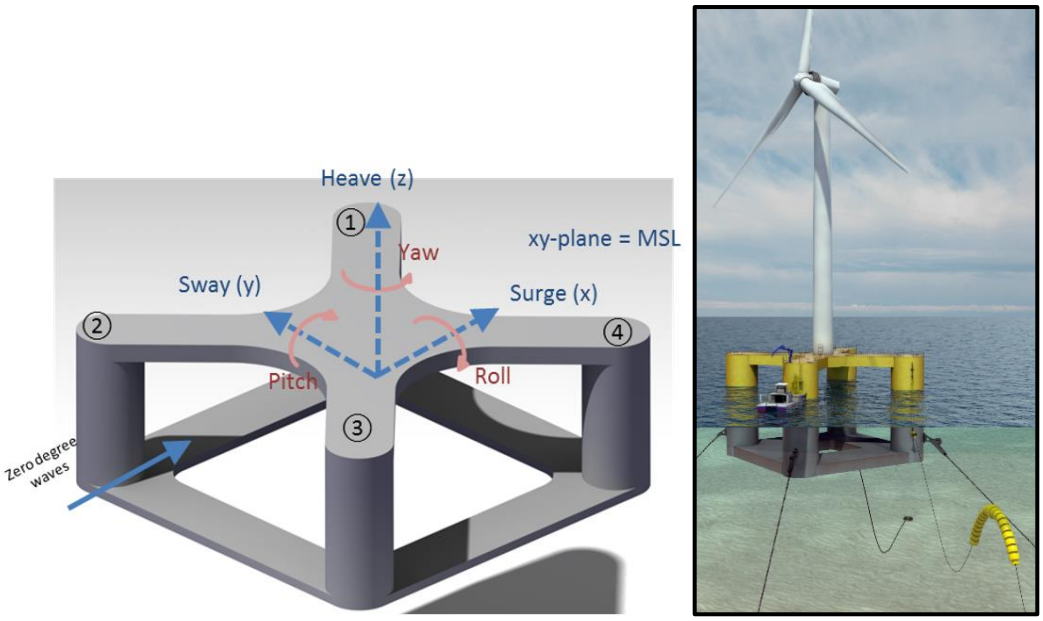


Figure 3.2: NAUTILUS-10 floating support structure concept (Yu, et al., 2018), (Müller, et al., 2018)

## 3.2 Considered environment

For the main simulation studies presented herein, reference environmental conditions are used. These are taken from the LIFES50+ project as well. The conditions analysed are of the LIFES50+ reference site B (medium severity), based on environmental data found at the Gulf of Maine, which is along the coast of the east coast in the United States of North America. The site is intended to be representative of the North Atlantic Ocean, about 25km at the southwest of Monhegan Island and 65 km east from Portland, Maine. It has a water depth of 130m and is characterised by a Weibull scale coefficient of 6.2 and a shape coefficient of 1.7, as derived by a measurement buoy. Table 3-2 summarizes key characteristics of the environmental parameters. The environmental conditions are defined in detail in (Krieger, et al., 2015) and (Ramachandran, et al., 2017).

**Table 3-2: site conditions (Ramachandran, et al., 2017)**

| Parameter | | Unit | Site B |
|---|---|---|---|
| Water depth conditions | Water depth | m | 130 |
| | Water level range (absolute) | m | 5.12 |
| Operational wind conditions | Mean air density | $kg/m^3$ | 1.225 |
| | Weibull scale parameter, A | m/s | 10.46 |
| | Weibull scale parameter, k | - | 1.701 |
| | Annual average wind speed, $v_{ave,hub}$ | m/s | 6.214 |
| | Wind shear exponent | - | 0.14 |
| | Mean free turbulence intensity at 15 m/s, $I_{15}$ | % | 8.5 |
| | Standard deviation of turbulence intensity | % | 4.9 |
| Extreme wind conditions | Mean air density | $kg/m^3$ | 1.225 |
| | 10 min. mean reference wind speed (50 years return period) at hub height, $v_{ref}$ | m/s | 44.0 |
| | 2 sec. gust wind speed (50 years return period) at hub height, $v_{e50}$ | m/s | 62.7 |
| | Extreme wind shear exponent | - | 0.11 |
| Normal Sea States (NSS) | See Section 7.5.1 of (Krieger, et al., 2015) | | |
| Extreme Sea States (ESS) | 50-year significant wave height, $H_{s50,3h}$ | m | 10.9 |
| | 50-year peak period range, $T_{p50,3hmin}$ - $T_{p50,3hmax}$ | s | 9.0 - 16.0 |
| | 1-year significant wave height, $H_{s1,3h}$ | m | 7.7 |
| | 1-year peak period range, $T_{p1,3hmin}$ - $T_{p1,3hmax}$ | s | 12.0 - 18.0 |
| Severe Sea States (SSS) | Significant wave height up to the rated wind speed | m | 7.7 |
| | Significant wave height beyond the rated wind speed | m | 10.9 |

## 3.3 Numerical model

The simulations were performed in the time domain using FAST v8.16 (Jonkman & Buhl, 2005). The system dynamics and elastodynamics are represented by a combined multibody and modal approach implemented in the ElastoDyn module (Jonkman & Buhl, 2005). The proposed model accounts for 21 Degrees Of Freedom (DOFs), where the flexible blades make use of 9 DOFs (most 3 relevant mode shapes by each blade) and the flexible tower accounts for 4 DOFs. The support structure is modelled as a rigid body, which generally leads to a non-conservative overestimation of the tower natural frequency, if the tower design is a stiff-stiff design (see also (Borg, et al., 2018) on including flexible substructures). The validity of this assumption is not investigated in detail in this study. The rotor-nacelle-assembly (RNA) aerodynamics are captured by traditional Blade-Element Momentum (BEM) theory and the common corrections included by AeroDyn (Laino & Hansen, 2002). Although the tower and floating platform aerodynamics can have some impact on the FOWT dynamics, both have been neglected in the model employed. TurbSim (Jonkman , 2009) was used to generate the random full-field turbulent wind fields. Periodic wind files have been used for turbulent wind simulations longer than 10 minutes since current memory RAM storage is limited and 3 hours wind files range in the size of gigabytes. As TurbSim produces periodic windfiles, the generated 10-min windfiles are simply repeated for all simulations longer than 10 minutes. It is noted that the cross section of the wind file (the grid) should be large enough to cover the entire rotor for all the range of motions that the platform has in surge, sway and heave.

For the hydrodynamics, the Hydrodyn module (Jonkman, 2007) was used, but different modeling was applied for the two platforms under consideration: For the *LIFES50+ OO-Star Wind Floater Semi 10MW*, first order potential-flow theory as well as Morison drag forces for hydrodynamics was

implemented as a function of the relative velocity of the substructure and water particles (considering both wave and current). For the *NAUTILUS-10*, hydrodynamics has been modelled by first order potential flow theory with the second-order addition from the Newman's approximation. Damping for this floater was achieved by linear and quadratic damping terms related to the floater absolute speed to represent the viscous effects. The additional hydrodynamic damping (AHD) approach leads to faster computation times compared to a Morison element model, but when implemented inside HydroDyn (Jonkman, 2007), presents the drawback of neglecting the sea current actions and viscous wave forcing. An alternative way to mitigate a hydrodynamic modelling of currents could be to define point forces on the substructure representing currents, but this has not been done in this study. For both floaters, a dynamic model is used for the mooring line forces with MoorDyn (Hall, 2017), which considers both inertial and viscous effects as well as line internal damping and line-to-seabed contact, but no seabed friction.

## 3.4 FLS Settings and parameters

The work in this document is based on the following assumptions and models.

Considered SN slope was always $m = 4$, even for blade loads. Hence, additional studies are required for the FLS of all materials different to steel, even if trends may be the same. Rainflow counting was used for fatigue load assessment, without consideration of mean load effects. The reference number of cycles used to calculate damage equivalent loads (DELs) was set to $N_{ref} = 2 \cdot 10^6$ and a lifetime of 25 years was assumed. Half cycles in DEL calculation are considered with a weight of 0.5.

## 3.5 Considered load cases

In contrast to complete design load calculation or certification load setup, a sensitivity analysis does not require absolute design load values and focusses more on qualitative results and comparability of the simulated data. Therefore, it is reasonable to apply a sub set of the complete standard load cases definition. Based on the preliminary load case study, three typically dimensioning load cases for floating wind turbines according to IEC 61400-3 have been selected for the sensitivity analysis. The selected load cases comprise fatigue load cases during normal operation between cut-in and cut-out wind speed (DLC 1.2) and two extreme load cases. The extreme situation of power production during a severe sea state (DLC 1.6) and idling during a 50-year storm event (DLC 6.1) generally produce critical loads for the rotor-nacelle assembly, the tower, the floater and the station keeping system. The transient failure load cases according to IEC 61400-3-2_Draft: DLC 9.x and DLC 10.x (e.g. loss of mooring line or leakage), could also generate dimensioning ULS loads as demonstrated in the *LIFES50+ OO-Star* simulations. However, since these load cases are depending strongly on the individual floater design and the station keeping system they have not been selected for the sensitivity analysis.

In Table 3-3 the design load cases to be performed are listed with the corresponding settings for the simulation studies. The explanation of the acronyms used in the table can be found in (Ramachandran, et al., 2016), (DNV-OS-J103 & DNVGL-ST-0119, 2013 & 2018) and (IEC/TS 61400-3-2 Ed.1.0 Wind turbines, kein Datum).

Table 3-3: Design load case table (Ramachandran, et al., 2017)

| Design situation | DLC | Wind condition | Marine Condition | | | | Type of Analysis | PSF |
|---|---|---|---|---|---|---|---|---|
| | | | Waves | Wind & wave directionality | Sea currents | Water level | | |
| Power production | 1.2 | NTM | NSS | MIS, MUL | NA | NWLR or ≥ MSL | F | ** |
| | 1.6 | NTM | SSS | COD, UNI | NCM | NWLR | U | N |
| Parked | 6.1 | Turbulent - EWM | ESS | MIS, MUL | ECM | EWLR | U | N |

# 4 FLS Simulation studies

## 4.1 FLS Simulation setup

### 4.1.1 Initial conditions

Establishing initial conditions (i.e. initial system conditions depending as a function of the mean wind speed and other environmental parameters with mean value different from zero) can reduce the run-in-time of the simulation runs. This is of particular benefit for power production load cases, as these are numerous in the design process of FOWT. As part of this deliverable, **two items were investigated: (1) the necessary length of initial condition simulations and (2) the necessary resolution of initial condition simulations** (i.e. the number of wind speeds that need to be evaluated to interpolate between them with sufficient accuracy). While this chapter focusses on the evaluation of a semi-submersible concept, the used methodologies are applicable as well for other concepts and for additional environmental conditions that are not part of this work, such as different directions of wind inflow, current, etc.).

For the typical FLS case DLC 1.2, considering no current and only direct inflow direction, the following degrees of freedom of the FOWT are considered of importance: rotor and generator speed, blade pitch angle, blade tip out of plane deflection, tower top fore-aft displacement, platform surge, platform heave and platform pitch.

Simulations were run considering steady wind speeds between 4 and 25 m/s with a resolution (bin-width) of 0.2 m/s, leading to a total number of 106 simulations. Wind speed was considered as uniform and aligned with the rotor and no wave heights or currents were considered as part of the initial condition calculations. For the initial conditions of these simulations, all displacements and velocities were set to zero in order to obtain the most conservative results possible. Simulation length was set to 3600 s in order to ensure the convergence of the mean values. Figure 4.1 exemplary shows the one-hour time series for the surge displacement as a function of different wind speeds for both concepts. Only a preliminary version of the tuned DTU baseline controller was available for the *NAUTILUS-10* concept in this study. With this version, some controller-induced excitation around rated wind speed is visible in the surge DOF (negative damping). As a similar interaction between controller and the environment is unlikely for a stochastic wind regime (much larger variation of inflow wind speed as well as additional damping introduced by the hydrodynamics), the controller was regarded of sufficient fidelity for this study. This way, it was also possible to investigate the usability of an imperfectly tuned controller. The

results from the power production sensitivity studies presented in chapter 4 and section 5.2.1 show no significant drawbacks of the preliminary controller.

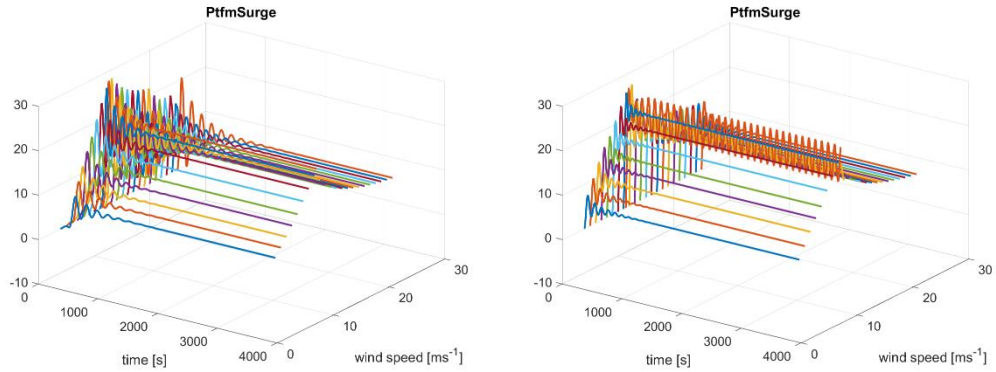


**Figure 4.1: Time series of platform surge displacement [m] in the z axis as a function of wind speed.**
**Left: *LIFES50+ OO-Star Wind Floater Semi 10MW***
**Right: *NAUTILUS-10***

#### 4.1.1.1 Simulation length requirements for initial condition calculations

A minimum simulation length for the initial condition simulations is required to ensure the convergence of the mean value of a given final time window which later will be used as simulation input. This was evaluated as part of this work for the abovementioned sensors. For the evaluation, for each considered wind speed, the convergence of the moving average $\boldsymbol{\mu}$ of different time windows of 10 min length along the time series $\boldsymbol{TS}$ was analysed. This was done by evaluating different starting points $\boldsymbol{t}_{start} \in \mathbb{R}^{1\times 30}$ for averaging windows. Here, we used 30 times windows of 10 minutes length each starting with a delay of 100s from the previous one:

$$\boldsymbol{t}_{start} = [1s, 101s, \dots, 2901s]$$

$$\boldsymbol{t}_{end} = \boldsymbol{t}_{start} + 600s$$

$$\boldsymbol{\mu}(\boldsymbol{t}_{start}, \boldsymbol{v}) = \overline{\boldsymbol{TS}([\boldsymbol{t}_{start} \dots \boldsymbol{t}_{end}], \boldsymbol{v})}$$

The results for each considered DOF were normalized using the mean value of the final window:

$$\boldsymbol{\mu}_{norm}(t_{start}, v) = \frac{\boldsymbol{\mu}(\boldsymbol{t}_{start}, \boldsymbol{v})}{\boldsymbol{\mu}(3000s, \boldsymbol{v})}$$

For the *LIFES50+ OO-Star Wind Floater Semi 10MW*, Figure 4.2 (left) shows the convergence of the normalized moving mean values for the different DOFs considered relevant and for all wind speeds. Already a starting time of 500s (leading to a total simulation time of 1100s) results in all mean values being within 5% of their final value. For the same sensor, the *NAUTILUS-10* response is shown in Figure 4.2 (right). There, some significant deviation from the final mean value is visible. This is due to the controller influence on platform dynamics around rated wind speed already seen in Figure 4.1. Also, it should be noticed that the absolute value of the mean platform pitch motion (shown later in Figure 4.4, bottom) is around an order of magnitude smaller than for the *LIFES50+ OO-Star Wind Floater Semi 10MW* concept. Thus, a larger relative error for some of the signals may still lead to useable steady states.

*LIFES50+ OO-Star Wind Floater Semi 10MW:* *NAUTILUS-10:*

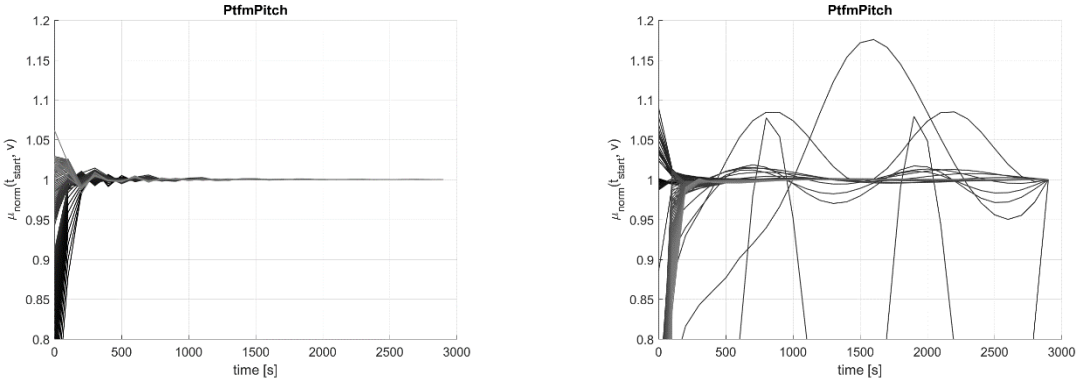


**Figure 4.2: Example steady state convergence for platform pitch motion for all wind speeds.**

Figure 4.2 summarizes the convergence behavior of the steady states for different signals, by plotting the maximum deviation of the mean value for each signal for each time step. For the *LIFES50+ OO-Star Wind Floater Semi 10MW* concept, it is visible, that the platform heave takes the longest to converge to its final value. It reaches a value with less than 10% deviation from the expected value with a starting time of 1101 seconds for the time window. At 1301 seconds starting time window it has converged below 5% of the expected mean value. The slow convergence may indicate that the heave is lightly damped compared to the other degrees of freedom, however, in this case it is more likely that the large relative error is linked to the small absolute value of the heave signal (close to 0.1 m). For the *NAUTILUS-10* response, most of the maximum values are observed around the rated wind speed, which is linked to the interaction of the preliminary controller used in this study with the uniform wind field. The platform and blade pitch show large relative errors, while all other signals seem to be within the 5% margin from the beginning (indicating that no calculation of initial conditions is required). Again, the small absolute values must be taken into account when relative errors are above the limiting threshold. Future comparisons of this type should refer to normalized values when convergence is to be investigated to allow a fair comparison between signals of different type.

Summarizing the findings, 1000-2000s are considered to lead to sufficiently converged steady states which may be used for load analysis.

*LIFES50+ OO-Star Wind Floater Semi 10MW:* *NAUTILUS-10:*

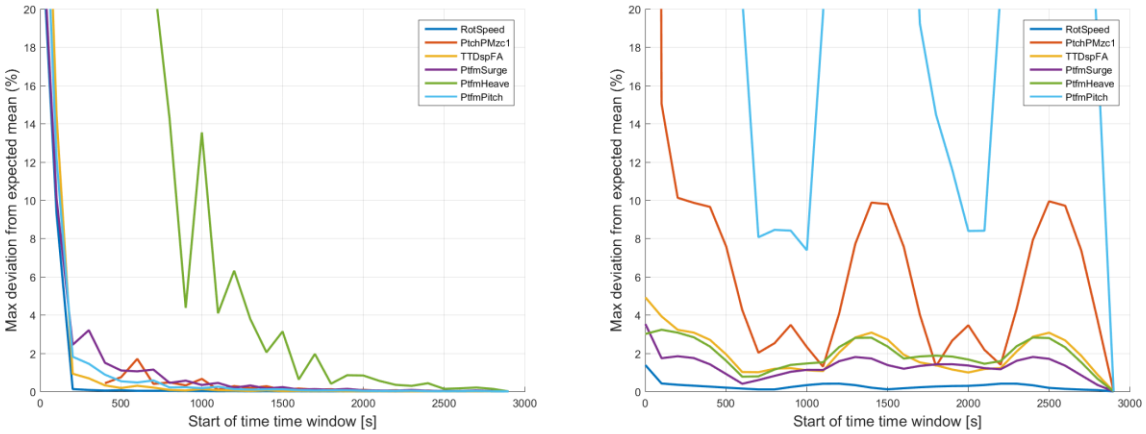


**Figure 4.3: Steady state convergence of absolute maximum deviation for all analysed sensors taking into account all wind speeds.**

#### 4.1.1.2 Resolution requirements of initial condition simulations

A certain resolution of the wind speed is necessary in order to capture the initial condition of the FOWT adequately. As a high resolution of 0.2 m/s was considered in the simulation setup, these simulations serve as quasi infinitive number of bins and as a reference for less detailed resolutions. As part of this study, with the considered concepts, a resolution of 2 m/s was found feasible for the *LIFES50+ OO-Star Wind Floater Semi 10MW*, if the cut-in, rated, and cut-out wind speeds are considered as well (see Figure 4.4). Based on this, the initial conditions for other wind speeds may be determined by interpolation. For the *Nautilus-10* concept in this study, a different controller was used than for the *LIFES50+ OO-Star Wind Floater Semi 10MW*. This included a higher number of wind speeds, where controller behaviour is adjusted (e.g. pitch activity starts already at 11.2 m/s wind speed). This leads to additional points which need to be considered for the initial conditions. Regarding the platform pitch, the *NAUTILUS-10* concept has around an order of magnitude less mean displacement overall, meaning that a higher percentage in the deviation should be acceptable for the convergence threshold (see Figure 4.4, bottom). Considering that for state-of-the-art binning of environmental conditions, the wind speed is typically binned with 2 m/s, a determination of the ICs for those wind speeds would be considered sufficient.

*LIFES50+ OO-Star Wind Floater Semi 10MW:*

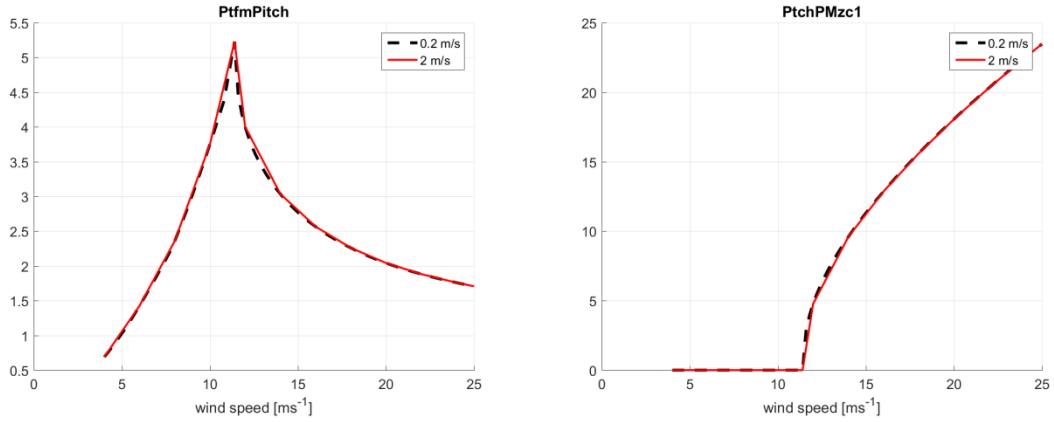


*NAUTILUS-10:*

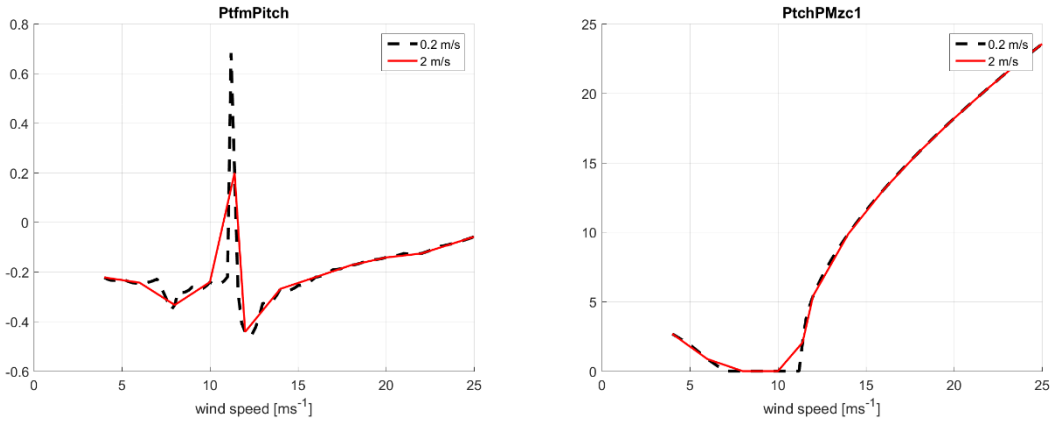


**Figure 4.4: Resolution requirements for wind speed for steady state simulations. Showing 2 different resolutions (0.2 m/s and 2 m/s). Both resolutions include cut-in, rated (11.4 m/s) and cut-out wind speed. Results are given for platform pitch (left, [°]) and blade pitch (right, [°]).**

### 4.1.2 Initial transient effects and required run-in-time

The load assessment in the design process is to be performed based on time series that are not affected by initial transients which take place at the start of a simulation. In this study, initial transients refer to settling effects, i.e. movements which are caused due to erroneous mean positions of the degrees of freedom of the system in the beginning of the simulation. Adding to this, settling of excitation of periodic

motions is required, e.g. the periodic surge displacement. To achieve exclusion of initial transients, a certain run-in-time is to be selected and disregarded in the post-processing. This run-in-time is typically chosen between 600 s and 1000 s, based on experiences from fixed-bottom offshore wind and case-specific studies. In normal operation simulations the decay of initial transients is also strongly depending on the individual controller algorithm applied. (Haid, et al., 2013) used 60 s additional simulation time considering proper initial conditions expected to be like the ones presented in section 4.1.1. Little documentation is available with respect to a generalized methodology for the assessment of the required run-in time, which is why a part of this work is to investigate and verify the results obtained elsewhere. To do this, it is necessary to investigate the convergence towards statistical stationarity of the time series of motions and loads of the considered systems. Figure 4.5 shows an example time series of the surge displacement for DLC 1.2 for the *LIFES50+ OO-Star Wind Floater Semi 10MW* concept. The initial transients are visible when comparing the surge behaviour in the beginning of the time series (red window) with the periodic behaviour later in the time series (green window). The settling periodic behaviour is linked to the use of repeating periodic wind fields of 10 min length each, which have a large influence on surge motion.

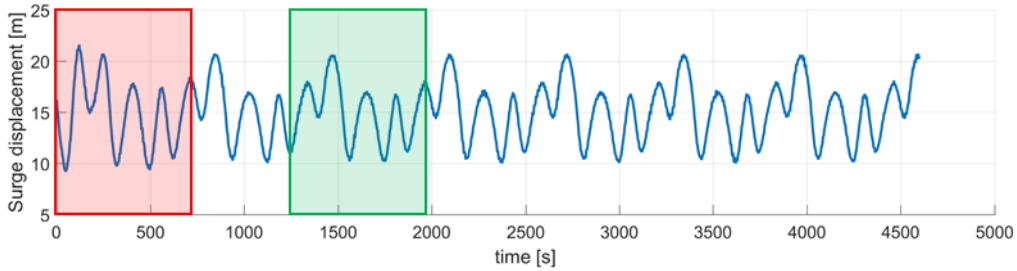


**Figure 4.5: Example time series of DLC 1.2 including initial transients (red window).**

It is not straight-forward to determine the length of the initial transient. Thus, different approaches were tested as part of this work to determine the required length of the run-in-time. These were for example (1) moving average analysis (as used for the initial condition simulations), (2) convergence of the frequency response, (3) forward and (4) backwards analysis of statistical characteristics. It was found that a backwards analysis of the standard deviation most efficiently gives valuable indication for the status of convergence of the time series towards stationarity (i.e. converged statistics). Equation (1) describes the calculation of the used standard deviation.

$$\sigma(t) = \sqrt{\frac{1}{T-t}\sum_{i=t}^{T}(x_i - \mu)^2} \qquad (1)$$

Here, $T$ represents the overall simulation length (total number of time steps) and $t$ the considered time step. A reference measure $\sigma(t = 2000\ s)$ is defined towards which the standard deviations are normalized (generally, $\sigma(t)$ shows constant values after some visible run-in time and diverges again for $t \rightarrow t_{sim}$. Hence $t = 2000\ s$ was chosen as a suitable reference value). With these values it is possible to investigate how the essential statistical properties of a time series behave.

For the present study, is not possible to obtain an exact value for the status of stationarity due to the limited data that is available (determination based on auto-comparison of each available time series, over 7+ different environmental conditions). Better results are to be expected if more seeds where available and considered for each of the performed simulations. Due to the limited data, some variation around the reference measure $\sigma(t = 2000s)$ is to be expected. Hence, the results documented here may

only be used as indicative, since significant deviations from the reference measure detected based on visual inspection where the basis of the analysis.

For the *LIFES50+ OO-Star Wind Floater Semi 10MW* concept, Figure 4.6 shows the run-in-time evaluation plot based on the simulation study of DLC 1.2 presented in section 4.2, where 10242 simulations are performed with variation of 7 environmental conditions. The standard deviation is shown for $t\epsilon[0\ s, 2000\ s]$ and normalized towards $\sigma(t = 2000s)$ for all simulations (Table 4-3) performed in this study (a single outlier is not shown in the figure). The fast convergence of tower top fore-aft and side-side displacement, platform heave, roll, and yaw are visible. Platform surge and sway motions require a longer time span to overcome the initial transients. From the results of this study, a run-in-period of 1000 s is considered advisable so that the larger oscillations of the surge motion transients are disregarded. However, the initial conditions used in this study were always assuming the same wind direction, which creates increased transients when the wind direction is changed (for the slow surge and sway motions), see section 4.2. This way a conservative case for the analysis of run-in-time is created, which may be used as reference, when no proper initial conditions are used.

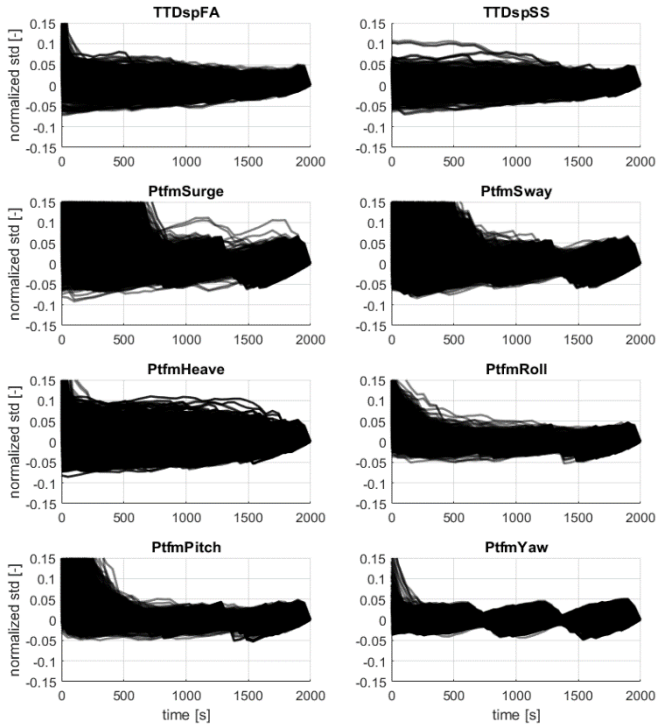


**Figure 4.6: *LIFES50+ OO-Star Wind Floater Semi 10MW* Run-in-time evaluation for DLC 1.2 considering 7 environmental conditions. Results are normalized using standard deviation of time series not considering first 2000 s of simulation (i.e. based on 4200 s total simulation time).**

For comparison, Figure 4.7 shows the same evaluation for the DLC 1.2 study with only 3 environmental parameters considered (wind speed, wave height and wave period) and considering wind speed dependent initial conditions. Comparing Figure 4.6 (no initial conditions/wrong initial conditions), with Figure 4.7 (using initial conditions) the plots indicate that when adequate initial conditions are applied, the required run-in-time may be reduced significantly. For in-depth studies on fatigue loads in this work, as the wind direction is in-line with initial conditions, a run-in-time of only 600 s was used. Note that this is considering the use of converged ICs (for which section 4.1.1 found 1000 s-2000 s of simulation time to be necessary).

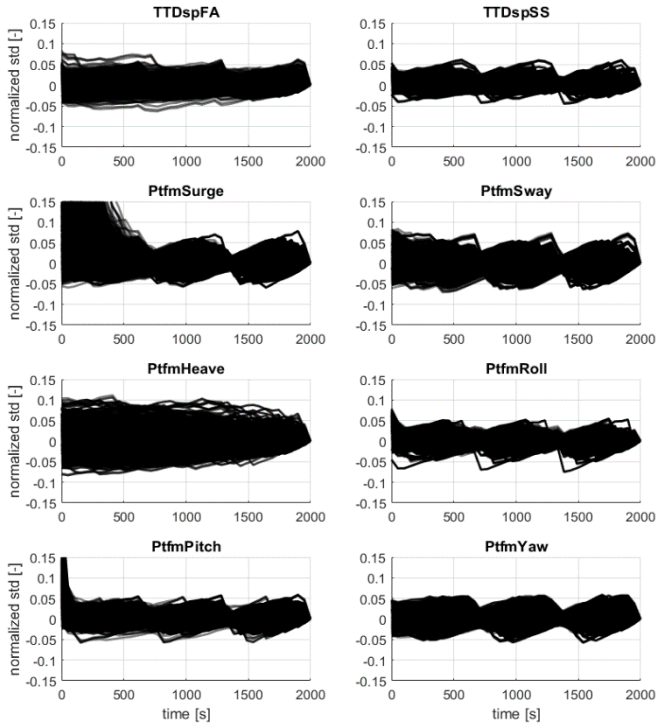


**Figure 4.7: *LIFES50+ OO-Star Wind Floater Semi 10MW* Run-in-time evaluation for DLC 1.2 considering 3 environmental conditions. Results are normalized using standard deviation of time series not considering first 2000 s of simulation (i.e. based on 4200 s total simulation time).**

Figure 4.8 shows the run-in-time evaluation for the *NAUTILUS-10* concept. For this concept, no initial conditions were used in order to add to the findings of the other platform (conservative and with initial conditions). The results show that around 500 s can be considered sufficient to remove initial transients from the time series.

For normal operation load cases the run-in-time length could be reduced significantly if the RNA operation parameters rotor speed and blade pitch angle have been setup according to the corresponding wind speed bin.

Summarizing the results, transients for floating wind turbines for DLC 1.2 are to be expected between 500-1000 s (with correct initial conditions regarding wind turbine performance and with and without correct initial conditions regarding positioning and displacements). Additional simulation time should reflect these changes to mitigate the presence of settling effects and include safety margins. If the times determined in this study are linked to the longest natural period of the floater (here: surge), they are expected to be within roughly 3-8 times the length of that period.

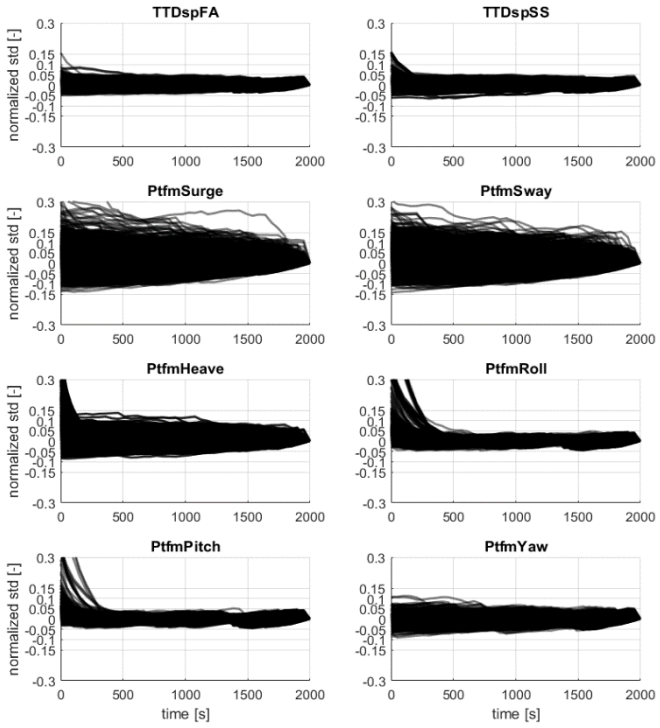


**Figure 4.8: *NAUTILUS-10* Run-in-time evaluation for DLC 1.2 considering 3 environmental conditions. Results are normalized using standard deviation of time series not considering first 2000 s of simulation (i.e. based on 4200 s total simulation time).**

## 4.2 FLS Sensitivity analysis

Sensitivity analyses (SA) are carried out in this study using FAST models based on the description from LIFES50+ Deliverable 4.2 (Yu, et al., 2018). The borders of the design space were determined from probabilistic analysis of the considered environment, taking into account three principal load ranges (LR): the partial load range or LR1 with wind speeds between cut-in and 85% of the rated wind speed, transitional load range or LR2 with wind speeds between 85% and 115% of the rated wind speed and the full load range or LR3 with wind speeds above 115% of the rated wind speed, see Figure 4.9. The load ranges are introduced here to allow a differentiated view on the behaviour of the turbine in different wind regimes. Due to the controller, the observed systems in the considered range are essentially different in their load response with increasing wind speed. This may also have implications on the relevance of environmental conditions on component loads which can only be investigated if the wind regimes are considered separately.

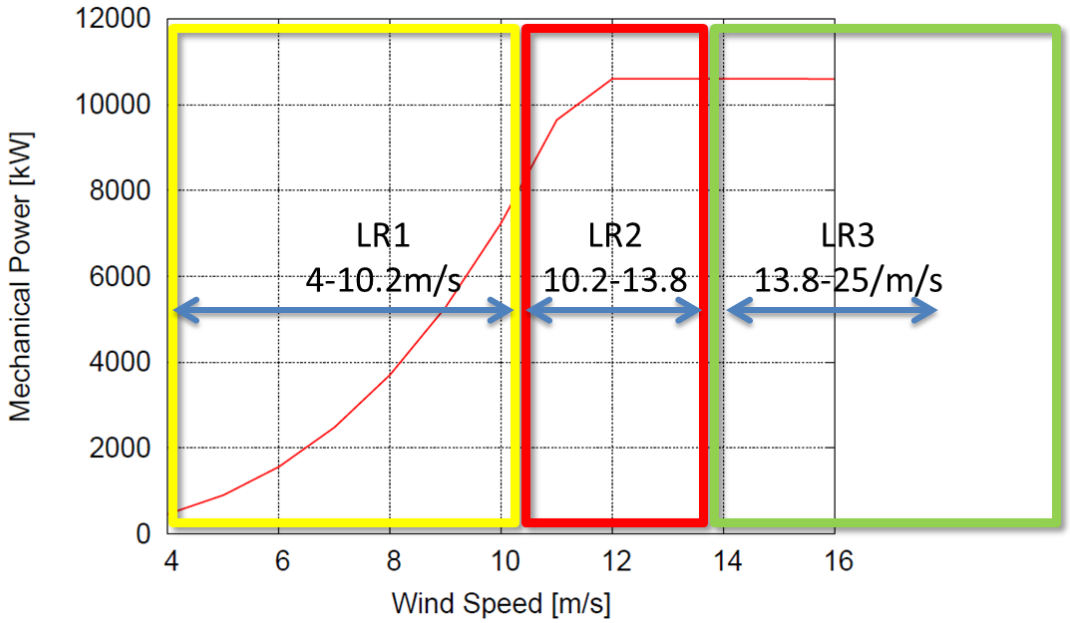


**Figure 4.9: Mechanical power based on the BEM based tool HAWTOPT for the DTU10MW reference turbine with load ranges used in this work (onshore turbine)**

For global sensitivity analyses, which aims at the determination of relevant influences, specific points of the analysis were selected using the Sobol's sampling method as described in (Müller & Cheng, 2017). The method provides an efficient coverage of the design space, allowing exploration of the system response over a wide range of parameters. For evaluation, chi-square testing was used as described in (Saltelli, et al., 2000). This allows the consideration of non-monotonic influences and a ranking of the different influencing factors. The chi-square test results in a p-value which gives the probability that the correlation between two observed variables is random. Hence, the smaller the p-value, the stronger the relationship between two investigated parameters is to be expected. The aim of the SA is to determine relevant environmental conditions for the different load cases under investigation.

For all sensitivity studies, representative locations for different major components of the system were evaluated. These were the blade root flapwise bending moment, tower base fore-aft and side-side moments (defined with respect to wind inflow direction) and tension of fairlead 1 for the *LIFES50+ OO-Star Wind Floater Semi 10MW* concept. For the *Nautilus-10* concept, the maximum of the loads of the four fairlead tensions was calculated as a representative load value for the mooring line system. This helped to identify more clearly the global load response and mitigate local effects on only one mooring line.

Regarding DLC 1.2 in this study, two global sensitivity analyses were performed with an increasing number of influencing parameters. In a first step (section 4.2.1), focus was put on the three main environmental parameters wind speed, wave height and wave period. In the second evaluation (section 4.2.2), the current speed as well as the directionalities of wind, waves and current were also considered. Next to these global analyses, in-depth analysis was done regarding specific parameters. This included the wave period (section 4.2.3), which was found to be of major importance in the first step, as well as the wave peak-shape-parameter (section 4.2.4) whose influence on the loads was found of interest.

### 4.2.1 Global sensitivity analysis on wind speed, wave height and wave period

For the first unidirectional analysis, which was only performed for the *LIFES50+ OO-Star Wind Floater Semi 10MW* concept, environmental parameters were selected based on the following: wind speed was defined according to boundaries of the considered load ranges. Borders for wave height -period were

chosen as the 1st and 99th percentile of available measurements related to the different load ranges in Site B: this means first all available environmental measurement data was filtered according to the wind speed defining the load range under consideration and from this data subset, 1st and 99th percentile values for wave height and wave period were used as boundaries. The resulting boundaries are summarized in Table 4-1. Figure 4.10 shows a scatterplot of the environmental conditions for the different load ranges. The reason the upper boundary of the wave period is the same for all load ranges is coincidental. The analysis is an extension of the load simulations required by the LIFES50+ design basis in the way that the environment is considered in much higher level of detail, but is based on it with respect to requirements towards simulation settings such as turbulence intensity, simulation time, number of seeds, etc.

**Table 4-1: environmental boundary conditions for sensitivity study considering spread of three environmental parameters for the *LIFES50+ OO-Star Wind Floater Semi 10MW* concept**

| Case | Environmental conditions | | Number of simulations [-] | Simulation time [s] |
|---|---|---|---|---|
| DLC 1.2 3 environmental conditions | Wind speed [m/s] | LR1: 4.0 : 0.1 : 10.2<br>LR2: 10.2 : 0.1 : 13.8<br>LR3: 13.8 : 0.1 : 25.0 | 2799 | 4600 (3600) |
| | Turbulence Intensity [-] | Class C | | |
| | Wind direction [°] | 0 | | |
| | Wind seeds [-] | 3 | | |
| | Wave height [m] | LR1: 0.3 : 0.1 : 3.1<br>LR2: 0.3 : 0.1 : 4.0<br>LR3: 1.2 : 0.1 : 6.6 | | |
| | Wave period [s] | LR1: 2.5 : 0.1 : 10.7<br>LR2: 2.5 : 0.1 : 10.7<br>LR3: 4.0 : 0.1 : 10.7 | | |
| | Wave direction [°] | 0 | | |
| | Wave seeds [-] | 3 | | |
| | Current speed [m/s] | 0 | | |
| | Current direction [°] | 0 | | |

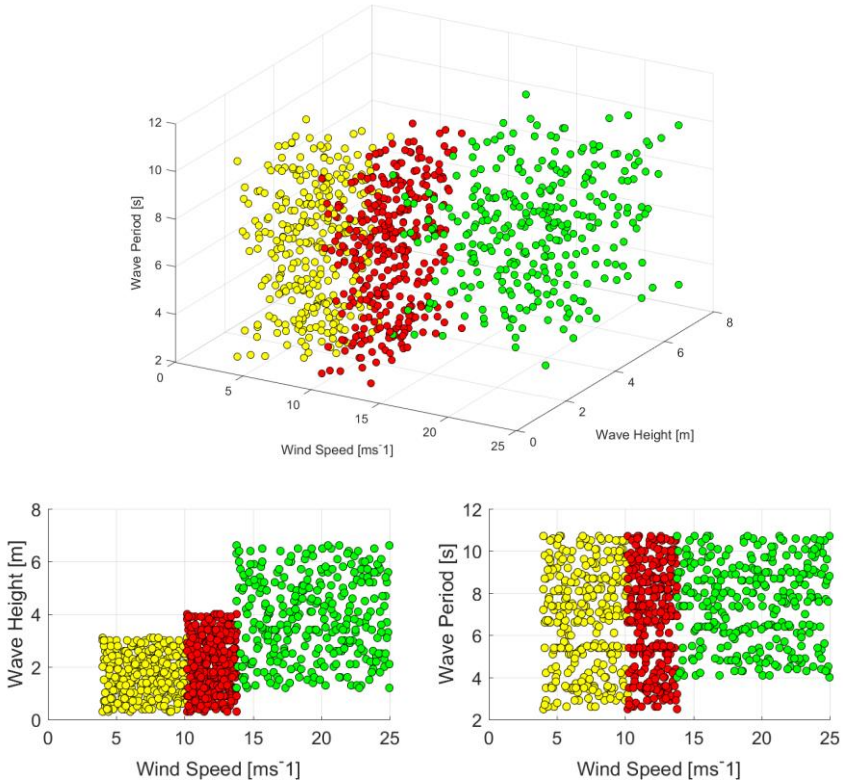


**Figure 4.10: 3D and 2D Scatterplot of environmental conditions used for DLC 1.2 global sensitivity analysis with three environmental parameters. Yellow: LR1, Red: LR2, Green: LR3**

Three seeds were simulated for each environmental condition, of which the average was used for evaluation. Figure 4.10 exemplarily shows the obtained DEL of the tower base fore-aft bending moment depending on environmental conditions (rows) and load ranges (columns).

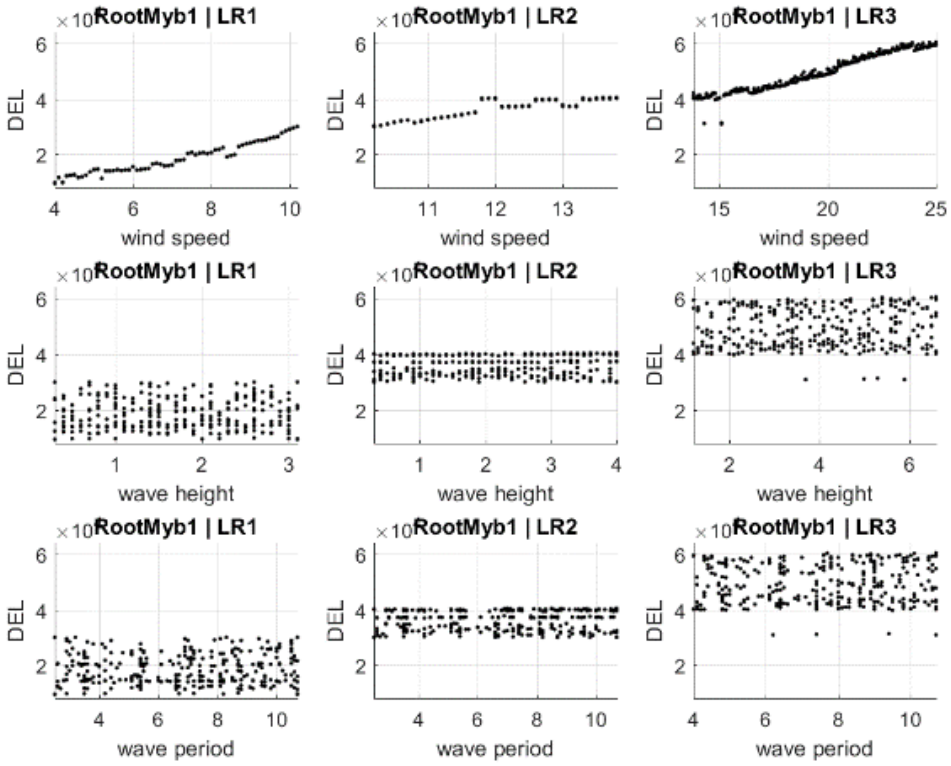
RootMyb1 | LR1
RootMyb1 | LR2
RootMyb1 | LR3
DEL
wind speed
wave height
wave period

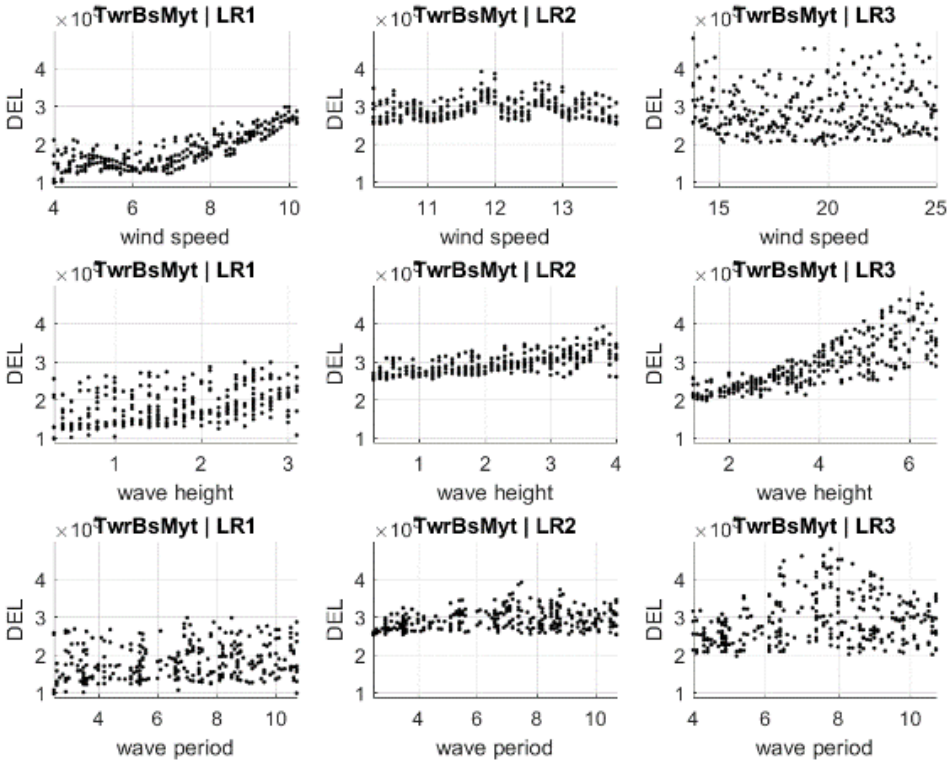
TwrBsMyt | LR1
TwrBsMyt | LR2
TwrBsMyt | LR3
DEL
wind speed
wave height
wave period

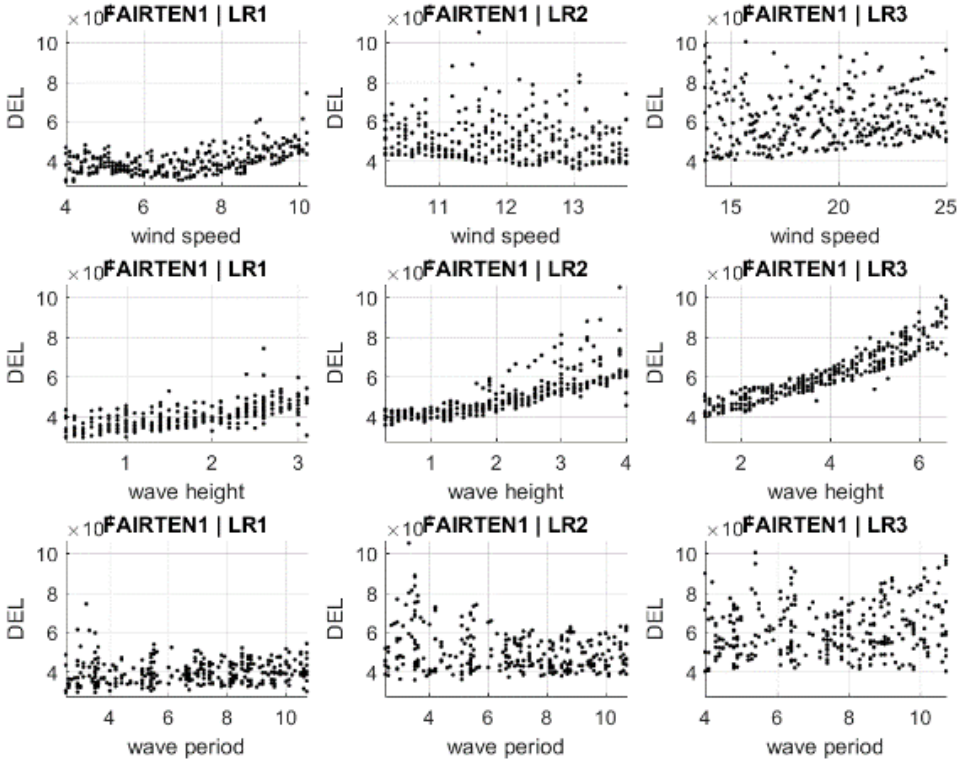


**Figure 4.11: *LIFES50+ OO-Star Wind Floater Semi 10MW* scatterplots of results of simulation study considering variation of wind speed, wave height and wave period for three different load ranges.**

Table 4-2 presents the ranking of environmental parameters and load ranges for all considered load locations (see introduction of section 4.2 for more details of methodology).

The results show the dominance of wind speed on **blade root loading** (p-value with order $<10^{-44}$ compared to larger values for other environmental conditions). For the **tower base loading**, different environmental conditions show significant impact. Wind speed has a relevance for LR1 (below rated), where it has the highest influence on tower base fore-aft fatigue loading. This is due to the controller action in this region, which aims at generating maximum power (and thus produces increased thrust with increasing wind speed). For LR2 and LR3 around and above rated wind speed this behaviour of the controller changes and thus, there, the wind speed is not of significant influence anymore. Rather, for increased wind speeds, the wave height increases generally and hence becomes of larger importance relative to wind speed and wave period. For LR3, wave height is the dominant influence on fatigue loading at the tower base. As wave heights increase, the wave period gains impact as well. For this study, it was found that a period at around 8 s will produce the largest fatigue loading on the tower base. This is of interest as the impact of the wave period is not dominantly monotonic as from the other environmental conditions (and a simple trend cannot be derived). For the **fairlead tension**, wave loading is dominant with some impact of wind loading from LR1. The impact of a specific wave periods is also visible for the fairlead (Figure 4.14), but the range of increased loading is much narrower. The impact of wave period is further investigated in Section 4.2.3.

**Table 4-2: Ranking table for most influential environmental parameters across different load ranges for OlavOlsen semi-submersible and DLC 1.2 considering wind speed, wave height and wave period.**

| *rank* | *region* | *p-value* |
|---|---|---|
| **Blade root flapwise** | | |
| 1 | LR1 / wind speed | 1.70E-51 |
| 2 | LR3 / wind speed | 9.64E-51 |
| 3 | LR2 / wind speed | 7.82E-44 |
| 4 | LR2 / wave period | 3.31E-01 |
| 5 | LR3 / wave height | 4.44E-01 |
| 6 | LR1 / wave period | 6.57E-01 |
| 7 | LR1 / wave height | 7.06E-01 |
| 8 | LR2 / wave height | 7.45E-01 |
| 9 | LR3 / wave period | 7.51E-01 |
| **Tower base fore-aft** | | |
| 1 | LR3 / wave height | 8.58E-36 |
| 2 | LR1 / wind speed | 1.61E-30 |
| 3 | LR2 / wave height | 9.94E-19 |
| 4 | LR2 / wind speed | 8.58E-09 |
| 5 | LR1 / wave height | 1.49E-05 |
| 6 | LR3 / wave period | 3.24E-04 |
| 7 | LR2 / wave period | 1.12E-02 |
| 8 | LR1 / wave period | 3.42E-01 |
| 9 | LR3 / wind speed | 7.73E-01 |
| **Fairlead 1 tension** | | |
| 1 | LR3 / wave height | 1.42E-43 |
| 2 | LR2 / wave height | 2.10E-41 |
| 3 | LR1 / wave height | 1.57E-18 |
| 4 | LR1 / wind speed | 3.34E-12 |
| 5 | LR3 / wave period | 1.68E-02 |
| 6 | LR1 / wave period | 8.68E-02 |
| 7 | LR2 / wave period | 3.62E-01 |
| 8 | LR2 / wind speed | 5.34E-01 |
| 9 | LR3 / wind speed | 7.78E-01 |

### 4.2.2 Global sensitivity analysis on more than 3 environmental conditions

For the second, more detailed study, which was performed for both selected concepts, current and directionalities are considered as well. The environmental parameters were selected in the same way as in section 4.2.1. Current was defined linked to the description in the design basis and directionalities were defined with a step size of 15°. The resulting boundaries are summarized in Table 4-3. The conditions presented in Table 4-3 were used for both concepts.

**Table 4-3: environmental boundary conditions for fatigue load sensitivity study with 7 environmental parameters for OlavOlsen semi-submersible[3]**

| Case | Environmental conditions | | Number of simulations [-] | Simulation time [s] |
|---|---|---|---|---|
| DLC 1.2 7 environmental conditions | Wind speed [m/s] | LR1: 4.0 : 0.1 : 10.2<br>LR2: 10.2 : 0.1 : 13.8<br>LR3: 13.8 : 0.1 : 25.0 | 10242 | 4600 (3600) |
| | Turbulence Intensity [-] | Class C | | |
| | Wind direction [°] | 0 : 15 : 345 | | |
| | Wind seeds [-] | 3 | | |
| | Wave height [m] | LR1: 0.3 : 0.1 : 3.1<br>LR2: 0.3 : 0.1 : 4.0<br>LR3: 1.2 : 0.1 : 6.6 | | |
| | Wave period [s] | LR1: 2.5 : 0.1 : 10.7<br>LR2: 2.5 : 0.1 : 10.7<br>LR3: 4.0 : 0.1 : 10.7 | | |
| | Wave direction [°] | 0 : 15 : 345 | | |
| | Wave seeds [-] | 3 | | |
| | Current speed [m/s] | 0 : 0.1 : 1 | | |
| | Current direction [°] | 0 : 15 : 345 | | |

Three seeds were simulated for each environmental condition, of which the average was used for evaluation. Figure 4.12 exemplarily shows the obtained DEL of the tower base fore-aft bending moment depending on environmental conditions (rows) and load ranges (columns). The results of the chi-square tests are included as well as the ranking (see introduction of section 4.2 for more details of methodology).

[3] Due to some minor variations, a total of 10368 was performed for the *Nautilus-10* concept. Also, as mentioned before, no current was considered for the *Nautilus-10* concept.

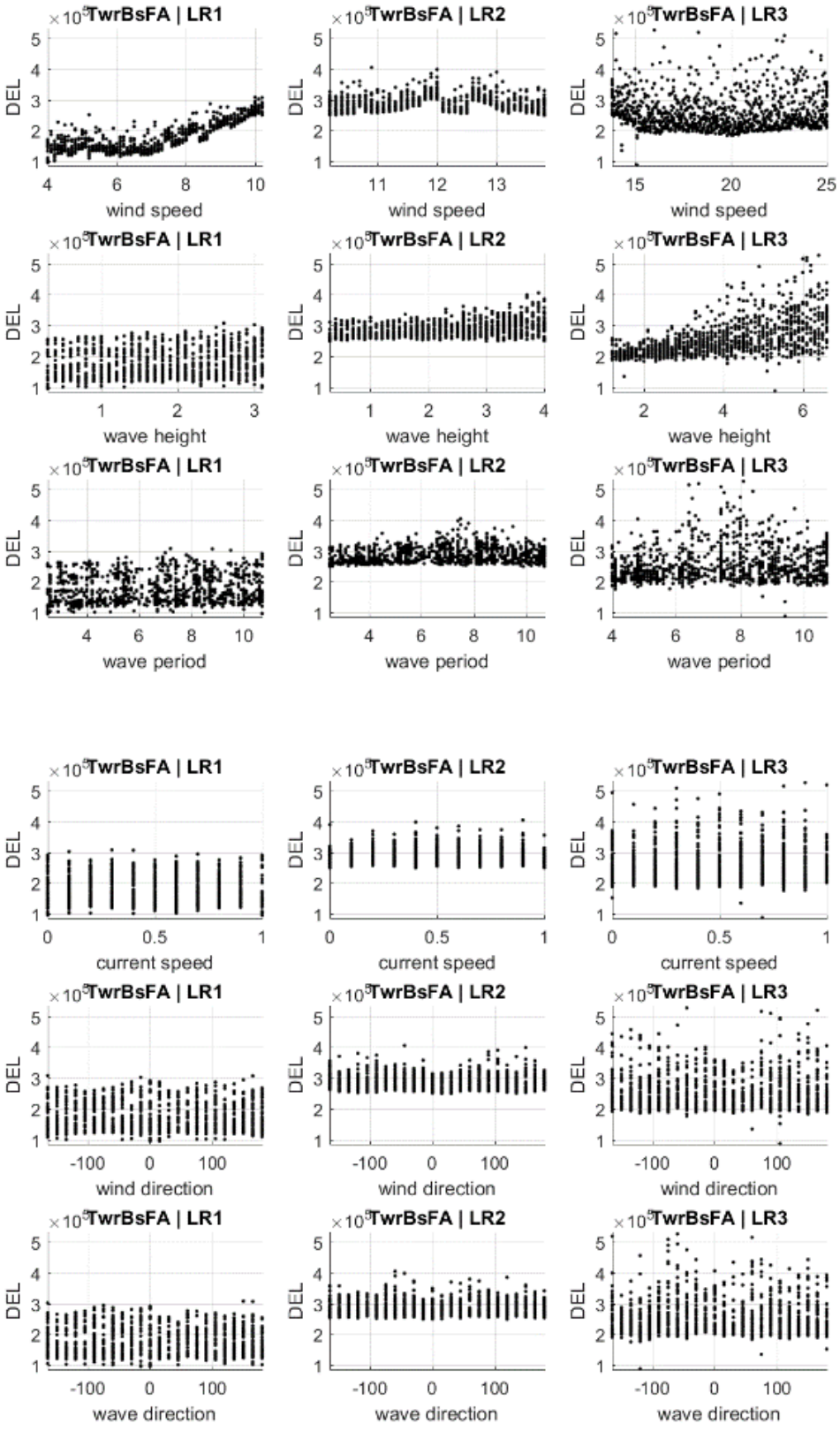
×10^5 TwrBsFA | LR1
×10^5 TwrBsFA | LR2
×10^5 TwrBsFA | LR3
DEL
wind speed
wave height
wave period
current speed
wind direction
wave direction

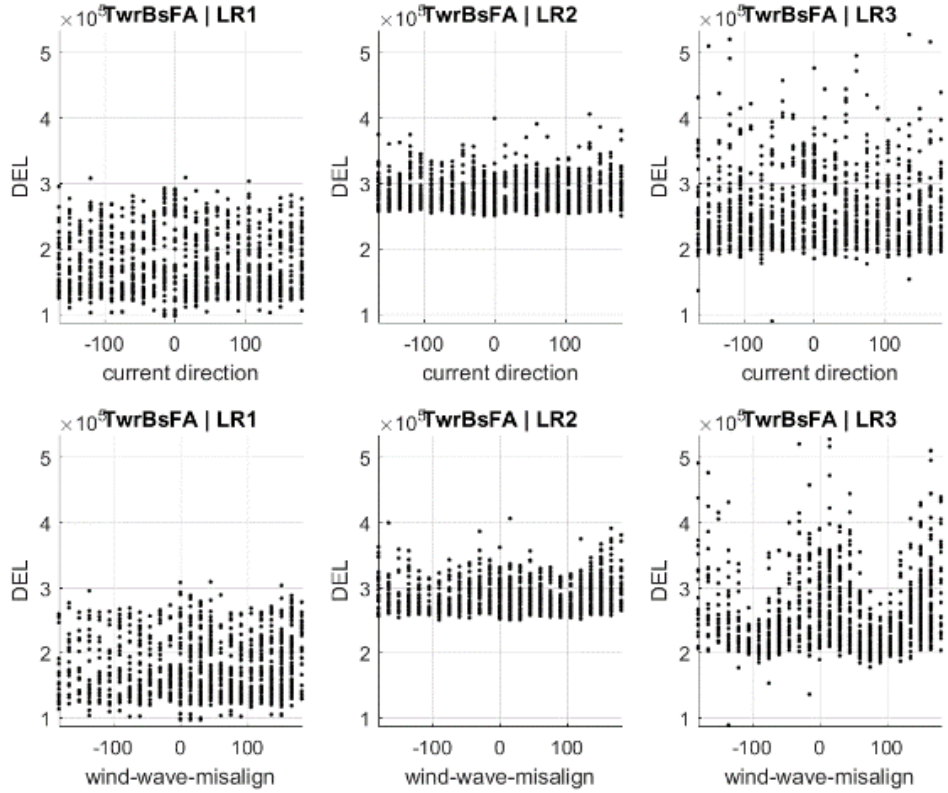


**Figure 4.12: OlavOlsen semi-submersible tower base fore-aft bending moment scatterplot results of simulation study conidering variation of wind speed, wave height, wave period, current and directionalities for three different load ranges.**

Table 4-4 presents the ranking of environmental parameters and load ranges for all considered load locations. Due to the large number of combinations, only the most relevant are included in this report.

Again, the results show the dominance of wind speed on **blade root loading** (p-value with order <-172 compared to values for other environmental conditions starting at order -5).
For the **tower base fore-aft loading**, different environmental conditions show significant impact. Wind speed has a relevance for LR1 (below rated), where it has the highest influence on tower base fore-aft fatigue loading. Wind speed remains important in LR2, but this is linked to the small load variation in this region and to controller action around rated which results in a drop of loading for a small range of wind speeds. Note that this effect is not visible when using a larger resolution for the wind speed (e.g. 1m/s). Hence, it is advised to use a high resolution of mean wind speed in the controller design and the load verification. For LR3 the wind speed is not of significant influence as for the study before, some small impact remains in this load range due to a drop close to rated condition which is more significant in this study than in the previous one. Also, as seen before, the wave height impact becomes more significant for larger wave heights, as well as the impact of the wave period, which is again showing distinctive values where increased loading occurs. Of interest in this study is the directionality, which mostly did not show any considerable impact on the tower base fore-aft fatigue loads. However, the wind-wave-misalignment has a considerable impact in LR3 (large wind speeds and wave heights) and the largest loads are resulting from misalignments of around 0° or 180°. This supports previous findings that linked maximum fatigue loads to co-aligned wind and wave direction.
The **tower base side-side moment** has somewhat reduced loading compared to the fore-aft moment. Here, the wave heights have an increased influence compared to the fore-aft bending moment, which

already is visible for small wave heights in LR1. The phenomena with specific wave periods is also repeated here for similar periods as for the fore-aft moment. The wind speeds play some role in LR1 from the statistical results, this is however linked to the low mean value and the small load variation in that range. Furthermore, wind-wave-misalignment is of high importance, here 90° and -90° produce the highest loads (smaller than for fore-aft bending moment).

For the **fairlead tension**, wave loading is relevant for all ranges with the highest impact for large waves. Due to the fairlead position, there is also significant impact from the directionality of wind (largest loading for 0° incoming direction, i.e. in-line with investigated fairlead). The impact of a specific wave periods is still visible in the scatterplots but becomes indistinct when considering directionality of the environmental loads. However, a clear trend of larger wave periods leading to larger loading is visible. The loading behaviour of the fairleads towards wave periods is not entirely in line with the previous study and should be investigated further with close focus on the directionality (i.e. relevance of specific periods). Figure 4.16 shows how the wave period load amplitude varies with different wind and wave impact direction. However, the observed increased loading with increased period cannot be explained with the wave period sensitivity alone, hence a closer look on the combined impact of wave height and wave period could be interesting in the future. Finally, some small increase of the loading due to increasing wind speed can be observed in LR1.

**Table 4-4: ranking table for most influential environmental parameters across different load ranges for OlavOlsen semi-submersible and DLC 1.2 considering wind speed, wave height, wave period, currents and directionalities.**

| *rank* | *region* | *p-value* |
|---|---|---|
| **Blade root flapwise** | | |
| 1 | LR3 / wind speed | 2.077E-203 |
| 2 | LR1 / wind speed | 3.095E-201 |
| 3 | LR2 / wind speed | 2.783E-172 |
| **Tower base fore-aft** | | |
| 1 | LR1 / wind speed | 3.783E-138 |
| 2 | LR2 / wind speed | 3.2437E-61 |
| 3 | LR3 / wave height | 1.2271E-45 |
| 4 | LR3 / wind-wave-misalign | 1.3628E-36 |
| 5 | LR2 / wave height | 5.0811E-32 |
| 6 | LR2 / wave period | 3.8842E-24 |
| 7 | LR3 / wind speed | 1.2774E-20 |
| **Tower base side-side** | | |
| 1 | LR3 / wave height | 4.3185E-73 |
| 2 | LR2 / wave height | 3.7211E-66 |
| 3 | LR2 / wave period | 1.7373E-56 |
| 4 | LR1 / wind speed | 2.0106E-52 |
| 5 | LR3 / wind-wave-misalign | 1.2764E-37 |
| 6 | LR2 / wind-wave-misalign | 2.1385E-26 |
| 7 | LR1 / wave height | 2.1281E-25 |
| **Fairlead 1 tension** | | |
| 1 | LR3 / wave height | 5.7734E-73 |
| 2 | LR2 / wind direction | 2.6273E-33 |
| 3 | LR2 / wave height | 8.5566E-33 |
| 4 | LR3 / wave period | 4.4066E-32 |
| 5 | LR1 / wave height | 2.7646E-27 |
| 6 | LR1 / wave period | 8.6283E-24 |
| 7 | LR2 / wave period | 6.5792E-21 |
| 8 | LR2 / wind speed | 4.8517E-20 |
| 9 | LR1, EnvC: wind direction | 6.8228E-18 |
| 10 | LR1, EnvC: wind speed | 1.1324E-17 |

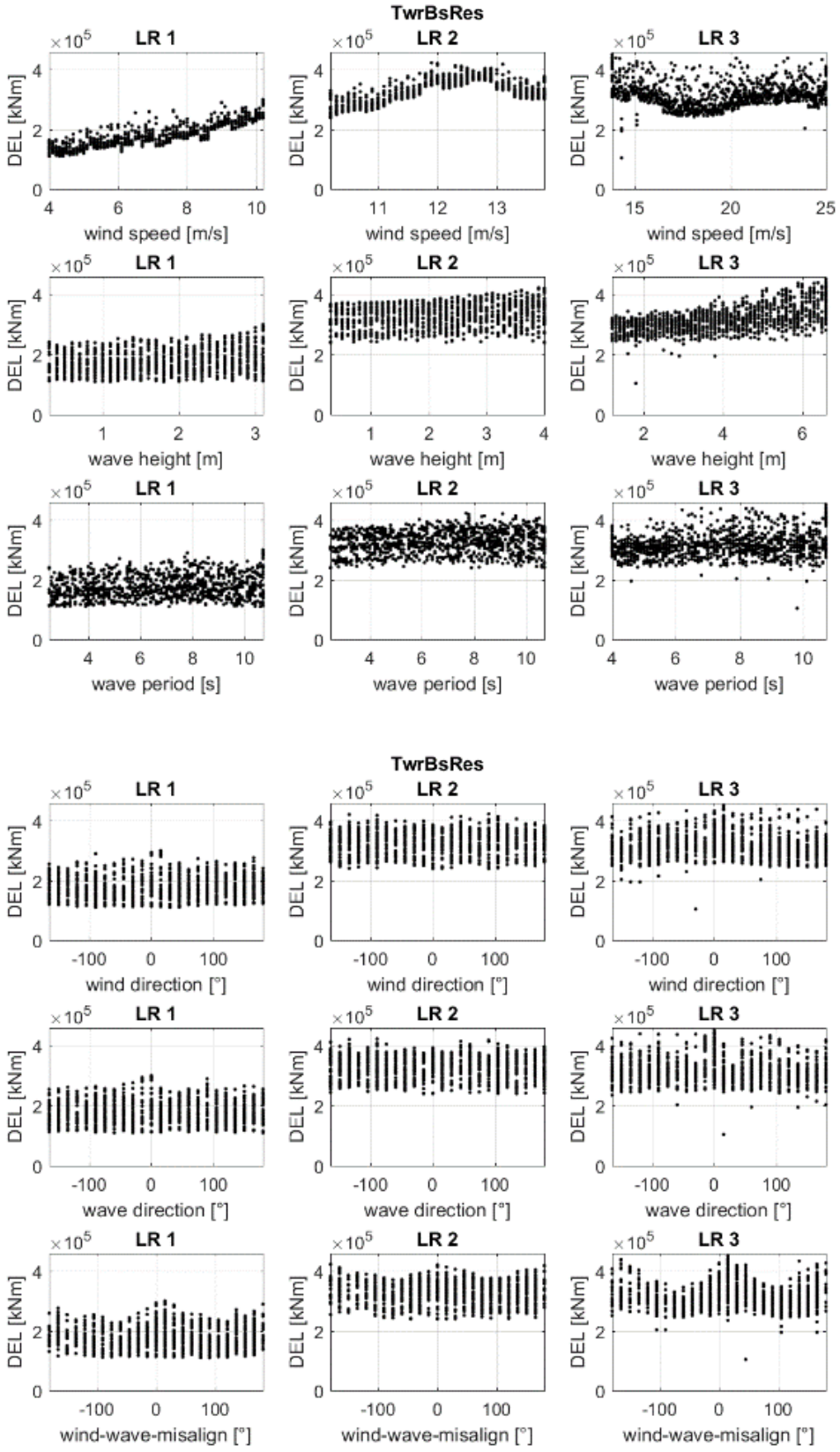


**Figure 4.13: *Nautlius-10* tower base resulting bending moment scatterplot results of simulation study considering variation of wind speed, wave height, wave period, and directionalities for three different load ranges.**

For the *Nautilus-10* concept, Figure 4.13 shows an example scatterplot of DLC 1.2 results for the tower base resulting bending moment. The large impact of wind speed in all load ranges is visible. Also, the DEL increases significantly with wind speed at wind speeds below rated. A more complex relationship between DEL and wind speed is visible around and above rated. The wave height becomes more relevant with larger wave heights (this trend starts at around three meters wave height). Regarding the wave periods, larger DELs are more likely around 8s. This effect is more distinctive for larger wind speeds / wave heights. A similar behaviour was found for the Olav Olsen platform and was investigated further in the following sections. Due to the appearance of a similar behaviour for both concepts, this effect may be related to the wind turbine (e.g. rated rotor speed has a period of 6.25 s for the DTU 10MW reference wind turbine but should not be important in ideal model) and hence could lead to a similar effect on both structures.

Table 4-5 shows the ranked environmental conditions for all considered signals. For the *Nautilus-10* concept the loads on the rotor blades are only influenced by the wind speed. For the tower base loading, the influence of wave height and wave period are important next to the wind speed as well as some impact of the wind-wave misalignment. For the fairleads, again wind speed is predominant for the fatigue loads (maximum DEL of all 4 fairlead signals was considered). Next to the wind speed, directionality plays a significant role due to the connection points of the fairleads as well as wave height and wave period, which become more important for increasing wave heights.

**Table 4-5: Ranking table for most influential environmental parameters across different load ranges for *Nautlius-10* concept and DLC 1.2 considering wind speed, wave height, wave period and directionalities.**

| *rank* | *region* | *p-value* |
|---|---|---|
| **Blade root flapwise** | | |
| 1 | LR3 / wind speed | 1.314E-186 |
| 2 | LR1 / wind speed | 1.027E-185 |
| 3 | LR2 / wind speed | 1.048E-169 |
| **Tower base resulting** | | |
| 1 | LR2 / wind speed | 3.561E-144 |
| 2 | LR1 / wind speed | 2.048E-135 |
| 3 | LR3 / wave height | 2.432E-37 |
| 4 | LR3 / wind speed | 3.156E-35 |
| 5 | LR3 / wind-wave-misalign | 3.563E-14 |
| 6 | LR2 / wave height | 3.289E-13 |
| 7 | LR2 / wave period | 2.994E-10 |
| **Fairlead tension maximum** | | |
| 1 | LR1 / wind speed | 5.54E-184 |
| 2 | LR3 / wind speed | 5.68E-95 |
| 3 | LR2 / wind speed | 2.37E-47 |
| 4 | LR2 / wind direction | 2.72E-36 |
| 5 | LR3 / wave height | 1.26E-23 |
| 6 | LR3 / wave period | 8.62E-13 |
| 7 | LR2 / wave direction | 1.70E-12 |

### 4.2.3 Wave period

During the simulation study presented in section 4.2.1 “Global sensitivity analysis on wind speed, wave height, wave period”, it was found that certain wave periods (specific to the considered component) may lead to larger fatigue loading (Figure 4.14) of the *LIFES50+ OO-Star Wind Floater Semi 10MW* concept. This effect was found to be more pronounced for larger wave heights. Figure 4.14 shows the results of the DEL for specific sensors for all load ranges.

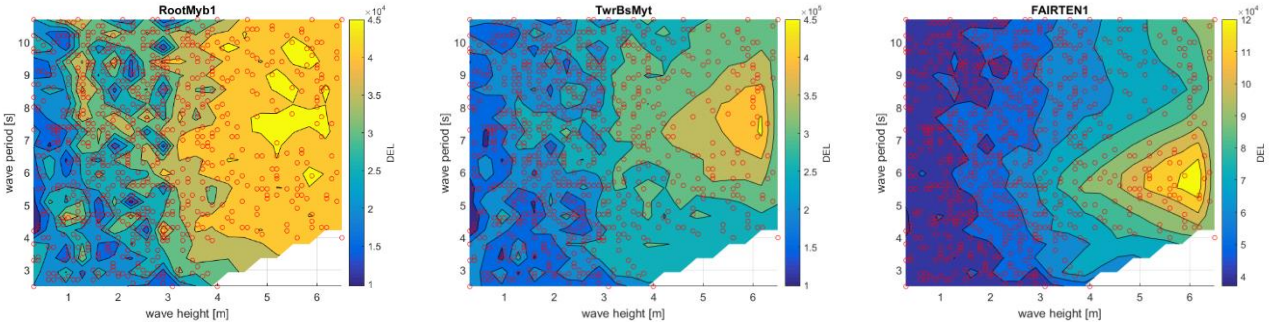


**Figure 4.14: DEL contour plots for blade root flap-wise bending moment, tower base fore-aft bending moment and fairlead 1 tension (leading mooring line). Plotted for all load ranges and showing channel-specific excitation periods. Red dots indicate performed simulations. Results are obtained independent of wind speed. *LIFES50+ OO-Star Wind Floater Semi 10MW***

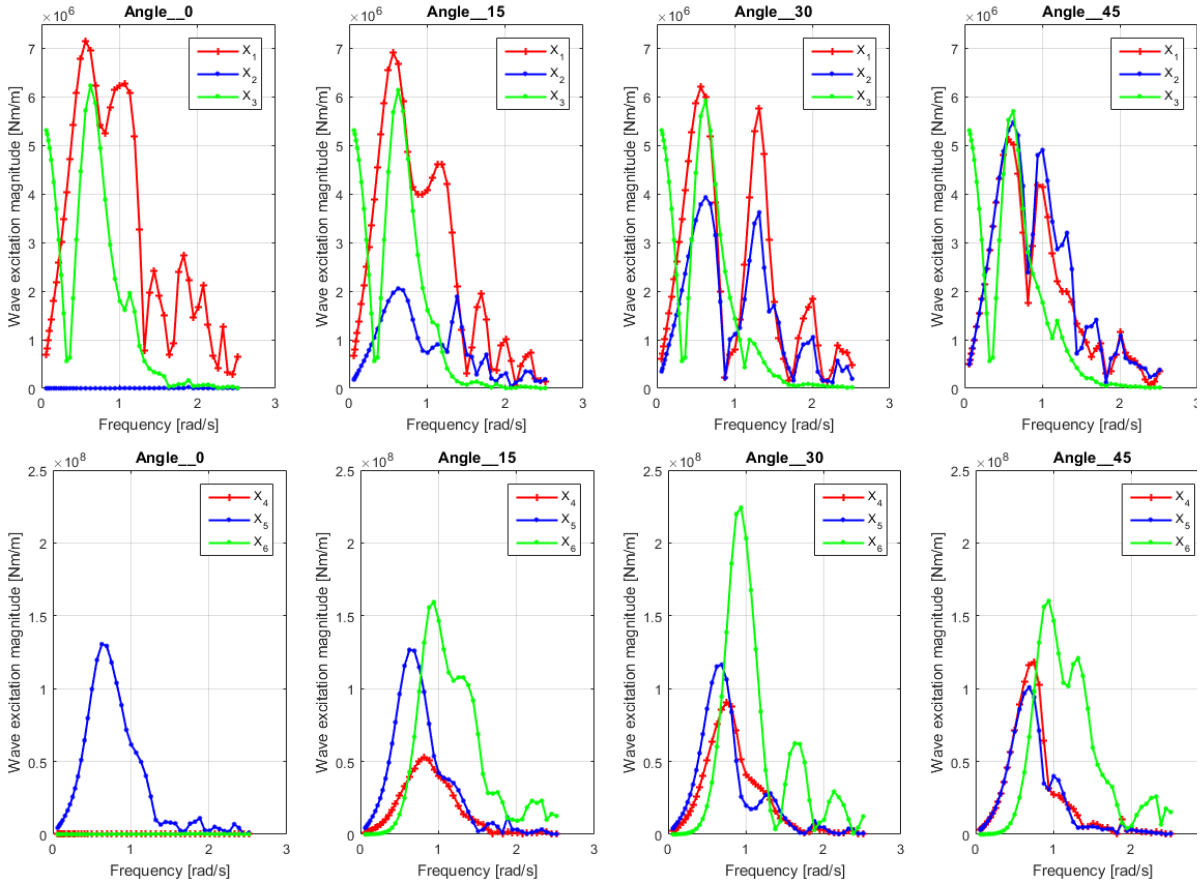


**Figure 4.15: Wave excitation magnitude of the investigated semi-submersible ($X_1$ = Surge, $X_2$ = Sway, $X_3$ = Heave, $X_4$ = Roll DOF, $X_5$ = Pitch DOF, $X_6$ = Yaw DOF), for different wave directions (0°, 30°, 60°), see also Figure 4.17. *LIFES50+ OO-Star Wind Floater Semi 10MW*.**

Further investigation for the *LIFES50+ OO-Star Wind Floater Semi 10MW* concept was done to find the connection between the peak periods and the DELs. Plotted is the frequency dependent wave excitation of the platform which is part of the hydrodynamic evaluation of the platform (Figure 4.15). This was carried out using the ANSYS AQWA software. The peak of the pitch excitation is found at about 0.65 rad/s or 9.67s, which is not equal to the periods with which the maximum loads were observed. Moreover, the period where maximum wave excitation is reached, does not alter with wave direction. This means that results from the frequency domain analysis of the platform alone cannot be taken directly for determination of conservative estimation of environmental parameters, due to not considering altered system dynamics by additional components (such as e.g. the mooring lines). Rather, evaluation of the coupled system is required so that a more complete interplay of physics within the considered system may be considered.

To investigate the mentioned effect, steady wind simulations at rated wind speed ($v_{hub} = 11.4\ m/s$) with aligned unit airy waves of 1m height and varying periods between 1 and 11 seconds with a step size of 0.1s were performed. The evaluated simulation length was 600s, with an additional 1000s of run-in-time. Using the rated wind speed was done to capture the effect during largest aerodynamic forcing. Due to the use of steady wind, however, a continuous switching of the controller between two regions may be expected as well. While this effect was not observed for the platform under investigation for still water conditions (see ICs in Figure 4.2) and thus is assumed negligible for the current investigation, it is considered that for future reference to perform the simulations from this study with wind speeds well above or below rated to ensure mitigation of such a region crossings.

Figure 4.16 shows the results of the simulation study for relevant displacements and loads. First it can be seen that no significant influence of wave period is observable on blade loads, tower side-side motion and on platform roll and yaw motions and loads. Next, the tower top displacement response peaks at about 7.5s as well as tower base fore-aft bending moment. Differing to this, the platform pitch response peaks at around 9.5s. Regarding translational motions in surge and heave, a peak does not seem to be reached for the largest considered wave period (natural period surge: 181.82s; heave: 20.41s). This suggests that translational responses (surge, heave) of the platform have a larger response with increasing wave period, which could be interesting when swell conditions are considered (not part of this study). Fairlead tendon load responses differ for different fairleads (meaning that the wave incident angle has an influence). The peak of the downwind fairlead tension is around periods with 3 s, the loads of the two “upwind” fair-leads also peak around the smallest physical wave periods.

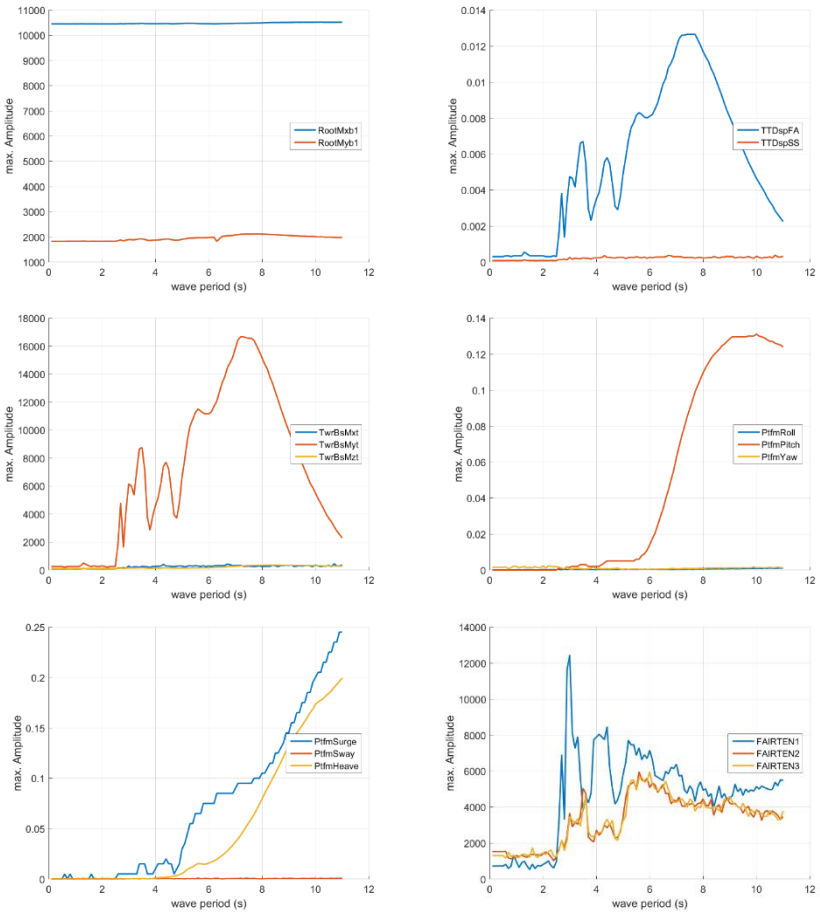


**Figure 4.16: Results of loads and movements of wave period sensitivity study for simulations at rated wind speed. *LIFES50+ OO-Star Wind Floater Semi 10MW***

A closer investigation was performed after analysis of the sensitivity study considering different wind and wave directions. There, a distinctive peak as seen in Figure 4.11 was not found. This indicates that the dynamic characteristics vary significantly with different incoming wind/wave directions. Three cases were analysed as shown in Figure 4.17 and the results are given in Figure 4.19.

Case 1: Wind: 0°, wave: 0° Case 2: Wind: 30°, wave: 30° Case 3: Wind: 60°, wave: 60°

**Figure 4.17: Cases of analysis to investigate platform dynamics for different environmental impact directions. *LIFES50+ OO-Star Wind Floater Semi 10MW***

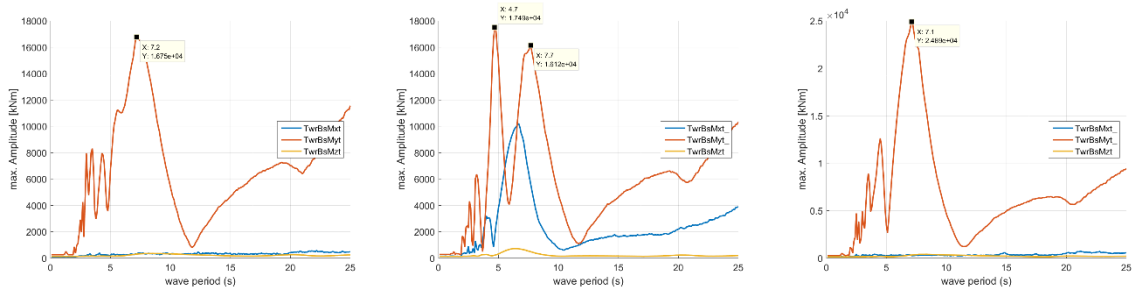


**Figure 4.18: Load response amplitudes for different environmental impact directions (left: case 1, center: case 2, right: case 3). *LIFES50+ OO-Star Wind Floater Semi 10MW.***

Overall, the results show the tendency towards varying relevant wave periods that are distinctive for different considered impact directions. Hence an approach of considering periods based solely on their occurrence probability (e.g. 10$^{th}$ percentile, mean and 90$^{th}$ percentile) is likely to lead to non-conservative results. The herein used procedure based on unit airy waves may support the determination of design driving periods for use in load analysis. Alternatively, the use of Monte Carlo analysis could also help to mitigate the negligence of important events while also considering their occurrence probability.

### 4.2.4 Wave peak shape parameter effect on fatigue loads

As stated in the guidelines IEC 61400-3 (International Electrical Commision, 2009), the Pearson-Moskowitz spectrum may be enhanced using the so-called peak shape parameter $\gamma$ to reach the Jonswap spectrum which is observed for developing sea states. The parameter may be defined between 1 and 5, where 1 results in the Pearson-Moskowitz spectrum. As part of this work, the sensitivity on this parameter was studied to quantify the uncertainty related to this parameter.

For the determination of the influence of the peak enhancement factor, two simulation studies of 246 simulations were performed (one based on power operation with normal sea state, one for power production with severe sea state), varying $\gamma$ continuously between values of 1 and 5 with a step of 0.1. For reference, the considered site and the considered wave characteristics lead to $\gamma = 5$ according to the definition of IEC 61400-3. For each value of gamma, 6 different wind and wave seeds were used to put the impact into perspective with the general statistical uncertainty. Table 4-6 lists other relevant simulation settings for the performed study. The analysis of the maximum and minimum loads based on DEL 1.6 are shown in a section later on in the report.

**Table 4-6: Simulation settings for peak shape parameter sensitivity study**

| Parameter | Analysis of DEL based on DLC 1.2 – power production with normal sea state | Analysis of maximum and minimum loads based on DLC 1.6 – power production with severe sea state |
|---|---|---|
| Number of simulations | 246 | 246 |
| Significant wave height | 6.3m | 11.2m |
| Wave period | 7.8s | 7.2s |
| Wind speed | 12.0 m/s | 12.0 m/s |
| Turbulence intensity | 14.6% | 14.6% |
| Run-in-time | 600s | 600s |
| Considered simulation time | 3600s | 3600s |

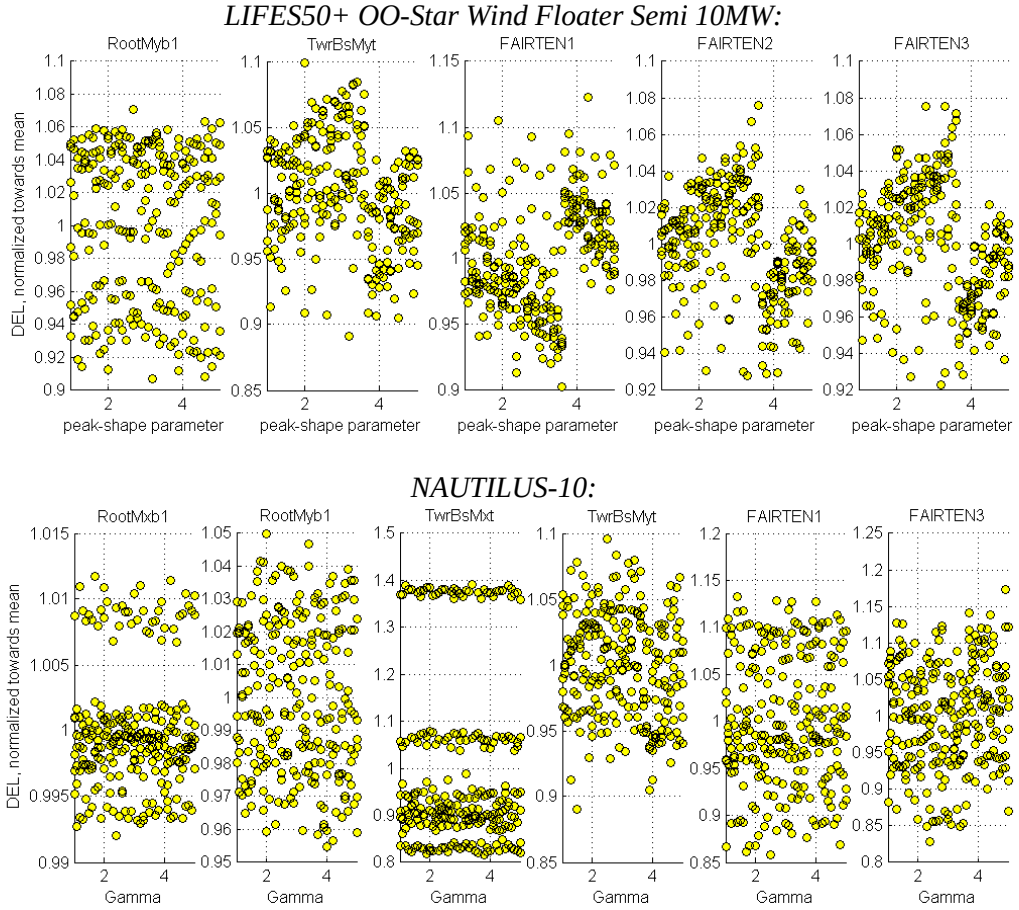


**Figure 4.19: Results of peak shape parameter sensitivity analysis for DEL of different load locations for significant wave height of 6.3m and wave period of 7.8s.**

The results are shown in Figure 4.19 and show only a minor influence of the peak shape parameter compared to the inherent uncertainty of the wind and wave environments. There is no influence visible at all for the blade flapwise damage equivalent loads (Figure 4.19, left) for both concepts. For tower base and mooring lines of the *LIFES50+ OO-Star Wind Floater Semi 10MW*, a minor influence is visible which is negligible for errors of $\gamma$- estimation around 10%. However, there is a considerable jump of the impact around $\gamma = 3.1$, which leads to a change of the mean of the results of around 10% in different directions for tower base fore-aft bending loads (decrease) and fairlead tension loads (increase or

decrease depending on the line being looked at). Overall an increasing $\gamma$ has an adverse effect on tower bending DELs and on leading fairlead DELS. With larger $\gamma$ leading to increased fatigue loading (with an exception of the observed jump around 3.1). For the *NAUTILUS-10* concept, no influence is visible for any of the signals. However, the noted jump observed for the *LIFES50+ OO-Star Wind Floater Semi 10MW* concept could also be reproduced when considering steady wind conditions. In this way, as the *LIFES50+ OO-Star Wind Floater Semi 10MW* concept shows a larger sensitivity towards the wave environment, the impact of $\gamma$ is also more pronounced.

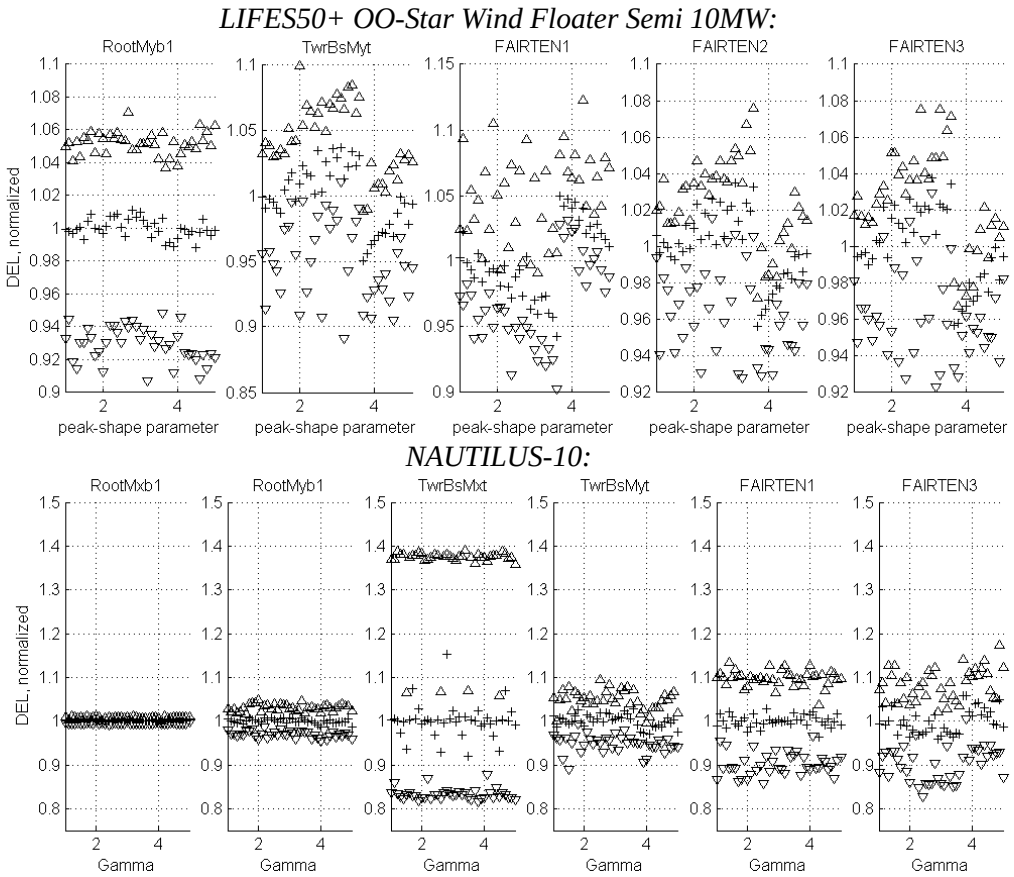


**Figure 4.20: Maximum, Mean and Minumum DEL from the 6 seeds of peak shape parameter sensitivity analysis for different load locations for significant wave height of 6.3m and wave period of 7.8s.**

A shortfall of this study which could be included in future work is firstly the investigation of impact of different wave directions and secondly, as mentioned above, the in-depth investigation of the origin of the jump in load response due to variation of $\gamma$ around $\gamma = 3.1$ for the DELs.

The conclusion for this work is that for most peak enhancement factors $\gamma$, and in the region close to $\gamma = 5$, there is no large impact on the fatigue loads expected due to reasonable errors (~10%) in the estimation of $\gamma$. An exception is the jump of DELs observed around $\gamma = 3.1$, which may lead to a noticeable jump in the load response, depending on the concept. This effect should be investigated in more depth in future studies to ensure it is of physical origin and not resulting from simulation settings (spectrum limits, resolution, etc.).

## 4.3 FLS Convergence studies

### 4.3.1 Seed number

As both wind and wave environment are stochastic processes, convergence is investigated for a varying number of seeds for three different cases: (1) wind only, (2) wave only and (3) wind and wave combined. Due to the large number of environmental conditions, the results of the FLS sensitivity study presented in section 4.2.1 were used to find the environmental conditions to be used for the different cases. Here, the environmental conditions that lead to the high DEL are used. The conditions themselves are expected to have a low probability of occurrence but are used here to provide a conservative estimate. The specific environmental conditions for the bootstrap analysis are given in Table 4-7, all other environmental conditions are set in accordance with (Krieger, et al., 2015). Blade root flap-wise bending moments (*RootMyb1*), tower base fore-aft bending moment (*TwrBsMyt*) and fairlead 1 (leading fairlead, *FAIRTEN1*) or fairlead 2 (*FAIRTEN2*, one of the leading fairleads for *Nautilus-10*) DELs were evaluated as part of this study. The results for the blade loads are to be seen as indicative results only, as a SN-slope of $m = 4$ was used, opposed to the typical value of $m = 10$ commonly used for composite structures.

It is noted one major difference in the approach for the two different floater concepts:

- For the *LIFES50+ OO-Star Wind Floater Semi 10MW*, stochastic environmental conditions are assumed for both wind and wave for all cases under investigation (i.e. for case 1, the same wave seed is used for all simulations and for case 2, the same wind seed is used for all simulations).
- For the *Nautilus-10*, only the environment with varying seeds is stochastic. (i.e. for case 1, still water conditions are assumed and for case 2, only waves are stochastic, while steady wind is applied.)

**Table 4-7: environmental conditions chosen for bootstrap evaluation of fatigue load simulations. Simulation length is 1 hour. 10 minutes are also added for run-in-time.**

| | Case 1: change wind seeds only | Case 2: change wave seeds only | Case 3: change wind and wave seeds |
|---|---|---|---|
| Wind speed [ms$^{-1}$] | 12 | 12 | 12 |
| Turbulence intensity[4] [%] | 14.6 | 14.6[5] | 14.6 |
| Wave height [m] | 6.3[5] | 6.3 | 6.3 |
| Wave period [s] | 7.8[5] | 7.8 | 7.8 |

**Methodology:** For each environmental setting, 1000 simulations were performed (1hr simulation length, 600s run-in-time, initial conditions applied). The bootstrap analysis was performed with increasing number of seeds based on 5,000 draws with replacement for each number of considered simulations $n_{Sim}$. Within each draw, the selected seeds were evaluated in a statistical sense, i.e. the median and 75$^{th}$ percentile values were determined. The visualization of the results for each $n_{Sim}$ was done using boxplots as shown in Figure 4.22, Figure 4.23, Figure 4.24 and Figure 4.25.

[4] According to IEC 61400-01 Class C turbulence
[5] Only applied for *LIFES50+ OO-Star Wind Floater Semi 10MW*

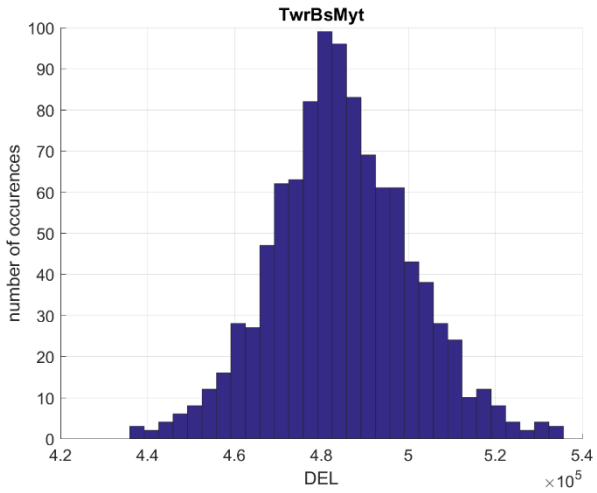


**Figure 4.21: *LIFES50+ OO-Star Wind Floater Semi 10MW* Overview of DEL values for bootstrap evaluation. Evaluation of case 3: wind & wave seeds.**

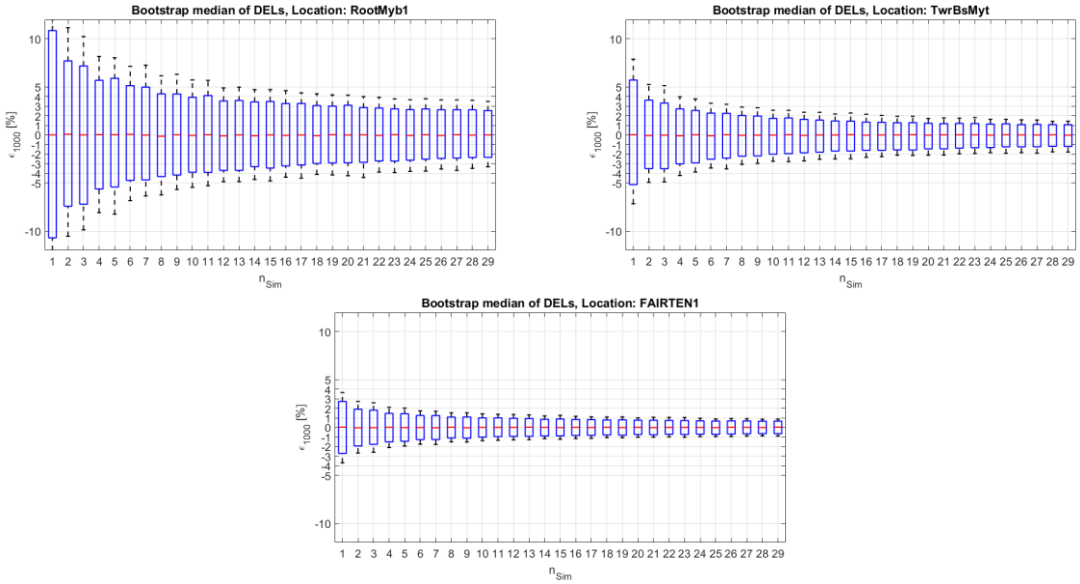


**Figure 4.22: *LIFES50+ OO-Star Wind Floater Semi 10MW* DEL bootstrap evaluation case 1 (wind only): median values after consideration of $n_{Sim}$ values. Red horizontal lines indicate median, box borders 95$^{th}$ percentile and whiskers 99$^{th}$ percentile values.**

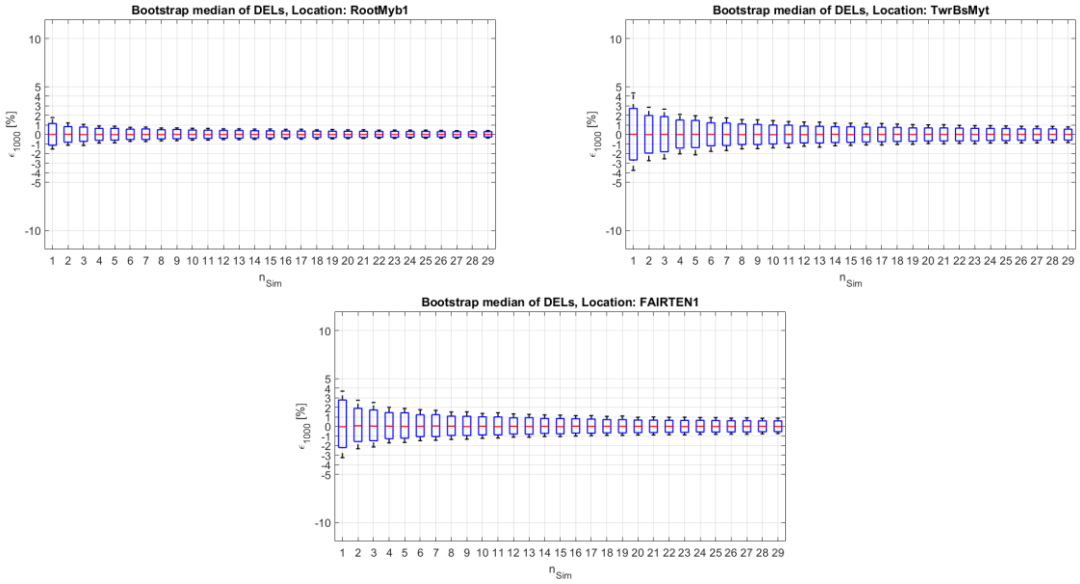


**Figure 4.23: *LIFES50+ OO-Star Wind Floater Semi 10MW* DEL bootstrap evaluation case 2 (wave only): median values after consideration of $n_{Sim}$ values. Red horizontal lines indicate median, box borders 95th percentile and whiskers 99th percentile values.**

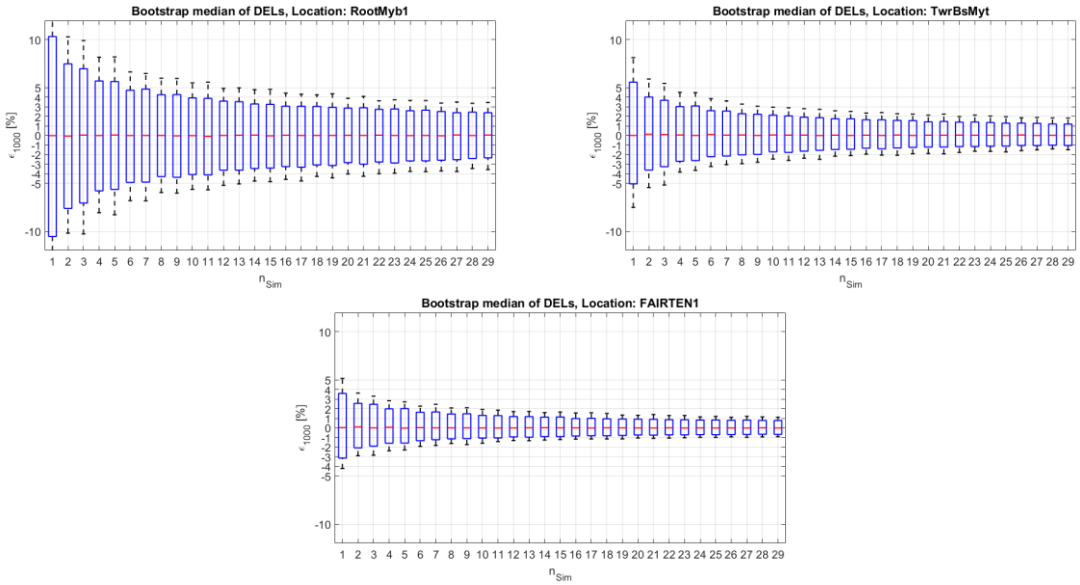


**Figure 4.24: *LIFES50+ OO-Star Wind Floater Semi 10MW* DEL bootstrap evaluation case 3 (wind and wave): median values after consideration of $n_{Sim}$ values. Red horizontal lines indicate median, box borders 95th percentile and whiskers 99th percentile values.**

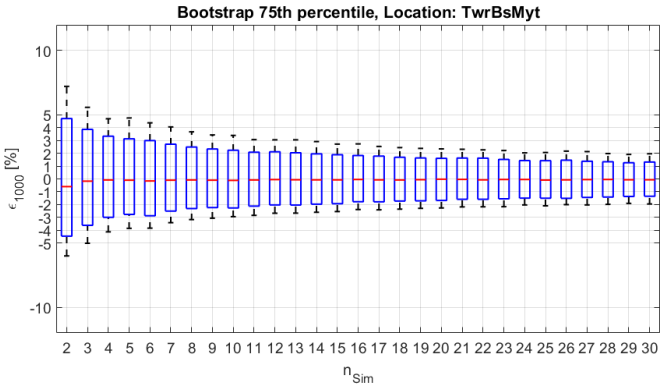


**Figure 4.25: *LIFES50+ OO-Star Wind Floater Semi 10MW* DEL bootstrap evaluation Case 3: 75th percentile values after consideration of $n_{Sim}$ values. Red horizontal lines indicate median, box borders 95th percentile and whiskers 99th percentile values.**

In Figure 4.21 to Figure 4.25, the flapwise blade root DEL shows the most variability, seen in case 1 and 3, (Figure 4.22, Figure 4.24). The results show that to reach below 5% uncertainty in the determination of the median DEL value, measured here by e.g. the 99th percentile, 8-10 simulations are required (Figure 4.23, *RootMyb1*). Using only three simulations, the uncertainty range of the DEL results may be around 20%, which may lead to non-conservative designs. It is possible to include the expected uncertainty in the estimation of statistical parameters either by application of safety factors or by estimating higher percentiles: For example, in Figure 4.25 the 75th percentile of the DEL distribution is estimated and the uncertainty linked to this estimate is like estimating the median value. If the 75th percentile is estimated, 5% of uncertainty will maintain conservative estimates of the DEL value (i.e. a bad estimate will still be above the real median value). Thus, from this evaluation it is advised to use the 75th percentile DEL as the representative value when using a small number of seeds.

Figure 4.26 to Figure 4.28 show the bootstrap results for the *Nautilus-10* concept. Compared to the *LIFES50+ OO-Star Wind Floater Semi 10MW* floater, uncertainty is reduced for the rotor blade loads which indicates a positive impact of the active ballast system. The increase of load uncertainty for both tower base and fairlead tension may be linked to the different geometries of the components.

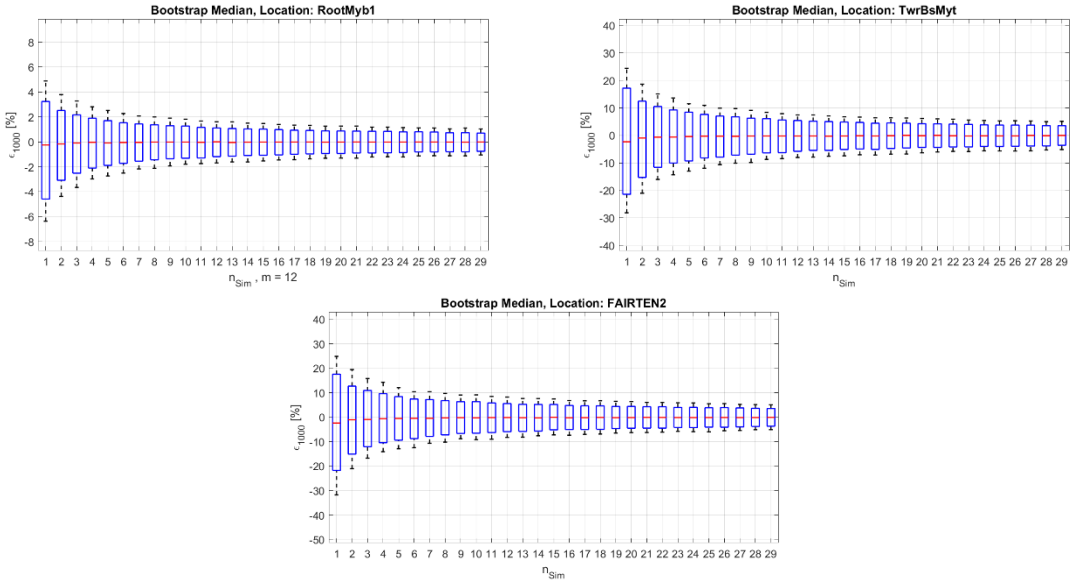


**Figure 4.26: *Nautilus-10* DEL bootstrap evaluation case 1 (wind only): median values after consideration of $n_{Sim}$ values. Red horizontal lines indicate median, box borders 95th percentile and whiskers 99th percentile values.**

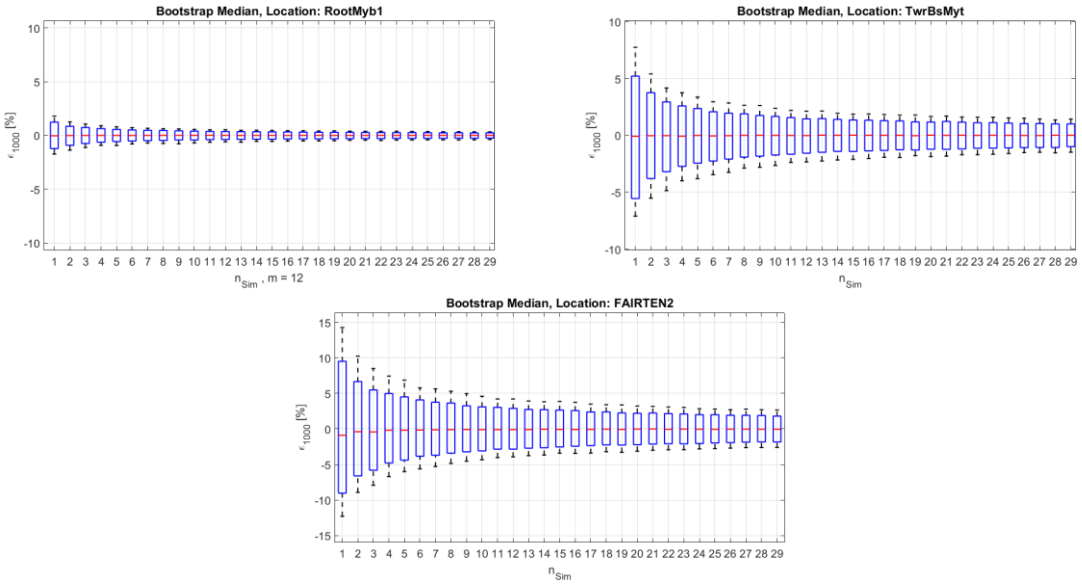


**Figure 4.27: *Nautilus-10* DEL bootstrap evaluation case 2 (wave only): median values after consideration of $n_{Sim}$ values. Red horizontal lines indicate median, box borders 95th percentile and whiskers 99th percentile values.**

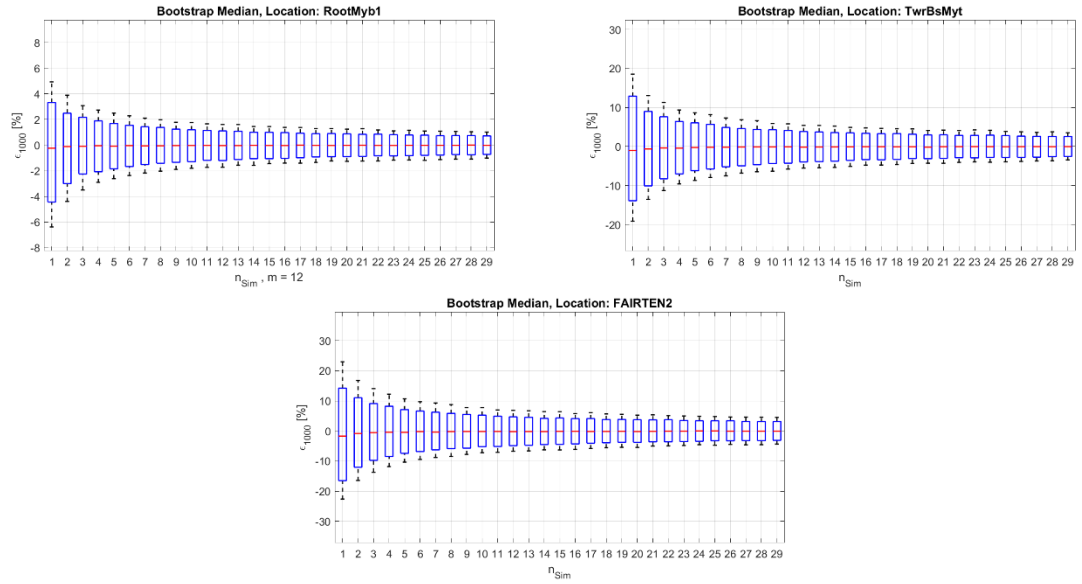


**Figure 4.28: *Nautilus-10* DEL bootstrap evaluation case 3 (wind and wave): median values after consideration of $n_{Sim}$ values. Red horizontal lines indicate median, box borders 95th percentile and whiskers 99th percentile values.**

It is important to remember that the error in the DEL will lead to exponentially larger errors in the estimated damage. This is seen in the following Eq. (2), which relates relative damage and relative DEL values:

$$\frac{DEL_1}{DEL_2} = \left(\frac{D_1}{D_2}\right)^{\frac{1}{m}}, \tag{2}$$

where D is the damage. Hence, a DEL error of 5% is equivalent to an error in the damage of $(1.05)^4 = 1.21$ or 21% for materials with SN-curve slope of $m = 4$.

It is noted that the observed uncertainty in the fatigue loads for more flexible structures (such as a semi-submersible) needs a more careful investigation in the future in order to determine whether an increased

uncertainty is to be expected in other components, which could require an increase of the considered seeds (e.g. blade fatigue loads, power production, rotor rotational speed, ultimate loads, etc.).

### 4.3.2 Simulation length

A question that remains unanswered with the studies performed in section 4.3.1 is the benefit of using an increased number of seeds rather than extending the simulation time of single seeds, when a total simulation time is required. According to the DNV offshore standard for design of floating wind turbines (DNV-OS-J103; DNVGL-ST-0119, 2013) , a minimum of 3 hours for fatigue calculations are to be simulated "*to adequately capture effects such as nonlinearities, second order effects, and slowly varying responses, and to properly establish the design load effects.*" This can be reached by combining seeds with varying simulation times.

**Table 4-8: Combination of simulation length and number of simulations.**

| Case | Number of Simulations to make 3,600s (FLS) | Number of Simulations to make 10,800s (ULS) |
|---|---|---|
| 300s | 12 | - |
| 600s | 6 | - |
| 900s | 4 | - |
| 1,200s | 3 | 9 |
| 1,800s | 2 | 6 |
| 2,700s | - | 4 |
| 3,600s | 1 | 3 |
| 5,400s | - | 2 |
| 10,800s | - | 1 |

In order to investigate the possible combinations of simulation time and number of seeds, parts of varying length of the available seeds for the three cases presented in Table 4-7 are considered, so that a combination of seeds can be used to reach a total of one hour of simulations (see Table 4-8, first column). Then, the statistics of the resulting combinations (e.g. 12 seeds of 300s time series) are determined. For each evaluation, the lifetime DEL defined by a reference cycle number of $N_{ref} = 2 \cdot 10^6$ of the considered sample is calculated to provide a comparison of equal values. For the statistics of 5,000 draws with replacement, the error towards the lifetime DEL of the 1000 available seeds with 3600s simulation time is calculated and are evaluated below.

For **case 1 (Table 4-7)**, only wind seeds are changed, meaning that only a singular wave seed was considered (*LIFES50+ OO-Star Wind Floater Semi 10MW*) or still water conditions (*Nautilus-10*). Figure 4.29 shows the statistical evaluation of the different combinations possible. It is visible that for the blade root bending moment, the uncertainty is smallest if many seeds are considered. For the lower positioned locations of the *LIFES50+ OO-Star Wind Floater Semi 10MW* concept (tower base fore-aft bending moment and fairlead tension), a bias is included, if the simulation time is too short. This is due to the use of a single wave seed where the wave environment needs more time to reach stationarity. The included bias shows the importance to include different wave seeds in the evaluation. For the *NAUTILUS-10* concept, still water conditions are considered. There, a benefit is visible for using a larger number of seeds for all signals.

*LIFES50+ OO-Star Wind Floater Semi 10MW:* *NAUTILUS-10:*

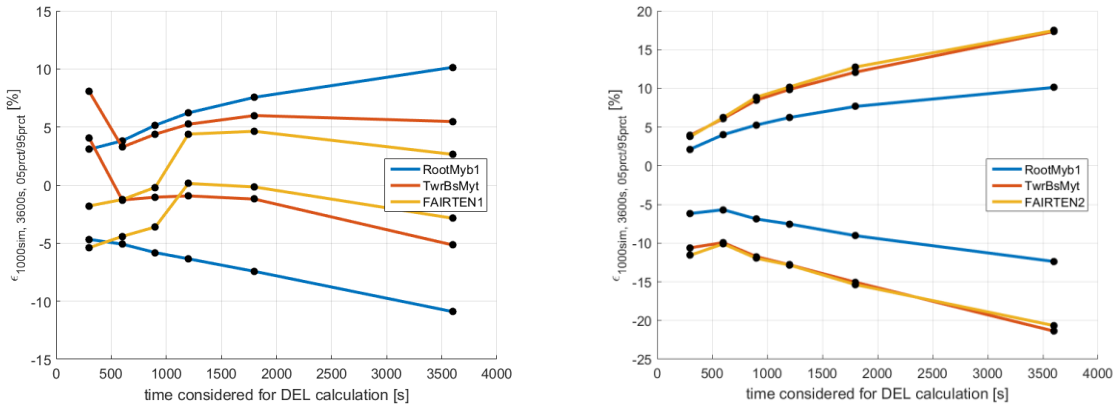


**Figure 4.29: error plot of DEL for 95th and 5th percentile for case 1, changing wind seeds only**

In **case 2**, only the wave seeds are changed, using a single wind seed (*LIFES50+ OO-Star Wind Floater Semi 10MW*) or steady wind (*Nautilus-10*) for all 1000 performed simulations. Hence, the uncertainty contribution from the wave environment is highlighted by the difference magnitude between 5th and 95th percentiles in Figure 4.30. For the *LIFES50+ OO-Star Wind Floater Semi 10MW* concept, this uncertainty can be reduced for the lower locations by almost 50% (7% difference for tower base fore-aft and 1200s simulations to 4% difference at 3600s). With respect to the wind environment, a bias towards underestimation of the damage is visible even though only one periodic wind file of 600s length is used. This is expected to be linked to the missing consideration of relevant load amplitudes that result from interaction of the wind and wave environment later in the time series. As can be seen in Figure 4.31, this effect is not of high importance if many wind seeds are considered. However, it adds to the overall

*LIFES50+ OO-Star Wind Floater Semi 10MW:* *NAUTILUS-10:*

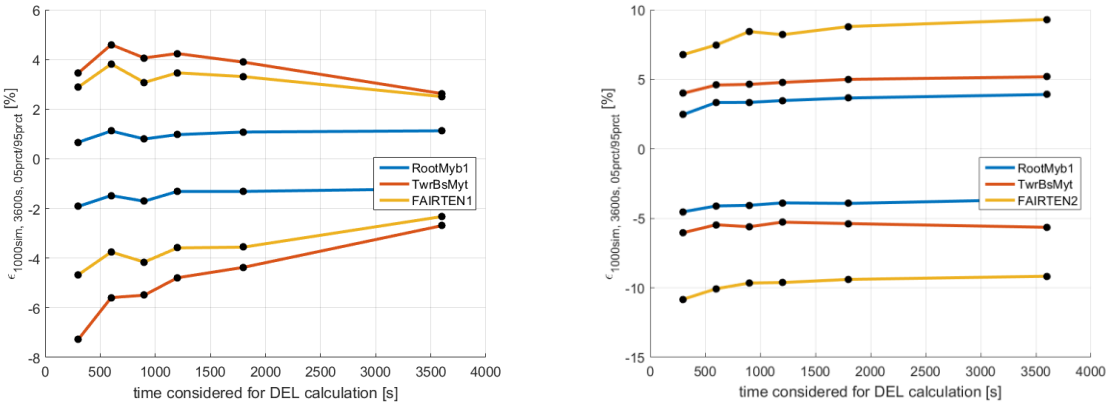


**Figure 4.30: error plot of DEL for 95th and 5th percentile of the 1000 simulations for case 2: changing wave seeds only ( single wind seed for LIFES50+ OO-Star Wind Floater Semi 10MW or steady wind for Nautilus-10)**

understanding that wind-wave interaction may cause significant impact even though periodic wind fields are applied. For the *Nautilus-10* concept, only minor changes in the uncertainty with increasing simulation time are visible, indicating that the wave environment has a limited impact overall.

In **case 3**, both wind and wave seeds are varied for each performed simulation. Here, a small bias (variation of median of estimation errors) for all locations is only observed for simulation lengths below 1200s for the *LIFES50+ OO-Star Wind Floater Semi 10MW*. The median of estimation errors is already low (<1%) for simulation times of 600s for the considered case. For the *NAUTILUS-10* concept, this

median is generally larger indicating that a larger number of seeds could be necessary to reach converged statistics. As the platform is more sensitive towards the wind environment, the greatest benefit is reached by including a full wind field in the simulation (i.e. simulation time > 600s). Overall this also leads to the conclusion that shorter simulations are to be preferred over a reduced number of seeds.

*LIFES50+ OO-Star Wind Floater Semi 10MW:* *NAUTILUS-10:*

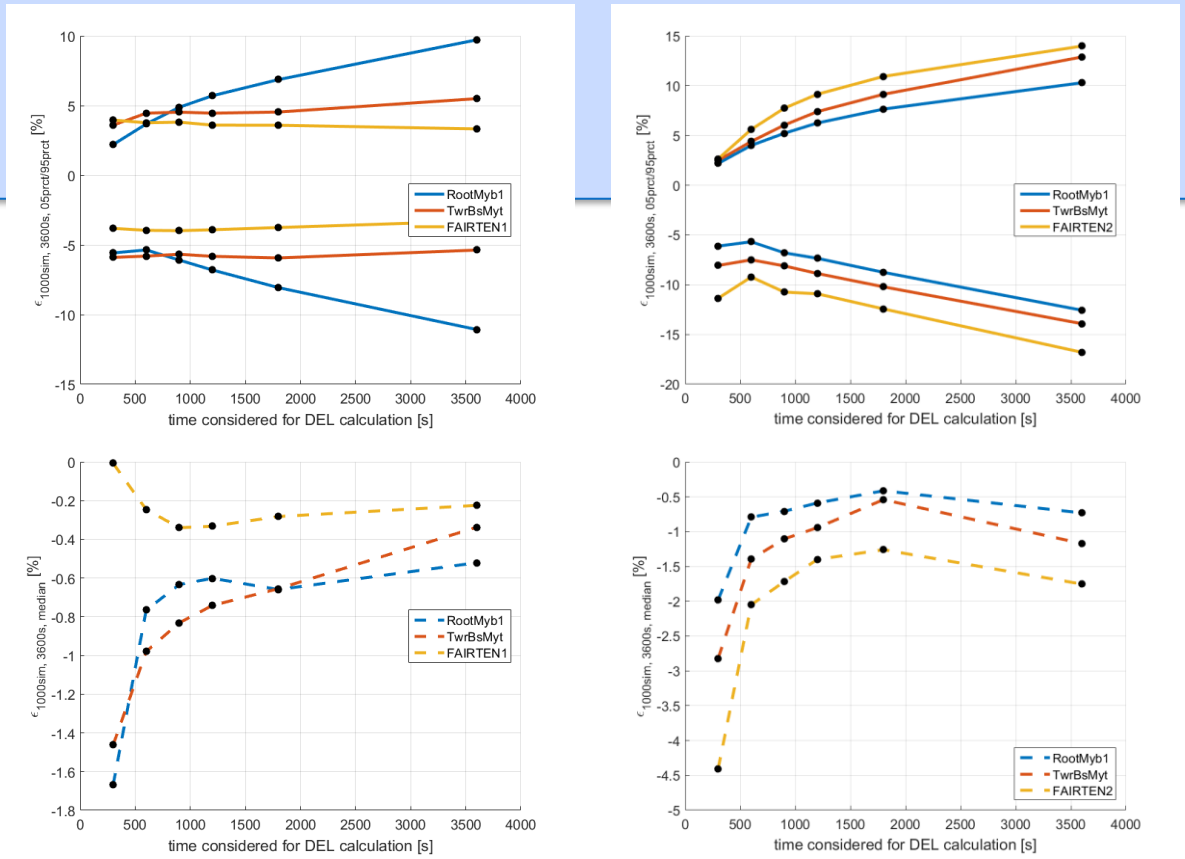


**Figure 4.31: error plot of DEL for 95th and 5th percentile (top) and median values (bottom) of the 1000 simulations for case 3: changing wind and wave seeds**

The results show that distributing a required overall simulation time over a larger number of seeds may lead to a reduction of the uncertainty and hence an improved load prediction for the considered setup if 10 min periodic wind seeds are used. Then, repeated periodic wind fields add no new information beyond their length of 10 min and hence an increase of seeds is to be preferred to achieve around 10% less uncertainty A significant bias is only introduced when reducing the simulation time below the time of a full wind-field (Figure 4.31, bottom). As shown in section 4.3.1, the uncertainty contribution from different wave seeds is limited (Figure 4.24) and only a limited bias-reduction can be reached by significantly extending simulation time (Figure 4.30). The impact of the wave time series is important (Figure 4.29), however the results of this study indicate that the impact is included sufficiently when considering multiple seeds rather than longer simulation times (Figure 4.31). It is to be expected that platforms more sensitive to low frequencies may show a different behaviour. For the *Nautilus-10* concept, all signals show a significantly smaller uncertainty when using a larger number of seeds rather than longer simulation times. Thus, the decision on where to put the focus is also depending on the sensitivity of the platform. If the wave environment has a large impact, it may well be that longer simulation times will lead to an increased benefit. For the platforms investigated in this study, this is however not the case. In this way, it is highlighted that the abovementioned results are very system specific and may change significantly if relevant natural periods are well within the wave spectrum.

# 5 ULS Simulation studies

For the close-up evaluation of ULS analysis, DLC 1.6 and DLC 6.1 were chosen in this work. DLC 1.6 is focussing on extreme load events during power production, which means that operation is taking place in parallel with a severe sea state. DLC 6.1 considers a parked wind turbine (implemented here by parked rather than idling turbine) in an extreme environment for both wind and waves. A summary of the load cases is given in Table 5-1.

**Table 5-1: DLC specification according to (Krieger, et al., 2015) for considered ULS cases in this document**

| Design Situation | DLC | Wind Condition | Marine Condition | | | | Other Conditions: | Type of Analysis | PSF |
|---|---|---|---|---|---|---|---|---|---|
| | | | Waves | Wind & wave directionality | Sea Currents | Water Level | | | |
| 1) Power Production: | 1.6 | NTM $V_{in} < V_{hub} < V_{out}$ | SSS $H_s = H_{s,SSS}$ | COD, UNI | NCM | NWLR | | U | N |
| 6) Parked (standing still or idling): | 6.1 | Turbulent - EWM $V_{hub} = V_{ref}$ | ESS $H_s = H_{s,50}$ | MIS, MUL | ECM $U = U_{50}$ | EWLR | | U | N |

**Table 5-2: Site B specific values for relevant environmental conditions**

| Environmental parameter | value |
|---|---|
| **Hs,sss / Hs,50 [m]** | 10.9 |
| **V_ref [m/s]** | 44.0 |
| **U50 [m/s]** | 1.13 |

Note that the wave height for the severe sea state was chosen equal to the extreme wave height in the LIFES50+ design basis (Krieger, et al., 2015). This resembles a very conservative approach due to the lack of more detailed information on the environment.

## 5.1 ULS Simulation setup

### 5.1.1 Minimum wave period for ULS sensitivity study

In DLC 6.1, and 1.6, the minimum peak wave period is chosen according to the physical breaking wave limit in deep waters according to (Det Norske Veritas AS, 2011). This results in $\frac{H_s}{\lambda} \leq \frac{1}{7}$ and using $\lambda = \frac{2\pi g}{\omega^2}$ and $\omega = \frac{2\pi}{T}$ leads to:

$$T \geq \sqrt{\frac{14\pi H_s}{g}}. \tag{3}$$

The obtained minimum wave period is then $T_{min} = 7.2\ s$ which is used as peak period for both DLC 6.1 and 1.6, taking into consideration the wave height at the considered site (i.e. 10.9m, see Table 5-2). The period may change slightly, if a range of wave heights is considered, see section 5.2.

It is noted that for the guidelines for the severe sea state as used for DLC 1.6, another range may be used according to (DNV GL AS, 2016):

$$11.1\sqrt{\frac{H_{s,sss}}{g}} \leq T, \tag{4}$$

which leads to a minimum peak period of $T_{min} = 11.7\ s$.

In this study, the physical breaking wave limit from equation (3) was considered, which is generally used only for one individual (maximum) wave. This is considered as a conservative option in place of the value derived from equation (4) to study more closely the impact of variation of wave periods. It is noted that this may lead to nonphysical wave periods in the evaluation.

The upper wave period is set to $T = 20\ s$, to give indication to the effect of swell waves on the structure.

It is acknowledged that the use of environmental contours is very common in the design of floating ocean structures and could potentially reduce the loading by using more realistic combinations of wave height and wave period. The focus of this work was a sensitivity analysis of the relevant parameters, considering a variation of 10 % of the significant wave height and a large range of the wave period. In this way, under the assumption that a certain wave height was detected, it is proposed to add a variation of wave periods and some variation of the determined wave height as well to consider all possible wave periods as well as some uncertainty in the prediction of the significant wave height. In conventional design, a range of periods is not considered as a monotonic behaviour of the response towards wave period is assumed. However, if concept specific response peaks for certain periods exist, these must be included in the design calculations.

### 5.1.2 Initial conditions

For ULS simulations in power production, the same initial conditions as obtained in section 4.1.1 may be used (i.e. for DLC 1.6). Focus in this section lies on the initial conditions that are required for simulations in extreme wind speed conditions. In this work, initial conditions are required for simulations of DLC 6.1, which uses wind speed with 50-year occurrence period. For the considered site Gulf of Maine, this amounts to $v_{50yrs} = 44\ \frac{m}{s}$. Some variation of the wind speed around the 50-year wind speed is considered for sensitivity studies, so wind speeds $v \in \mathbb{R}: 41 \leq v \leq 47$ were taken into account here. Due to the stable condition of the FOWT (idling position), a monotonic relationship of the system dynamic behaviour is expected, and a resolution of 1 m/s was chosen. Figure 5.1 exemplarily shows the time series of the surge displacement for the simulations used in this chapter.

*LIFES50+ OO-Star Wind Floater Semi 10MW:* *NAUTILUS-10:*

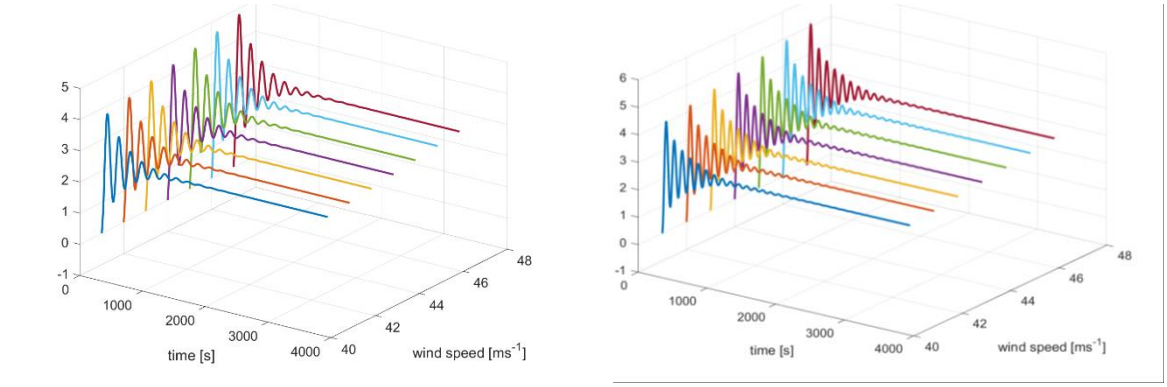


**Figure 5.1: Time series of surge displacement [m] as a function of wind speed.**

#### 5.1.2.1 Simulation length requirements for initial condition calculations

The same procedure as presented in section 4.1.1.1 was used here, to determine the required length for simulations around the 50-year occurrence period. This means wind speed was considered as uniform and aligned with the rotor and no wave heights or currents were considered as part of the initial condition calculations. Also, because of the high wind speeds, the rotor is idling, which is different from section 4.1.1.1.

Figure 5.2 shows exemplary the convergence of the normalized moving mean values for the platform pitch motion for all wind speeds considered. As a summary, Figure 5.3 shows the maximum deviation from the mean value for all relevant signals. In this plot, a large deviation is documented for the rotor speed, which is to be ignored because the rotor speed is close to zero in this load case. For the *LIFES50+ OO-Star Wind Floater Semi 10MW,* already the mean of the first 600s (indicated in Figure 5.3 with starting time equal to 0 seconds) results in the mean values of all positions to being within 5% of their final value. All signals quickly converge, and faster than for the power production load cases as presented in Figure 4.3. This indicates that using the same time constraints for idling conditions as for power production load cases is feasible. One difference between the concepts is the platform pitch motion, which is larger for the *NAUTILUS-10* concept. This signal needs some significant time in the range of power production cases, which should be considered when determining the initial conditions. An improved version of the ballast distribution should help mitigating this behaviour. Also, as mentioned before, if the reference value is close to zero (which is the case for the platform pitch angle of the *NAUTILUS-10* concept), error values may be very large, and the interpretation may be more difficult.

*LIFES50+ OO-Star Wind Floater Semi 10MW:* *NAUTILUS-10:*

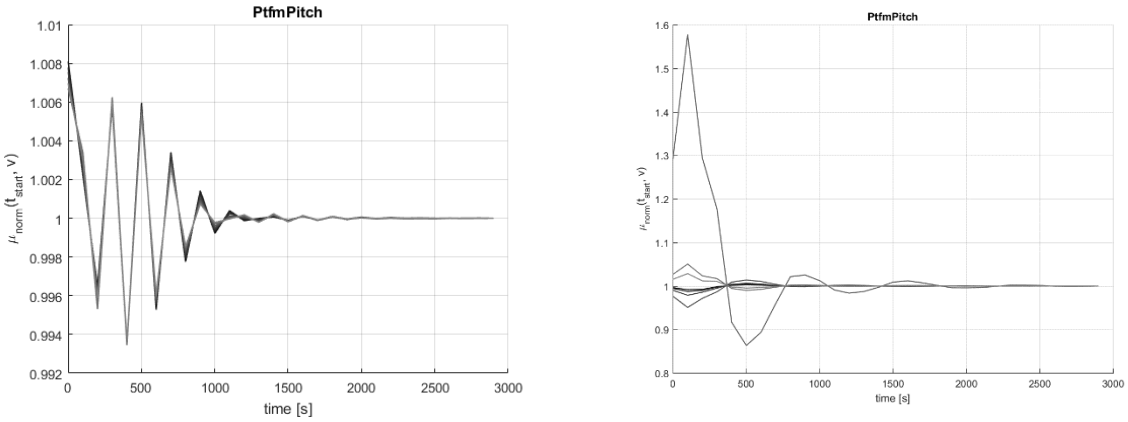


**Figure 5.2: Convergence of normalized mean value for platform pitch motions, all wind speeds**

*LIFES50+ OO-Star Wind Floater Semi 10MW:* *NAUTILUS-10:*

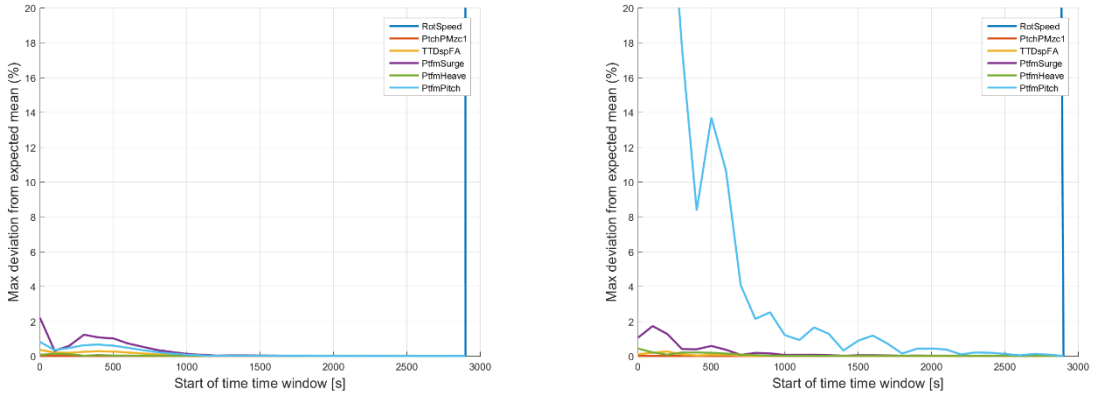


**Figure 5.3: Convergence of normalized mean value for relevant FOWT DOFs, maximum across all wind speeds**

### *5.1.2.1 Resolution requirements of initial condition simulations*

For idling simulations, the initial conditions will be less sensitive towards changes of wind speed, as only the reduced (blades feathering) and static (no rotor revolution) impact of thrust is acting on the turbine. Figure 5.4 shows the small difference between a resolution of 1m/s and only considering the extreme values of the range of wind speeds to be considered. A direct comparison with the results from Figure 4.4 show that absolute platform pitch displacement is a magnitude smaller for 50-year winds compared to peak values during power production, which further justifies the use of a coarser resolution.

*LIFES50+ OO-Star Wind Floater Semi 10MW:* *NAUTILUS-10:*

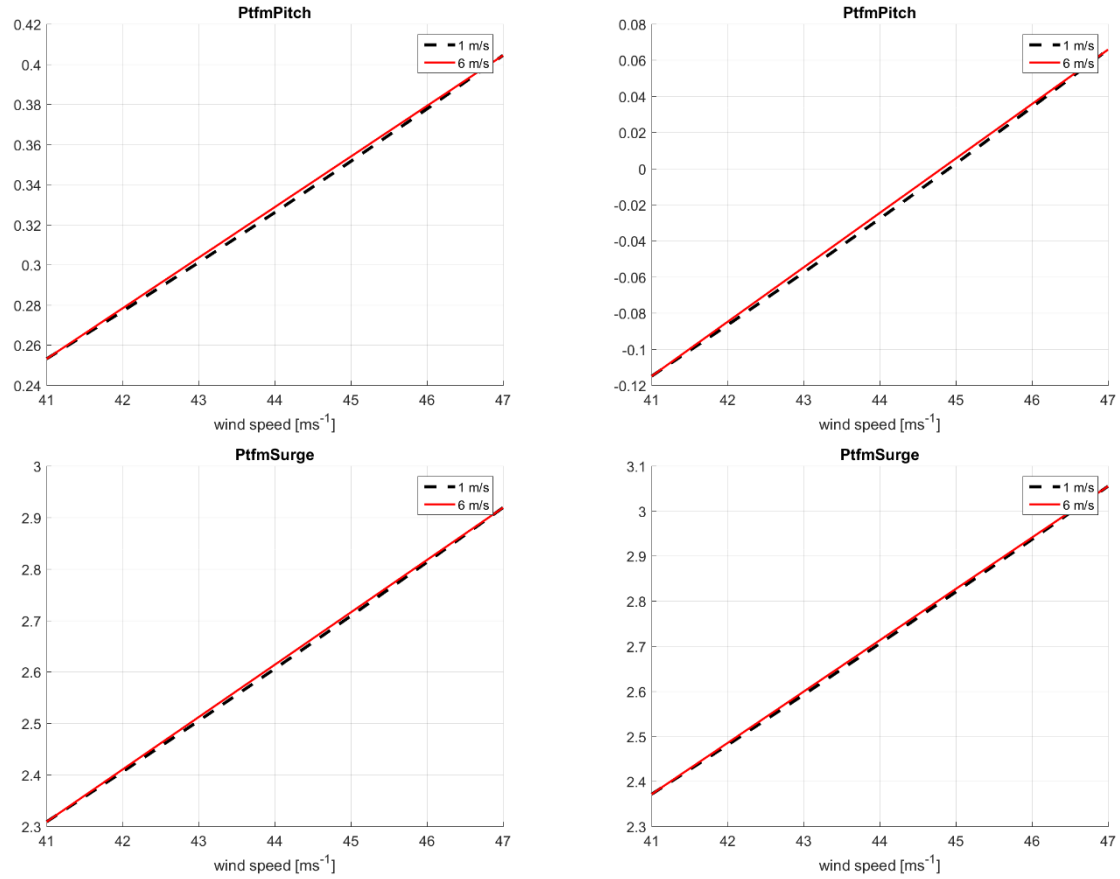


**Figure 5.4: Resolution requirements for wind speed for steady state simulations. Showing 2 different resolutions (1 m/s and 6 m/s). Showing results for platform pitch (left, [°]) and platform surge (right, [m]).**

As a summary of the results for initial condition assessment of idling load cases, the following points are highlighted:

- Using the same time length for the determination of initial conditions as for power production load cases is expected to lead to feasible results.
- If multiple wind speeds are considered, a coarse resolution is possible (i.e. consider only minimum and maximum wind speeds). Initial conditions for other wind speeds may then be interpolated.

### 5.1.3 Initial transient effects and required run-in-time

The same methodology was used here as introduced in section 4.1.2. in which the backwards standard deviation is used to analyse the initial transient effects run-in time. Again, the same initial conditions were used for all simulations, meaning that the observed transients are considered a conservative estimate.

#### *5.1.3.1 DLC 1.6*

The results for DLC 1.6 are based on the simulation study addressed in section 5.2.1. There, simulations are performed to investigate the impact of eight varying environmental conditions (wind speed/direction, wave height/period/direction, current speed/direction and water depth). Using the manifold different environmental conditions produced in that analysis is considered to give meaningful insight into the possible transient time and the resulting required simulation run-in-time. Figure 5.5 visually assesses the transient behaviour of various degrees of freedom of the *LIFES50+ OO-Star Wind Floater Semi 10MW* structure.

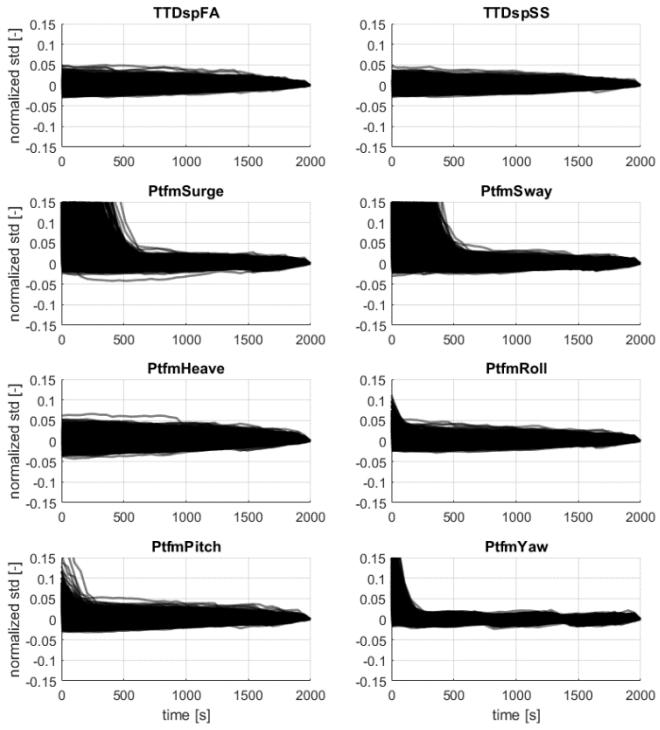


**Figure 5.5: *LIFES50+ OO-Star Wind Floater Semi 10MW* Run-in-time evaluation for DLC 1.6. Results are normalized using standard deviation of time series not considering first 2000s of simulation (i.e. t=2000s).**

The results from Figure 5.5 show that the degrees of freedom with the larges transients are the platform surge and the platform sway. Surge and sway motions are converged around 600 s. Overall, based on the results from section 4.1.2, 1000s is taken here as well as a reasonable time for convergence to be achieved for all sensors, which may be significantly reduced by proper initial conditions.

Figure 5.6 shows the run-in-time evaluation for the *NAUTILUS-10* concept. As mentioned before, for this concept, no initial conditions were used to add to the findings of the other platform. Also, no influences of currents were considered. The results show that the reduced influence of the wind speed for this platform leads to a faster convergence of the standard deviation than documented in DLC 1.2. For this load case this means that again around 500s can be considered sufficient to remove initial transients from the time series.

It is interesting to mention that for the *NAUTILUS-10,* less time is required for the final value to be achieved for stochastic simulations than for the initial conditions in the previous section. Note however, that in the previous section, the behaviour of the moving average was investigated to identify the required overall simulation time while in this section the backwards standard deviation is the focus of study in order to determine the required run-in-time. Hence these values serve very different purposes and are also different in their character and hence should not be compared directly.

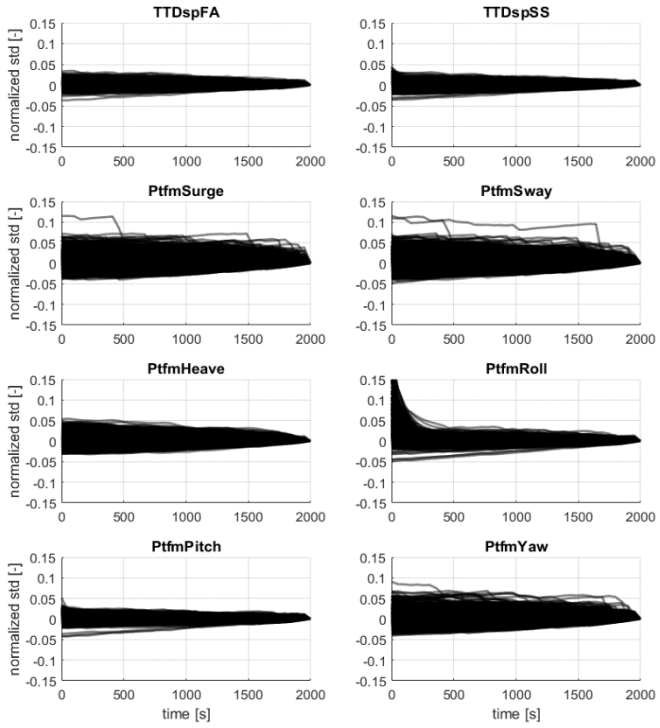


**Figure 5.6: *NAUTILUS-10* Run-in-time evaluation for DLC 1.6. Results are normalized using standard deviation of time series not considering first 2000s of simulation (i.e. t=2000s).**

#### 5.1.3.1 DLC 6.1

The results for DLC 6.1 are based on the simulation study addressed in section 5.2.2. There, simulations are performed to investigate the impact of seven varying environmental conditions (wind speed/direction, wave height/period/direction, current direction and water depth). Using the manifold different environmental conditions produced in that analysis is considered to give meaningful insight into the possible transient time and the resulting required simulation run-in-time. Figure 5.7 visually assesses the transient behaviour of various degrees of freedom of the *LIFES50+ OO-Star Wind Floater Semi 10MW* structure.

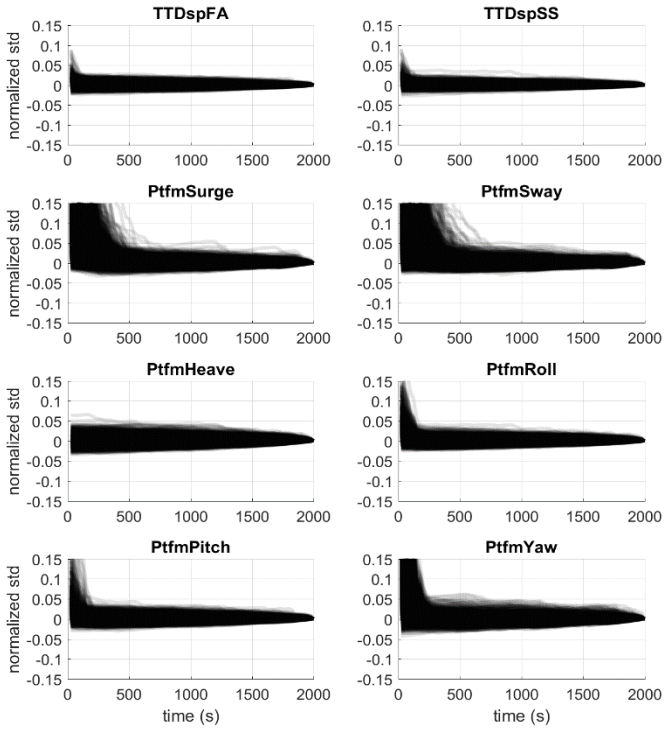


**Figure 5.7: *LIFES50+ OO-Star Wind Floater Semi 10MW* Run-in-time evaluation for DLC 6.1. Results are normalized using standard deviation of time series not considering first 2000s of simulation (i.e. t=2000s).**

As with DLC 1.6, the results from Figure 5.7 show that the sensors that take the longest to reach a stable standard deviation are the platform surge and the platform sway (around 600 s). Overall, based on the results from section 4.1.2 to give a coherent value, 1000s is taken as a reasonable time for convergence to be achieved for all sensors, which may be significantly reduced by proper initial conditions.

This analysis was initially performed for both concepts. However, due to numerical difficulties with the mooring line modelling and reduced time, the results for the *NAUTILUS-10* platform are left out in this evaluation.

As a conclusion, a run-in-time of around 500-1000s is to be expected for different semi-submersible concepts, if no proper initial conditions apart from the correct rotor speed are applied. Additional safety margins are recommended (e.g. use 2000s), if no concept specific experience or results of sensitivity analyses is available.

## 5.2 ULS Sensitivity analysis

The following section outlines the sensitivity analysis carried out to investigate the relationship between the environmental conditions and the loads for specific load cases.

### 5.2.1 DLC 1.6 Global sensitivity analysis on more than 3 environmental conditions

For DLC 1.6, 13698 simulations are performed with eight varying environmental conditions for the *LIFES50+ OO-Star Wind Floater Semi 10MW* concept: wind speed/direction, wave height/period/direction, current speed/direction and water depth. Again, due to minor adjustments, for the *Nautilus-10* concept only 11520 simulations were performed, without consideration of current. For both concepts, turbulence intensity is kept as a function of wind speed, as per turbulence class C. The variation of wave height is limited around +/- 5% of the 50-year wave height.

Table 5-3 provides the ranges and resolution of environmental conditions used for the simulations for the *LIFES50+ OO-Star Wind Floater Semi 10MW* concept. The values for the *Nautilus-10* concept are the same with the limitations described above. As for DLC 1.2, misalignments in the directionalities are implemented indirectly through random selection of the impact direction for the different parameters.

**Table 5-3 Simulation settings for DLC 1.6 *LIFES50+ OO-Star Wind Floater Semi 10MW***

| Case | Environmental conditions | | Number of simulations [-] | Simulation time [s] |
|---|---|---|---|---|
| DLC 1.6<br>8 environmental conditions | Wind speed [m/s] | LR1: 4.0 : 0.1 : 10.2<br>LR2: 10.2 : 0.1 : 13.8<br>LR3: 13.8 : 0.1 : 25.0 | 13698 | 11800 (10800) |
| | Turbulence Intensity [-] | Class C | | |
| | Wind direction [°] | 0 : 15 : 345 | | |
| | Wave height [m] | 10.4 : 0.1 : 11.4 | | |
| | Wave period [s] | 7.2 : 0.1 : 20 | | |
| | Wave direction [°] | 0 : 15 : 345 | | |
| | Current speed [m/s] | 0 : 0.1 : 1 | | |
| | Current direction [°] | 0 : 15 : 345 | | |
| | Water depth [m] | -134.3 : 0.1 : -129.2 | | |

#### 5.2.1.1 Results

Example scatterplots for the maximum resulting tower base bending moment are shown in Figure 5.8 for the *LIFES50+ OO-Star Wind Floater Semi 10MW* concept.

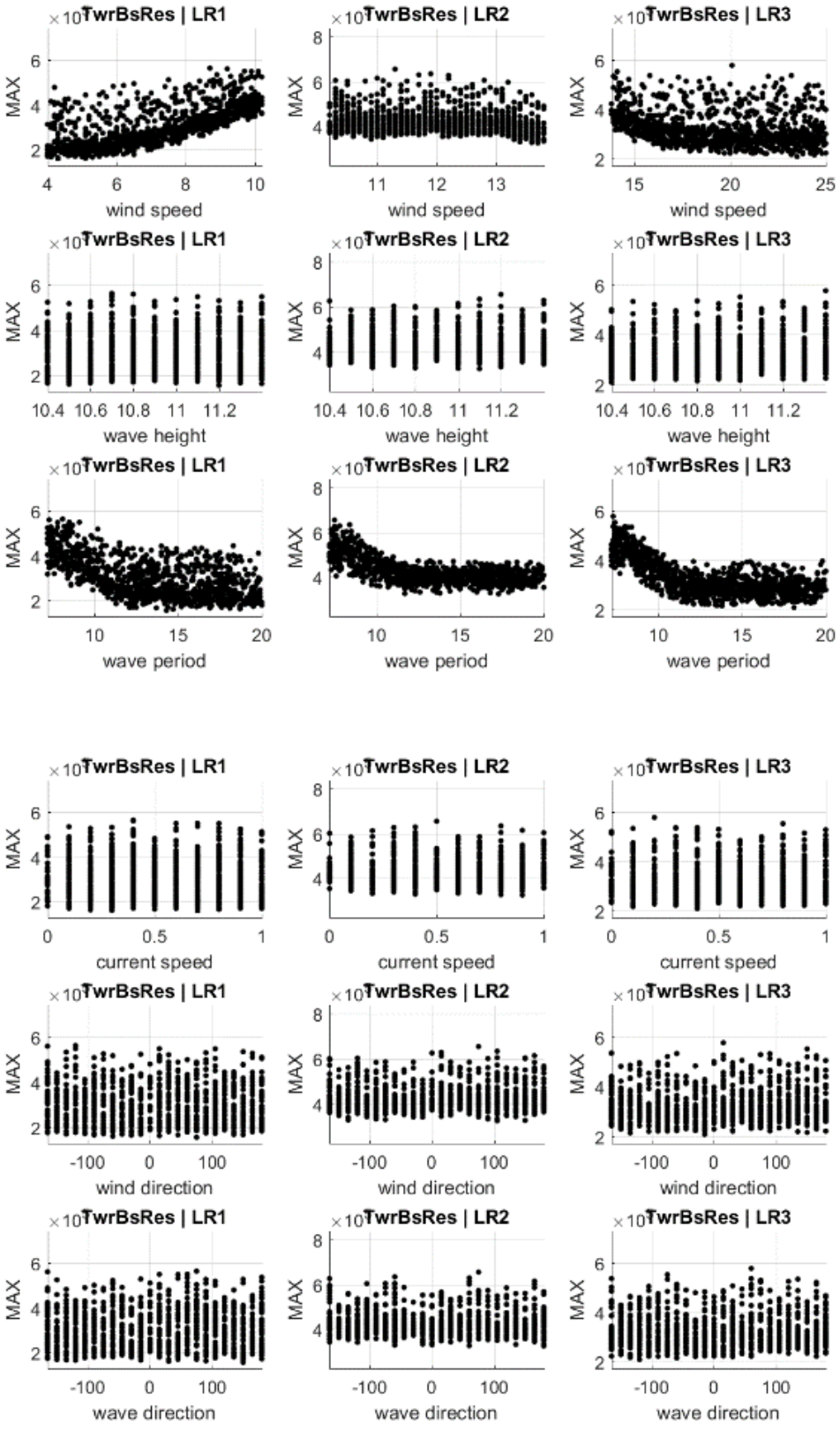
×10 TwrBsRes | LR1
×10 TwrBsRes | LR2
×10 TwrBsRes | LR3
MAX
wind speed
wave height
wave period
current speed
wind direction
wave direction

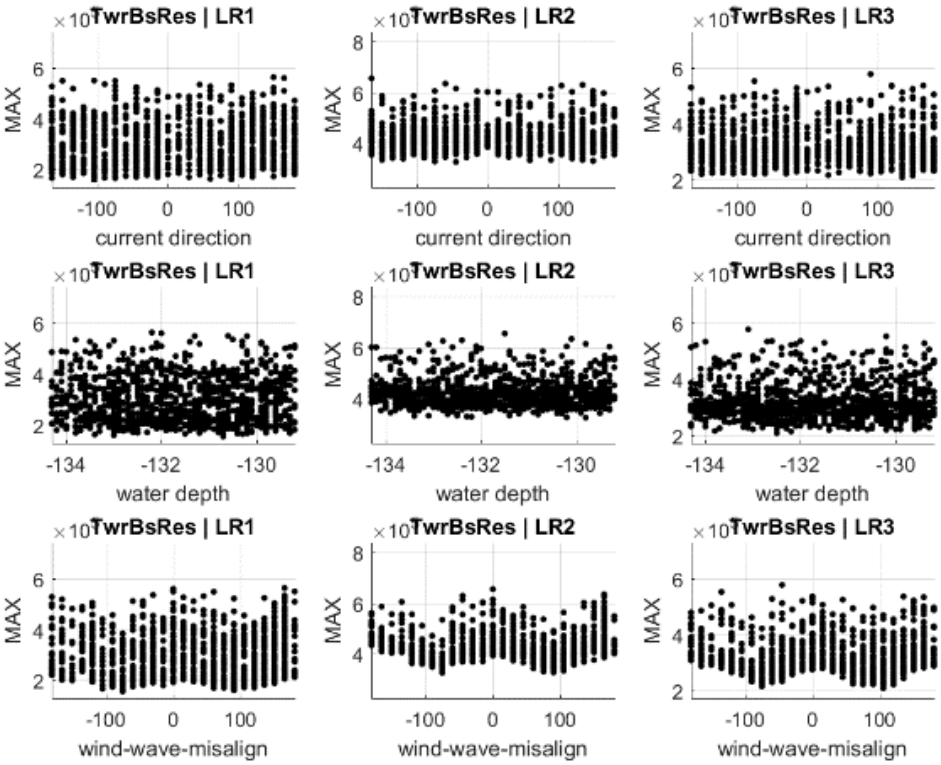


**Figure 5.8: *LIFES50+ OO-Star Wind Floater Semi 10MW* results of sensitivity study for maximum tower base resulting bending moment (TwrBsRes). Results are shown for different load ranges (columns) and environmental conditions (rows).**

The impact ranking of environmental parameters is given in Table 4-2 (*LIFES50+ OO-Star Wind Floater Semi 10MW*).

**Table 5-4: Ranking tables of environmental conditions for different load sensors. Small p-values indicate increased significance of environmental variables. Showing significant candidates only.**

| *rank* | *region* | *p-value* |
|---|---|---|
| **Blade root flapwise** | | |
| 1 | LR1 / wind speed | 1.133E-169 |
| 2 | LR3 / wind speed | 1.6951E-76 |
| 3 | LR2 / wind speed | 6.2664E-52 |
| **Tower base resulting** | | |
| 1 | LR1 / wind speed | 2.852E-95 |
| 2 | LR3 / wave period | 3.3414E-60 |
| 3 | LR1 / wave period | 7.3801E-55 |
| 4 | LR2 / wave period | 3.1116E-48 |
| 5 | LR2 / wind-wave-misalign | 1.0123E-43 |
| 6 | LR3 / wind speed | 3.7833E-32 |
| 7 | LR3 / wind-wave-misalign | 2.8693E-16 |
| 8 | LR2 / wind speed | 4.2815E-05 |
| **Fairlead 1 tension** | | |
| 1 | LR3 / wave direction | 7.9053E-72 |
| 2 | LR1 / wave direction | 3.7196E-64 |
| 3 | LR2 / wave direction | 5.6218E-36 |
| 4 | LR1 / wave period | 3.682E-25 |
| 5 | LR2 / wave period | 8.908E-22 |
| 6 | LR3 / wave period | 5.2414E-20 |

Based on the obtained scatterplots and the ranking tables, the following results can be summarized:
**Blade root flapwise bending moment:** The results show the predominant importance of wind speed with the largest loading around rated wind speed.

**Tower base resulting bending moment**: wind speed, wave height and wind-wave-misalignment have the largest impact. The impact of wave periods may be significantly lower, if only the period range as proposed in (DNV GL AS, 2016) is considered (lowest period around 11s, see section 5.1.1). The small influence of wave height is linked to the small variation of that variable. It shows that an estimation error of the 50-year wave does not lead to any large error in the damage prediction. Largest loads are expected around rated wind speed, for small periods, and for wind-wave-misalignments of 0° and/or 180°.

**Fairlead 1 tension:** wave direction and wave period are the variables with the most significant impact. The directional results can be directly linked to the position of the fairlead, with maximum loads occurring, when the fairlead is directly opposing the impact direction of wind or waves (i.e. 0°). For the wave periods, a monotonous trend results from the study with smaller wave periods leading to higher loads. Opposing to the tower base, this trend continues for larger wave periods as well. Only a small impact of the wind speed is visible, however the largest loads are found around rated wind speed for the fairlead tension as well.

Example scatterplots for the maximum fairlead tension are shown in Figure 5.9 for the *NAUTILUS-10* concept.

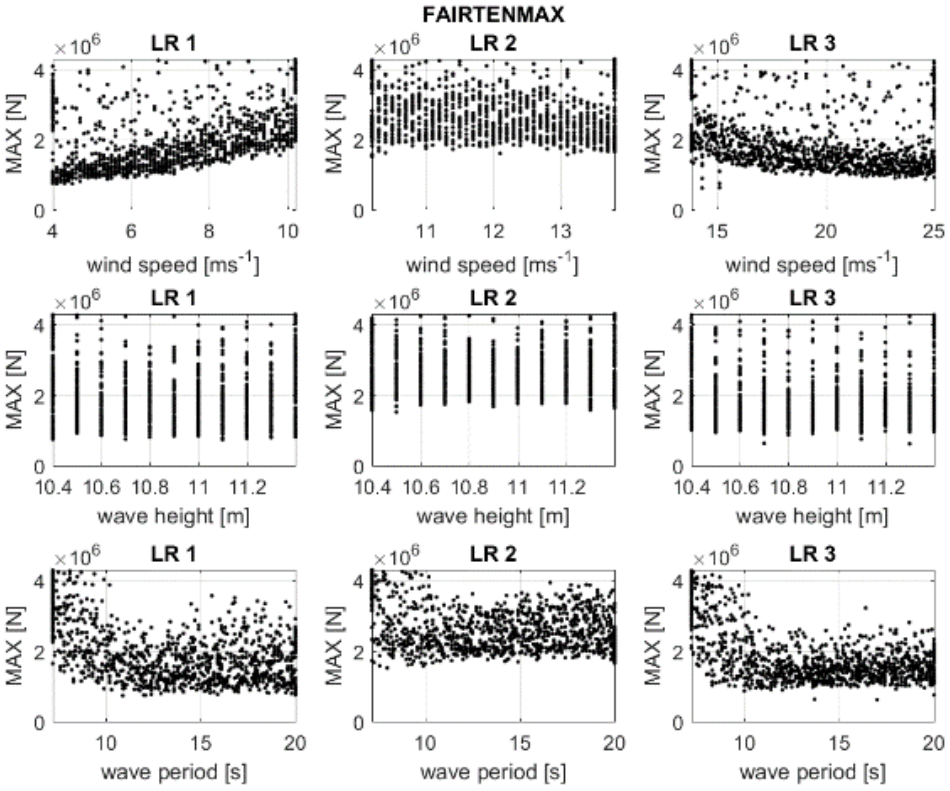
FAIRTENMAX
LR 1
LR 2
LR 3
MAX [N]
wind speed [ms-1]
wave height [m]
wave period [s]

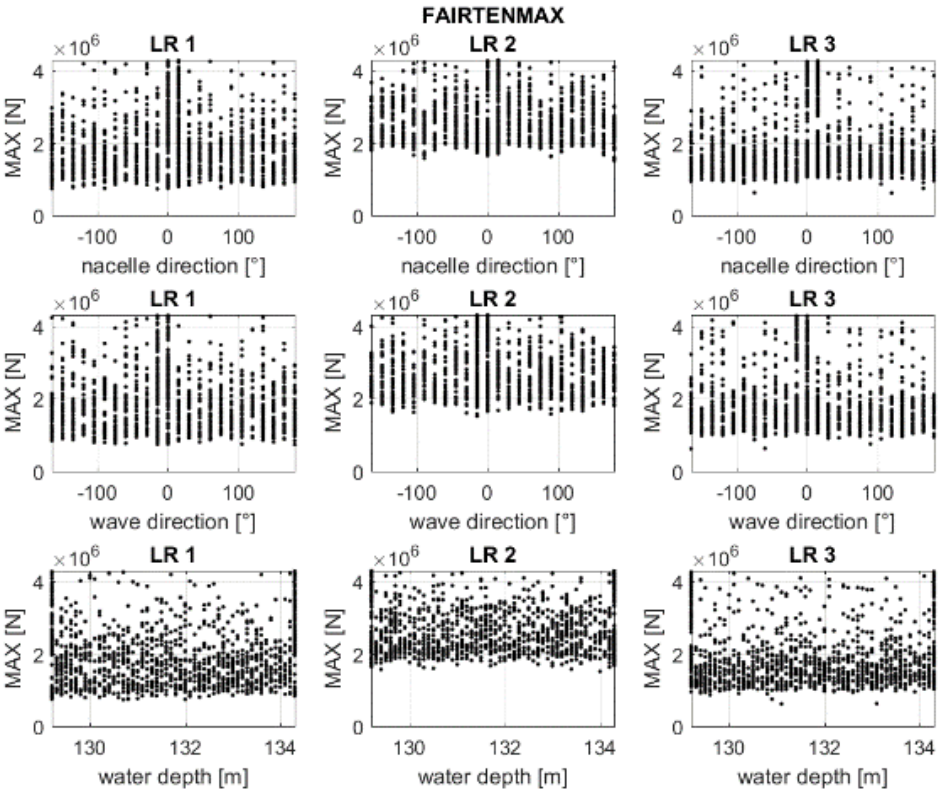
FAIRTENMAX
LR 1
LR 2
LR 3
MAX [N]
nacelle direction [°]
wave direction [°]
water depth [m]

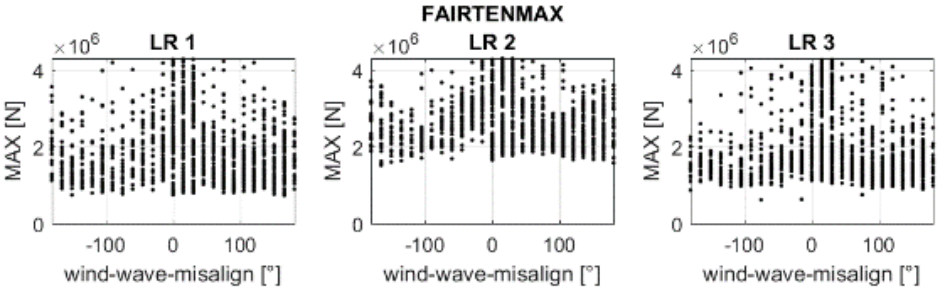


**Figure 5.9: *NAUTILUS-10* results of sensitivity study for maximum fairlead tension (FAIRTENMAX). Results are shown for different load ranges (columns) and environmental conditions (rows).**

The impact ranking of environmental parameters on all investigated signals is given in Table 4-2 (*NAUTILUS-10).*

**Table 5-5: *NAUTILUS-10* ranking tables of environmental conditions for different load sensors. Small p-values indicate increased significance of environmental variables. Showing significant candidates only.**

| *rank* | *region* | *p-value* |
|---|---|---|
| **Blade root flapwise** | | |
| 1 | LR1 / wind speed | 1.806E-198 |
| 2 | LR2 / wind speed | 4.187E-107 |
| 3 | LR3 / wind speed | 1.204E-94 |
| **Tower base resulting** | | |
| 1 | LR3 / wave period | 4.250E-147 |
| 2 | LR1 / wave period | 7.818E-123 |
| 3 | LR2 / wave period | 1.405E-109 |
| 4 | LR3 / wind speed | 9.688E-36 |
| 5 | LR1 / wind speed | 2.297E-32 |
| 6 | LR2 / wind-wave-misalign | 1.227E-19 |
| 7 | LR3 / wind-wave-misalign | 3.243E-19 |
| 8 | LR2 / wind speed | 1.853E-15 |
| 9 | LR1 / wind-wave-misalign | 2.081E-14 |
| **Fairlead tension maximum** | | |
| 1 | LR1 / wind speed | 1.47E-60 |
| 2 | LR3 / wave period | 3.79E-60 |
| 3 | LR3 / wind speed | 3.49E-56 |
| 4 | LR1 / wave period | 3.77E-55 |
| 5 | LR3 / wind-wave-misalign | 4.14E-29 |
| 6 | LR1 / wind-wave-misalign | 1.60E-20 |
| 7 | LR2 / wave period | 1.86E-18 |
| 8 | LR2 / wind-wave-misalign | 5.12E-16 |

Based on the obtained scatterplots and the ranking tables, the following results can be summarized for the *NAUTILUS-10* concept:

Again, for the maximum loads of the **blade root bending moment**, largely only the wind speed is detected to have a significant impact. However, some impact is also detected for the wave periods as well as a minor impact of wind-wave misalignment (load range 3).

For the **tower base resulting bending moment**, the relevant loads are wave period (all load ranges), wind speed (all load ranges) and wind-wave misalignment (second and third load range). No significant impact of wave height is visible, which may be linked to the small range investigated (+/- 5% of 50-year wave height)

For the **maximum fairlead tension**, the largest impact of wind speed is in the first and the third load range (LR1 and LR3). Maximum loads increase significantly with wind speed at wind speeds below rated and decline with increasing wind speed above rated. No significant impact of wave height is

visible, which may be linked to the small range investigated (+/- 5% of 50-year wave height). This indicates that errors in the design assumptions may not lead to large errors in the predicted load. An in-depth analysis of the combined effect of wave period and wave height showed, however, that there is some increased impact of the wave height for small wave periods visible. Contrary to the fatigue loads, the wave period has a large effect on the maximum loads in the way that very small wave periods (all load ranges) as well as large periods (first and second load range) lead to increased maximum loads. This is expected to be related to the RAO with peaks at lower periods (see, e.g. Figure 4.15). Wind-wave-misalignment also seems to be important with a misalignment of 0° leading to the highest loads. For load range two, a misalignment of 180° may also lead to high loading. The sensitivity is quite high on wind-wave misalignment and wave periods, which indicates that a probabilistic approach considering the probability of occurrence of the environmental parameters may lead to less conservative designs (then, not only the scenario leading to the highest load is to be considered).

Overall for DLC 1.6 and based on the investigated parameters in this study, wind speed, wave period and wind-wave-misalignment are seen of major importance for all components and both concepts. For both concepts, it is interesting to see the impact of the wave period. There is a significant decrease in overall loading when neglecting the range between physical breaking wave limit and the minimum period required for severe sea states by standards (see also section 5.1.1). Even though the different concepts show different sensitivity to the wave period, this margin is expected to have an important effect on the predicted loads of the systems. Increasing the peak periods towards 20s and larger again led to increased loadings. In this way, the wave period as parameter with large uncertainty for this load case is assumed to be of interest in future studies. Moreover, a more detailed study on the impact of the wave height may be of interest which was assumed to vary only within a narrow range in this study. It is noted that due to insufficient measurement data, the ESS was used for this load case, which is likely producing overly conservative results and may also influence the sensitivities obtained in this work.

### 5.2.2 DLC 6.1 Global sensitivity analysis on more than 3 environmental conditions

This analysis was initially performed for both concepts. However, due to numerical difficulties with the mooring line modelling and reduced time, the results for the *NAUTILUS-10* platform are left out in this evaluation. Thus, all results presented below refer to the *LIFES50+ OO-Star Wind Floater Semi 10MW* concept.

For DLC 6.1, 6768 simulations are performed with seven varying environmental conditions: wind speed/direction, wave height/period/direction, current direction and water depth. Turbulence intensity is kept as a function of wind speed, as per turbulence class C. The variation of wave height is limited around the 50-year wave height, which helps to determine the error resulting from insufficient accuracy of the estimation of the extreme environmental conditions. As opposed to analysis for DLC 1.6, water depth was only varied with maximum values and evaluated separately using ANOVA. As for DLC 1.2, misalignments in the directionalities are implemented indirectly through random selection of the impact direction for the different parameters.

Table 5-6 provides the ranges and resolution of environmental conditions used for the simulations.

Table 5-6: Simulation settings for DLC 6.1

| | Simulation Settings | | | |
|---|---|---|---|---|
| **Case** | **Environmental conditions** | | **Number of simulations [-]** | **Simulation time [s]** |
| DLC 6.1<br>7 environmental conditions | Wind speed [m/s] | 41.8 : 46.2 | 6768 | 11800 (10800) |
| | Turbulence Intensity [-] | Class C | | |
| | Wind direction [°] | 0 : 15 : 345 | | |
| | Wave height [m] | 10.4 : 0.1 : 11.4 | | |
| | Wave period [s] | 7.2 : 0.1 : 16 | | |
| | Wave direction [°] | 0 : 15 : 345 | | |
| | Current speed [m/s] | 1.13 | | |
| | Current direction [°] | 0 : 15 : 345 | | |
| | Water depth [m] | -134.32 / -129.21 | | |

#### 5.2.2.1 Results

The results are shown as scatterplots for the considered components in Figure 5.10. The impact ranking of environmental parameters is given in Table 5-7.

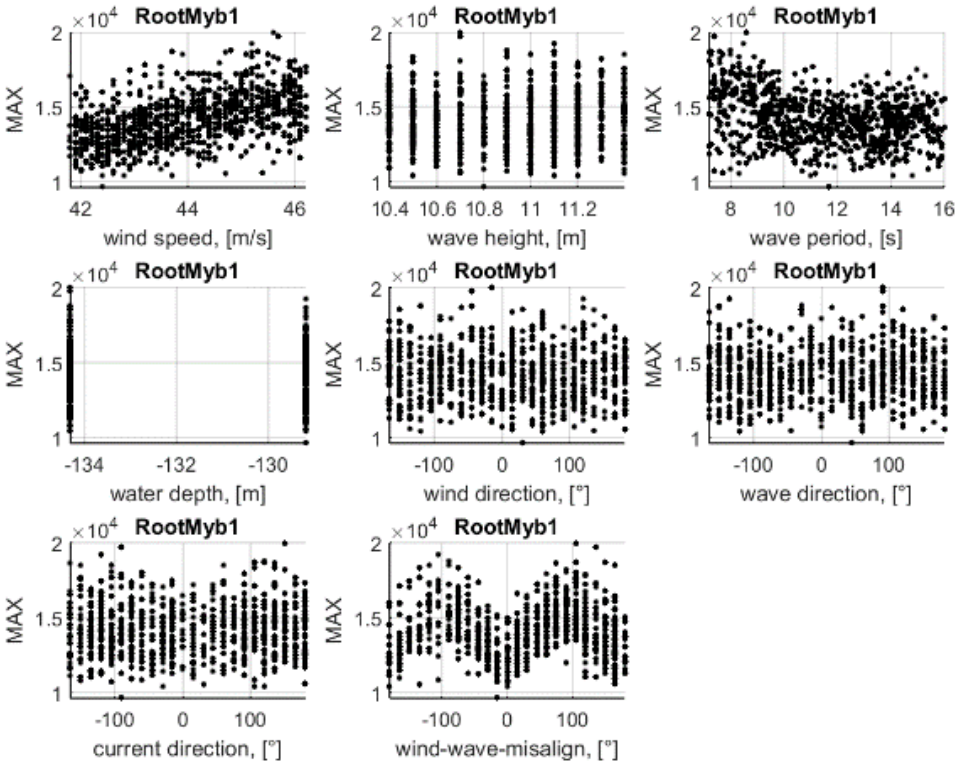
RootMyb1
MAX
wind speed, [m/s]
wave height, [m]
wave period, [s]
water depth, [m]
wind direction, [°]
wave direction, [°]
current direction, [°]
wind-wave-misalign, [°]

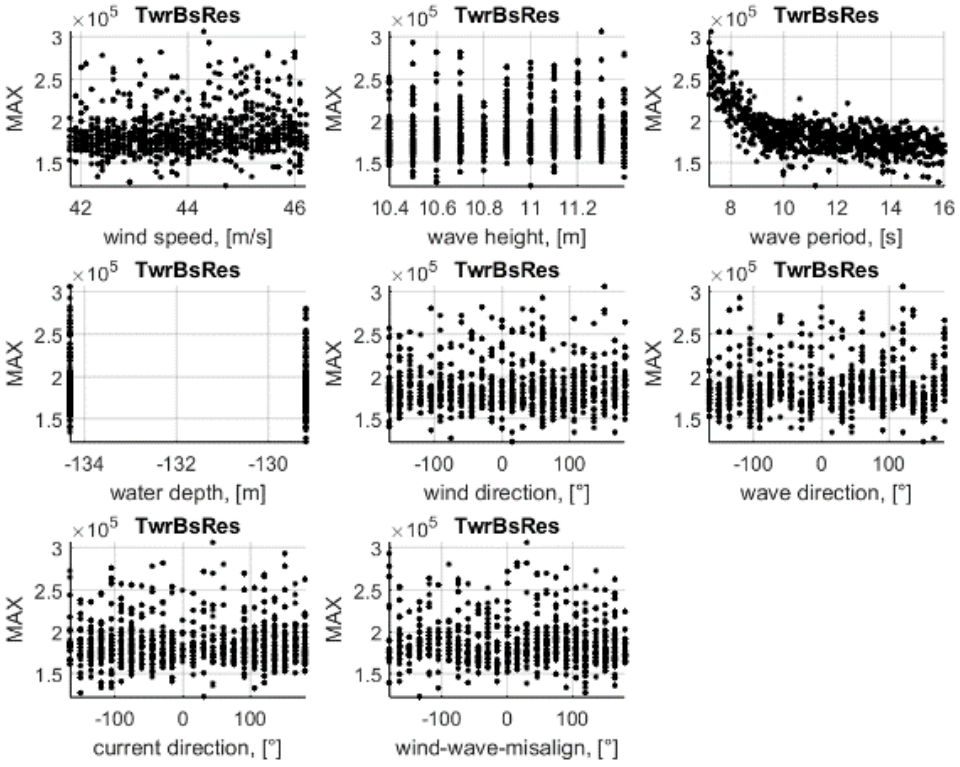
TwrBsRes
MAX
wind speed, [m/s]
wave height, [m]
wave period, [s]
water depth, [m]
wind direction, [°]
wave direction, [°]
current direction, [°]
wind-wave-misalign, [°]

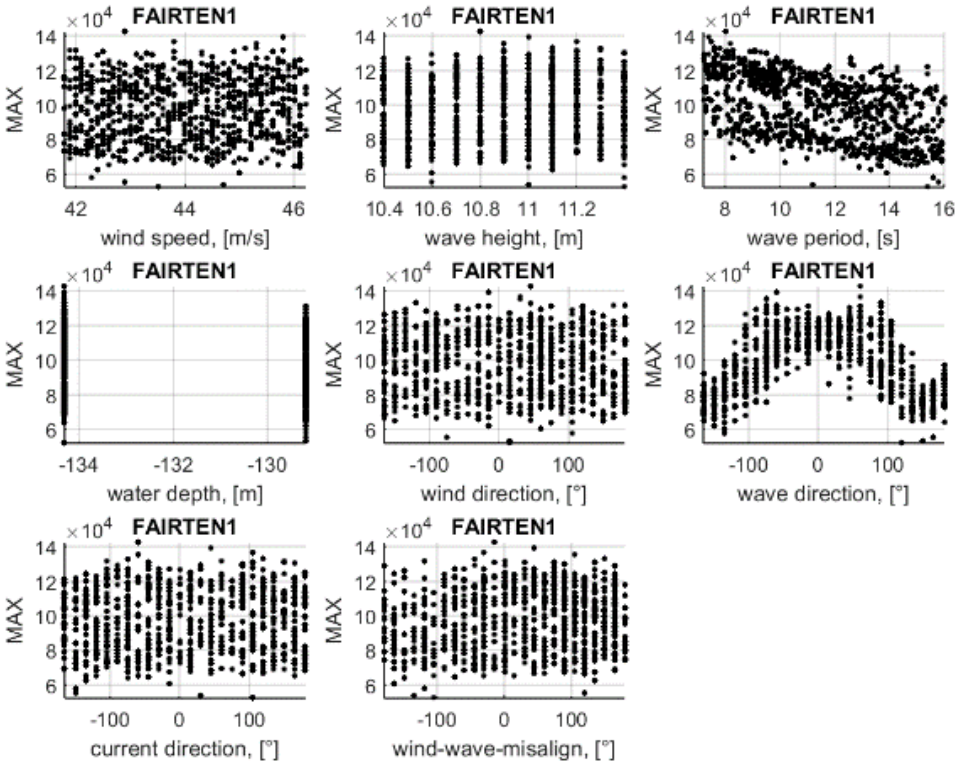


**Figure 5.10:** ***LIFES50+ OO-Star Wind Floater Semi 10MW*** **Results of sensitivity study for maximum blade 1 flapwise root bending moment (RootMyb1), tower base resulting bending moment (TwrBsRes) and fairlead 1 tension (FAIRTEN1). Results are shown for different environmental conditions.**

**Table 5-7: Ranking tables of environmental conditions for different components. Small p-values indicate increased significance of environmental variables.**

| *rank* | *region* | *p-value* |
|---|---|---|
| **Blade root flapwise** | | |
| 1 | wind speed | 4.19E-30 |
| 2 | wind-wave-misalign | 1.99E-28 |
| 3 | wave period | 2.32E-09 |
| 4 | wave direction | 1.96E-02 |
| 5 | current direction | 2.31E-01 |
| 6 | wave height | 4.37E-01 |
| 7 | wind direction | 4.81E-01 |
| **Tower base resulting** | | |
| 1 | wave period | 9.57E-39 |
| 2 | wave direction | 1.90E-07 |
| 3 | wind-wave-misalign | 1.54E-03 |
| 4 | wave height | 1.08E-02 |
| 5 | wind speed | 1.52E-02 |
| 6 | wind direction | 8.69E-02 |
| 7 | current direction | 9.47E-01 |
| 8 | water depth | 9.98E-01 |
| **Fairlead 1 tension** | | |
| 1 | wave direction | 2.04E-85 |
| 2 | wave period | 1.75E-13 |
| 3 | wind-wave-misalign | 9.25E-04 |
| 4 | wind direction | 2.48E-02 |
| 5 | wave height | 5.13E-01 |
| 6 | current direction | 7.08E-01 |
| 7 | wind speed | 8.52E-01 |

Based on the obtained scatterplots and the ranking tables, the following results can be summarized:

**Blade root flapwise bending moment:** The results show the predominant importance of wind speed even for the small variation of wind speed and for a parked rotor. Next to this, wind-wave-misalignment has a significant impact with the largest loads occurring at around 90° misalignment. Interestingly, for this load case the wave periods also have a noticeable influence on the blade loads with smaller periods leading to increased loading.

**Tower base resulting bending moment**: Wave period and –direction show the highest impact. Small wave periods lead to the highest loads, with a significant change of impact around $T_P = 9s$. For periods $T_P > 10s$, there is a small influence, with larger wave periods leading to lower maximum loads. The (minor) impact of wave direction is periodic with directions of multiples of 60° leading to increased loads.

**Fairlead 1 tension:** As for DLC 1.6, the wave direction is of high importance for the fairlead tension. Again, the highest loads are expected, when the fairlead is facing the impact direction (i.e. 0°). Wave period is of some importance, with a seemingly linear trend with decreasing loads for increasing wave periods.

Overall, wind speed, wave period and wind-wave-misalignment are found to have the largest effect on loading for DLC 6.1 and should be considered carefully. In future studies it could be interesting to investigate a larger range of wave periods to determine the possible impact of low-frequency swell waves. As for DLC 1.6, any uncertainty with respect to the lower end of possible wave periods is expected to have an impact on the loads.

### 5.2.3 DLC 1.6 Peak shape parameter effect on maximum loads

As mentioned in section 4.2.4 the peak shape parameter of the JONSWAP spectrum has been investigated to find out its effect on maximum loads and DELs. For this, the environmental parameters in Table 4-6 have been used for the simulation study, based on DLC 1.6. The following figures show the results of the maximum loads from the 6 seeds of the peak shape parameter sensitivity analysis.

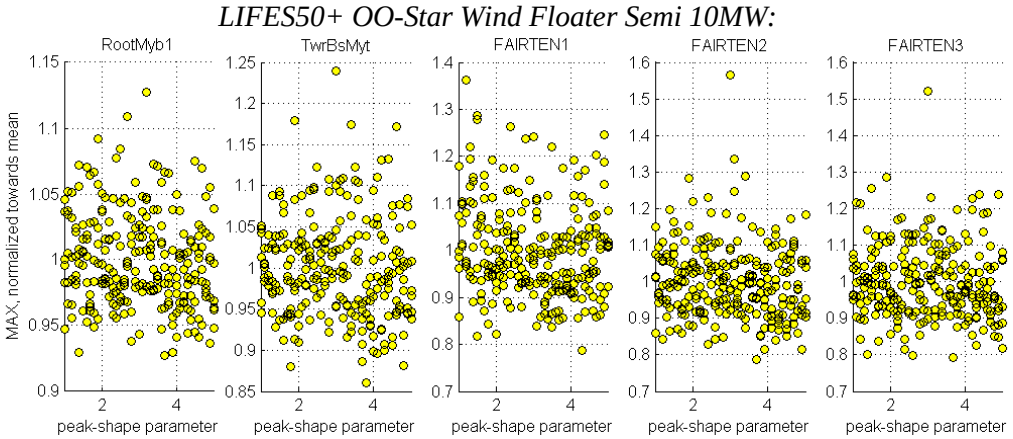

*NAUTILUS-10:*

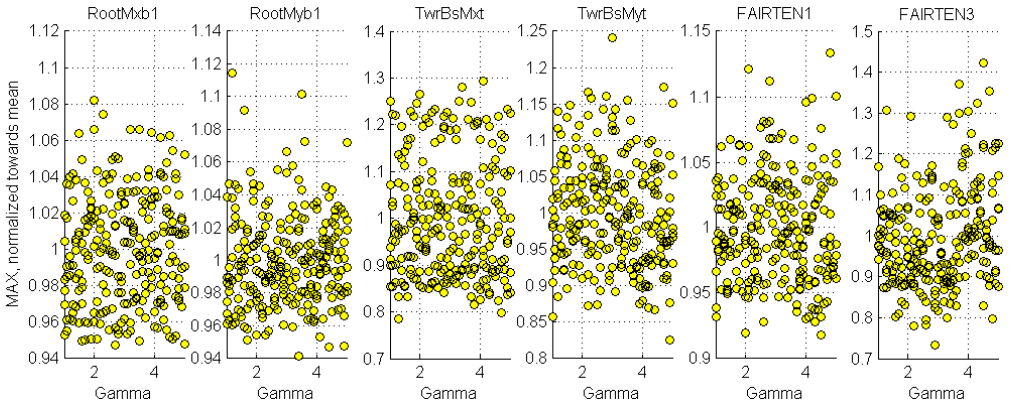


**Figure 5.11: Results of peak shape parameter sensitivity analysis of maximum loads for different load locations for significant wave height of 11.2m and wave period of 7.2s.**

*LIFES50+ OO-Star Wind Floater Semi 10MW:*

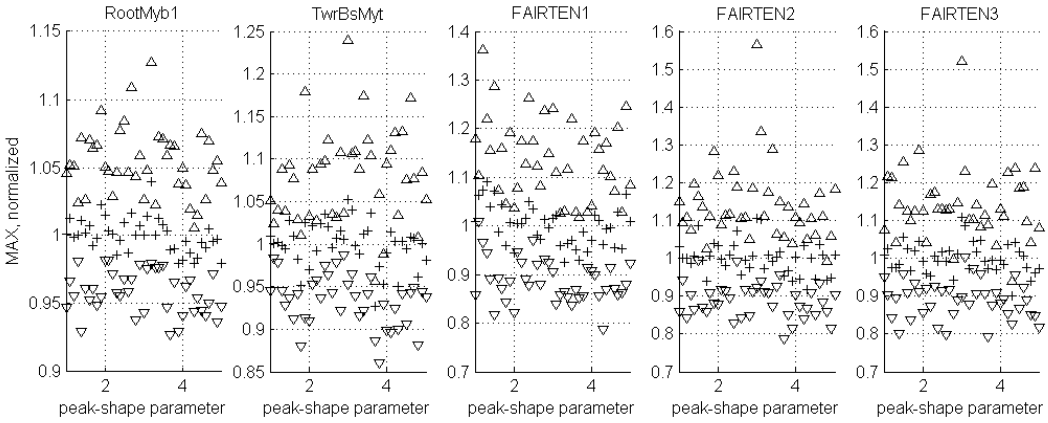


*NAUTILUS-10:*

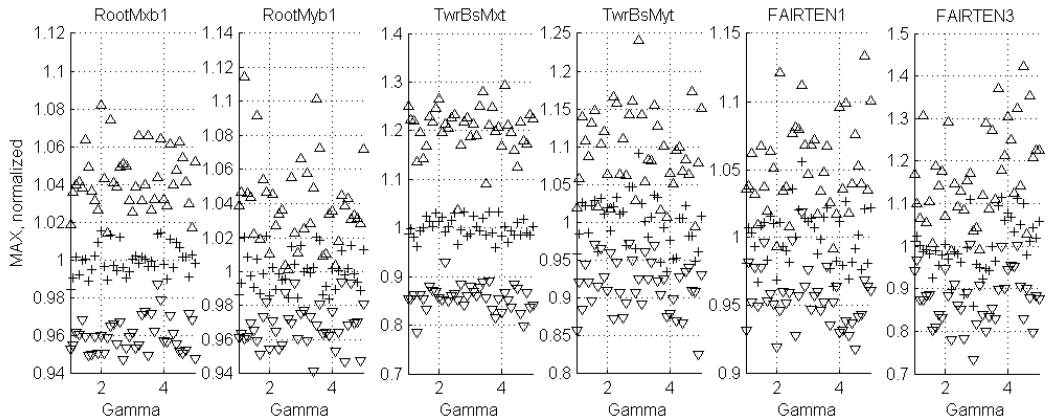


**Figure 5.12: Maximum, Mean and Minimum of the maximum loads from the 6 seeds of peak shape parameter sensitivity analysis for different load locations for significant wave height of 11.2m and wave period of 7.2s.**

After a visual analysis, the results shown in Figure 5.11 and Figure 5.12 show no influence of the peak shape parameter on the maximum loads recorded for both concepts. Here, the inherent uncertainties of the wind and wave environments, and the random nature of their seeds and time series, seem to have a larger effect leading to the randomly distributed maximum loads.

### 5.2.4 DLC 1.6 Marine growth sensitivity

The growth of marine organisms affects all structures installed offshore and causes an increment of loadings due to additional weight, increased diameter and rougher surface (DNV, May 2014). In this section, an overview on marine growth and the existing studies are given. Subsequently, the influence of marine growth on mooring line loading of FOWTs is examined.

The type and intensity of marine growth varies with different factors, such as geological location, water depth, water temperature and season, ocean current, platform design and operation. The most wide-spread classification of marine growth is into hard and soft growth. Mussels, oysters, barnacles and tubeworms are considered hard growth, while soft growth includes seaweeds, soft corals, sponges, anemones and algae. (Msut & Frina, 1996) Examples for marine growth species of the North Sea can be found in (Msut & Frina, 1996) and (Schoefs, 2002). Another, aspects of marine growth are thickness and density of the layer, which are strongly influenced by location, water depth and type of marine growth. The layer is assumed to increase linearly over a period of 2 years until stabilize on a certain value after the structure is placed into the sea (Standards Norway, 2007). Table 5-8 shows established values of marine growth thickness in Norwegian and UK waters.

**Table 5-8: marine growth thickness in Norwegian and UK waters (Standards Norway, 2007)**

| Depth below MWL [m] | Marine growth thickness [mm] | |
|---|---|---|
| | Central and Northern North Sea (56° to 59° N) | Norwegian Sea (59° to 72° N) |
| -2 to 40 | 100 | 60 |
| > 40 | 50 | 30 |

The effects of marine growth on loading of offshore structures are due to the enhancement of structural diameters, force coefficients, hydrodynamic added mass and flow instability, among others (Msut & Frina, 1996). Experiments with smooth cylinders resulted in an increase of diameter and roughening of the surface, in which marine growth thicknesses of 50-100 mm (full scale) and 70 % higher drag coef-ficients are observed (Wolfram & Theophanatos, 1985). While the dynamic response of offshore wind turbine considering marine growth are studied in (Wei, et al., 2012) and (Salvesen Fevåg, 2012).

In (Wei, et al., 2012) the NREL offshore 5MW wind turbine is examined by simulating different cases of marine growth varying the thickness and density of the marine growth layer on the OC4 jacket. More-over, the influence of drag and inertia coefficients are studied. The resulting mass of marine growth in the case of largest thickness and density amounted 9 % of the total wind turbine mass. When considering the individual parameters, the different thickness had strong influence on hydrodynamic loads, but the density less. The natural frequencies showed no dependency on drag coefficient, but the second and third fore-aft and side-to-side natural frequencies are strongly affected by the inertia coefficients. In (Salvesen Fevåg, 2012) the dynamic response of the NOWITECH 10 MW reference turbine with lattice tower is investigated when marine growth is considered. The study concludes that the impact of marine growth on hydrodynamic loads is not negligible and points out a fatigue lifetime reduction from the X-brace of the jacket up to 50% for 0.20 m thick marine growth. Table 5-9 shows the difference between the mentioned studies.

**Table 5-9: Comparison of studies (Wei, et al., 2012) and (Salvesen Fevåg, 2012)**

| Study | Study on the Marine Growth Effect on the Dynamic Response of Offshore Wind Turbines (Wei, et al., 2012) | Influence of marine growth on support structure design for offshore wind turbines (Salvesen Fevåg, 2012) |
|---|---|---|
| Object of study | NREL offshore 5MW | NOWITECH 10 MW |
| Type of tower | Jacket | jacket |
| Program | Bladed V3.85 | Fedem Windpower |
| Simulation time [s] | - | 180 |
| Wind speed [m/s] | 8 | 13 |
| Turbulence intensity [%] | - | 16 |
| Power law exponent [-] | - | 0.14 |
| Wave height [m] | 4 | 4 |
| Wave period [s] | 6 | 9 |
| Current speed [m/s] | 1.5 | |
| Variables | Thickness, Density, Drag coefficient, inertia coefficient | Thickness |
| Thickness [mm] | 0, 50, 100, 150 | 50, 100, 150, 200 |
| Density [kg/m$^3$] | 900, 1100, 1300 | 1300 |
| Drag coefficient | 0.8, 1.0, 1.2 | 1.00 |
| Inertia coefficient | 1.6, 1.8, 2.0 | 2.00 |

The presented studies serve as a starting point to determine the influence of marine growth on the dynamic response of the LIFES50+ OO-Star Wind Floater Semi 10MW. In this case, the submerged members of the wind turbine are parts of the platform and the mooring lines. Before the sensitivity study a rough calculation of the added mass due to marine growth was done for the submerged parts in order to determine the proportion of marine growth weight to the resulting total mass of the component. Therefore, the submerged area of the platform is determined by a computer-aided design (CAD) program and multiplied with thickness and density of the marine growth resulting into the additional mass. To determine the additional marine growth weight on the mooring lines, the thickness is added to the radius and multiplied with the corresponding mass per length. Considering the maximum values of Table 5-8 for thickness and the standard value of 1325 kg/m$^3$ for density (Standards Norway, 2007), the marine growth weight results being 5 % of the resulting total mass of the platform and 17 % of the resulting total mass of mooring lines. As the additional mass due to marine growth on the platform is percentage small the effects on the dynamic response of the WEA are negligible in this study. According to this, the simulation parameters are thickness and density of marine growth, as well as drag and inertia coefficient of the mooring lines. As no site-specific information is available, a wide range of values around the recommended value by standards are used to cover all possibilities. The simulation parameters for the study are given in Table 5-10, which are used for both concepts.

**Table 5-10: Simulation settings for the marine growth sensitivity study**

| Case | Environmental conditions | | Number of simulations [-] | Simulation time [s] |
|---|---|---|---|---|
| DLC 1.6 In-Depth Marine Growth | Wind speed [m/s] | 12 | 1200 | 4200 (3600) |
| | Turbulence Intensity [-] | 0.146 | | |
| | Wind direction [°] | 0 | | |
| | Wave height [m] | 11.4 | | |
| | Wave period [s] | 7.2 | | |
| | Wave direction [°] | 0 | | |
| | Current speed [m/s] | 0 | | |
| | Current direction [°] | 0 | | |
| | Diameter Mooring lines [m] | 0,24675 : 0.44675 | | |
| | Mass per length Mooring lines [kg/m] | 375,38 : 522,44 | | |
| | Drag coefficient | 1.8 : 2.4 | | |
| | Inertia coefficient | 1,6 : 2,0 | | |

The results of the impact of the considered variables are shown in Figure 5.13. It is visible, that the changes in the mooring lines related to marine growth do not have any significant impact on the tower base loads (< 1% for *LIFES50+ OO-Star Wind Floater Semi 10MW* depending on diameter and no significant influence visible for *NAUTILUS-10)*. For the mooring line loads, a significant impact is visible from the increased diameter, leading to a total load increase of over 5% for *LIFES50+ OO-Star Wind Floater Semi 10MW* and even up to 30% for the *NAUTILUS-10* concept. It is also visible that the variation of loading increases with increasing diameter, indicating some higher order dependencies.

*LIFES50+ OO-Star Wind Floater Semi 10MW:*

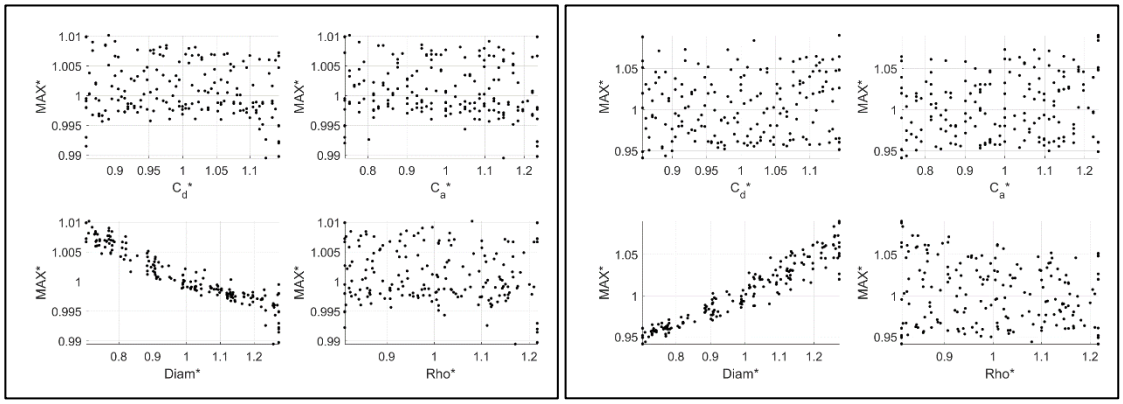


*NAUTILUS-10:*

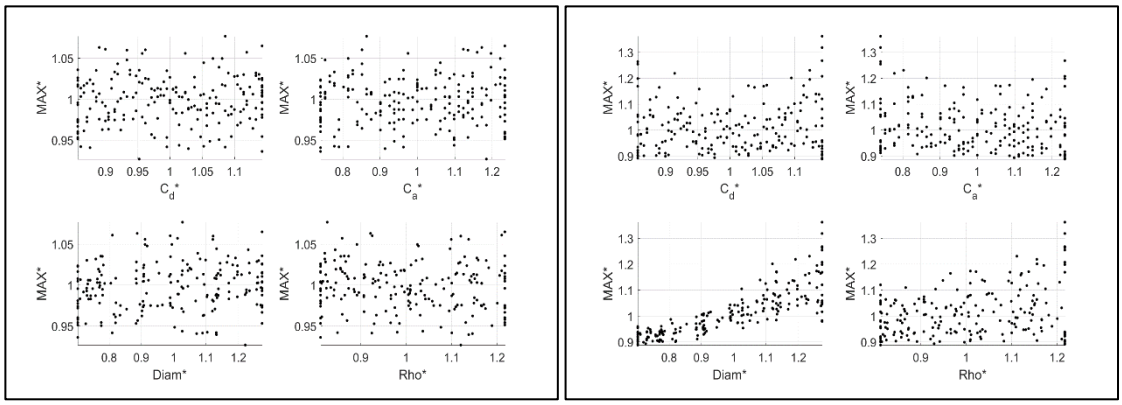


**Figure 5.13: Scatterplots for normalized maximum loads for tower base resulting bending moment (left) and fairlead1 tension (right)**

The second order (i.e. combined effects from two independent variables) impacts can be visualized via contourplots as shown in Figure 5.14. These show that for the *LIFES50+ OO-Star Wind Floater Semi*

*10MW* concept, increased loading is to be expected by a combination of large diameters and low marine growth densities, as well as large diameters and large values for added mass.

Interestingly, even though marine growth leads to larger loading for the *NAUTILUS-10* concept as well, the origin of this increase is somewhat different as well as the overall impact (i.e. note the maximum loading for Nautilus being up to some 115% while it is only 106% for the *LIFES50+ OO-Star Wind Floater Semi 10MW*). For the *NAUTILUS-10*, increased diameters with small added masses and increased marine growth densities lead to increased loading.

*LIFES50+ OO-Star Wind Floater Semi 10MW:*

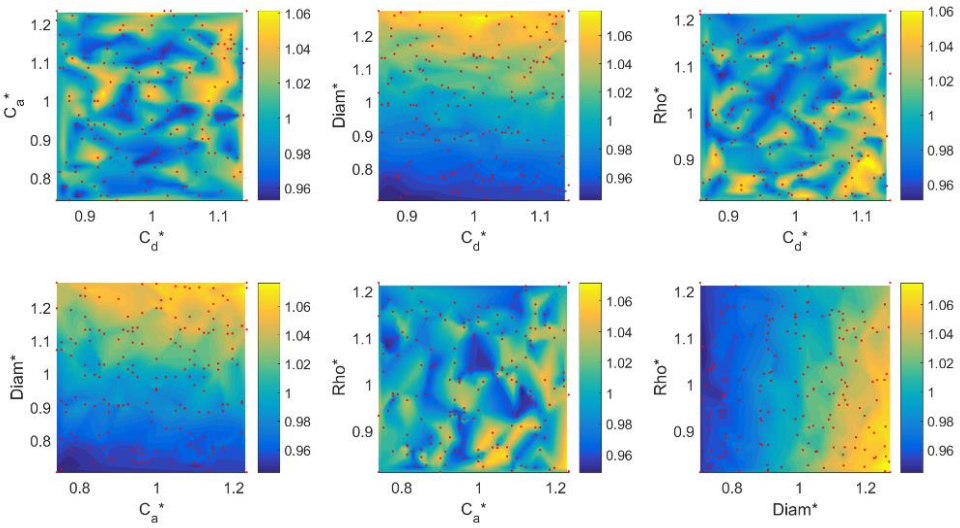


*NAUTILUS-10:*

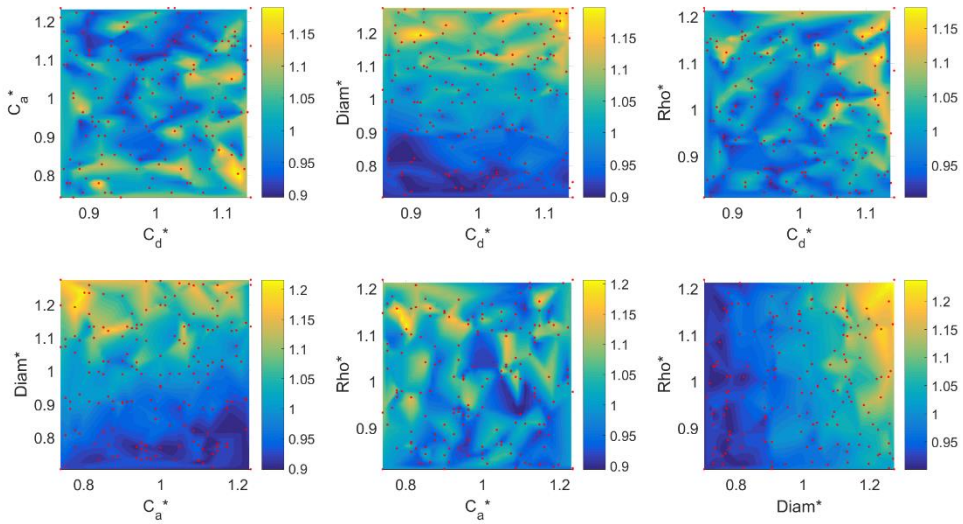


**Figure 5.14: Contourplots for normalized maximum loads for fairlead1. Red dots indicate performed simulations.**

The results show a significant contribution of mooring line marine growth to system dynamics and loading for the mooring lines (up to 30% increased maximum loads for the fairleads). Marine growth is mainly significant due to the added diameter. Adding to the impact of the diameter, interaction effects between increased diameter, marine growth density and added mass that may be concept specific may further increase the loading.

## 5.3 ULS Convergence studies

As both wind and wave environment are stochastic processes, convergence is investigated for a varying number of seeds for three different cases: (1) wind only, (2) wave only (3) wind and wave combined. Blade root flap-wise bending moments (*RootMyb1*), tower base fore-aft bending moment (*TwrBsMyt*) and fairlead 1 (leading fairlead, *FAIRTEN1*) or fairlead 2 (*FAIRTEN2*, one of the leading fairleads for *Nautilus-10*) tension maximum loads were evaluated as part of this study.

One major difference should be taken into account in the approach for the two different concepts regarding the study for DLC 1.6.:

- For the *LIFES50+ OO-Star Wind Floater Semi 10MW*, stochastic environmental conditions are assumed for both wind and wave for all cases under investigation (i.e. for case 1, the same wave seed is used for all simulations and for case 2, the same wind seed is used for all simulations).
- For the *Nautilus-10*, only the environment with varying seeds is stochastic. (i.e. for case 1: still water conditions & stochastic wind, for case 2, stochastic waves & steady wind, for case 3: stochastic wind and wave.)

Note also that due to numerical difficulties and reduced time, the *NAUTILUS-10* platform is not included in the DLC6.1 evaluation.

### 5.3.1 Seed number

For the investigation of necessary seeds, a bootstrap evaluation of the calculated maximum loads (1000 simulations for DLC 1.6 and 750 simulations for DLC 6.1) was performed as described in section 4.3.1. The used environmental conditions for the different cases under consideration are summarized next to the key results in Table 5-11. Note that for DLC 6.1, a new approach was used, using still water / steady wind conditions for the cases in which only one environmental parameter was investigated. The evaluated variable of each sample of seeds was the average maximum load (rather than the maximum of the maximum), to conserve the probability characteristics of the load case.

**Table 5-11: environmental conditions chosen for bootstrap evaluation of ultimate load simulations. Simulation length is 3 hours. 10 minutes are also added for run-in-time. Percentile results give errors towards the reference median of max calculation (MoM) considering all available simulations**

| | | Case 1: change wind seeds only | Case 2: change wave seeds only | Case 3: change wind and wave seeds |
|---|---|---|---|---|
| DLC 1.6 | Wind speed [ms$^{-1}$] | 12 | 12 | 12 |
| | Turbulence intensity[6] [%] | 14.6 | 14.6[7] | 14.6 |
| | Wave height [m] | 11.4[7] | 11.4 | 11.4 |
| | Wave period [s] | 7.2[7] | 7.2 | 7.2 |
| DLC 6.1 | Wind speed [ms$^{-1}$] | 46.2 | 46.2 | 46.2 |
| | Turbulence intensity[2] [%] | 0.11 | Steady wind | 0.11 |
| | Wave height [m] | still water | 11.4 | 11.4 |
| | Wave period [s] | still water | 7.2 | 7.2 |

[6] According to IEC 61400-01 Class C turbulence
[7] Only applied for *LIFES50+ OO-Star Wind Floater Semi 10MW*

Figure 5.15 and Figure 5.16 show the results of the bootstrap study for cases 3 of DLC 1.6 and DLC 6.1 of the *LIFES50+ OO-Star Wind Floater Semi 10MW* concept. Figure 5.17 shows the results of the bootstrap study for cases 3 of DLC 1.6 for the *NAUTILUS-10* concept.

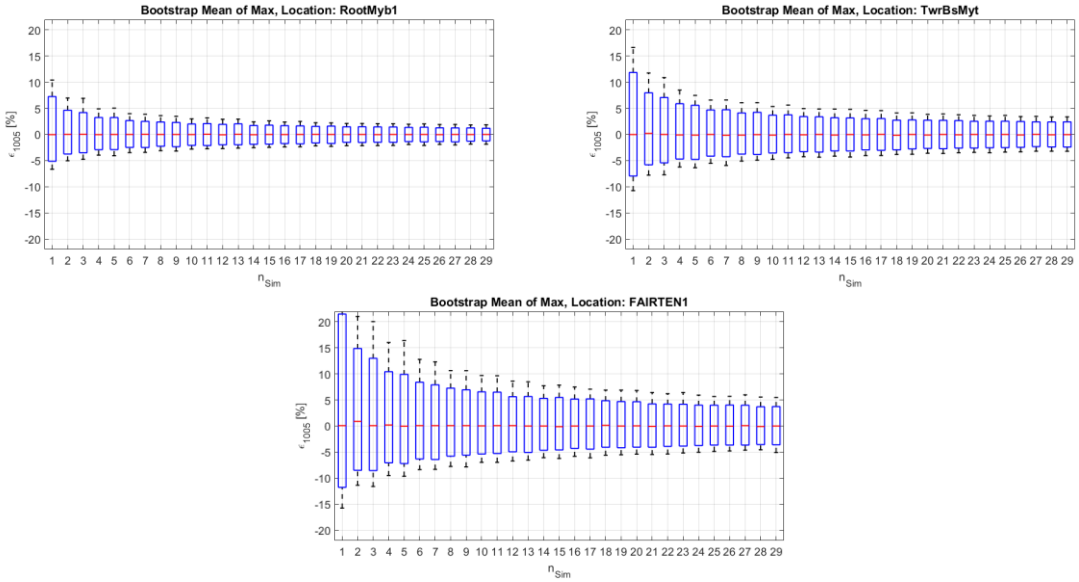


**Figure 5.15: *LIFES50+ OO-Star Wind Floater Semi 10MW* DLC 1.6 ULS bootstrap evaluation case 3 (wind and wave): median values after consideration of $n_{Sim}$ values. Red horizontal lines indicate median, box borders 95th percentile and whiskers 99th percentile values.**

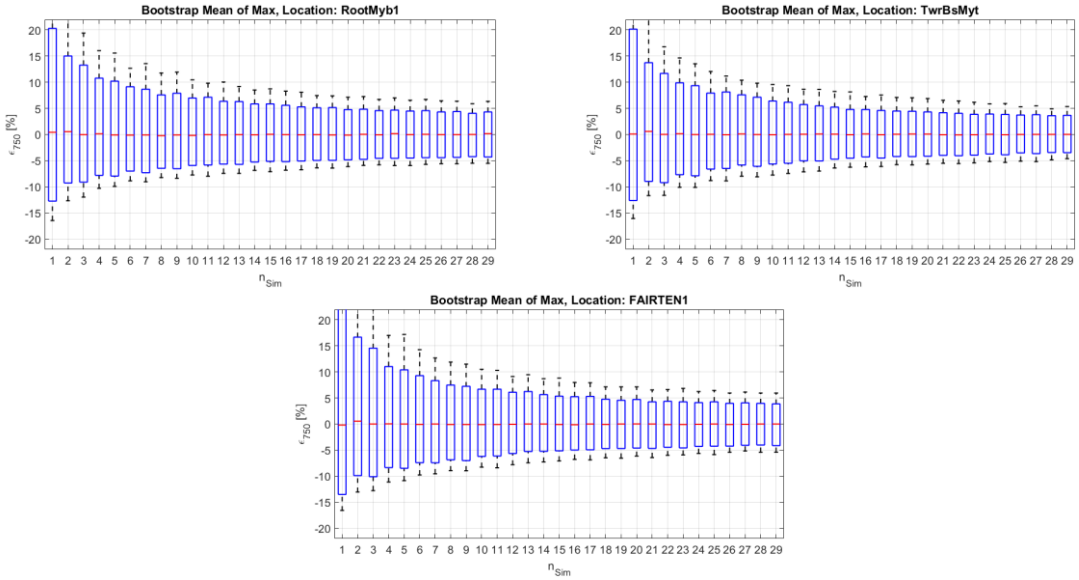


**Figure 5.16: *LIFES50+ OO-Star Wind Floater Semi 10MW* DLC 6.1 ULS bootstrap evaluation case 3 (wind and wave): median values after consideration of $n_{Sim}$ values. Red horizontal lines indicate median, box borders 95th percentile and whiskers 99th percentile values.**

For DLC 1.6 and for both concepts, a larger uncertainty is observed for fairlead tensions than for the other component loads. For DLC 6.1, uncertainties are similar for all component loads. For DLC 6.1 it is also visible how the wind loading predominates the loads of the rotor blades, while the load uncertainty of the other components about equal for wind and wave.

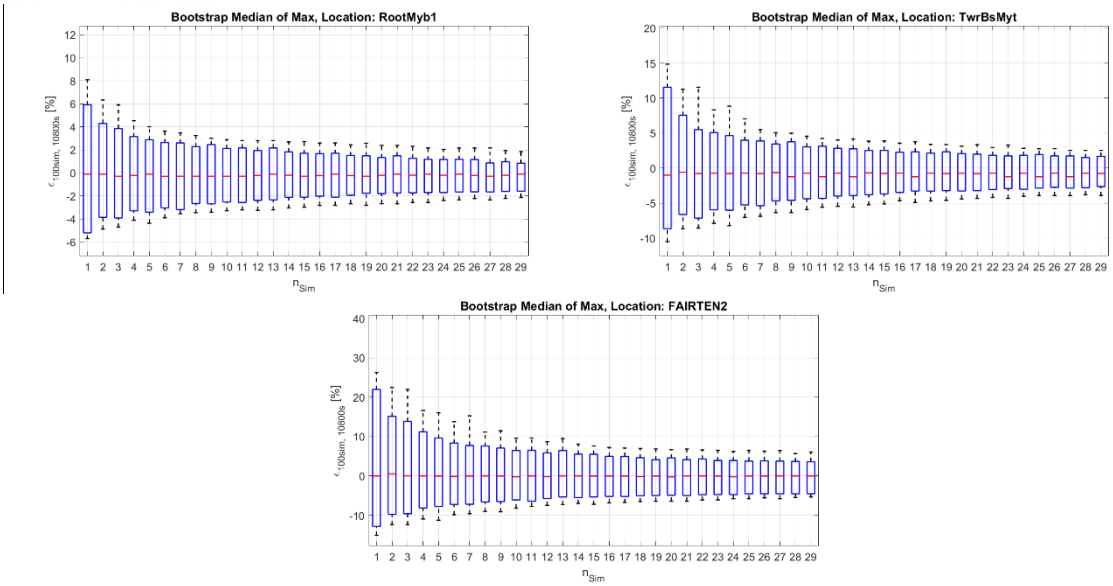


**Figure 5.17: *NAUTILUS-10* DLC 1.6 ULS bootstrap evaluation case 3 (wind and wave): median values after consideration of $n_{Sim}$ values. Red horizontal lines indicate median, box borders 95$^{th}$ percentile and whiskers 99$^{th}$ percentile values.**

### 5.3.2 Simulation length

The obtained time series of the simulations performed in section 5.3.1 were used in a follow-up study to investigate the compromise between simulation length and number of considered seeds. This is not as straightforward for ultimate as for fatigue loads. It must be taken into account that (1) the overall considered time series stays the same for the compared cases and (2) that the number of seeds compared is the same for the compared cases. Otherwise, the obtained (median) maximum will increase for longer time intervals and for larger seed numbers. Taking this into account, the following procedure was applied:

1) Determine the number of "short" seeds that fit into the longest seed for different values of considered simulation time (e.g. 3 seeds of 3600s are equal to 1 seed of 10800s regarding overall simulation time).
2) Subdivide all available seeds of shorter simulation lengths into tuples that resemble the total simulation length (e.g. the first 3 seeds of 3600s length will represent the first tuple with 10800s overall simulation time, and so on).

In the post processing of the simulations, only one value for each time length was used for the calculation of the statistical values of the simulated time series. This means that for the convergence studies, an equal amount of 3600s seeds is available as 10800s. As a result, when the shorter seeds have to be combined, the total number of full-length (10800s) simulations which can be used for the comparison is decreased. For this study, we chose several 100 seeds as the most feasible compromise between the number of available full-length seeds and the considerable simulation times. A larger number of seeds would lead to a decrease of number of considered simulation times (e.g. considering 900s for simulation times requires 36 seeds alone for one realization of 10800s simulation time. As only 1000 seeds are available, this means that for the 10800s case, only 1000/36=27 seeds are available. Hence, 900s were not considered for this study). The use of this limited number of seeds leads to some added uncertainty in the results. Hence, a more comprehensive study in the future would be of interest.

Simulations were performed like section 4.3.2. For brevity, focus of this section is put on the evaluation of combined variation of wind and wave seeds.

**DLC 1.6:** Figure 5.18 shows the 5th and 95th percentiles of the median maximums obtained from bootstrap evaluation (1000 draws) each considering 10800s of simulation time. As mentioned before, seeds with shorter single simulation times than 10800s were collected in tuples with 10800s overall time. Overall the uncertainty of the load response seems to be indifferent to the way seeds are combined, if the overall simulation time stays the same. A slightly larger uncertainty is to be expected for fairlead tension, highlighting the possible importance of longer simulation times for locations that are sensitive towards the wave environment.

*LIFES50+ OO-Star Wind Floater Semi 10MW:* *NAUTILUS-10:*

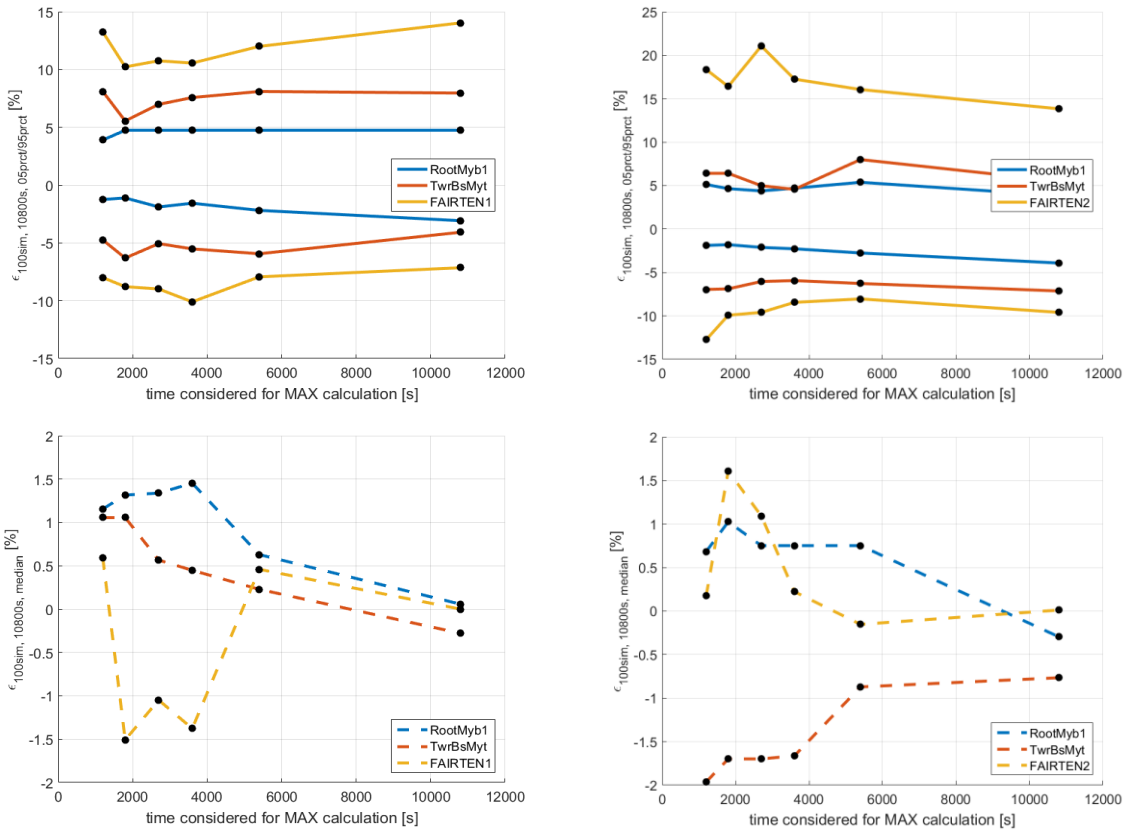


**Figure 5.18: DLC1.6 error plot of median maximum loading for 5th and 95th percentiles for changing wind and wave seeds**

**DLC 6.1:** Figure 5.18 (left) shows the 5th and 95th percentiles of the median maximums obtained from bootstrap evaluation (1000 draws) each considering 10800s of simulation time. As mentioned before, seeds with shorter single simulation times than 10800s were collected in tuples with 10800s overall time. For DLC 6.1 it is clearly visible how the wind environment has a large impact on the blade root loads. Using shorter simulation times automatically leads to a consideration of more wind seeds (since wind fields are implemented periodically in the simulation). Hence, for DLC 6.1 using shorter simulations but a larger number of seeds seems to be the conservative option for blade loads (Note that from this work DLC 6.1 is typically not the load case with the highest loads on the blades, but DLC 1.6 with increased loads by a factor >2). The opposite can be observed for tower base and fairlead loading. There, a general underestimation of the loading is visible for short simulation times. Figure 5.18 (right) shows the median error as a function of increasing simulation length. The median error for tower base and fairlead max loads from short simulation times is around -5%. This may be however within the uncertainty introduced by considering a reduced amount of seeds for increased simulation times.

From the results of this study, the uncertainty of the load response for DLC 1.6 loads seems to be indifferent to the way seeds are combined if the overall simulation time stays the same. A slight increase of uncertainty is visible only for fairlead tension loads, indicating that care should be taken for components strongly influenced by the wave environment. Load uncertainties can be expected the same for all components, while blade loads show overestimation of loading when increasing the number of considered seeds. It is noted that due to insufficient measurement data, the ESS was used for this load case, which is likely producing overly conservative results and may also influence the sensitivities obtained in this work.

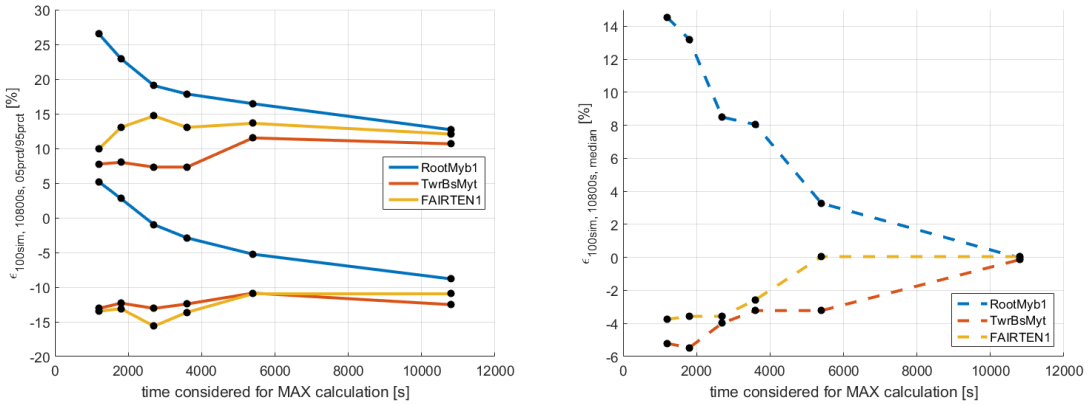


**Figure 5.19: DLC 6.1 error plot for changing wind and wave seeds of median maximum loading for 5th and 95th percentiles (left) and median error (right)**

# 6 LCOE and upscaling considerations

## 6.1 Impact of environmental conditions on LCOE

Due to the direct implications of the environmental loading on the system dimensions, a question that arises is in how far the overall cost of the design are impacted through the LCOE. This interdisciplinary question was addressed in LIFES50+ in an effort to combine the findings from WP2 on LCOE and WP4 on environmental loading. This section summarizes these efforts and provides indication, how a link between environment and LCOE may be drawn. The values presented in this study are strongly indicative, due to the extremely simplified models that are used. The workflow is outlined by three steps:

1) Determine the impact of platform loading on the system cost for a given environment
2) Determine the impact of environmental conditions on the platform loading for a given platform design
3) Determine the overall impact of costs resulting from design variation on the system LCOE

The **Impact of platform loading on the system cost** was investigated as part of (Lemmer, et al., 2016). Figure 6.1 shows the results of a design variation study of the SWE TripleSpar with the platform cost as a dependent variable, depending on the platform geometric variables column radius, distance of columns to platform center, heave plate thickness and heave plate ratio. As can be seen, a simplified linear relationship between variation of the DEL of the platform for the site under investigation and platform costs of can be assumed for simplification which is used in this work as a thumb rule. In this way, the cost increases with 60% of the DEL increase. If we consider that a variation of DEL is linked to a

variation of damage through the S-N-curve exponent $m$, then a damage decrease for a given site by 10% is transferred to a reduction of DEL by roughly 46% (assuming $m = 4$), which leads to an increase of costs of 27%. This means that a damage reduction for a given site through concept variation comes at significant expense (even though the study found that smart optimization may lead to more cost-efficient load reduction, we use here the more simple relationship which assumes that simply increasing the dimensions of the platform will lead to reduced motions and hence reduced damage).

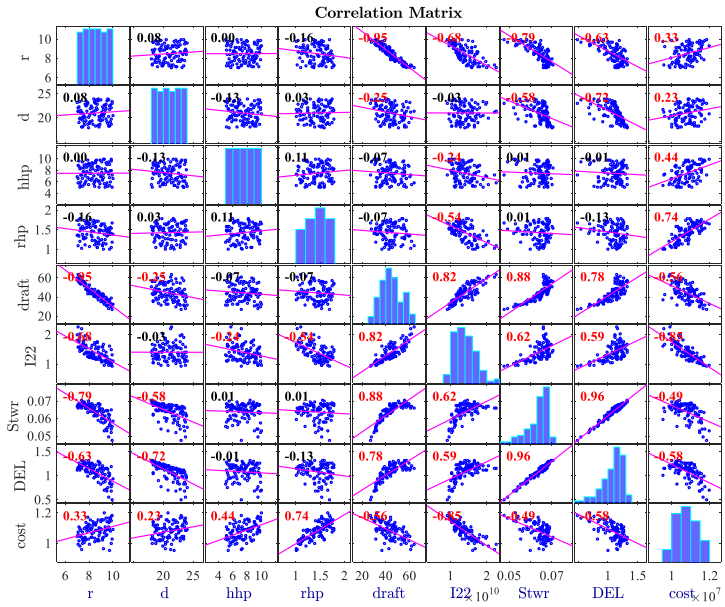


**Figure 6.1: Results from sensitivity study. Correlation matrix of free variables (column radius r, distance from column to platform center d, heave plate thickness h, heave plate ratio rhp) and results (draft, mass moment of inertia I22, standard deviation of tower-top displacement Stwr, DEL of tower-top displacement and cost of platform), (Lemmer, et al., 2016)**

The **impact of environmental conditions on the platform loading for a given platform design** may be investigated based on surrogate models as used in (Müller & Cheng, 2018). A surrogate model may be based on a sensitivity study as performed in e.g. section 4.2 and produces a DEL response for a given combination of environmental conditions. To identify the impact of the environment on the LCOE one may vary the marginal distributions of a given environment (e.g. Gulf of Maine) and determine the increase in lifetime damage based on Monte Carlo simulations (this may be performed fast using the surrogate model). In this study, we tailored the marginal probability distributions of the Gulf of Maine environment, available as Nataf model. Through this, a variation of the mean value for the three environmental variables wind speed, wave height and wave period were possible and the resulting evaluation points could be fed into the surrogate model (here: *LIFES50+ OO-Star Wind Floater Semi 10MW*), leading to a prediction of the lifetime damage equivalent load. Table 6-1 summarizes the performed study. A variation of the mean wind speed has the strongest impact on predicted damage (ca. 30%) followed by mean significant wave height (ca. 10%) and mean wave peak period (1%). Note that these results are based on a surrogate model and not real simulations. Hence, a simulation study is required to confirm these values.

**Table 6-1: Results of Monte Carlo study on the predicted lifetime damage equivalent load for different environments. Evaluations performed using surrogate model resembling tower base fore-aft bending moment DEL response of *LIFES50+ OO-Star Wind Floater Semi 10MW* system for Gulf of Maine and DLC 1.2 under consideration of wind speed, wave height and wave period.**

| | Gulf of Maine | Environment 1 (*10% decreased mean wind speed*) | Environment 2 (*10% decreased mean wave height*) | Environment 3 (*10% decreased mean wave period*) |
|---|---|---|---|---|
| Mean wind speed [$ms^{-1}$] | 7.55 | 6.79 | 7.55 | 7.55 |
| Mean sign. wave height [m] | 1.36 | 1.41 | 1.22 | 1.35 |
| Mean peak period [s] | 6.70 | 6.62[8] | 6.70 | 6.02 |
| Resulting lifetime DEL (Tower base fore-aft bending moment)[9] [kNm] | $4.23 \cdot 10^6$ | $3.95 \cdot 10^6$ | $4.13 \cdot 10^6$ | $4.22 \cdot 10^6$ |
| Resulting decrease in predicted damage[9] | - | 29.2 % | 9.8 % | 1.0 % |

Finally, **the overall impact of costs resulting from variation of the design or environmental conditions on the system LCOE** was investigated in WP2. A floating offshore wind turbine should be designed to withstand even the most extreme environmental conditions at a specific location. However, a more robust design may lead to higher material usage and result in increased manufacturing cost. As Figure 6.3 shows, the manufacturing cost has the highest contribution to the life cycle cost (LCC) of a floating offshore wind farm (FOWF) and the substructure cost represents the second largest portion of the manufacturing cost after the wind turbine. Therefore, a variation of the design and dimensions would have a significant impact on the overall cost of the system.

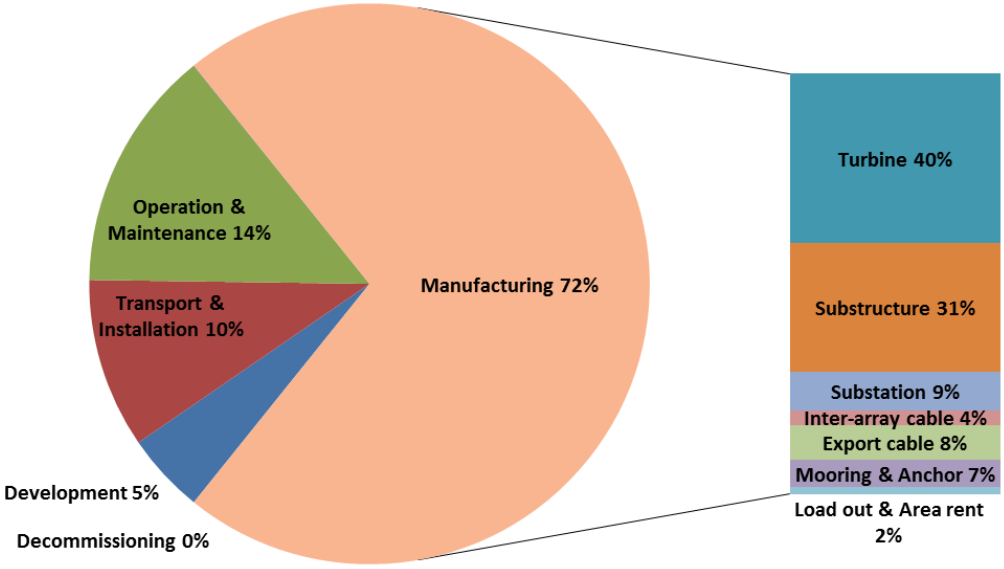


**Figure 6.2: Life cycle cost and manufacturing cost breakdown of a 500MW floating offshore wind farm. Calculation based on mean values of the 4 floating wind turbine designs considered in LIFES50plus.**

[8] Note that as wave height and wave period are correlated to wind speed, some (minor) change of the mean wave parameters is induced by changing the wind environment.
[9] Based on surrogate model. Results need to be verified by simulations.

In the deliverable 7.6 of the LIFES50plus project a sensitivity analysis has been performed on over 325 parameters to determine the ones that most influence the LCOE. Is has been found that, besides financial parameters such as the discount rate, the ones that relate to the manufacturing phase have the largest impact on the LCOE due to the capital-intensive investment required at the beginning of the life cycle. For instance, by increasing the substructure cost by 50% the LCOE increases by more than 15% depending on the type of floating wind turbine studied. In comparison, by changing the manufacturing cost of the mooring lines or inter-array cables by the same rate, the LCOE would only rise by 1.6% or 3.1% respectively. However, it has also been found that the variation of turbine manufacturing cost has a significant influence on the LCOE. For example, by raising the turbine cost by 50% the LCOE increases up to 21% depending on the floating wind turbine concept studied.

The environmental conditions of an offshore site have also a significant impact on the cost of a floating offshore wind farm. Figure 6.3 shows the life cycle cost breakdown of two types of floating wind farms for three different locations.

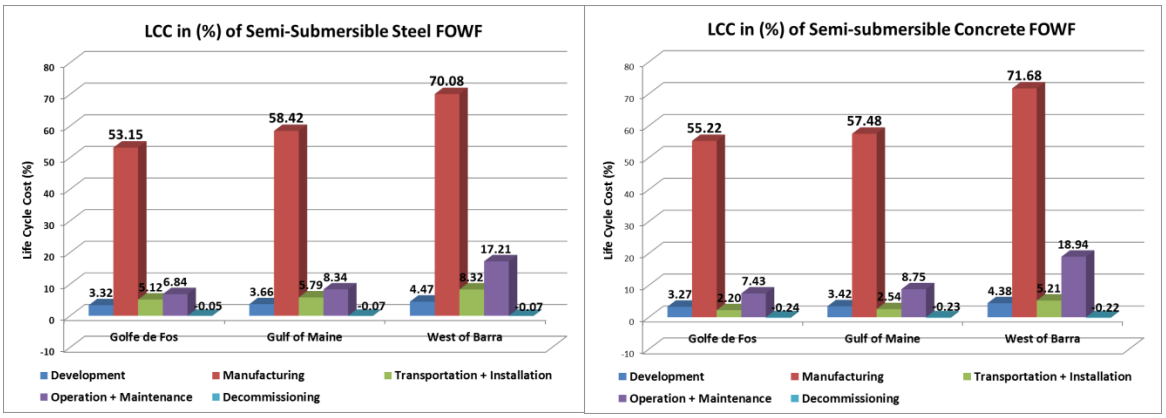


**Figure 6.3: Life cycle cost breakdown for a Semi-Submersible Steel and a Semi-Submersible Concrete Floating Offshore Wind Farm for the offshore locations Golfe de Fos, Gulf of Maine and West of Barra. Total life cycle cost of Golfe de Fos and Gulf of Maine are in proportion to West of Barra.**

The offshore sites represent different met-ocean conditions; namely Golfe de Fos moderate, Gulf of Maine medium and West of Barra severe conditions (Ramachandran, et al., 2017). A significant increase in manufacturing cost is observable for West of Barra, where the harsh environment demands a more robust design of the structures. Besides that, since the seabed at this site is more challenging a different type of anchor is required and depending of the design an increase in the number of mooring lines might be required. This results in higher cost for the anchor and mooring system. However, a large part of the increased manufacturing cost is based on the longer export cable required at this remote offshore site. Finally, the environmental conditions of an offshore site effect also transportation and installation of floating offshore wind turbines since suitable weather windows must be found where operations can be safely executed. This has contributed to higher cost in West of Barra for transportation and installation since the severe conditions at this site restrict operations to certain time intervals.

Summarizing this chapter, it can be said that manufacturing costs have a significant contribution to the overall LCOE of a FOWT system. The manufacturing costs are closely linked the design which is typically important for the resulting loads on the structure. Additionally, the loads on the structure are significantly linked to the conditions experienced at site. Variations of the main properties of the environment may have large impact on the loading which again increases the structural costs. While more detailed investigations are necessary to find more reliable figures in the future, this showcase study showed the usefulness of sensitivity analyses and surrogate models for finding the correct answers.

## 6.2 Upscaling

Considerations linked to upscaling a given substructure are already addressed in previous work WP7 and LIFES50+ (see, e.g. (Müller, et al., 2016) for a high-level overview). Additionally, in WP1, it was also found that scaling of physical properties did not have significant effects on the overall concept design and the design procedure. Furthermore, it was reported that the design driving load cases remained the same as for the same floaters designed to support smaller wind turbines. Items of interest linked to upscaling are in the design of the tower and the water depth (minimum depth required for umbilical & mooring line design), industrialization (manufacturing and logistics for increasing component size), assembly (WT and tower erection), wind farm considerations (turbine spacing, wind farm layout, wake turbulence models, power production) and mooring/umbilical design. These items are seen to be of interest for more detailed research in the future.

# 7 Recommendations

General recommendations for the setup of the critical DLCs are collected here. See also the Conclusions for specific design assumptions

## 7.1 FLS (DLC 1.2)

### 7.1.1 Relevant environmental conditions

The environmental conditions at offshore sites that can have a significant effect on FOWT fatigue loading are generally wind, waves, current and water level. The combinations of variables such as directions and magnitudes will lead to an overwhelming number of simulations to consider and so it is expected that the data is reduced in some way, ideally backed up by sensitivity studies as presented above.

Environmental conditions at site are complex. The values that are expected to be variable for fatigue load cases are:

**Wind**

- Wind speed
- Wind direction
- Turbulence intensity

**Waves**

- Significant wave height
- Period parameter
- Wave direction

**Current** (for both wind driven and tidal)

- Current velocity
- Current direction

**Miscellaneous**

- Water level
- Yaw error
- Control modes (like active ballast on/off)

In general, the environmental aspects can be split into two groups that, for load analysis purposes, can be assumed to be independent from each other. But within each group the relevant interdependencies are important and should be considered at some point in the design process.

**Tidal driven**

- Water level
- Tidal current

**Local wind driven**

- Wind
- Waves
- Wind induced current

Storm surge

To reduce the numerical effort, global sensitivity analysis as applied in this study is a feasible tool to reduce the design space effectively.

### 7.1.2 Simulation settings

#### *7.1.2.1 Run-in-time*

For the observed systems, a run-in-time of 1000s (or 6-8 times longest natural period in this work) is recommended for fatigue load simulations. Run-in-time is expected to be reduced significantly by proper initial conditions. Further research should investigate the effect of ramping up environmental loads, which potentially could further reduce transient effects.

#### *7.1.2.2 Simulation length*

A sensitivity study to determine the sufficient simulation length is recommended. For the tower and RNA components a duration as low as 10 minutes could be sufficient if enough seeds or number of environmental condition bins are considered so that the overall simulation time does not change. For specific floater types 10 minutes simulations in combination with a high number of seeds could be sufficient even for the floater and station keeping system load convergence, as shown in Figure 4.29. Generally, for floater loads and mooring lines, a simulation duration of three hours could potentially be necessary because of the large surge motions are quite slow.

#### *7.1.2.3 Seed number*

To select an appropriate number of seeds for FLS load cases, a convergence study as shown in chapter 4.3.2 should be performed. The analysis shows that a faster convergence of FLS results is achieved when increased the number of seeds rather than an increase of the simulation length. Alternatively, this consideration can be thought of in terms of environmental condition bin size and a convergence study performed using a fixed number of seeds per bin but with reducing bin size. Due to practical limitations in terms of computational capacities, only a limited number of FLS simulations is possible. Therefore, it is recommended to increase the number of environmental bins (reducing bin sizes) to a sufficient level before increasing the number of seeds per bin.

### 7.1.3 Post-processing

It is advised to estimate a higher percentile (e.g. 75$^{th}$ percentile, backed up by bootstrap analysis) for the DEL-response estimation of a given load case when using a small number of seeds. This way, a conservative estimate is ensured. See section 4.3.1.

## 7.2 ULS (DLC 1.6, 6.1)

### 7.2.1 Relevant environmental conditions

#### *7.2.1.1 Load driving environmental parameters*

The following site specific environmental conditions are deemed necessary to be known to define the extreme load cases:

- Normal Sea State (NSS)

Normally, there is a range of wave periods associated with a pre-defined wave height. For load cases with NSS of bottom fixed structures, it might be acceptable that for a set of wind speeds and wave heights, a value of wave periods is considered. For FOWT, the responses might be sensible to wave periods. Therefore, a range of wave periods derived from the scatter diagram shall be considered. Any peak period, which is close to any eigenfrequencies of the system shall also be considered. For the current, a conservative value of current speed can be assumed.

- Extreme Sea State (ESS) and Severe Sea State (SSS)

For ESS and SSS, all the points on the environmental contour of (wave height, wave period) shall be considered including small and concept specific wave periods and not just the largest wave heights and associated wave periods as shown in Figure 5.10.

For SSS, the sea state is conditioned on an operational wind speed. If sufficient information is not available, ESS parameters can be used as a guidance.

50-year return current speed can be assumed as conservative assumption.

Another relevant environmental effect is marine growth on the station keeping system e.g. on mooring lines and catenaries. Marine growth could have significant effect on loading due to the enhancement of structural diameters, force coefficients, hydrodynamic added mass and flow instability, see section 5.2.4

### 7.2.2 Simulation settings

#### *7.2.2.1 Run-in-time*

For the observed systems and model fidelities used in this study, a run-in-time of 1000s is recommended for extreme load simulations. Run-in-time may be reduced significantly by proper initial conditions. Further research should also investigate the effect of ramping up environmental loads, which potentially could further reduce the scale of transient effects.

#### *7.2.2.2 Simulation length*

For design of the RNA components and tower, it may for some structures be sufficient with simulation duration of 10 minutes. However, the applicability of the selected duration should be documented by sensitivity studies.

For floater and station keeping design typically longer simulation time than 10 minutes are necessary to enable the full frequency range and maximum wave heights of the applied sea state spectrum within the simulation time. Contrarily, the findings in this study shows that shorter simulation times than e.g. 3 hours may be possible, if the overall simulation time is held the same, see e.g. Figure 5.18. However, in case no sensitivity study is present a minimum duration of three hours is recommended.

For transient cases (emergency shutdowns, etc.) sufficient simulation length should be given to allow for a full decay of the triggered motions. The duration is strongly depending on natural periods and the damping of floater. For catenary and rope mooring systems, it is recommended to apply at least 600-second total simulation time for transient load cases.

#### 7.2.2.3 Seed number

The number of seeds for ULS cases should be high enough to sufficiently well estimate the sought characteristic values. This depends on the sensitivity to the random variables that are varying with each seed, as well as the simulation length. The number of seeds could therefore be set based on a sensitivity study as shown in chapter 5.3.1. A simplification of the sensitivity study could be to use the minimum number of seeds as suggested by the standards and then compare the results with those obtained using the double number of seeds. For example, if 6 seeds are required, then simulating an additional 6 seeds will result in a total of 12 seeds. If there is no significant difference in the estimated characteristic values, then it may be assumed that 6 seeds are sufficient.

# 8 Conclusions and Outlook

The sensitivity studies on several floater types performed within this report demonstrate consistently that the load simulation of FOWT today is far away from a standardised and uniform process. The manifold site specific environmental conditions and the differences in floater and station keeping design concepts require an individual analysis of each concept and a careful load case setup in order to meet the FOWT concept peculiarities. This leads to comprehensive statistical considerations with high computational efforts in terms of data volume and calculation time. The convergence studies performed for FLS and ULS simulations, see chapter 4.3 and 5.3, point out that for achieving an accuracy of +-5% in the final load result requires a remarkable amount of simulations is needed. Some of the concise results are:

- 500 to 1000 seconds run-in-time in advance of every load case to exclude transient effects (initial operational parameters already predefined, otherwise 2000 s might be required)
- 3 hours simulation time for all components with significant impact of sea states to design loads or split of the 3 hours into shorter simulation packages with different seeds.
- 24 wind-wave misalignment combinations at least in case of sensitivity of the floater type to directionality
- Resolution of the environment:
    - Wind speed: 2.0 m/s wind bin size at least, additionally include controller-specific wind speeds
    - Wave height: 1.5 m wave height bin at least
    - Wave period: 2.0 s wave period bin at least
- The full spectrum of wave periods of each wave height bin to be considered with special focus on interaction with low frequency floater motions

On the other hand, some potentials for reducing load case variations could be identified within this study;

- For calculation of RNA loads on FOWT 10 minutes simulation time appears sufficient
- For known floater behaviour regarding wind waves directionality a reduced setup could be the conservative application of unidirectional wind and waves, 180° misalignment or design specific misalignments such as 60 or 90°.
- The influence of the variation of the wave peak shape factor to final load results is marginal

- For determining ULS idling wind speed variations a coarse resolution is possible (i.e. to consider only minimum and maximum wind speed)

In summary, this study underlines the need of understanding the characteristic system behaviour of a FOWT design concept in question and to configure the integrated load simulation setup accordingly. A complete load setup for a FOWT according to one of the referenced certification standards requires at least the double amount of load case variations than for of a comparable sized bottom fixed offshore wind turbine. A reduction of load cases and parameter variations are only possible when detailed knowledge about the dynamic interaction of the floater type with environmental conditions is present. A known sensitivity for instance regarding specific, critical wave periods or wind wave misalignment angles could reduce the load setup significantly.

Further comparisons and code validations against measurements from full scale FOWT are necessary in order to increase confident level and accuracy of current load calculation procedures. Real life operational experiences from demonstrator projects and semi commercial floating wind farms will provide valuable inside into the relevant load aspects of FOWT. In the near future, a few floater designs concepts will turn out as the most reliable and cost-effective concepts and reduce the diversity of today's floating concepts. The alignment of load simulation procedures with the gained experiences in operating of full scale FOWT's will support the reduction of load simulations effort significantly and in line with that the overall LCOE of floating wind.

Some improvements to the applied methodologies are possible in the future:

- For the **assessment of initial transient effects**, an additional comparison to frequency domain simulations may be helpful. Also, the evaluation would better be based on the averaged results of different seeds rather than on an auto-comparison (i.e. reference value from same time series rather than averaged over all simulations).
- For the **simulation length assessment**, simulations should not be cut after a given time but rather be simulated for different times. This way, the stochastic time series for wind and waves are tailored towards the correct simulation length and relevant frequencies are included. Also, for the ultimate loads, only 100 seeds could be used for the longest simulation time. There, a more extensive simulation study could help to obtain more robust results. The inclusion of second order hydrodynamics and forces for both platforms and a flexible support structure would help to make the evaluation more complete (i.e. longer periods may then have a larger impact than in this study)
- For the **sensitivity analysis**, the effect of further environmental conditions could be considered (in the wind regime) next to a convergence analysis of the sensitivity measures. Also, the impact of further load cases could be of interest (e.g. mooring line failure). An additional finding was the impact of the controller, which is assumed constant in this study, but could be varied next to other significant design parameters.
- The **number of considered load cases** in this study have been limited to three basic load case definitions (DLC 1.2, 1.6 and 6.1). Transient load cases between intact and redundancy condition, e.g. loss of mooring line or leakage, as suggested by several standards for FOWT could be included in future investigations.
- Beside the semi-submersible floater design concept there are spar buoy, barge or tension leg platform designs on the market. These **different floater concepts** and their characteristic influence on design loads would be interesting to evaluate in future studies.
- In this study the turbine controller of the 10 MW reference wind turbine applied for the two semi-submersible simulation models has been tuned to a preliminary design stage. **Advanced,**

**integrated controller design for FOWT** might reduce FLS and ULS loading significantly e.g. by applying active damping to characteristic motion modes. The impact and comparison of specific FOWT control features will be a relevant question for future FOWT developments.

- The **FLS blade root loads** have been evaluated with an S/N curve inclination of m=4 because of simulation and post-processing efficiency reasons. An additional FLS post-processing routine with m=10 is recommended for following analysis.
- The study revealed a sensitivity of the station keeping system (here multiple mooring lines) to specific wave periods. This effect should be highlighted in future studies in more detail.
- The application of DELs in this report is purely for academic and for comparative purposes. For a detailed fatigue damage assessment, the use of stress time series at specific details is proposed in combination with rainflow counting, appropriate concentration factors and safety factors. For mooring lines, the mean loading may also be of influence for the fatigue loading.
- With respect to the **FLS bootstrap studies,** the evaluation is only a small view on a much larger problem. For a full picture, the evaluation needs to take into account the full range of environmental variables which have a significant influence on the FOWT loads. Also, different system characteristics and their influence on the uncertainty of fatigue loading need to be studied (different substructures, turbines, controllers, mooring systems, etc.). Focus has been given here on settings which were considered to give conservative estimated loads and load variation for the tower base fore-aft bending moment. For this component, the obtained results should be applicable in a conservative way for other environmental events as well. For other components, a different combination of environmental parameters may lead to increased uncertainties. Questions to be addressed in future studies are the impact of varying absolute values in the normalization procedure (i.e. if smaller DELs are observed, the uncertainty resulting from an offset may be considered much larger due to normalization than for larger DELs), as well as the influence of simulation length with each varying number of considered seeds.

# 9 Dissemination activities

The results presented in this document have been included in the following publications:

- Müller, Cheng, 2018. *Application of a Monte Carlo procedure for probabilistic fatigue design of floating offshore wind turbines*, Wind Energ. Sci., 3, 149–162, 2018, https://doi.org/10.5194/wes-3-149-2018
- Faerron Guzmán, Müller, Vita, Cheng. *Simulation requirements and relevant load conditions in the design of floating offshore wind turbines*, Proceedings of the 37th International Conference on Ocean, Offshore & Arctic Engineering OMAE, June 2018, Madrid, Spain.
- Müller, Cheng. *A surrogate modelling approach for fatigue damage assessment of floating wind turbines*, Proceedings of the 37th International Conference on Ocean, Offshore & Arctic Engineering OMAE, June 2018, Madrid, Spain.
- Müller, Faerron Guzmán, Cheng, Galván, Sánchez Lara, Rodríguez Arias, Manjock. *Load Sensitivity analysis for a floating wind turbine on a steel semi-submersible substructure*, Proceedings of the 1st International Offshore Wind Technical Conference, IOWTC, November 2018, San Francisco, USA, *under review*

# 10 Bibliography

Bachynski, E. E., Kvittem, M. I., Luan, C. & Moan, T., 2014. Wind-Wave Misalignment Effects on Floating Wind Turbines: Motions and Tower Load Effects. *Journal of Offshore Mechanics and Arctic Engineering*, November, 136(4).

Bak, C., 2013. *Description of the DTU 10 MW reference wind turbine,* s.l.: DTU Wind Energy, DTU Wind Energy Frederiksborgvej 399 4000 Roskilde, Denmark, I–0092.

Bak, C. et al., 2013. *Description of the DTU 10 MW Reference Wind Turbine,* s.l.: DTU Wind Energy.

Barj, L. et al., 2014. *Wind/Wave Misalignment in the Loads Analysis of a Floating Offshore Wind Turbine.* s.l., s.n.

Borg, M. et al., 2018. Models for advanced load effects and loads at component level. *LIFES50+ Deliverable 4.7*, May.

Det Norske Veritas AS, 2011. Modelling and Analysis of Marine Operations. *DNV-RP-H103*, April.

DNV GL AS, 2016. Loads and site conditions for wind turbines. *DNVGL-ST-0437*, November.

DNV, May 2014. *Design of Offshore Wind Turbine Structures,* s.l.: s.n.

DNV-OS-J103; DNVGL-ST-0119, 2013. *Design of Floating Wind Turbine.* s.l.:Det Norske Veritas AS.

DNV-OS-J103, 2013. Design of Floating Wind Turbine Structures. *DNV-OS-J103*.

DNV-OS-J103 & DNVGL-ST-0119, 2013 & 2018. *Design of floating wind turbine structures,* s.l.: s.n.

Frias Calvo, J., 2017. *Response analysis of an offshore floating 10MW wind turbine support structure, M.Sc. thesis*, Kgs. Lyngby, Denmark: DTU Wind Energy M-0184.

Haid, L. et al., 2013. *Simulation-Length Requirements in the Loads Analysis of Offshore Floating Wind Turbines.* Nantes, s.n.

Hall, M., 2017. *MoorDyn User's Guide.* University of Prince Edward Island: School of Sustainable Design Engineering, University of Prince Edward Island.

Hansen, M. & Henriksen, L., 2013. *Basic DTU Wind Energy controller*, s.l.: DTU, Department of Wind Energy, DTU, Denmark, E-0028.

IEC/TS 61400-3-2 Ed.1.0 Wind turbines, n.d. *Part 3-2: Design requirements for floating offshore wind turbines,* s.l.: s.n.

International Electrical Commision, 2009. *IEC 61400 - Part 3: Design requirements for offshore wind turbines.* s.l.:International Electrical Commision.

International Electrotechnical Commission , 2009. Wind Turbines - Part 3: Design Requirements for Offshore Wind Turbines. *61400-03.*

Jonkman , B., 2009. *TurbSim User's Guide: Version 1.50..* NREL: Golden, CO.: NREL/EL-500-46198..

Jonkman, J., 2007. *Dynamics Modeling and Loads Analysis of an Offshore Floating Wind Turbine..* NREL/TP-500-41958: NREL: Golden, CO..

Jonkman, J. & Buhl, M., 2005. *FAST User's Guide..* NREL: Golden, CO..: NREL/EL-500-38230..

Jonkman, J., n.d. *Overview of the ElastoDyn structural-dynamics module, NREL Wind turbine modelling workshop, Bergen, Norway, 11-sep-2014.,* s.l.: s.n.

Kim, T. H. A. B. K., 2013. Development of an anisotropic beam finite element for composite wind turbine blades in multibody system. *Renewable Energy*, Volume 59, pp. 172-183.

Krieger, A. et al., 2015. *LIFES50+ D7.2 Design Basis*, s.l.: s.n.

Kvittem, M. I. & Moan, T., 2015. Time domain analysis procedures for fatigue assessment of a semi-submersible wind turbine. *Marine Structures*, Issue 40, pp. 38-59.

Laino, D. & Hansen, A., 2002. *AeroDyn user's guide version 12.50,* s.l.: s.n.

Larsen, T. M. H. L. G. H. K., 2013. Validation of the dynamic wake meander model for loads and power production in the Egmond aan Zee wind farm. *Wind Energy*, Volume 16, pp. 605-624.

Lemmer, F. et al., 2016. Optimization framework and methodology for optimized floater design. *LIFES50+ Deliverable 4.3*.

Msut, I. J. & Frina, J. W., 1996. Effect of Marine Growth and hydrodynamic loading on offshore structures. *Jurnal Mekanikal*, pp. Vol. 1, No. 1, pp. 77-96.

Müller, K. & Cheng, P. W., 2016. Validation of uncertainty in IEC damage calculations based on measurements from alpha ventus. *13th Deep Sea Offshore Wind R&D Conference, EERA DeepWind*.

Müller, K. & Cheng, P. W., 2017. Application of a Monte Carlo Procedure for Probabilistic Fatigue Design of Floating Offshore Wind Turbines, under review. *Wind Energy Science*.

Müller, K. & Cheng, P. W., 2018. A Surrogate Modeling Approach for Fatigue Damage Assessment of Floating Wind Turbines. *Proceedings of the 37th International Conference on Ocean, Offshore & Arctic Engineering*, June.

Müller, K. et al., 2018. Load Sensitivity Analysis for a Floating Wind Turbine on a Steel Semi-Submersible Substructure. *Proceedings of the 1st International Offshore Wind Technical Conference IOWTC2018*, November.

Müller, K. et al., 2016. LIFES50+ D7.5 Guidance on platform and mooring line selection installation and marine operation. *Project Report*, August.

Natarajan, A. H. M. W. S., 2016. *Design load basis for offshore wind turbines,* Roskilde, Denmark: DTU Wind Energy Report E-0133.

Olsen, O., n.d. *OO-Star Wind Floater.* [Online] Available at: http://www.olavolsen.no/nb/node/149 [Accessed 09 05 2017].

Pegalajar-Jurado, A., J., M. F., Borg, M. & Bredmose, H., 2018. *State-of-the-art models for the two LIFES50+ 10MW floater concepts,* Kgs. Lyngby, Denmark: LIFES50+ Deliverable 4.5, DTU Wind Energy.

Ramachandran, G. K. V., Vita, L., Krieger, A. & Mueller, K., 2017. *Design basis for the Feasibility evaluation of Four Different Floater Designs.* s.l., s.n.

Ramachandran, G. K. V. et al., 2016. *LIFES50+ Deliverable D7.2: Design Basis*, s.l.: s.n.

Saltelli, A., Chan, K. & Scott, E. M., 2000. *Sensitivity analysis.* s.l.:Wiley New York.

Salvesen Fevåg, L., 2012. *Influence of marine growth on support structure design for offshore wind turbines,* s.l.: s.n.

Schoefs, F., 2002. *Sensitivity and Uncertainty Studies for the Modelling of Marine Growth Effect on Offshore Structures Loading.* Oslo, s.n.

Söker, H., Kauffeld, N., Kensche, C. & Krause, O., 2004. *Introducing Low Cycle Fatigue in IEC Standard Range Pair Spectra.* s.l., Proceedings DEWEK .

Standards Norway, 2007. Actions and action effects. *NORSOK STANDARD N-003*.

Stewart, G., 2016. *Design Load Analysis of Two Floating Offshore Wind Trubine Concepts.* University of Massachusetts - Amherst: Doctoral Dissertations.

Stewart, G. et al., 2013. *Assessing fatigue and ultimate load uncertainty in floating offshore wind turbines due to varying simulation length.* s.l., s.n.

Wei, S. et al., 2012. Study on the marine growth effect on the dynamic response of offshore wind turbines. *International Journal of precision engineering and manufacturing*, July, pp. Vol.13, No.7, pp. 1167-1176.

Wolfram, J. & Theophanatos, A., 1985. *The effects of marine fouling on the fluid loading of cylinders: some experimental results.* s.l., s.n.

Yu, W., Müller, K. & Lemmer, F., 2018. *LIFES50+ Deliverable D4.2: Public Definition of the Two LIFES50+ 10MW Floater Concepts,* s.l.: s.n.

Yu, W. et al., 2018. Public Definition of the Two LIFES50+ 10MW Floater Concepts. *LIFES50+ Deliverable 4.2*.

# 11 Appendix

## 11.1 Scatter plots for Olav Olsen 7D sensitivity study for DLC 1.2

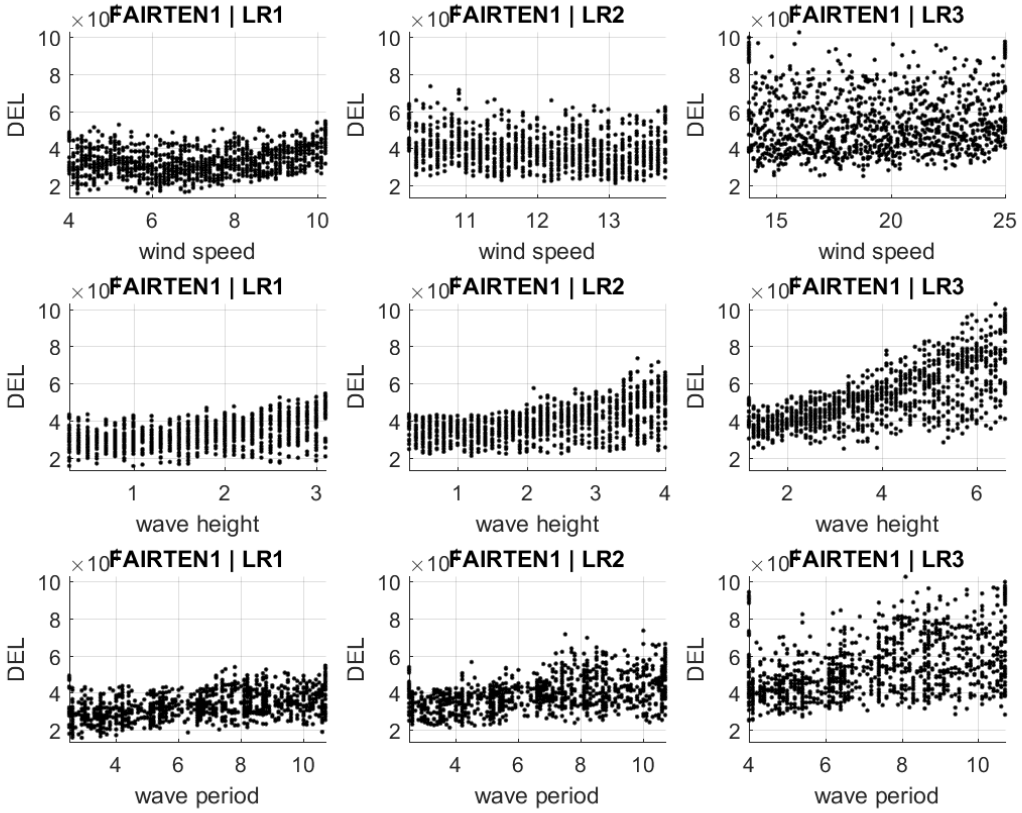

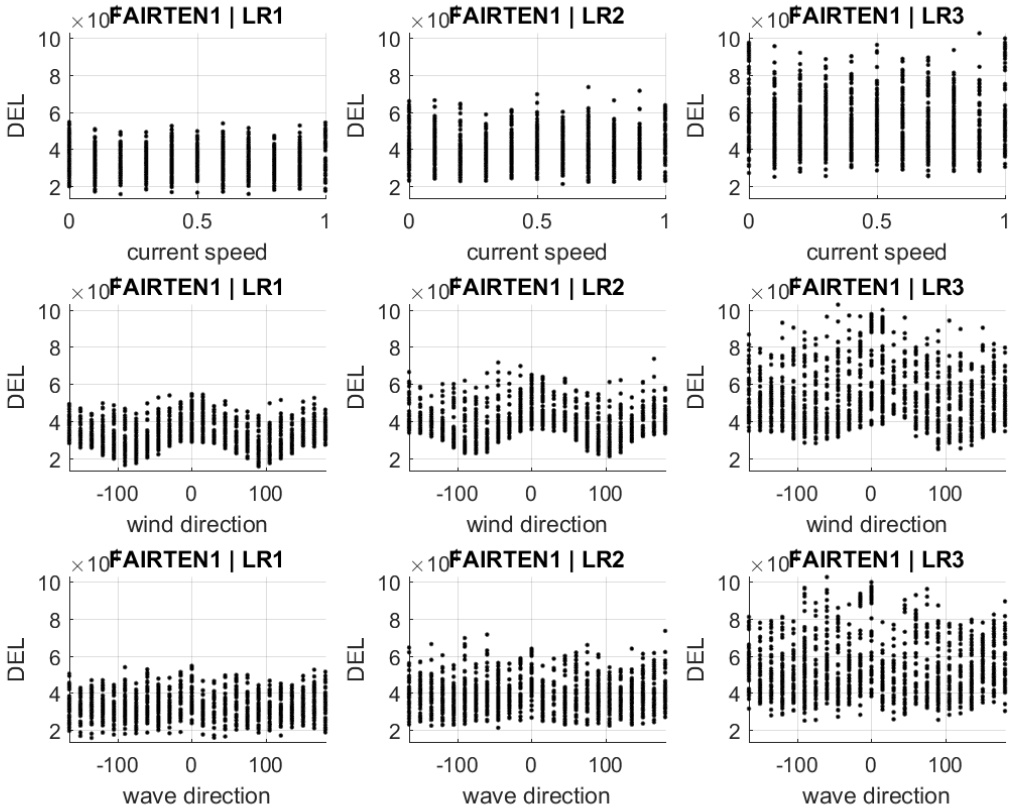
FAIRTEN1 | LR1
FAIRTEN1 | LR2
FAIRTEN1 | LR3
DEL
current speed
wind direction
wave direction

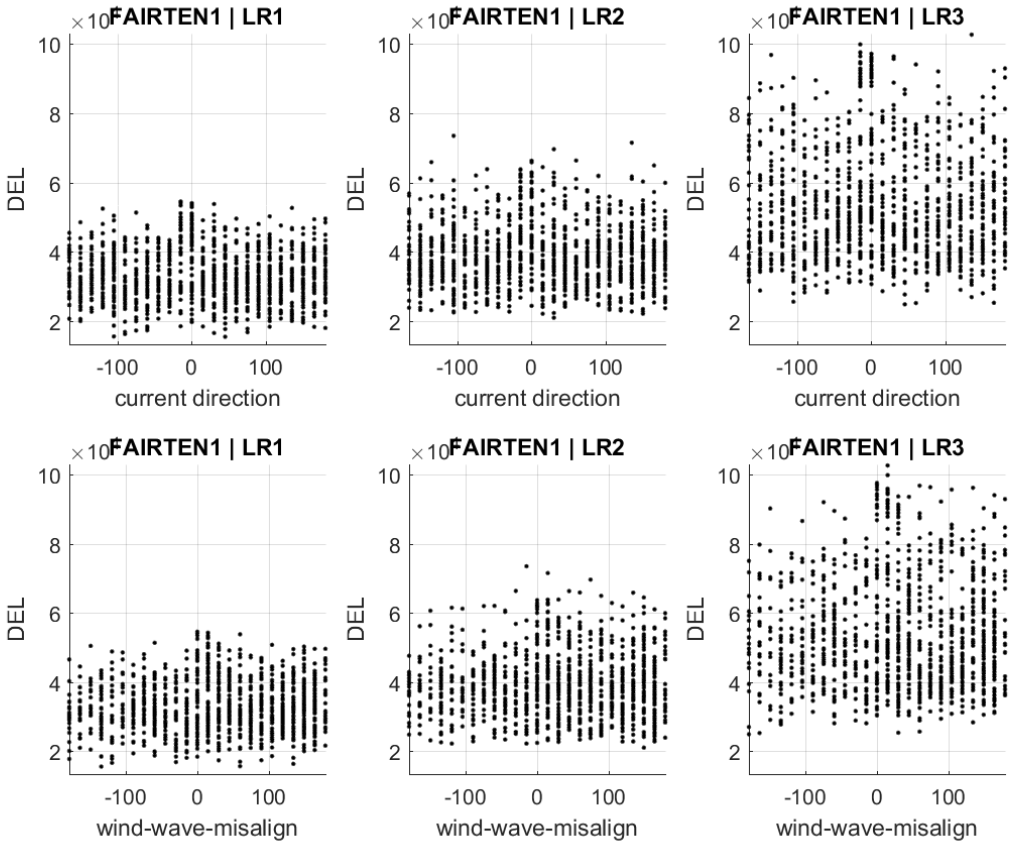
FAIRTEN1 | LR1
FAIRTEN1 | LR2
FAIRTEN1 | LR3
DEL
current direction
wind-wave-misalign

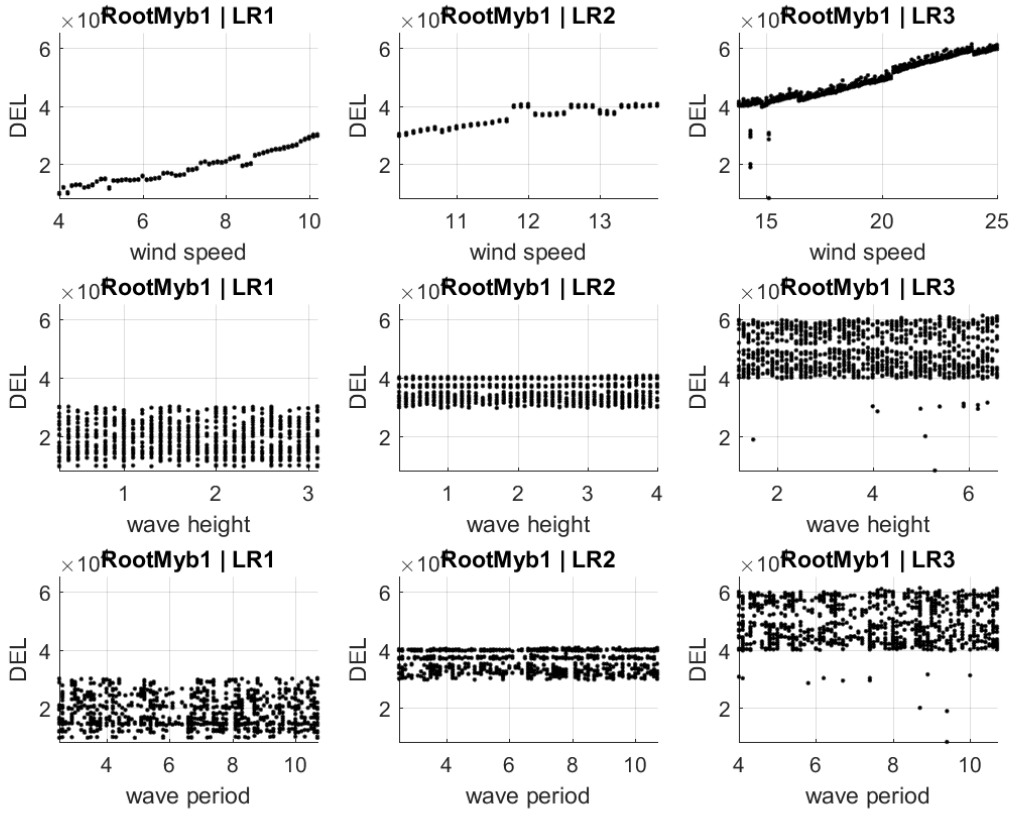
×10 RootMyb1 | LR1
×10 RootMyb1 | LR2
×10 RootMyb1 | LR3
DEL
wind speed
wave height
wave period

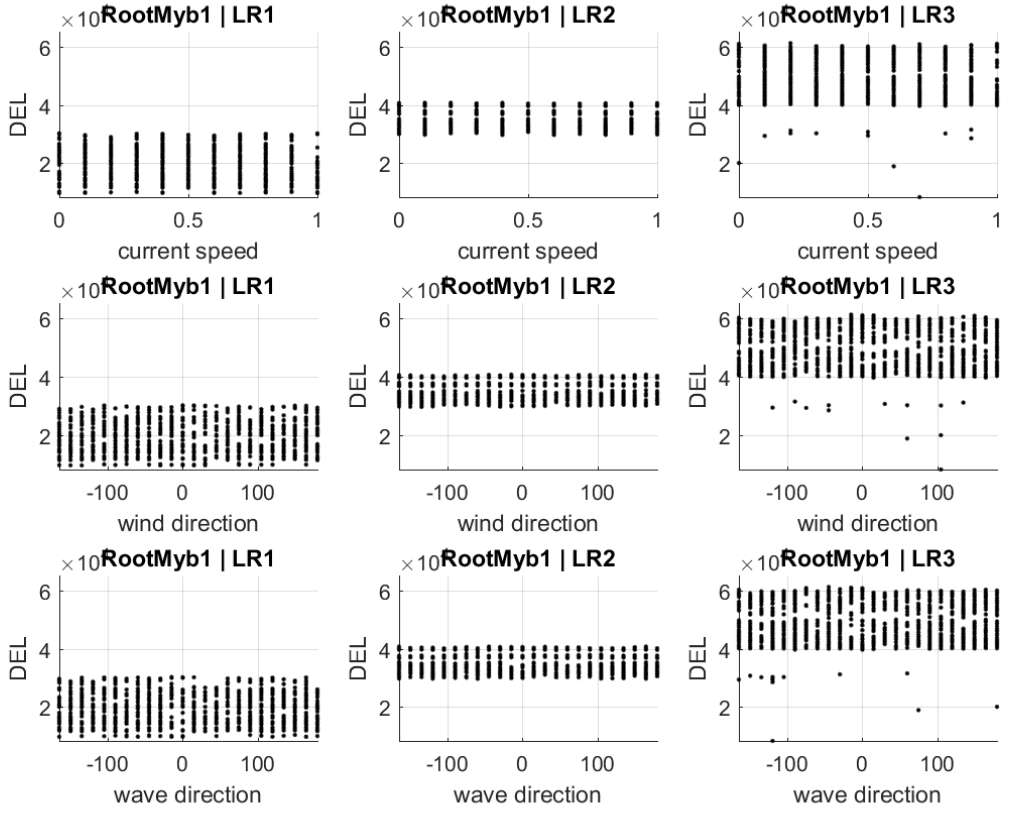
×10 RootMyb1 | LR1
×10 RootMyb1 | LR2
×10 RootMyb1 | LR3
DEL
current speed
wind direction
wave direction

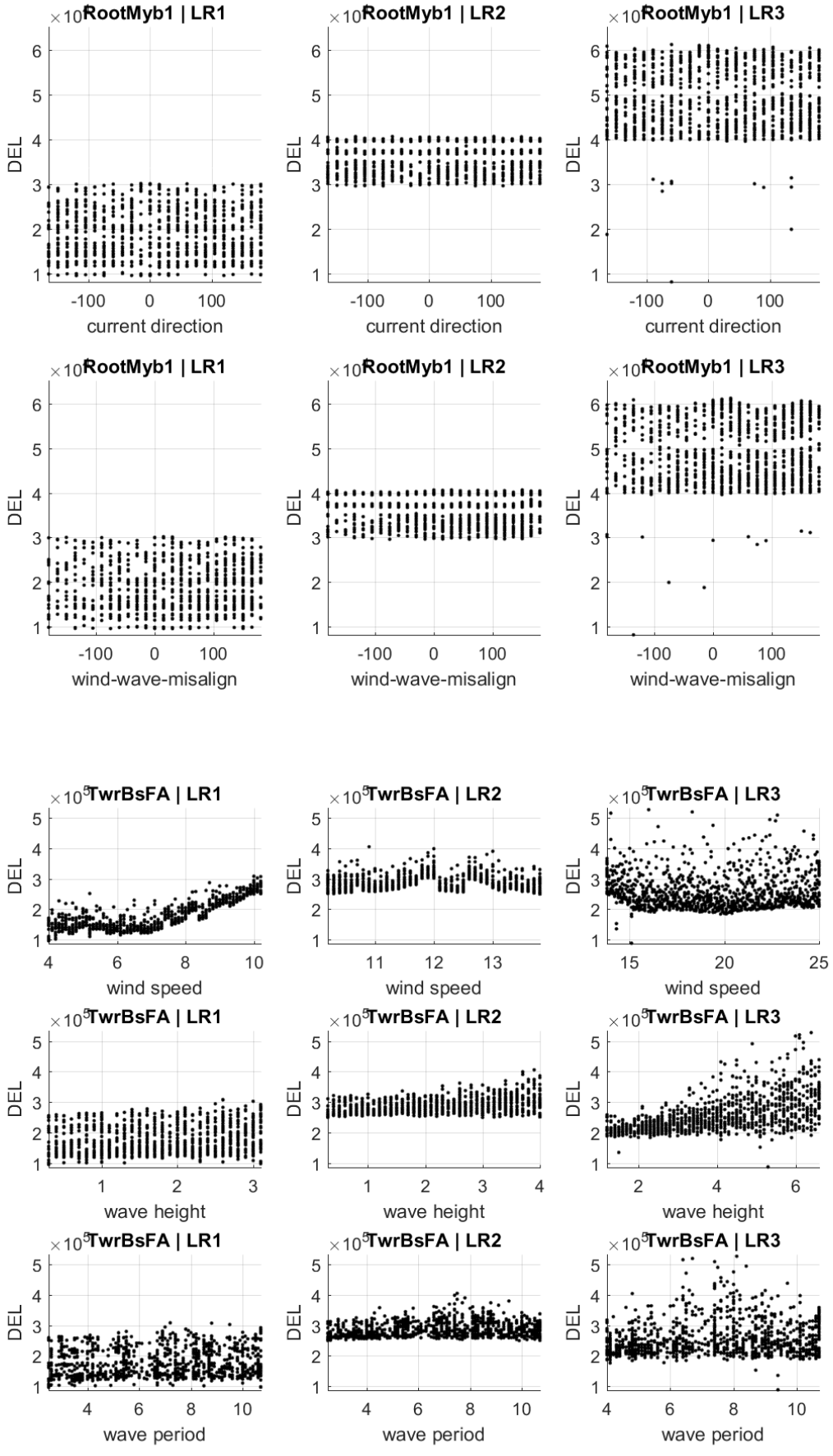
×10^6 RootMyb1 | LR1
×10^6 RootMyb1 | LR2
×10^6 RootMyb1 | LR3
DEL
current direction
wind-wave-misalign
×10^5 TwrBsFA | LR1
×10^5 TwrBsFA | LR2
×10^5 TwrBsFA | LR3
wind speed
wave height
wave period

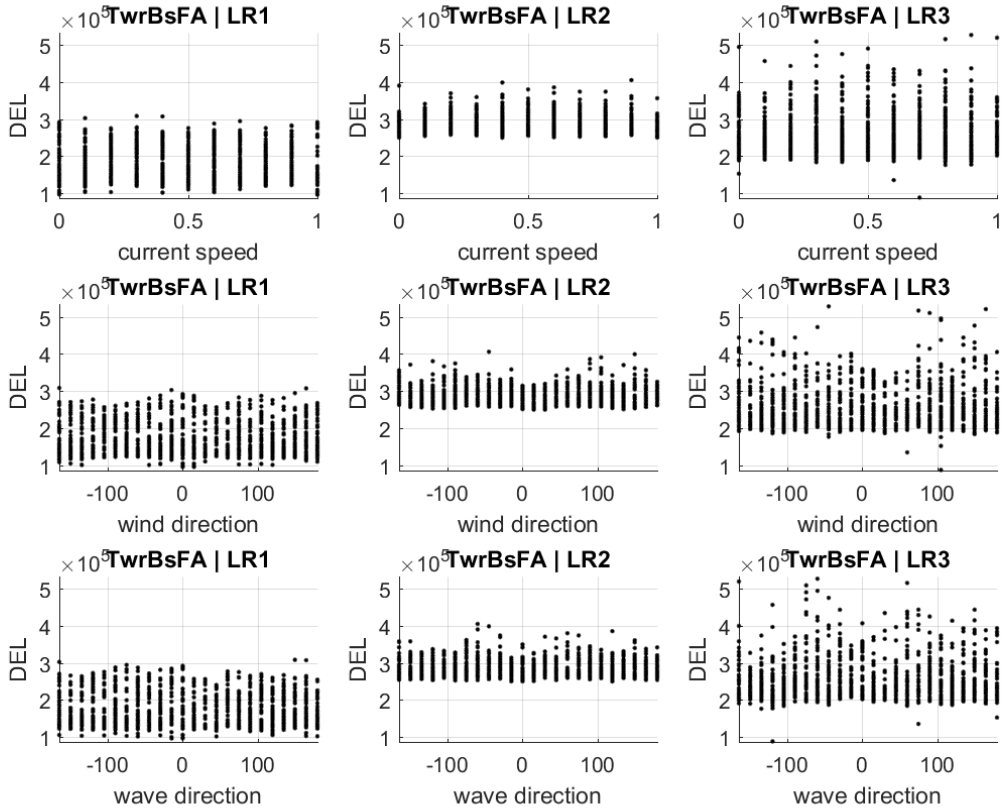
×10^5 TwrBsFA | LR1
×10^5 TwrBsFA | LR2
×10^5 TwrBsFA | LR3
DEL
current speed
wind direction
wave direction

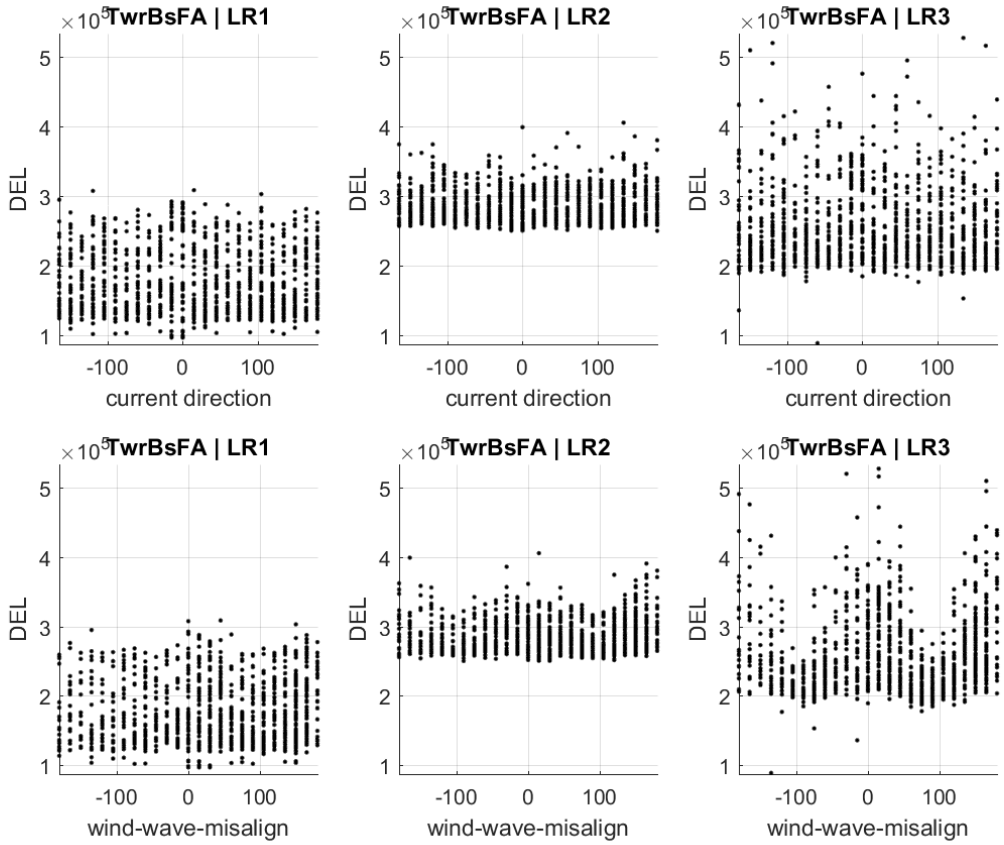
×10^5 TwrBsFA | LR1
×10^5 TwrBsFA | LR2
×10^5 TwrBsFA | LR3
DEL
current direction
wind-wave-misalign

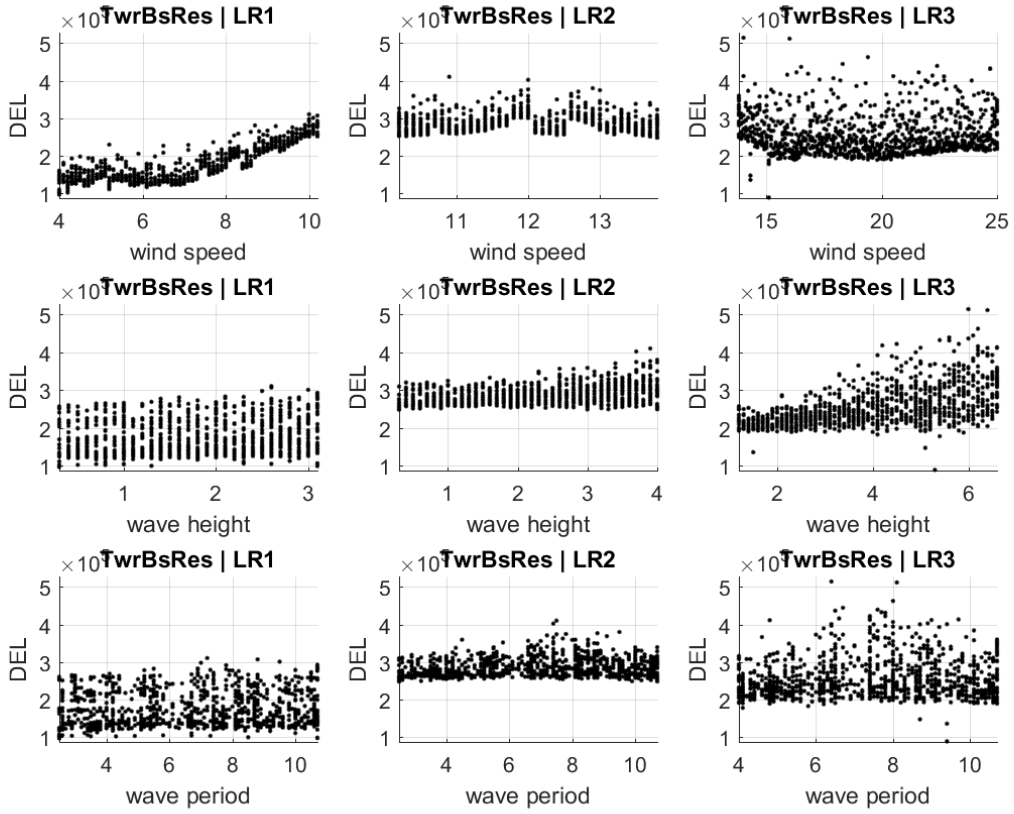
TwrBsRes | LR1
TwrBsRes | LR2
TwrBsRes | LR3
DEL
wind speed
wave height
wave period

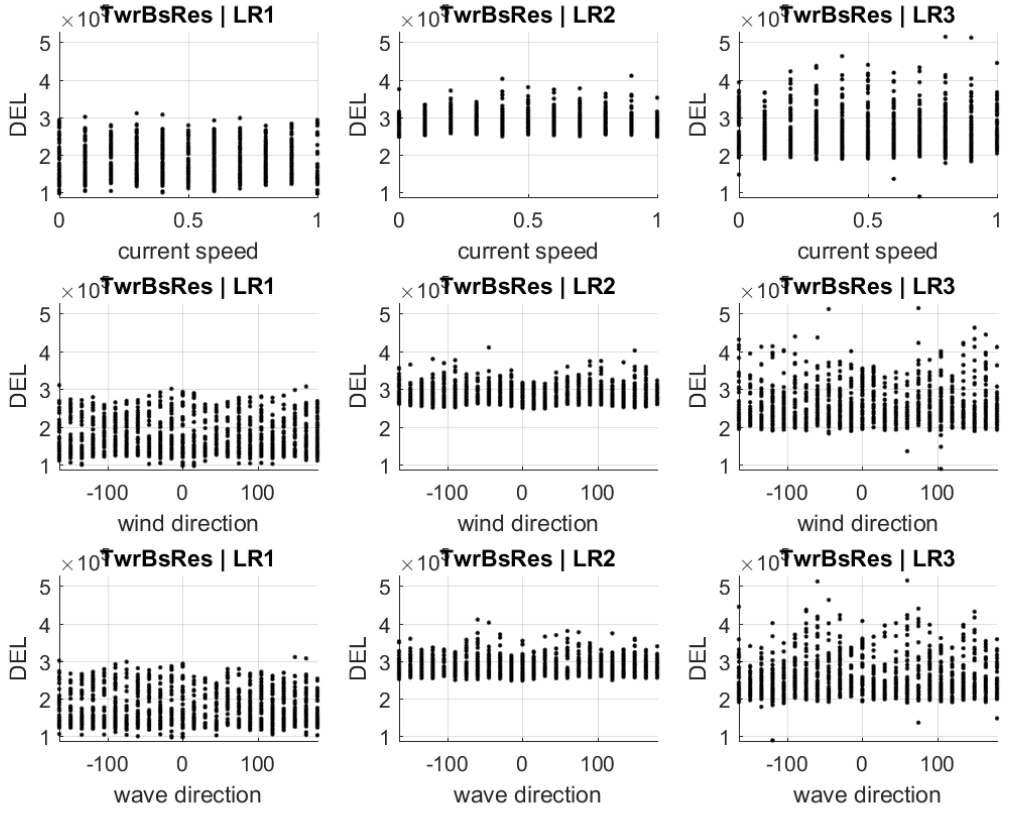
TwrBsRes | LR1
TwrBsRes | LR2
TwrBsRes | LR3
DEL
current speed
wind direction
wave direction

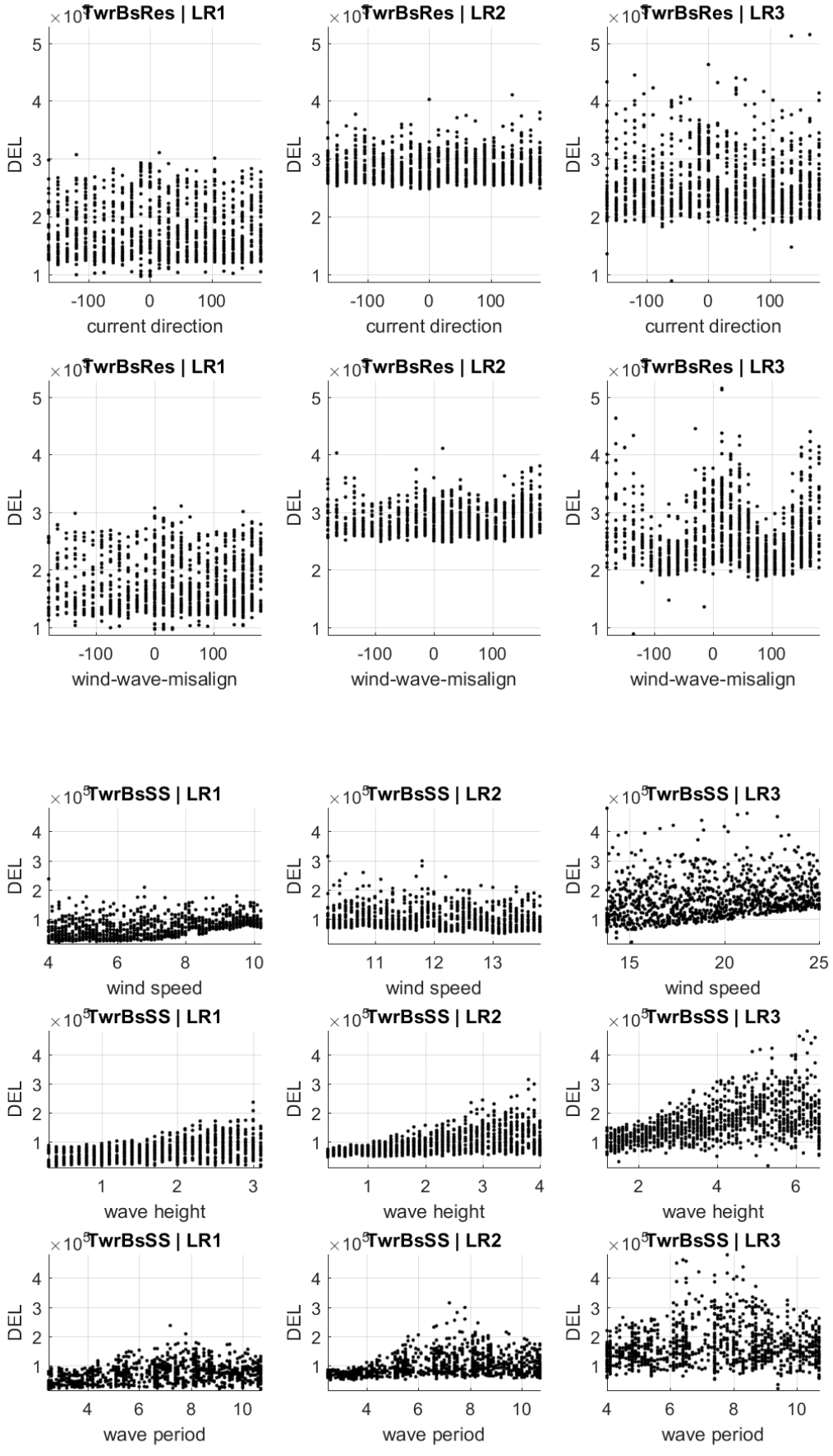
×10^5 TwrBsRes | LR1
×10^5 TwrBsRes | LR2
×10^5 TwrBsRes | LR3
DEL
current direction
wind-wave-misalign
×10^5 TwrBsSS | LR1
×10^5 TwrBsSS | LR2
×10^5 TwrBsSS | LR3
wind speed
wave height
wave period

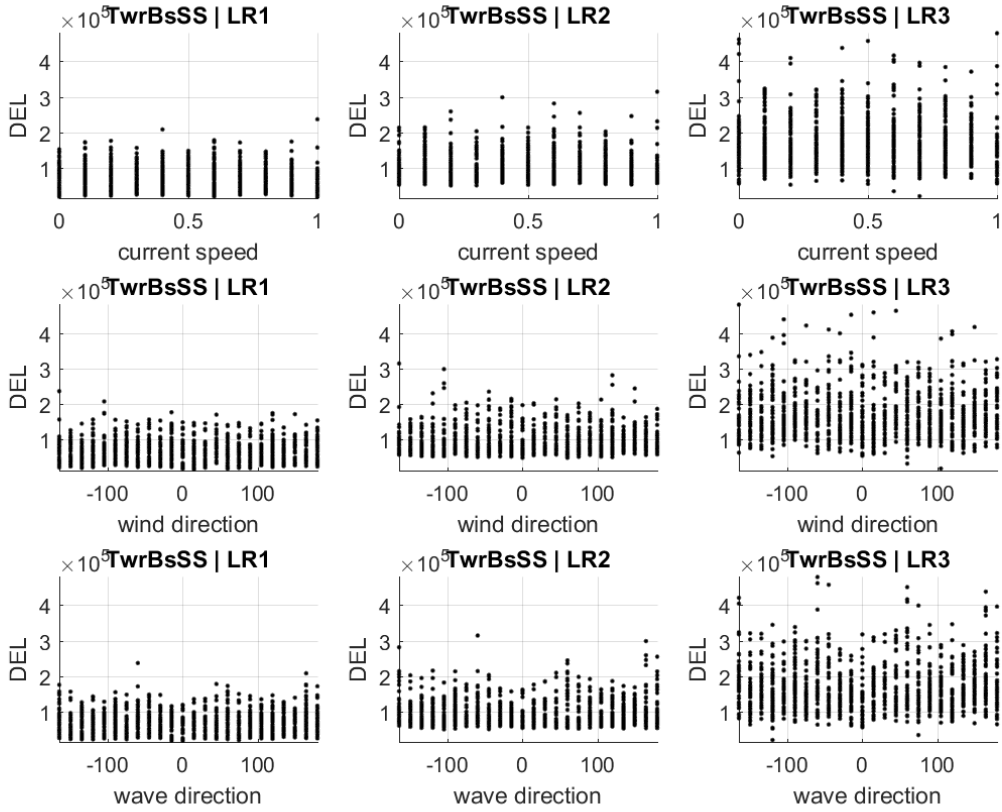
×10^5 TwrBsSS | LR1
×10^5 TwrBsSS | LR2
×10^5 TwrBsSS | LR3
DEL
current speed
wind direction
wave direction

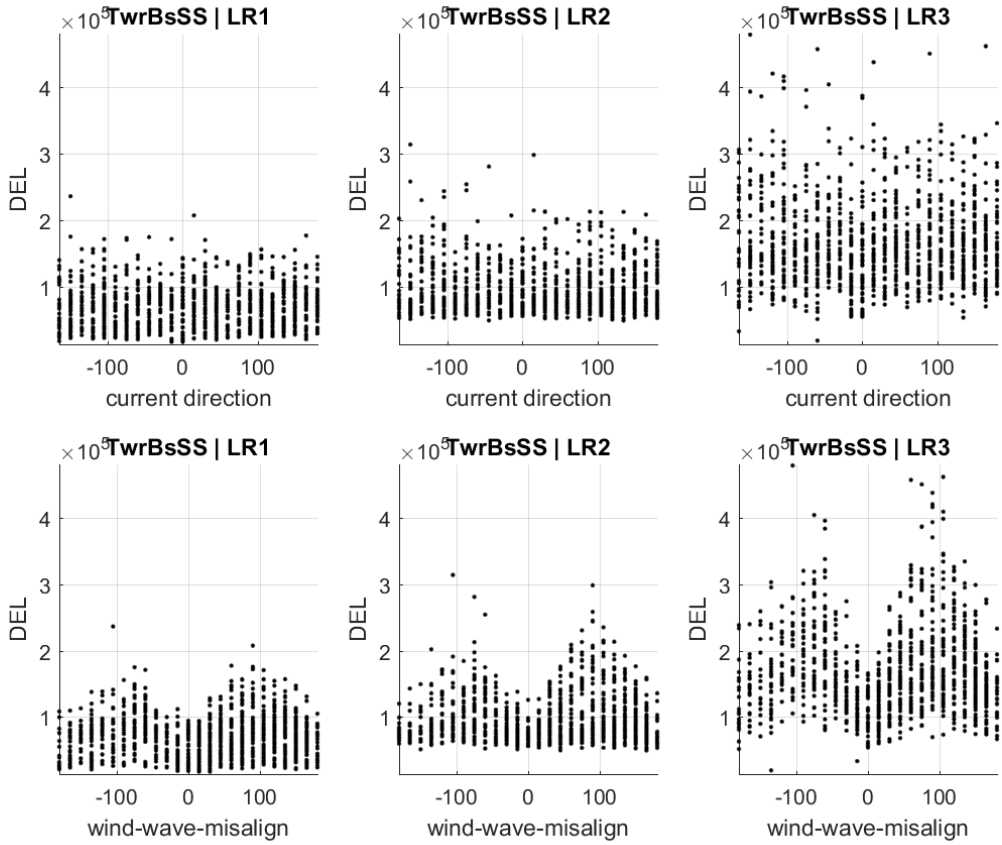
×10^5 TwrBsSS | LR1
×10^5 TwrBsSS | LR2
×10^5 TwrBsSS | LR3
DEL
current direction
wind-wave-misalign

## 11.2 Scatter plots for Olav Olsen 8D sensitivity study for DLC 1.6

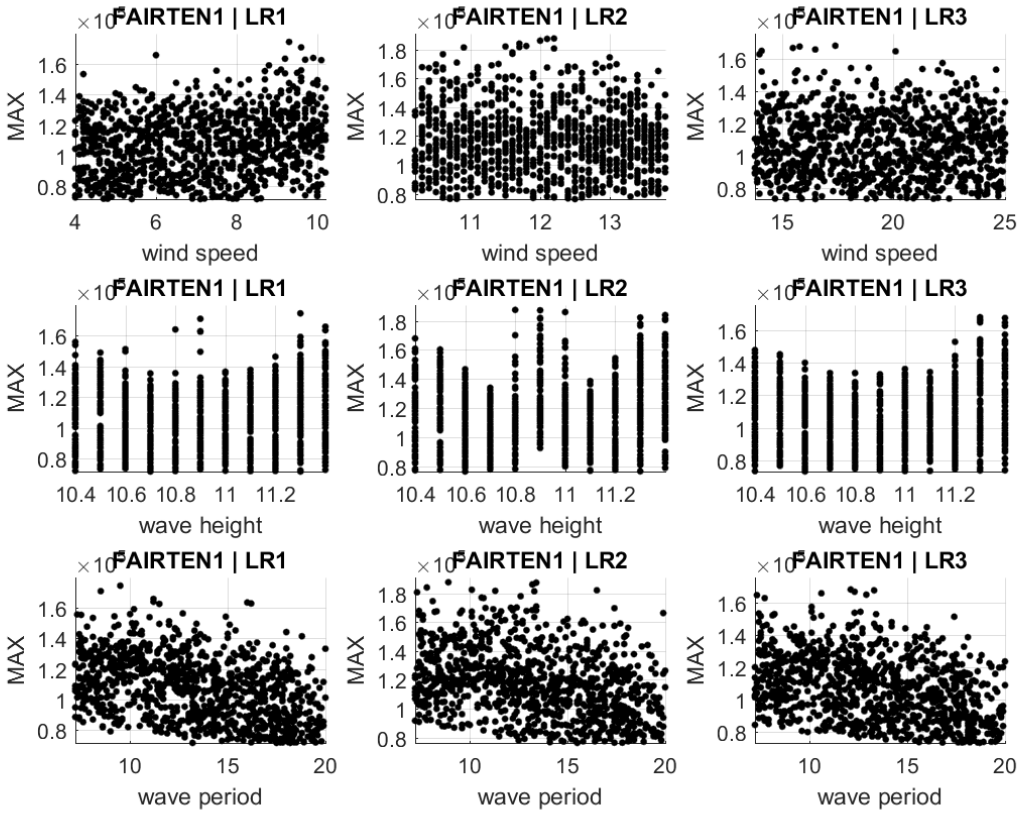

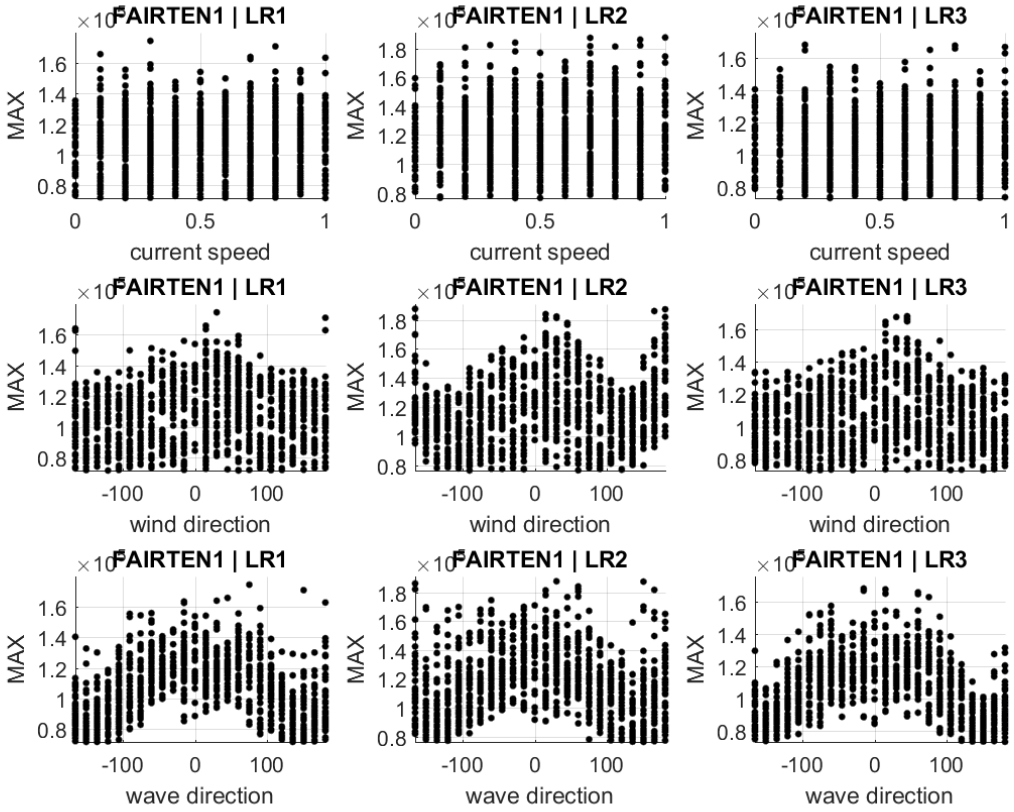
FAIRTEN1 | LR1
FAIRTEN1 | LR2
FAIRTEN1 | LR3
MAX
current speed
wind direction
wave direction

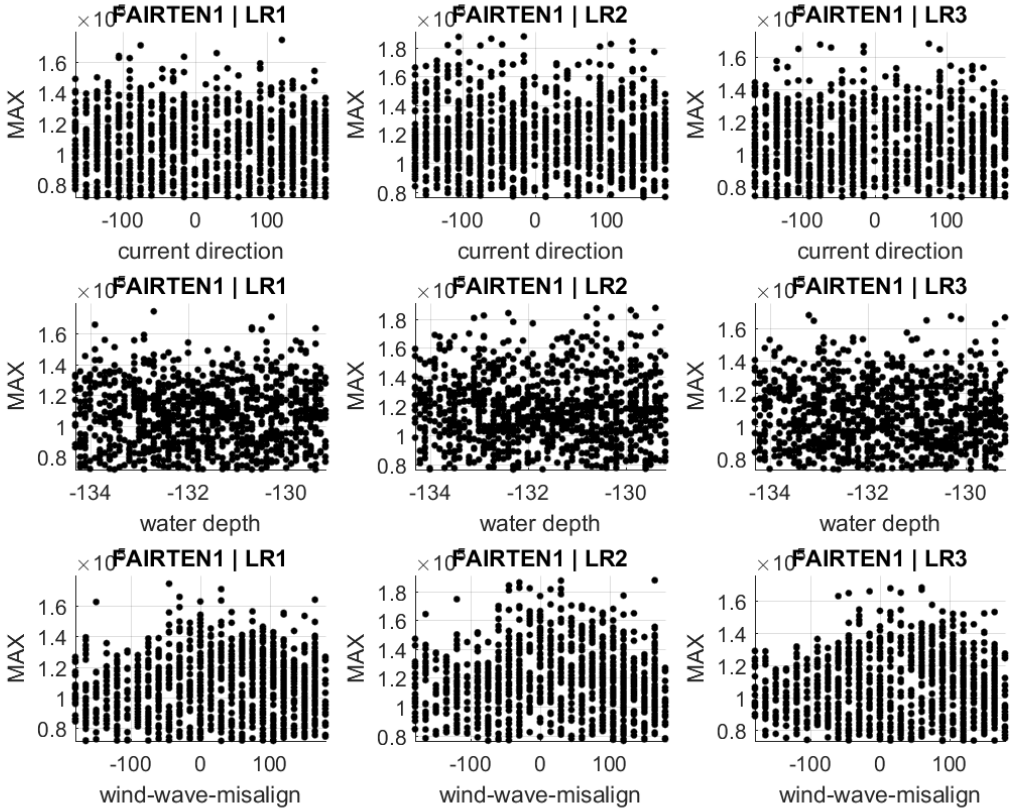
FAIRTEN1 | LR1
FAIRTEN1 | LR2
FAIRTEN1 | LR3
MAX
current direction
water depth
wind-wave-misalign

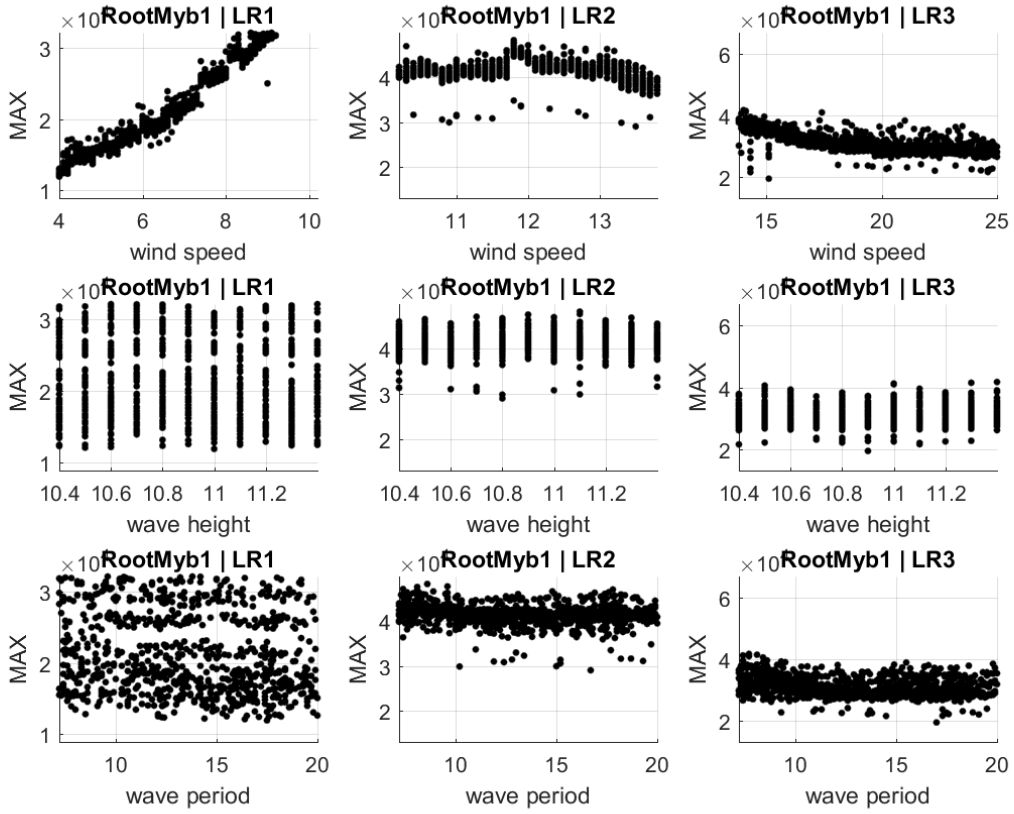
×10 RootMyb1 | LR1
MAX
wind speed
×10 RootMyb1 | LR2
MAX
wind speed
×10 RootMyb1 | LR3
MAX
wind speed
×10 RootMyb1 | LR1
MAX
wave height
×10 RootMyb1 | LR2
MAX
wave height
×10 RootMyb1 | LR3
MAX
wave height
×10 RootMyb1 | LR1
MAX
wave period
×10 RootMyb1 | LR2
MAX
wave period
×10 RootMyb1 | LR3
MAX
wave period

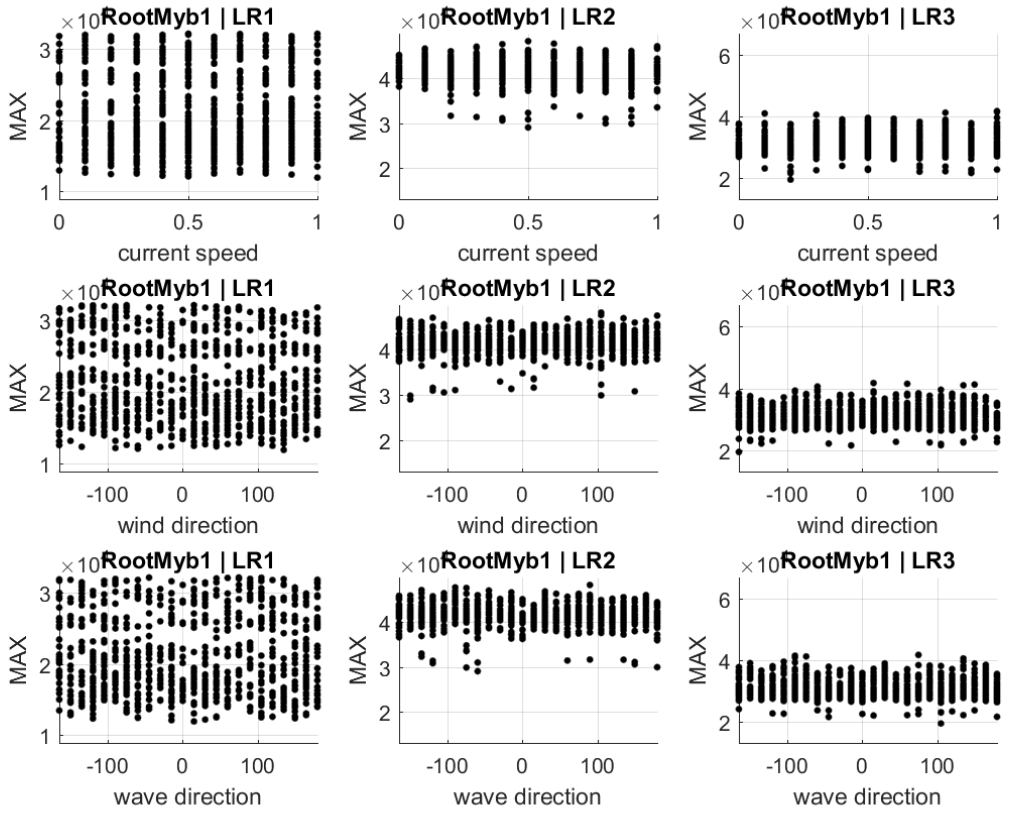
×10 RootMyb1 | LR1
MAX
current speed
×10 RootMyb1 | LR2
MAX
current speed
×10 RootMyb1 | LR3
MAX
current speed
×10 RootMyb1 | LR1
MAX
wind direction
×10 RootMyb1 | LR2
MAX
wind direction
×10 RootMyb1 | LR3
MAX
wind direction
×10 RootMyb1 | LR1
MAX
wave direction
×10 RootMyb1 | LR2
MAX
wave direction
×10 RootMyb1 | LR3
MAX
wave direction

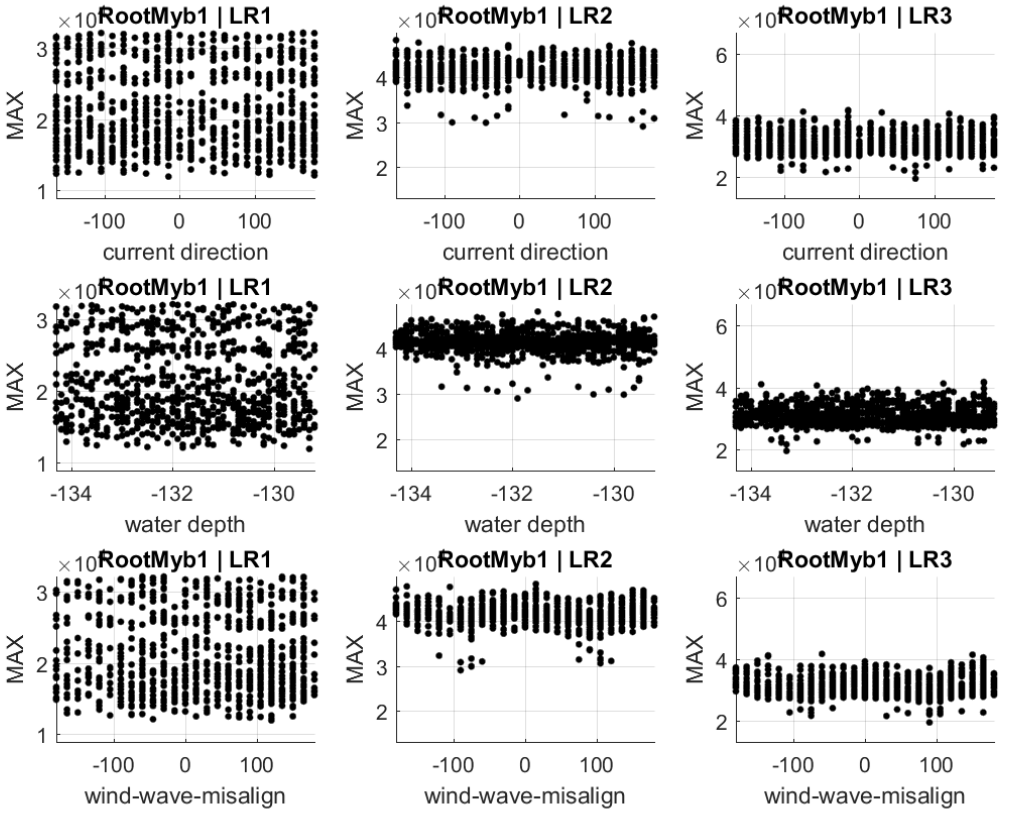
RootMyb1 | LR1
RootMyb1 | LR2
RootMyb1 | LR3
MAX
current direction
water depth
wind-wave-misalign

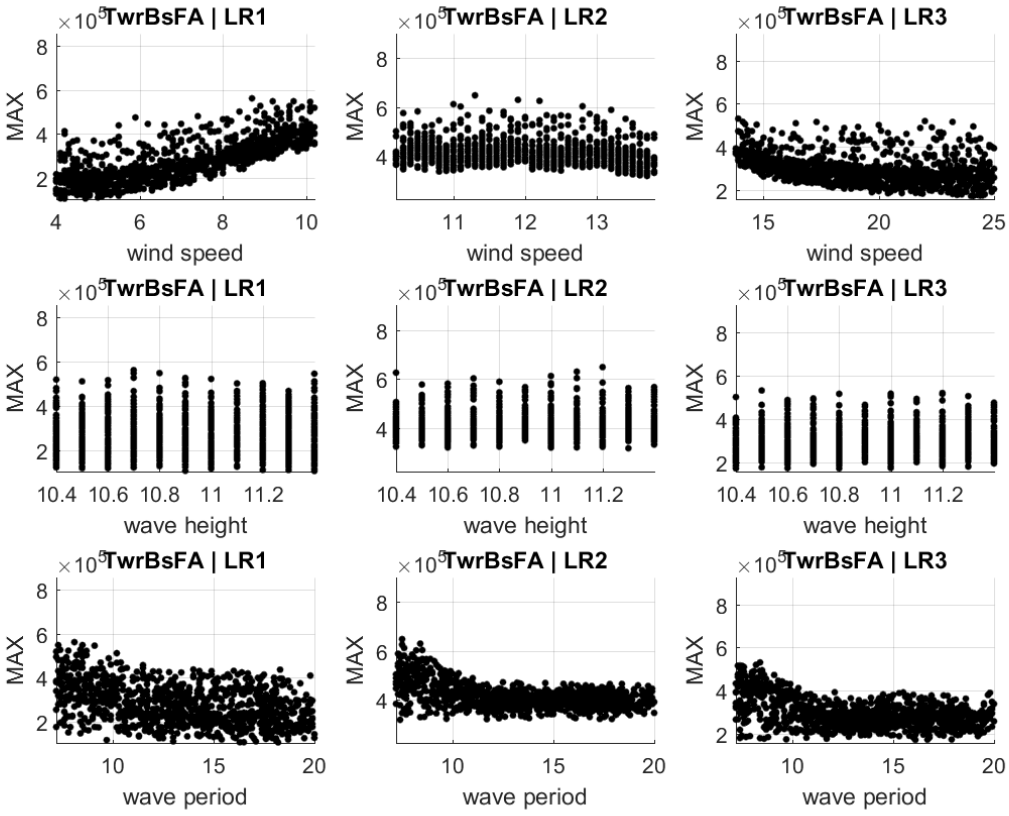
TwrBsFA | LR1
TwrBsFA | LR2
TwrBsFA | LR3
MAX
wind speed
wave height
wave period

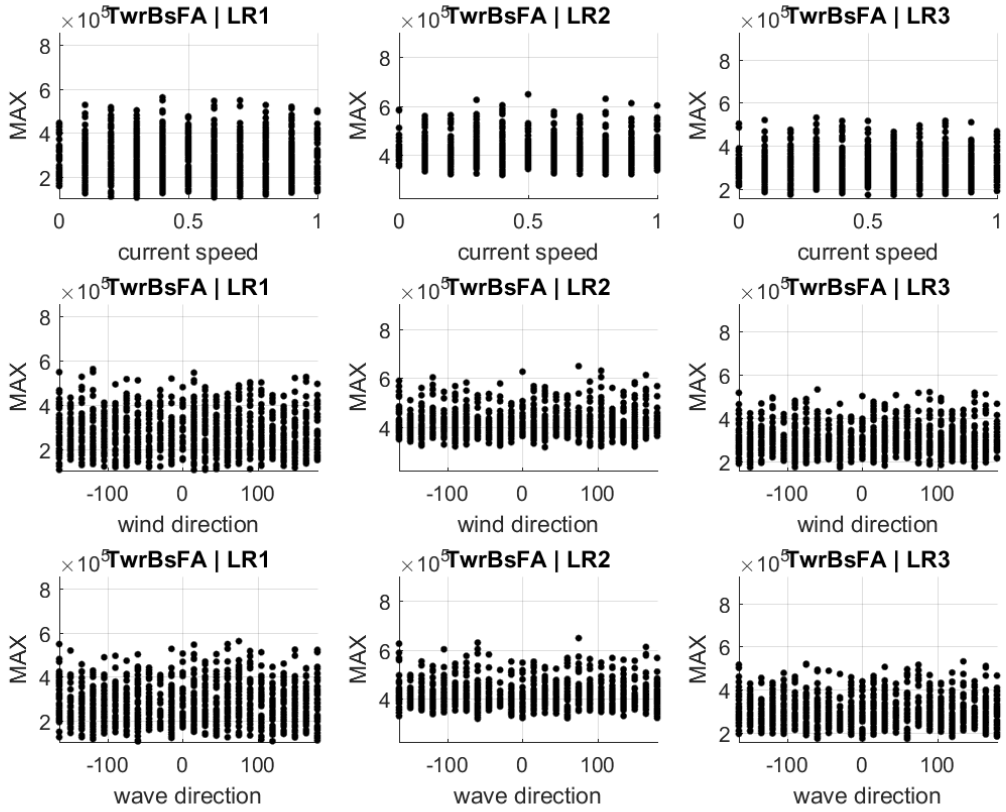
×10^5 TwrBsFA | LR1
×10^5 TwrBsFA | LR2
×10^5 TwrBsFA | LR3
MAX
current speed
wind direction
wave direction

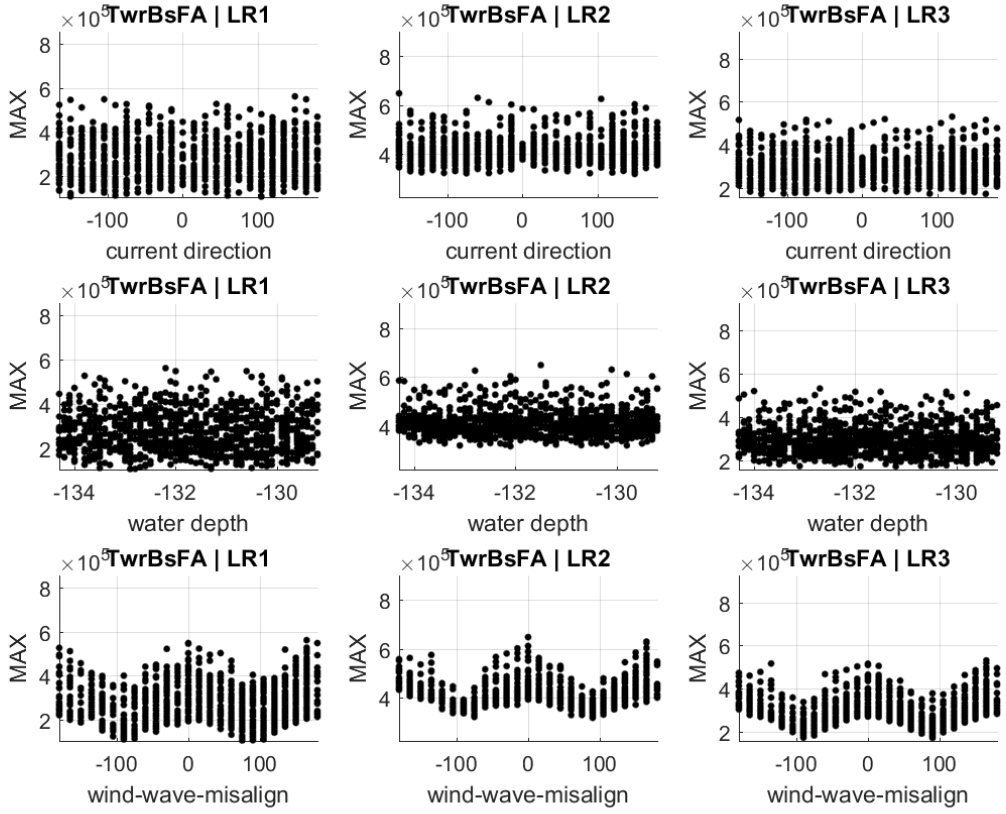
×10^5 TwrBsFA | LR1
×10^5 TwrBsFA | LR2
×10^5 TwrBsFA | LR3
MAX
current direction
water depth
wind-wave-misalign

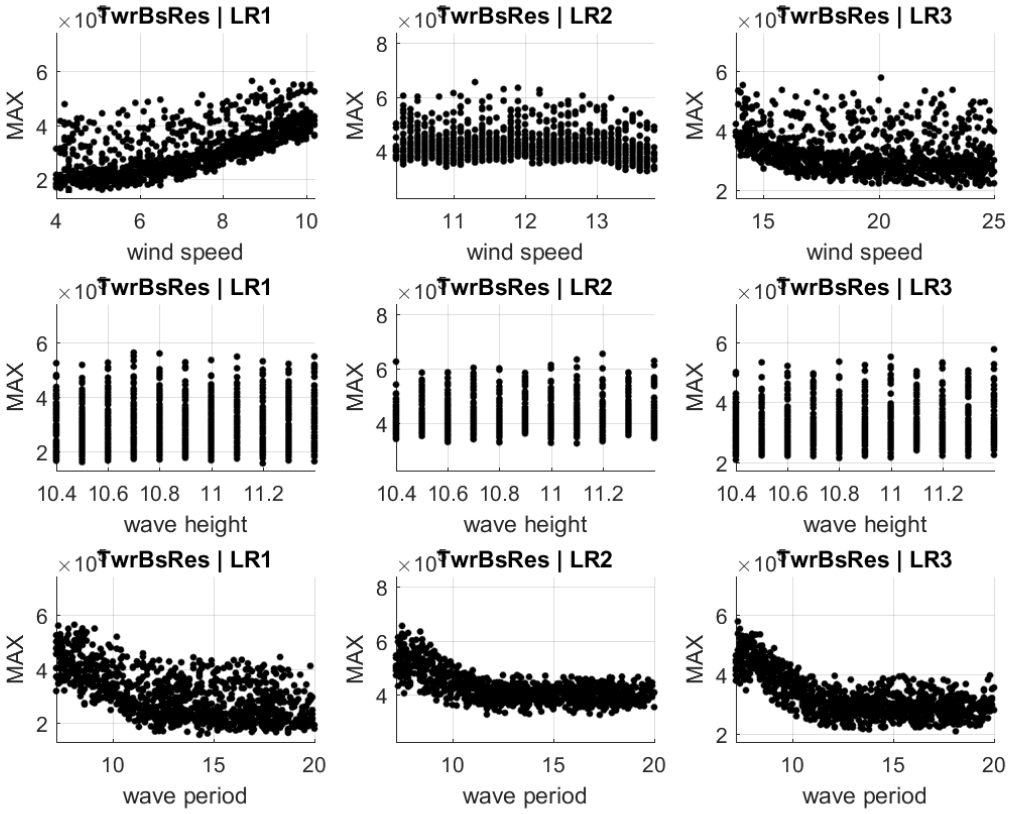
×10^6 TwrBsRes | LR1
×10^6 TwrBsRes | LR2
×10^6 TwrBsRes | LR3
MAX
wind speed
wave height
wave period

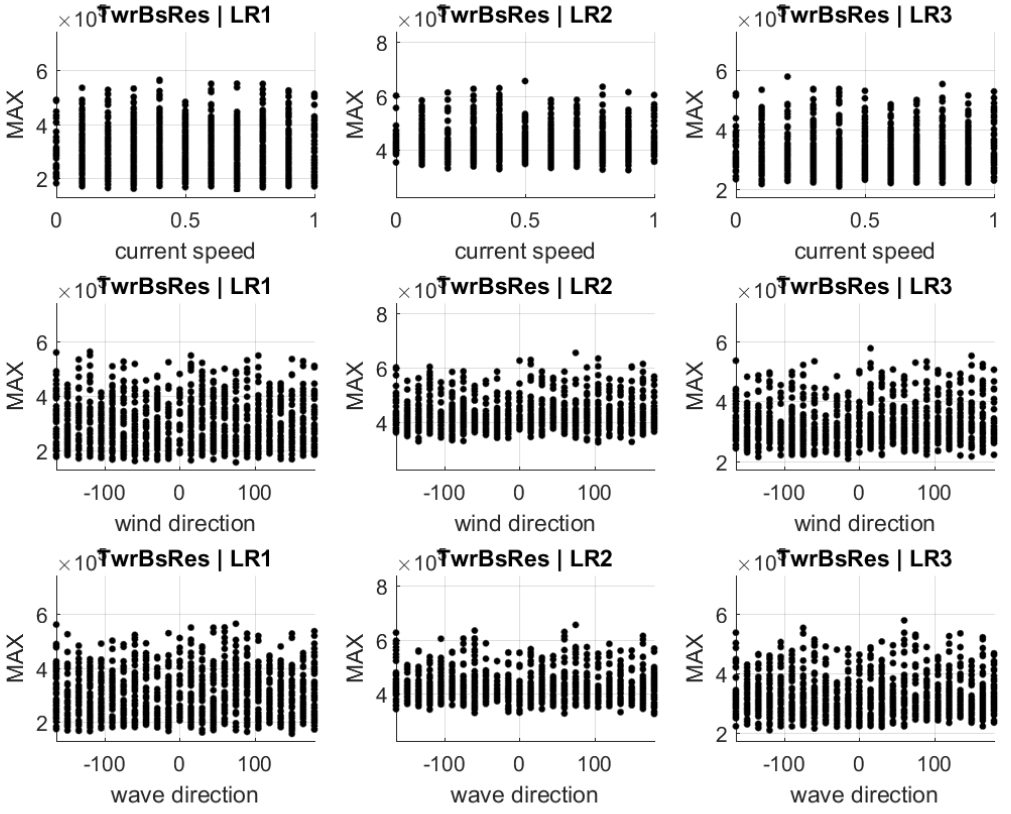
×10^6 TwrBsRes | LR1
×10^6 TwrBsRes | LR2
×10^6 TwrBsRes | LR3
MAX
current speed
wind direction
wave direction

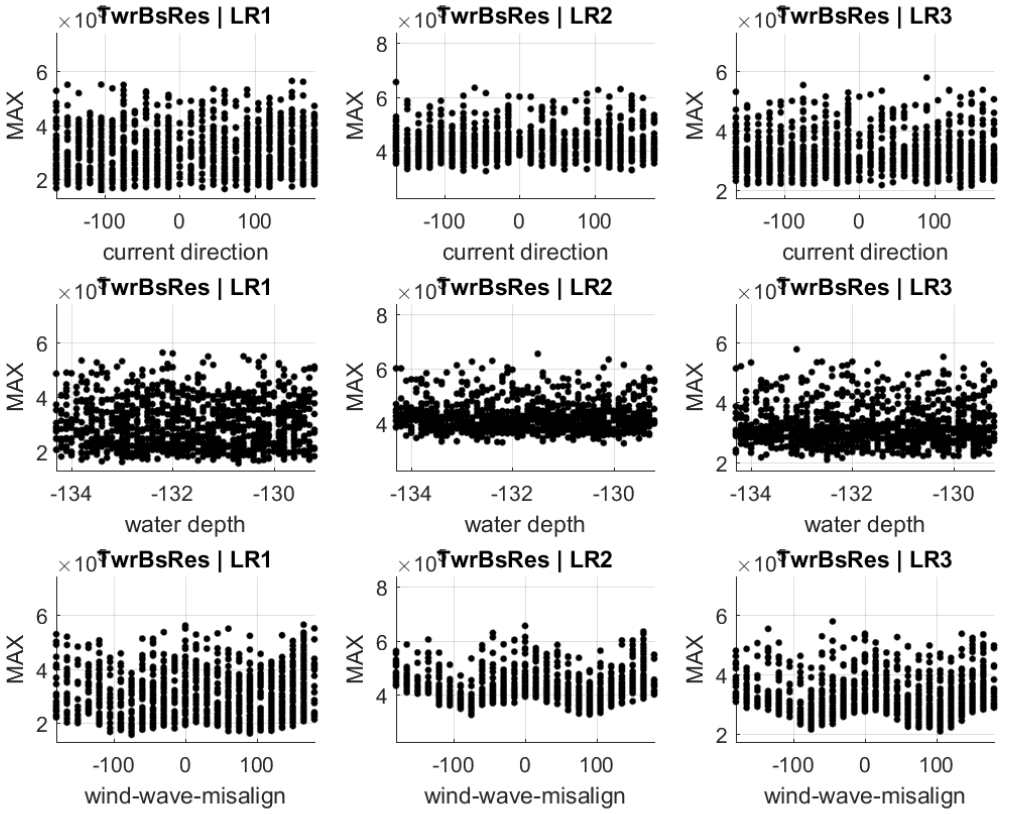
×10^5 TwrBsRes | LR1
×10^5 TwrBsRes | LR2
×10^5 TwrBsRes | LR3
MAX
current direction
water depth
wind-wave-misalign

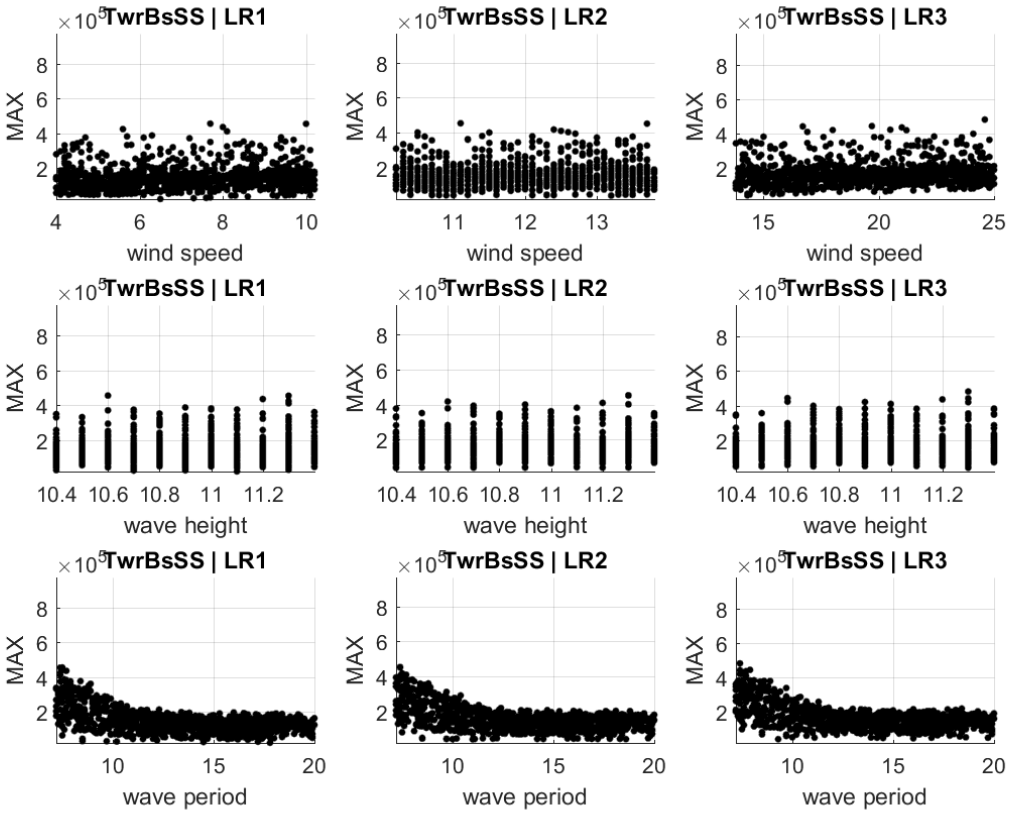
×10^5 TwrBsSS | LR1
×10^5 TwrBsSS | LR2
×10^5 TwrBsSS | LR3
MAX
wind speed
wave height
wave period

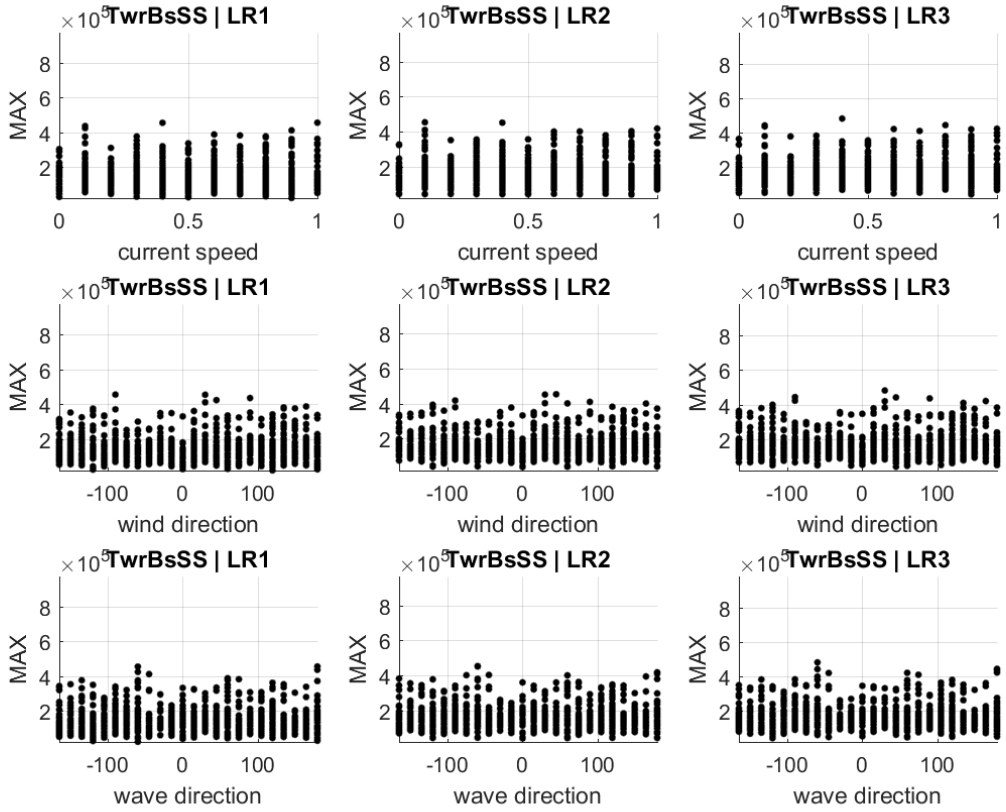
×10^5 TwrBsSS | LR1
×10^5 TwrBsSS | LR2
×10^5 TwrBsSS | LR3
MAX
current speed
wind direction
wave direction

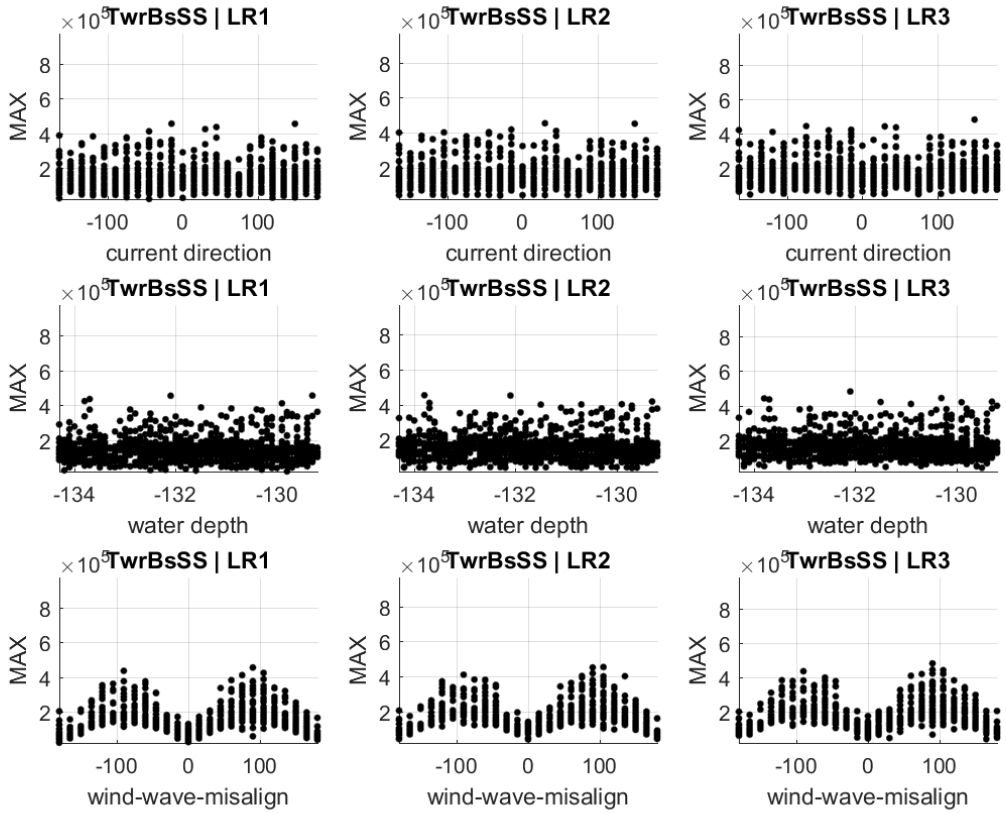
×10^5 TwrBsSS | LR1
×10^5 TwrBsSS | LR2
×10^5 TwrBsSS | LR3
MAX
current direction
water depth
wind-wave-misalign

## 11.3 Scatter plots for Olav Olsen 7D sensitivity study for DLC 6.1

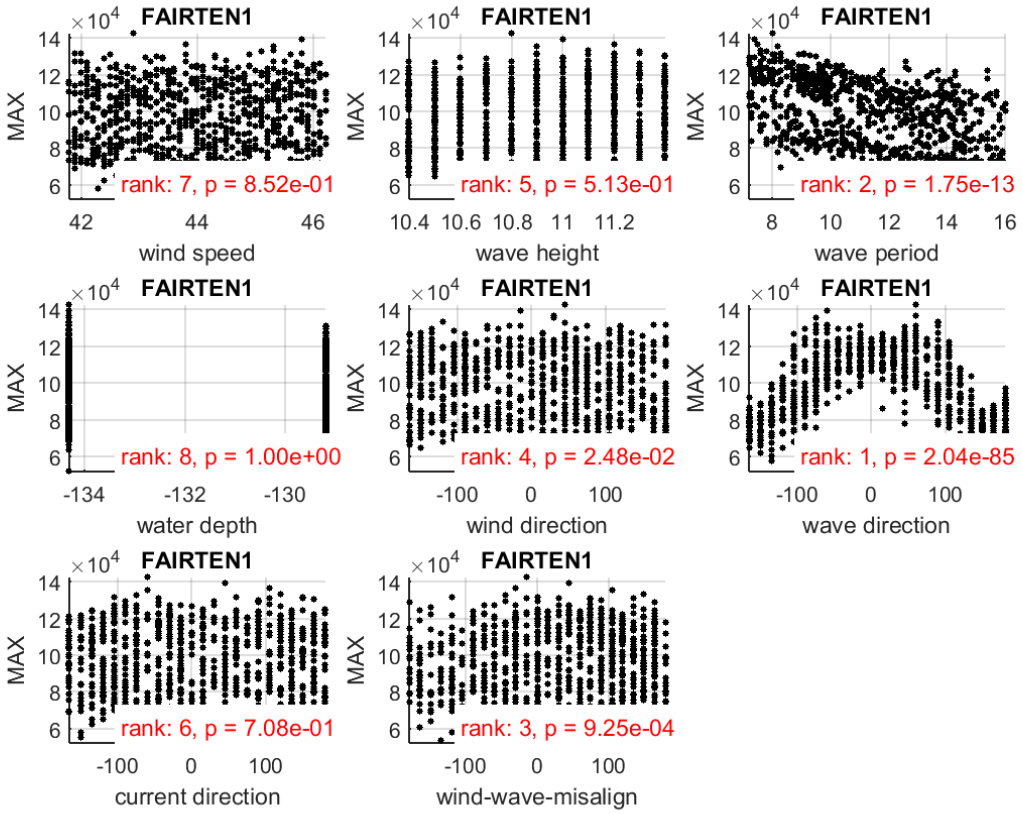

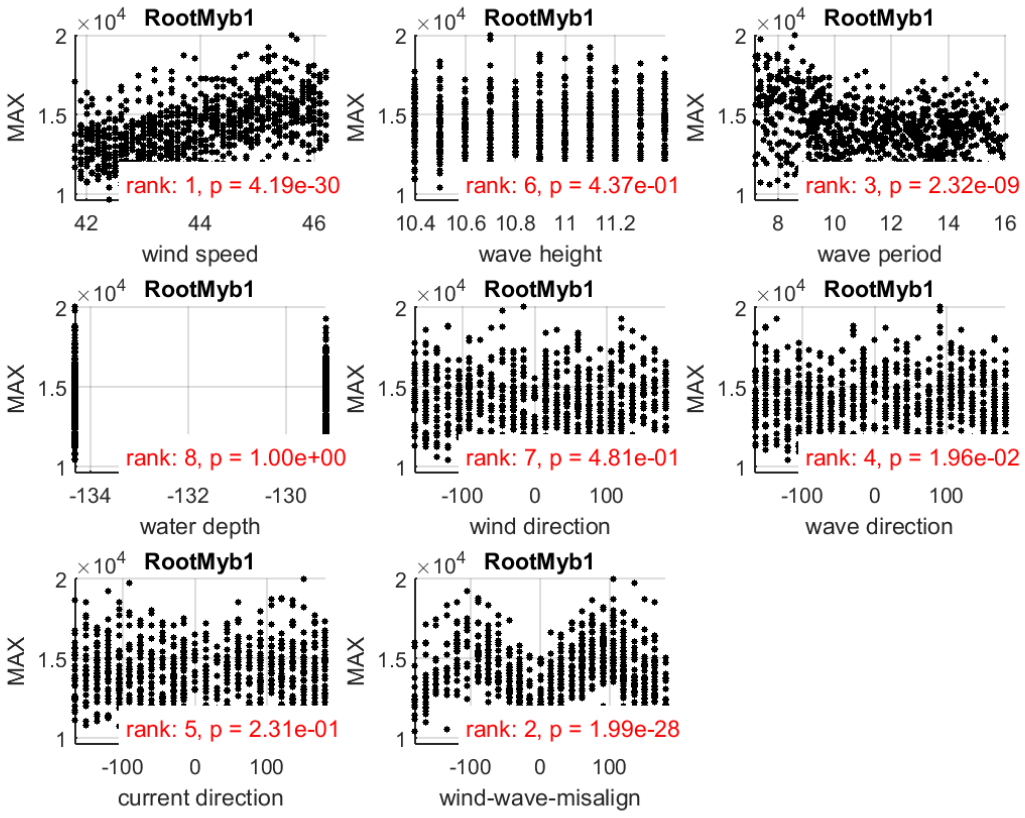
RootMyb1
MAX
rank: 1, p = 4.19e-30
wind speed
rank: 6, p = 4.37e-01
wave height
rank: 3, p = 2.32e-09
wave period
rank: 8, p = 1.00e+00
water depth
rank: 7, p = 4.81e-01
wind direction
rank: 4, p = 1.96e-02
wave direction
rank: 5, p = 2.31e-01
current direction
rank: 2, p = 1.99e-28
wind-wave-misalign

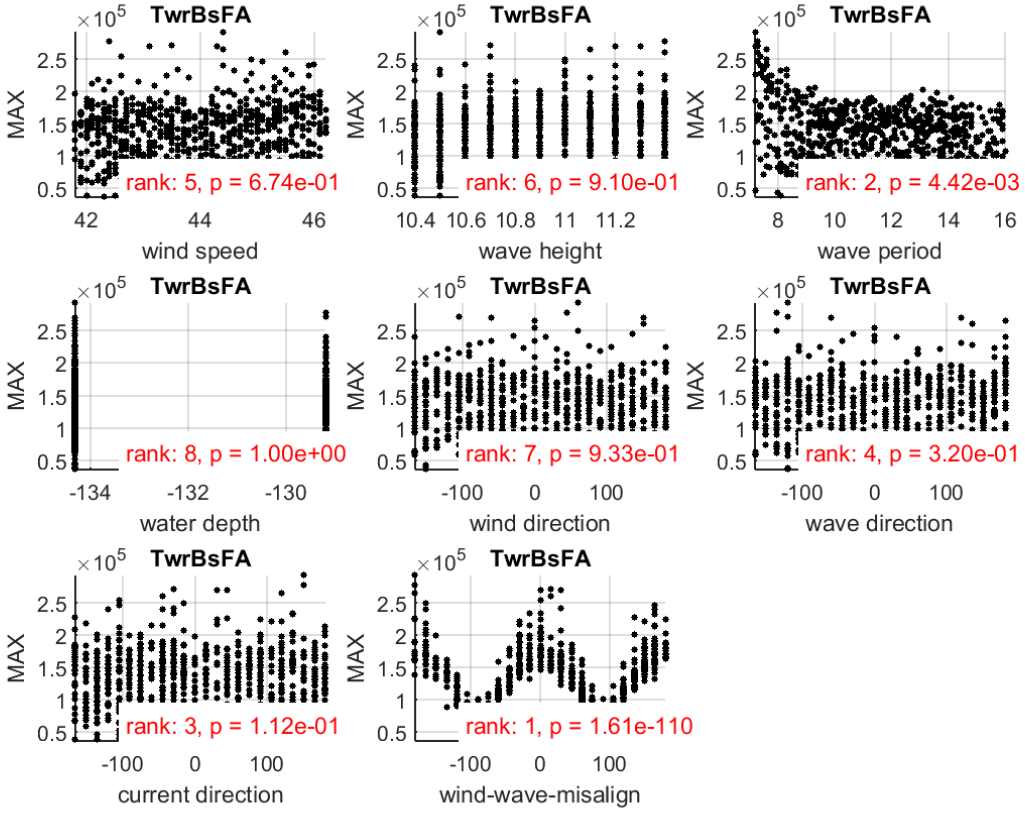
TwrBsFA
MAX
rank: 5, p = 6.74e-01
wind speed
rank: 6, p = 9.10e-01
wave height
rank: 2, p = 4.42e-03
wave period
rank: 8, p = 1.00e+00
water depth
rank: 7, p = 9.33e-01
wind direction
rank: 4, p = 3.20e-01
wave direction
rank: 3, p = 1.12e-01
current direction
rank: 1, p = 1.61e-110
wind-wave-misalign

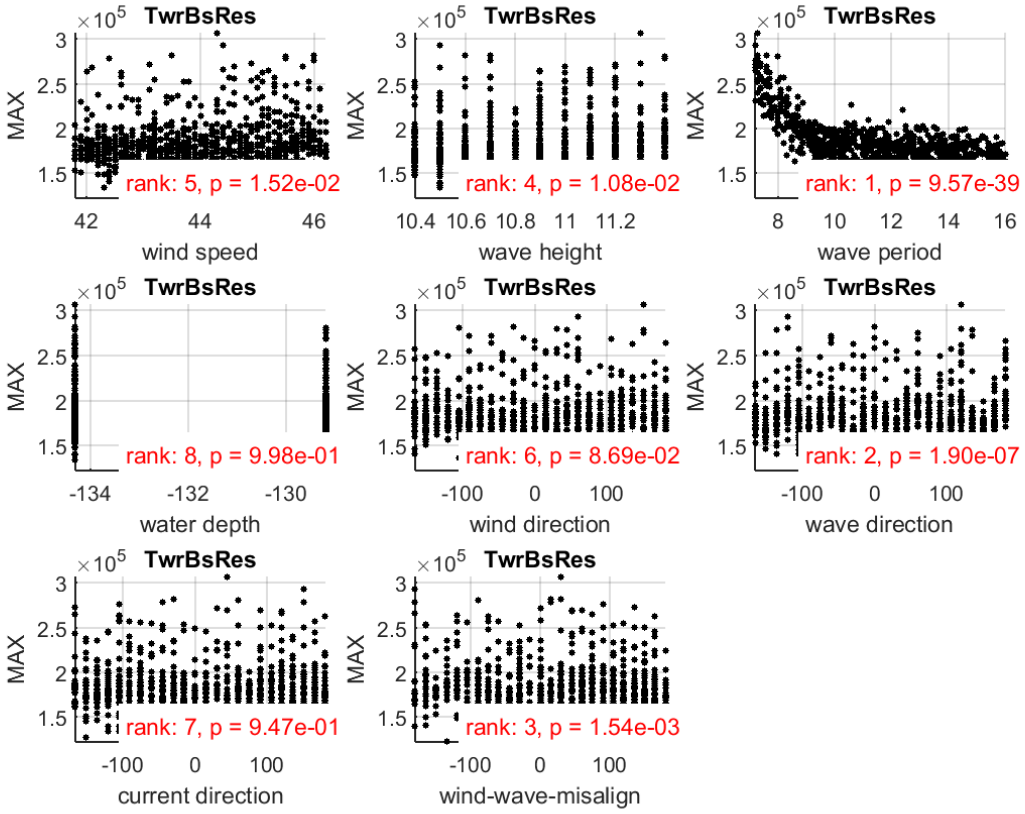
TwrBsRes
MAX
rank: 5, p = 1.52e-02
wind speed
rank: 4, p = 1.08e-02
wave height
rank: 1, p = 9.57e-39
wave period
rank: 8, p = 9.98e-01
water depth
rank: 6, p = 8.69e-02
wind direction
rank: 2, p = 1.90e-07
wave direction
rank: 7, p = 9.47e-01
current direction
rank: 3, p = 1.54e-03
wind-wave-misalign

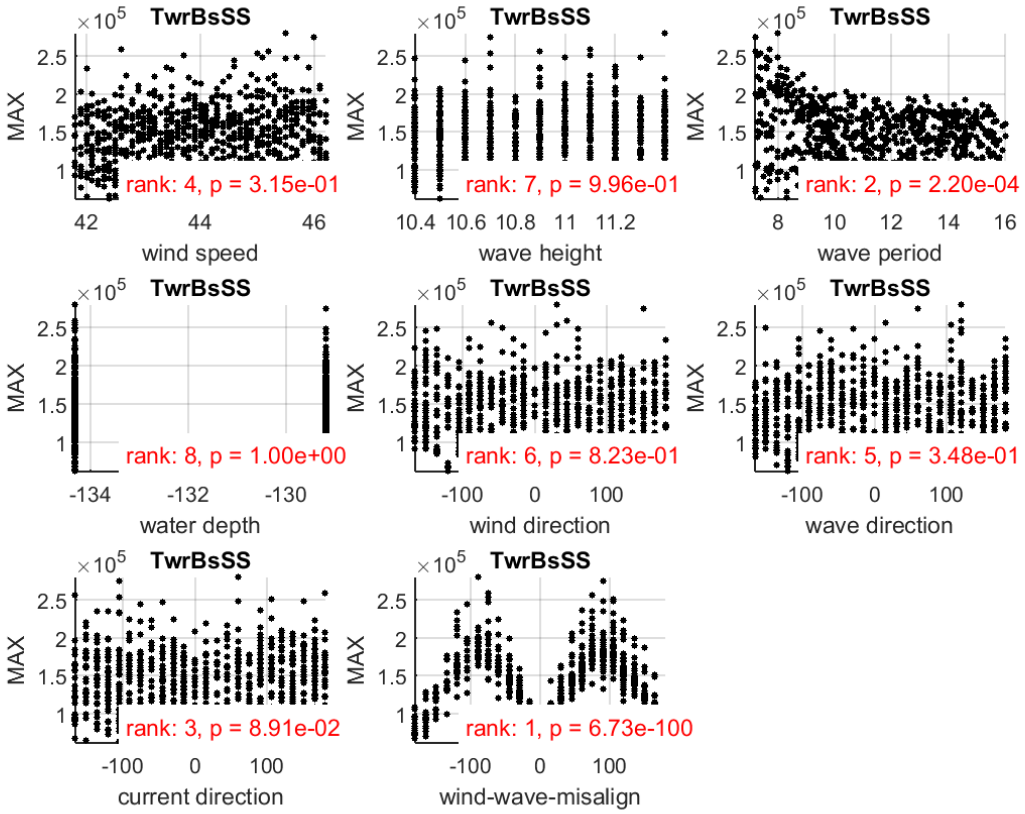
TwrBsSS
MAX
rank: 4, p = 3.15e-01
wind speed
rank: 7, p = 9.96e-01
wave height
rank: 2, p = 2.20e-04
wave period
rank: 8, p = 1.00e+00
water depth
rank: 6, p = 8.23e-01
wind direction
rank: 5, p = 3.48e-01
wave direction
rank: 3, p = 8.91e-02
current direction
rank: 1, p = 6.73e-100
wind-wave-misalign

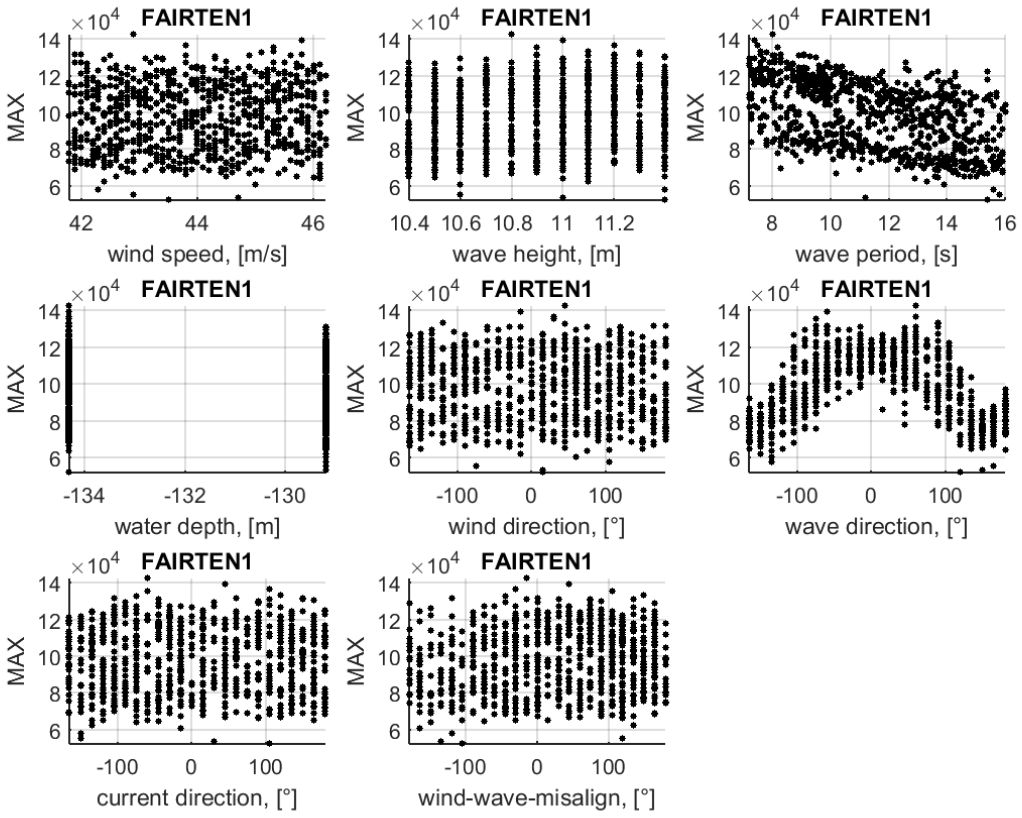
FAIRTEN1
×10^4
MAX
wind speed, [m/s]
wave height, [m]
wave period, [s]
water depth, [m]
wind direction, [°]
wave direction, [°]
current direction, [°]
wind-wave-misalign, [°]

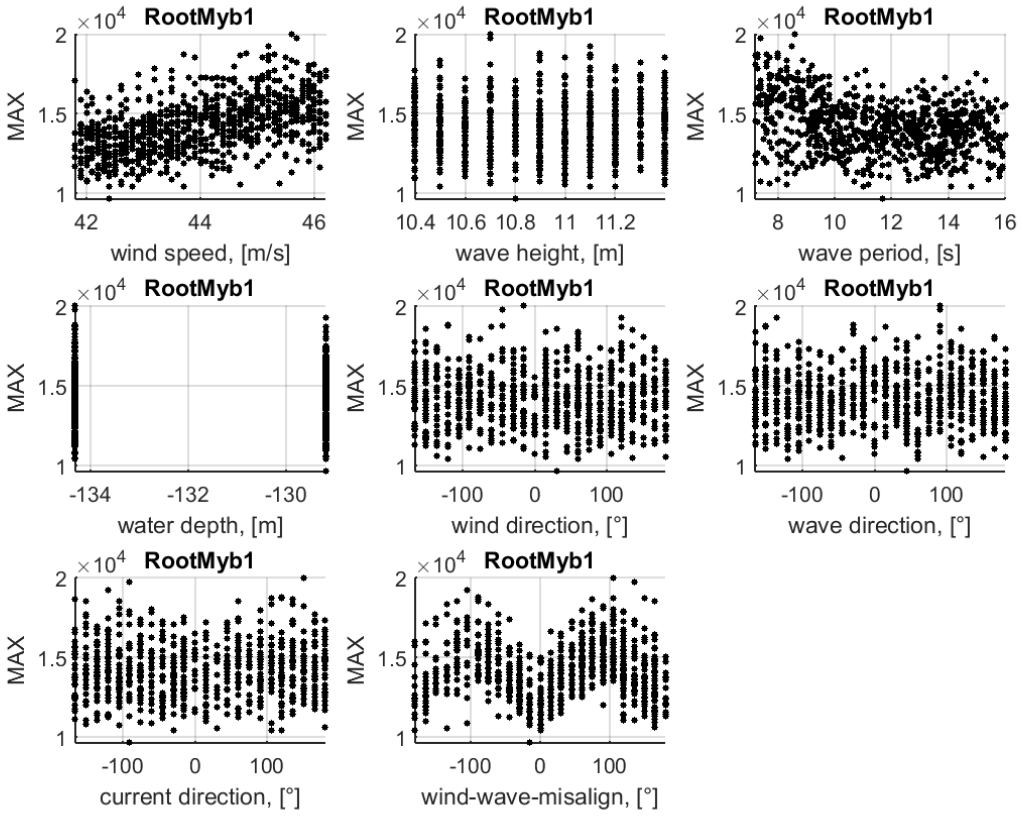
RootMyb1
×10^4
MAX
wind speed, [m/s]
wave height, [m]
wave period, [s]
water depth, [m]
wind direction, [°]
wave direction, [°]
current direction, [°]
wind-wave-misalign, [°]

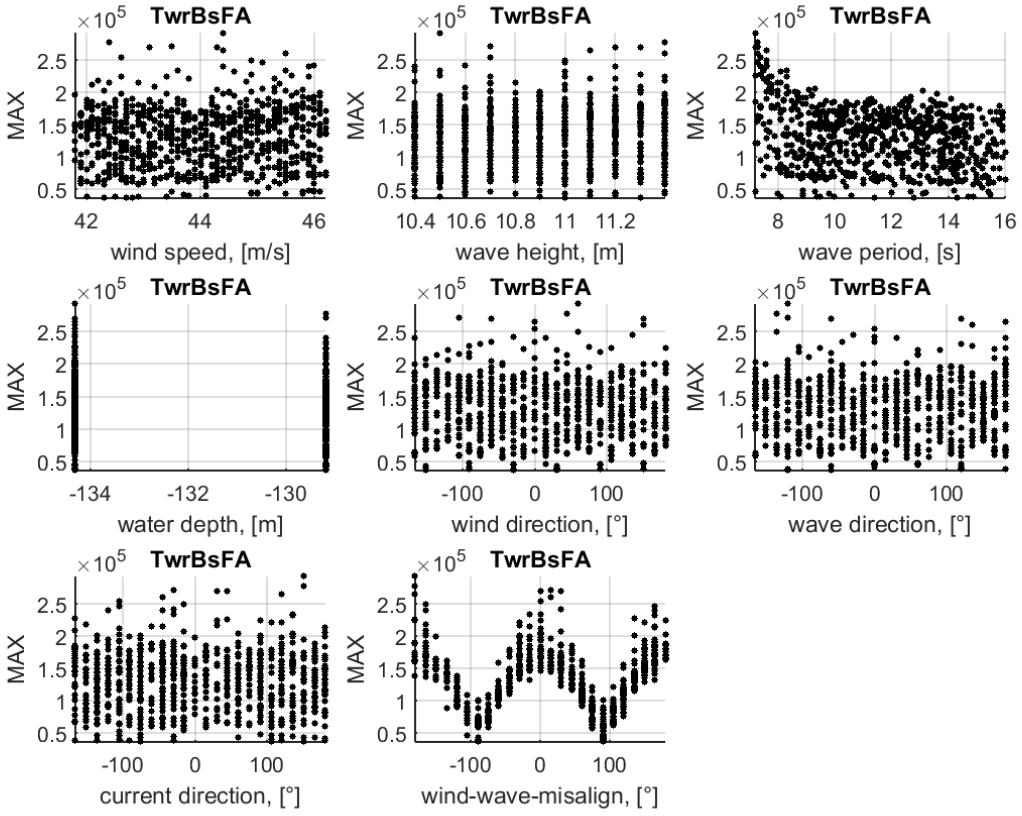
TwrBsFA
×10^5
MAX
wind speed, [m/s]
wave height, [m]
wave period, [s]
water depth, [m]
wind direction, [°]
wave direction, [°]
current direction, [°]
wind-wave-misalign, [°]

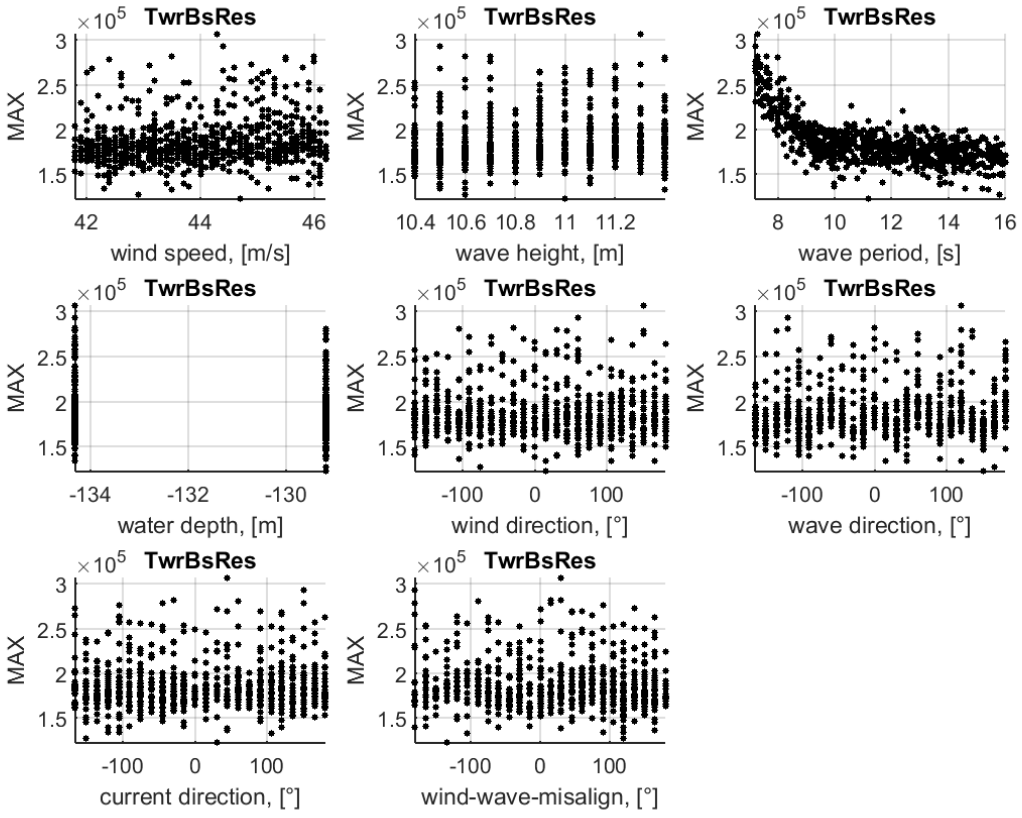
TwrBsRes
×10^5
MAX
wind speed, [m/s]
wave height, [m]
wave period, [s]
water depth, [m]
wind direction, [°]
wave direction, [°]
current direction, [°]
wind-wave-misalign, [°]

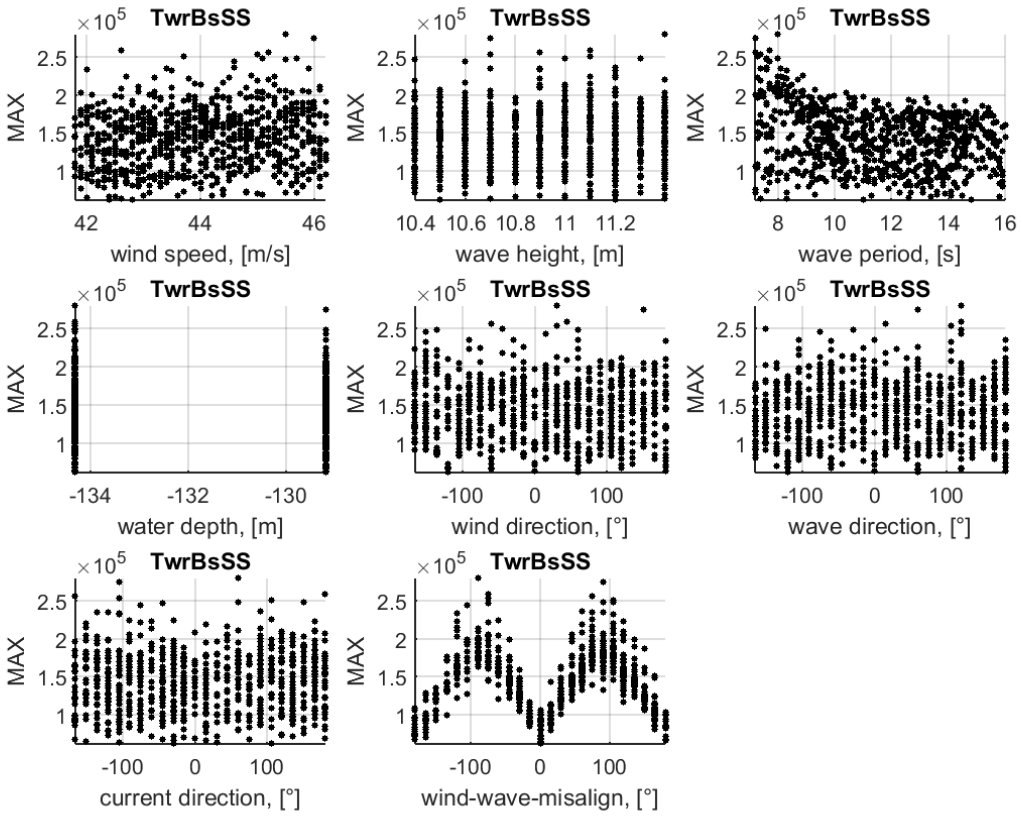
TwrBsSS
×10^5
MAX
wind speed, [m/s]
wave height, [m]
wave period, [s]
water depth, [m]
wind direction, [°]
wave direction, [°]
current direction, [°]
wind-wave-misalign, [°]

## 11.4 Scatter plots for Nautilus 7D sensitivity study for DLC 1.2

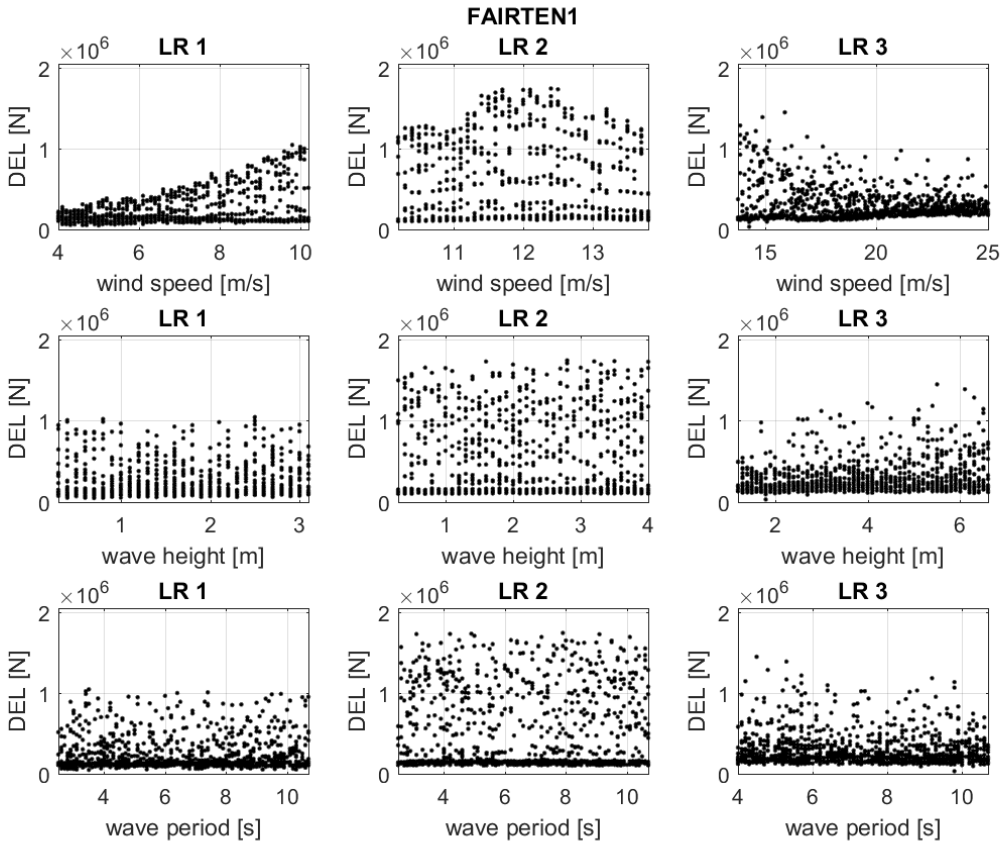

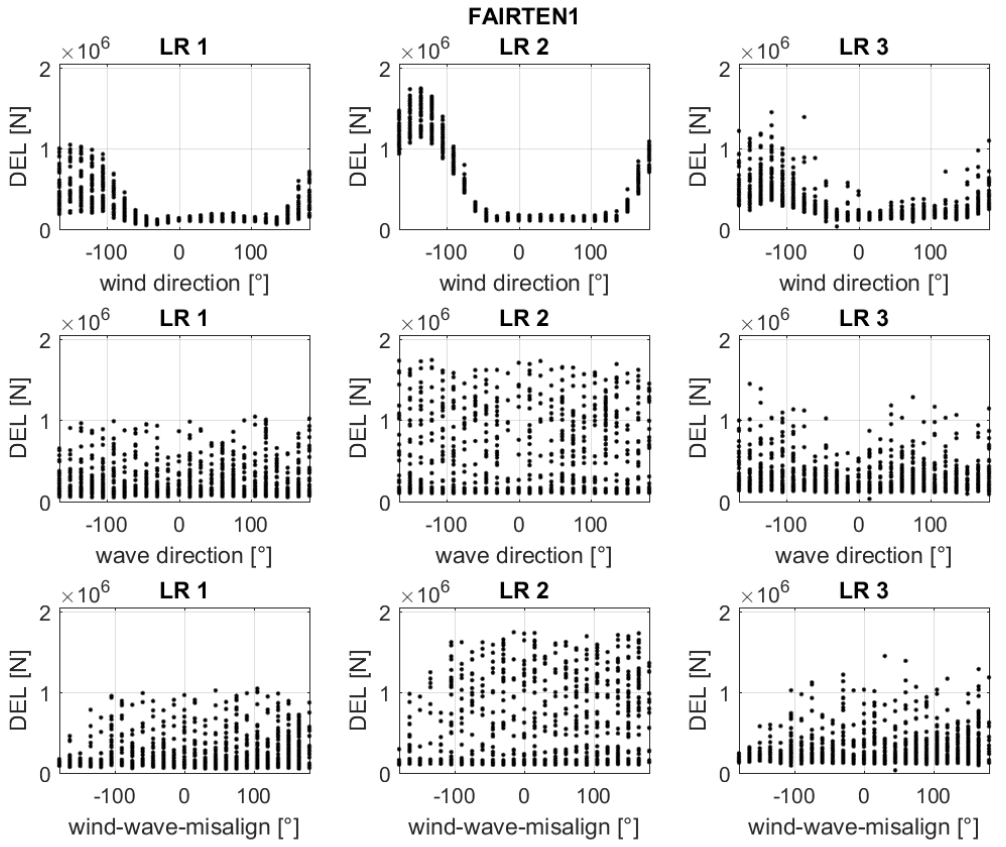
FAIRTEN1
LR 1
LR 2
LR 3
DEL [N]
×10^6
wind direction [°]
wave direction [°]
wind-wave-misalign [°]

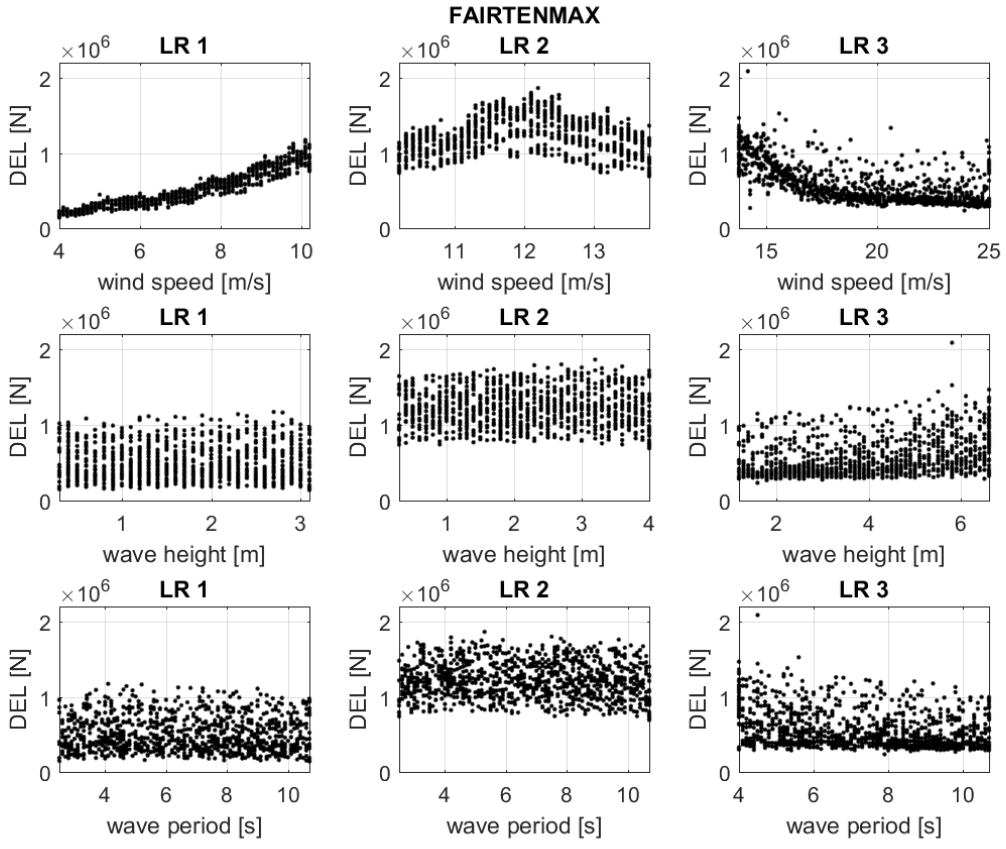
FAIRTENMAX
LR 1
LR 2
LR 3
DEL [N]
×10^6
wind speed [m/s]
wave height [m]
wave period [s]

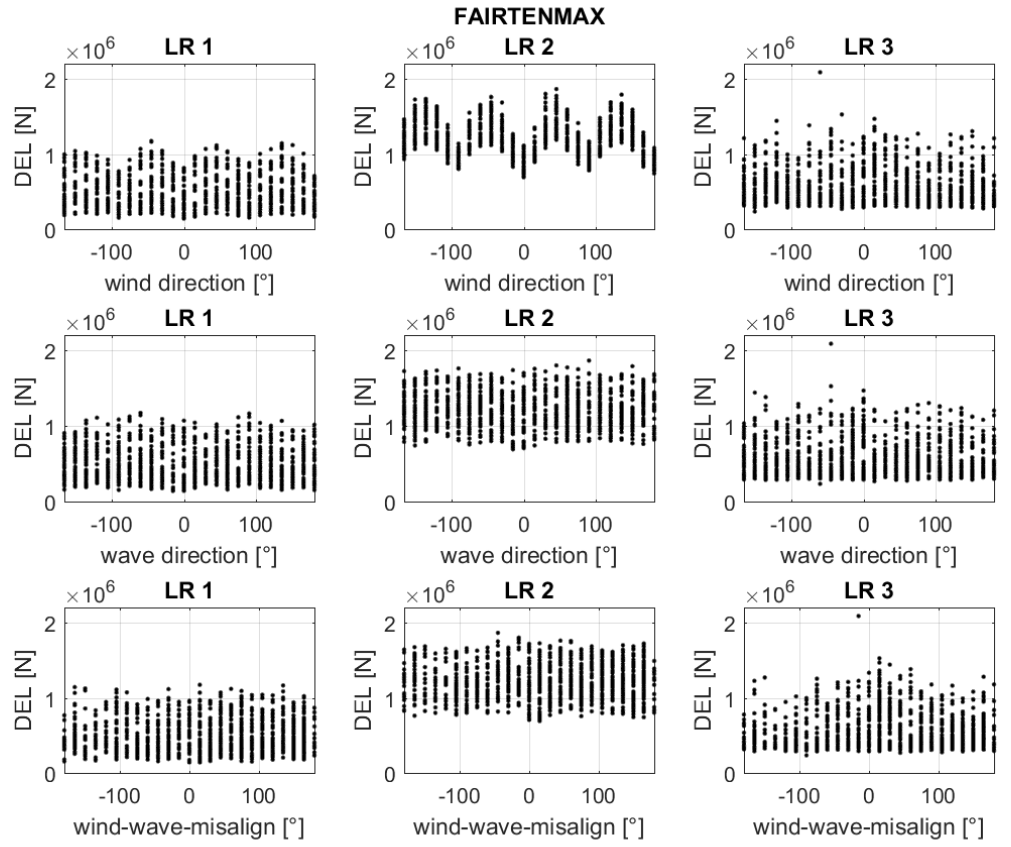
FAIRTENMAX
LR 1
LR 2
LR 3
DEL [N]
wind direction [°]
wave direction [°]
wind-wave-misalign [°]

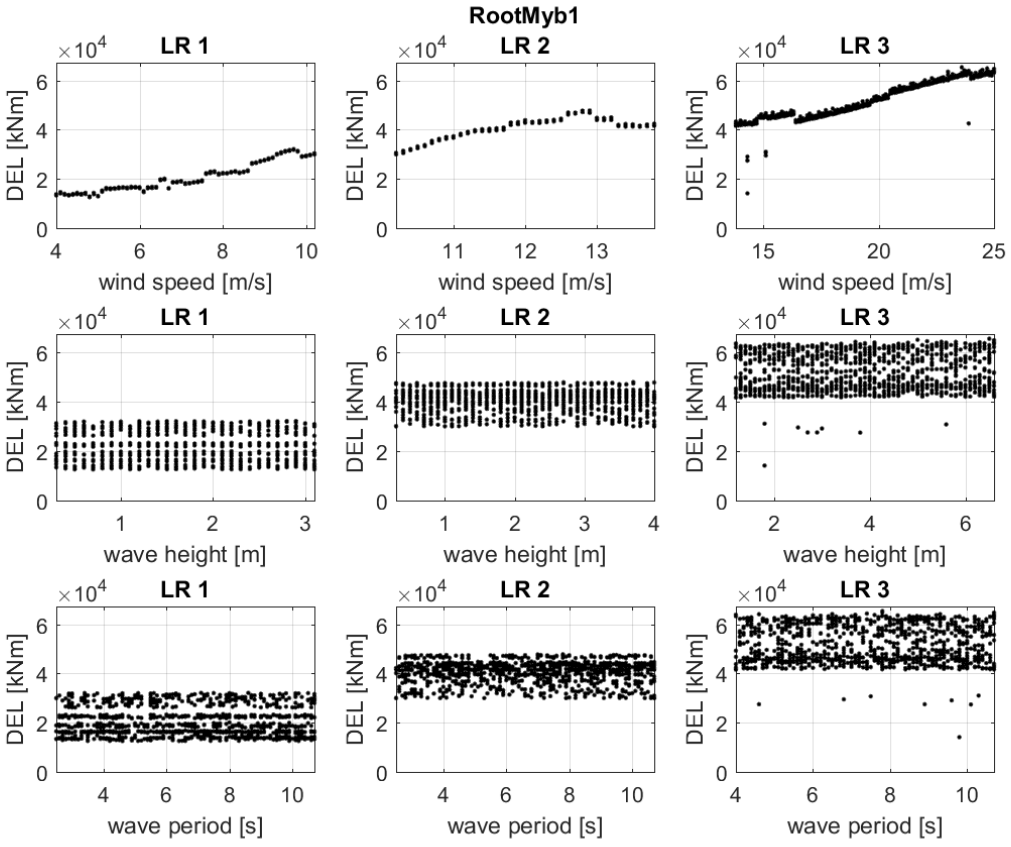
RootMyb1
LR 1
LR 2
LR 3
DEL [kNm]
wind speed [m/s]
wave height [m]
wave period [s]

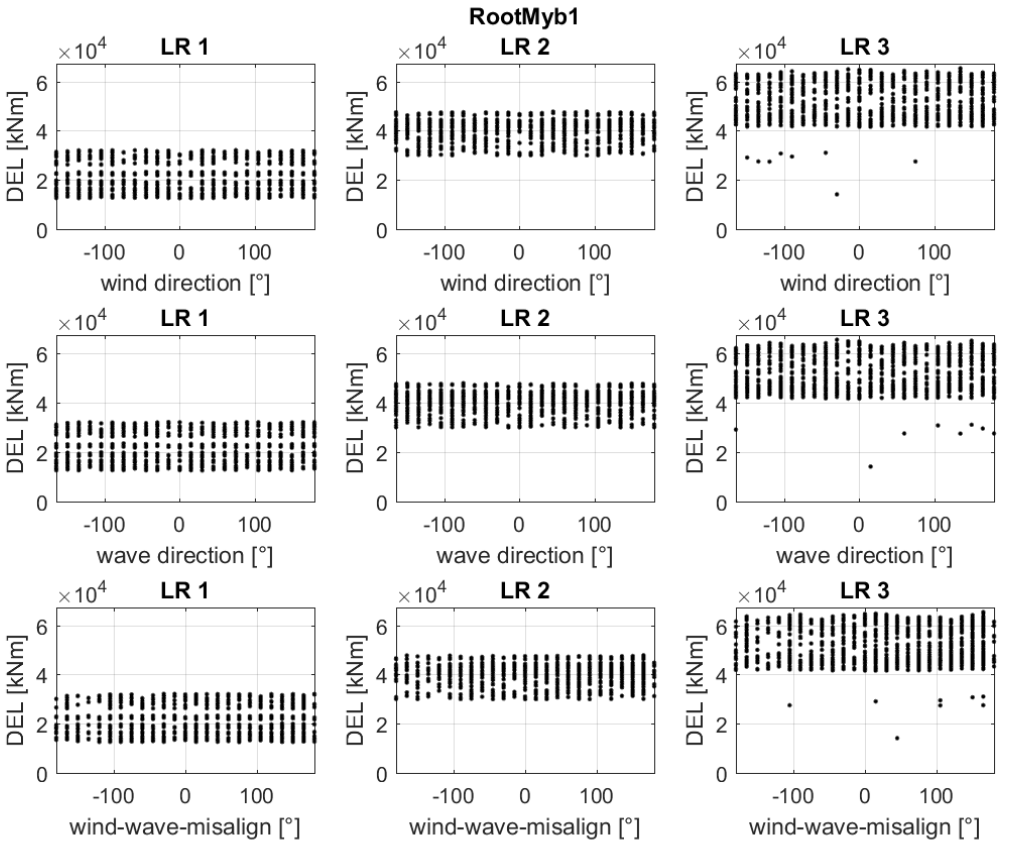
RootMyb1
LR 1
LR 2
LR 3
DEL [kNm]
wind direction [°]
wave direction [°]
wind-wave-misalign [°]

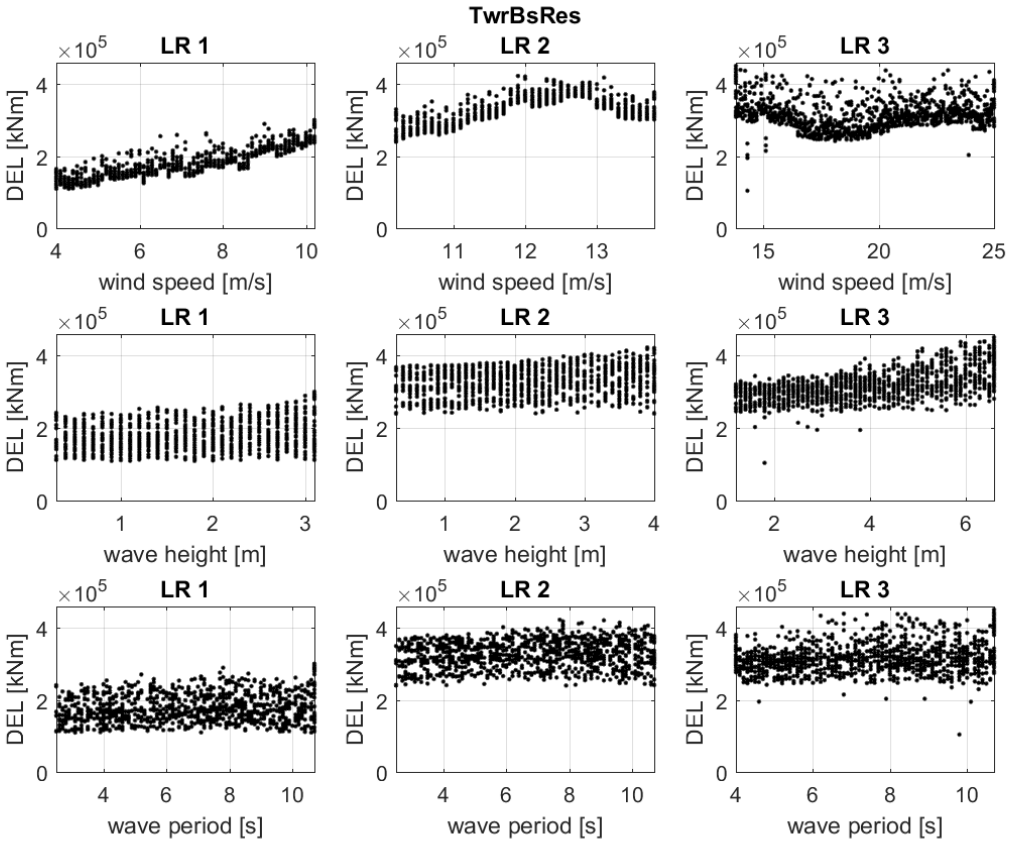
TwrBsRes
LR 1
LR 2
LR 3
DEL [kNm]
wind speed [m/s]
wave height [m]
wave period [s]

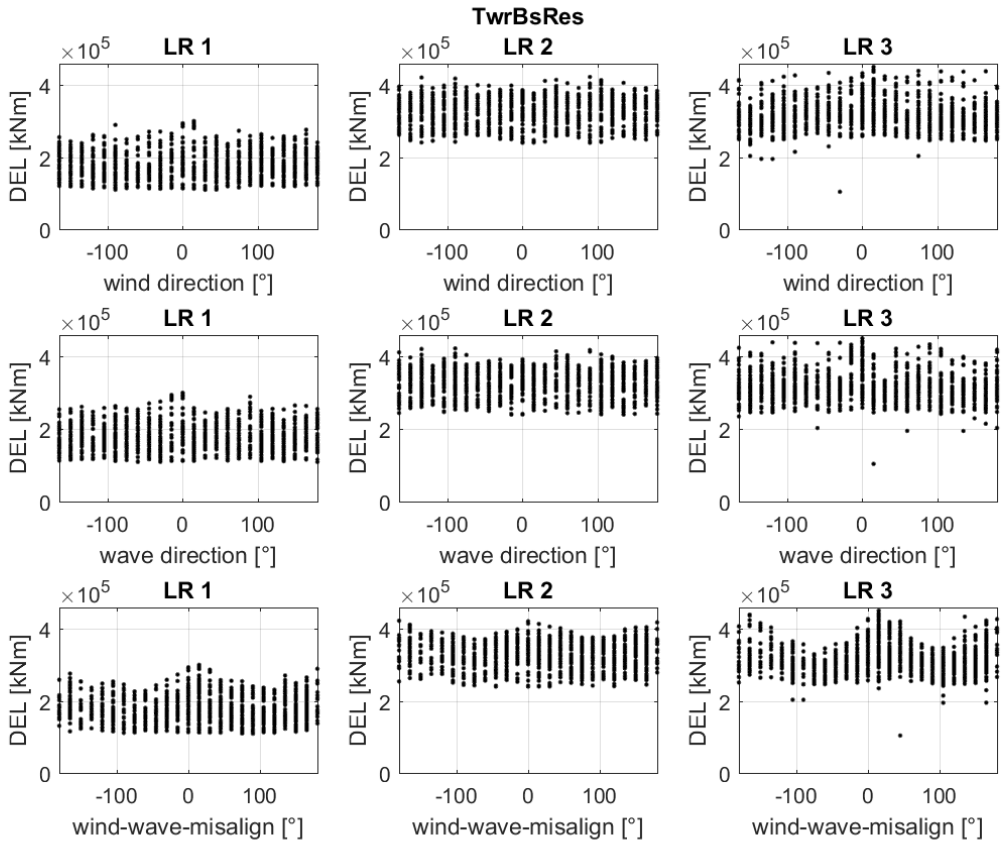
TwrBsRes
LR 1
LR 2
LR 3
DEL [kNm]
×10^5
wind direction [°]
wave direction [°]
wind-wave-misalign [°]

## 11.5 Scatter plots for Nautilus 8D sensitivity study for DLC 1.6

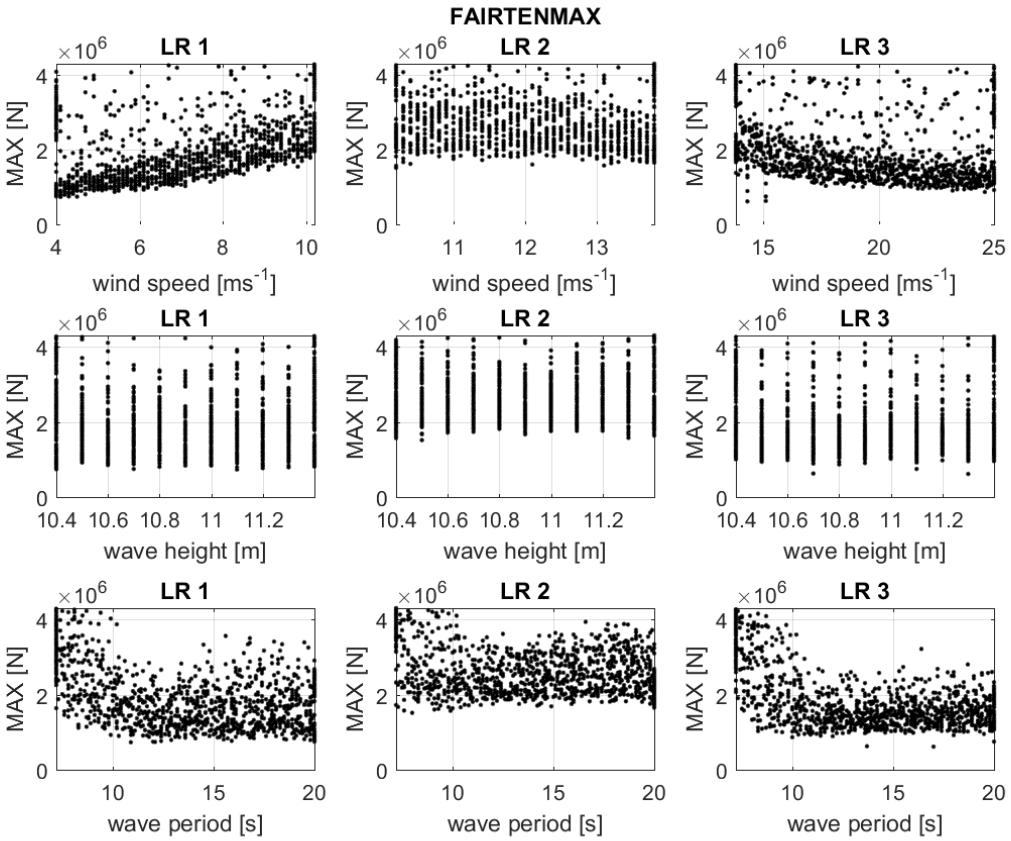

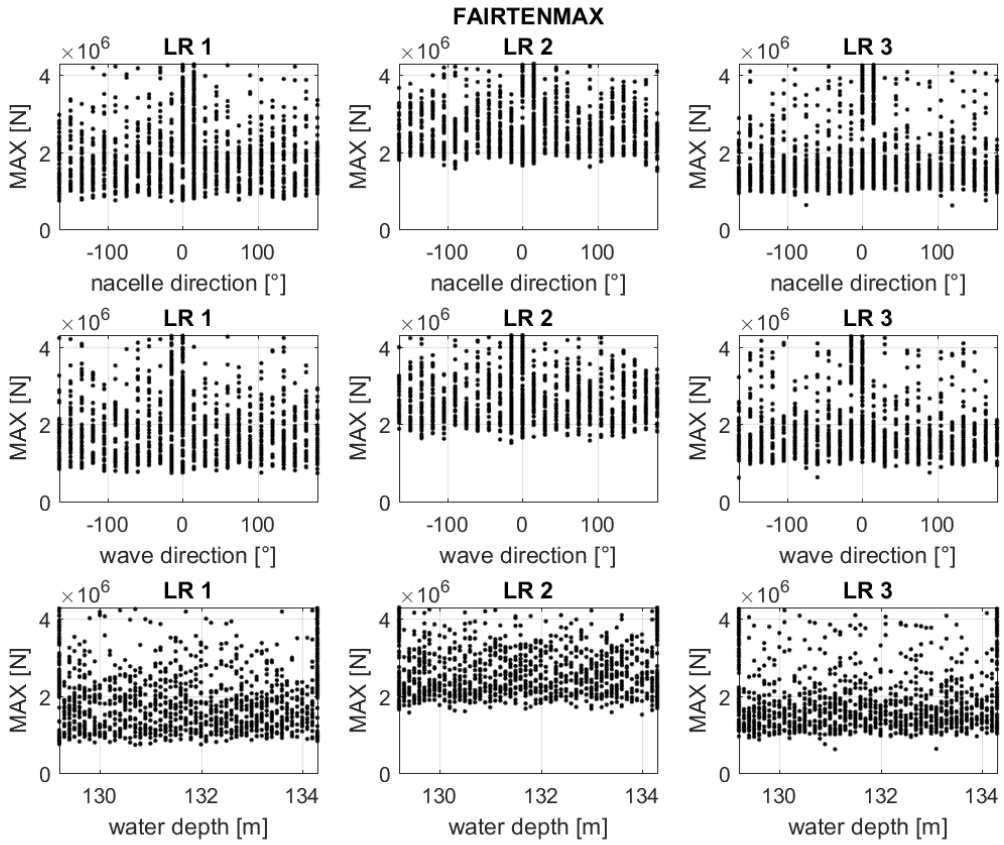
FAIRTENMAX
LR 1
LR 2
LR 3
MAX [N]
×10^6
nacelle direction [°]
wave direction [°]
water depth [m]

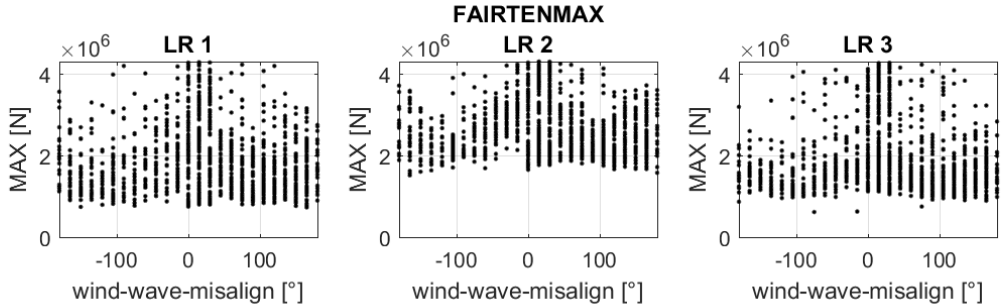
FAIRTENMAX
LR 1
LR 2
LR 3
MAX [N]
×10^6
wind-wave-misalign [°]

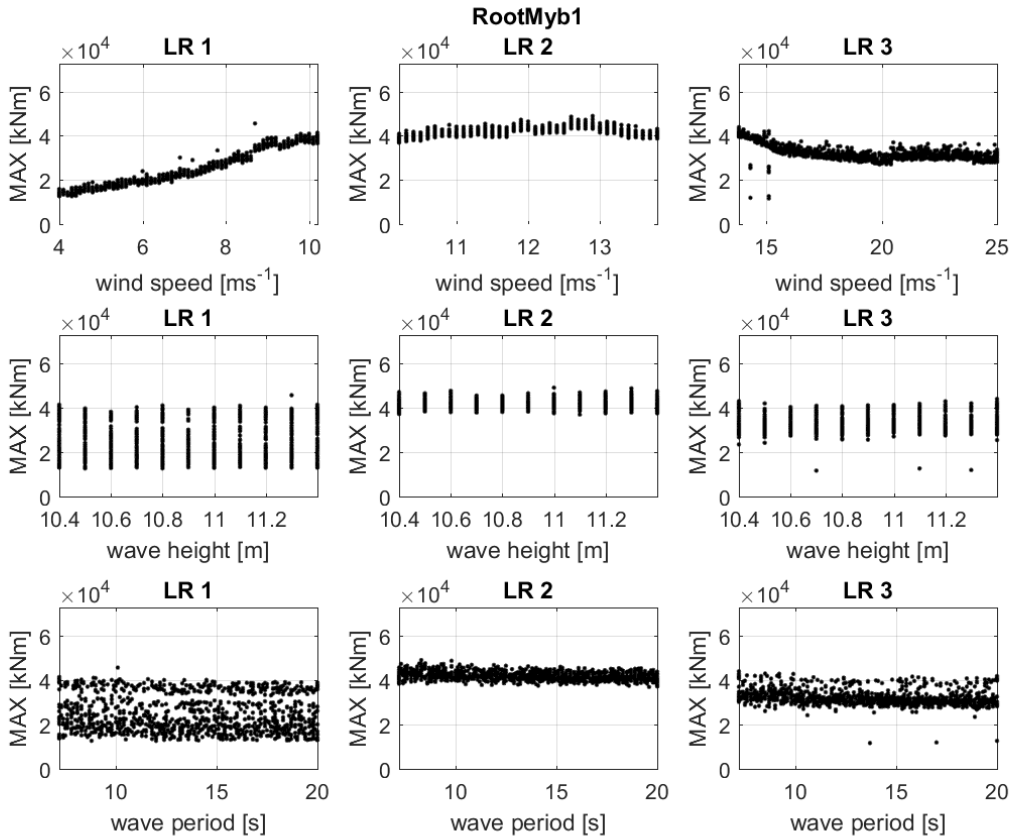
RootMyb1
LR 1
LR 2
LR 3
MAX [kNm]
wind speed [ms-1]
wave height [m]
wave period [s]

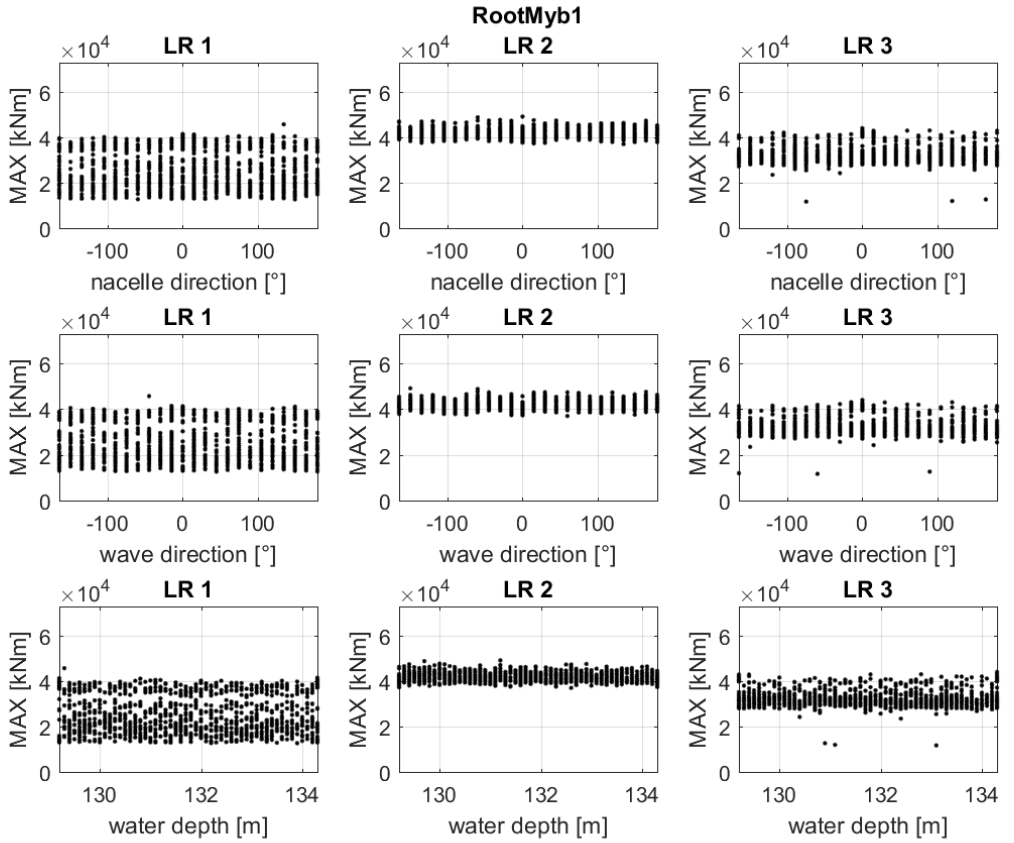
RootMyb1
LR 1
LR 2
LR 3
MAX [kNm]
nacelle direction [°]
wave direction [°]
water depth [m]

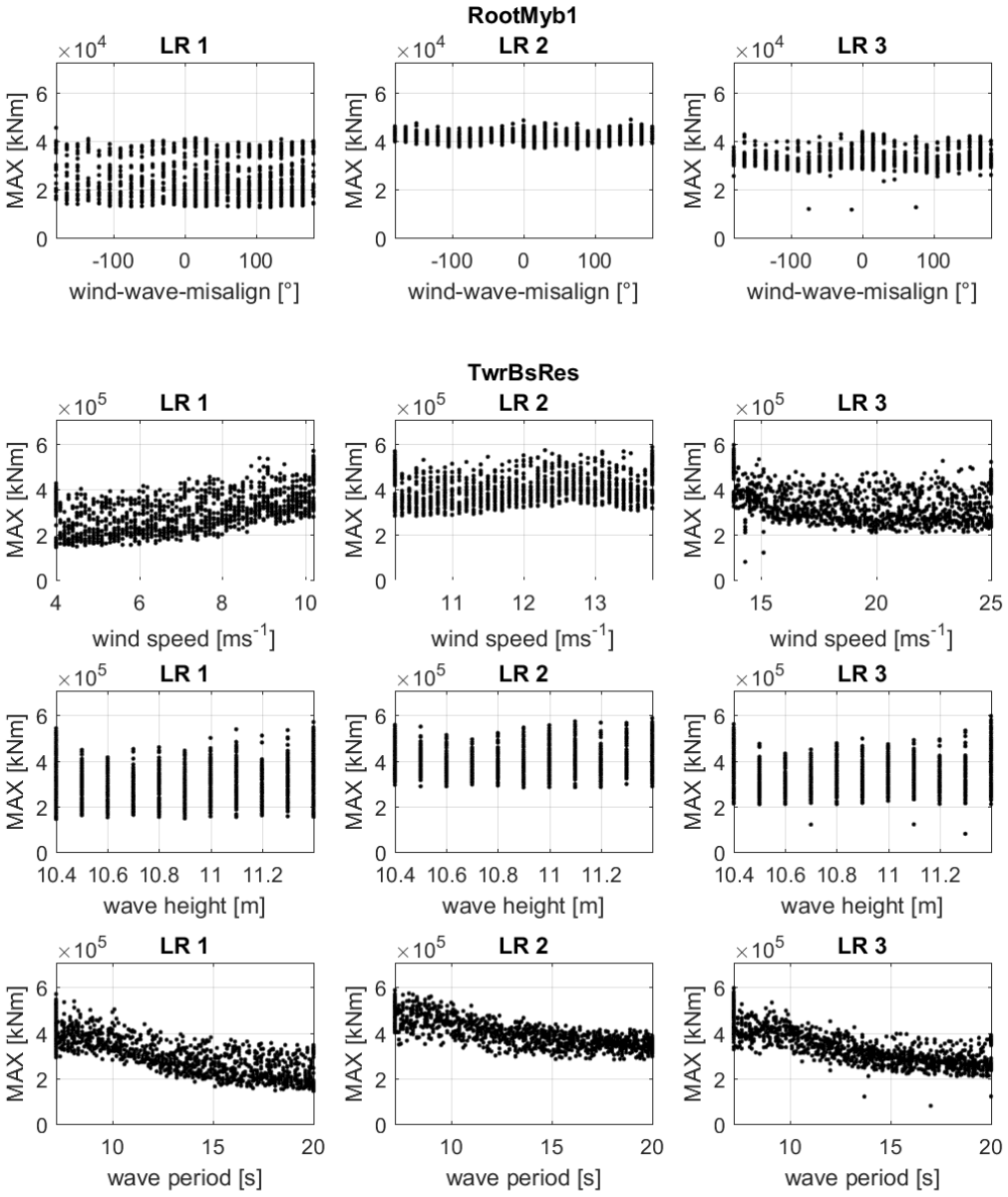
RootMyb1
LR 1
LR 2
LR 3
MAX [kNm]
wind-wave-misalign [°]
TwrBsRes
wind speed [ms-1]
wave height [m]
wave period [s]

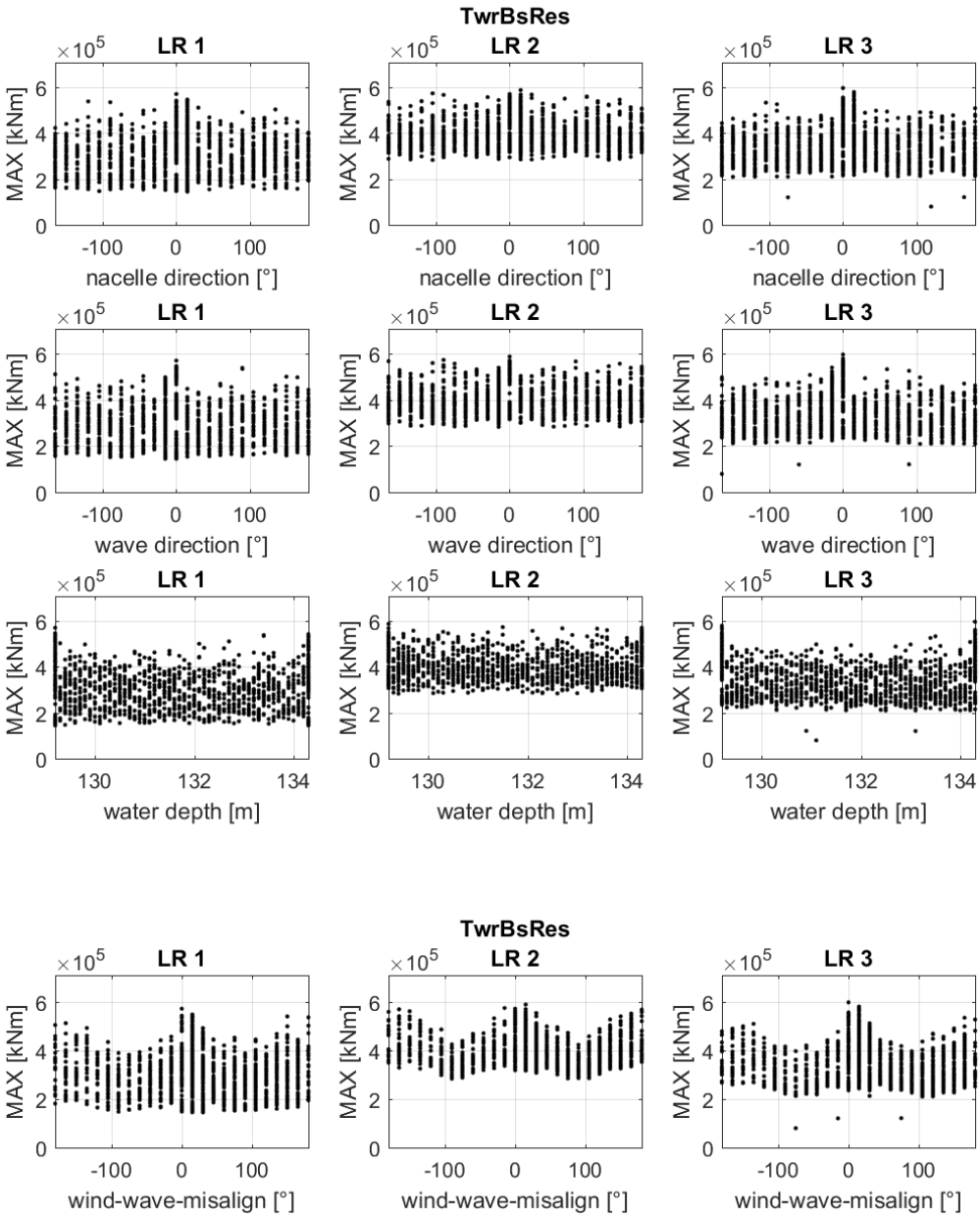
TwrBsRes
LR 1
LR 2
LR 3
MAX [kNm]
nacelle direction [°]
wave direction [°]
water depth [m]
wind-wave-misalign [°]